Discovery of New Scaffolds for GABA$_A$ Receptor Modulators from Natural Origin

Inauguraldissertation

zur
Erlangung der Würde eines Doktors der Philosophie
vorgelegt der
Philosophisch-Naturwissenschaftlichen Fakultät
der Universität Basel

von

Janine Michèle Zaugg

aus Trub, Bern

Basel, 2011

Genehmigt von der Philosophisch-Naturwissenschaftlichen Fakultät
auf Antrag von

Prof. Dr. Matthias Hamburger

Prof. Dr. Veronika Butterweck

Basel, den 21.06.2011

<div align="right">
Prof. Dr. Martin Spiess

Dekan
</div>

creative commons

Attribution-Noncommercial-No Derivative Works 2.5 Switzerland

---

You are free:

to Share — to copy, distribute and transmit the work

Under the following conditions:

Attribution. You must attribute the work in the manner specified by the author or licensor (but not in any way that suggests that they endorse you or your use of the work).

Noncommercial. You may not use this work for commercial purposes.

No Derivative Works. You may not alter, transform, or build upon this work.

- For any reuse or distribution, you must make clear to others the license terms of this work. The best way to do this is with a link to this web page.

- Any of the above conditions can be waived if you get permission from the copyright holder.

- Nothing in this license impairs or restricts the author's moral rights.

Quelle: http://creativecommons.org/licenses/by-nc-nd/2.5/ch/deed.en   Datum: 3.4.2009

Table of Contents

LIST OF ABBREVIATIONS

BBB	Blood-brain barrier
BW	Bodyweight
BZD	Benzodiazepine
CD	Circular dichroism
CD_{50}	Half maximal convulsant concentration
CHO *cells*	Chinese Hamster Ovary *cells*
CNS	Central nervous system
DMSO	Dimethyl sulfoxide
EC_{50}	Half maximal effective concentration
ECD	Electronic circular dichroism
ELSD	Evaporative light scattering detection
FDA	Food and Drug Administration
GABA	Gammaaminobutyric acid
$GABA_A$ *receptor*	Gammamaniobutyric acid type A *receptor*
HEK cells	Human endothelial kidney cells
hERG	Human ether-a-go-go related gene
HPLC	High performance liquid chromatography
HTS	High-througput screening
IR *spectroscopy*	Infrared *spectroscopy*
LGIC	Ligand gated ion channels
LTK- *cells*	Leukocyte tyrosine kinase *cells*
MS	Mass spectrometry
NDA	New drug approval
NMR *spectroscopy*	Nuclear magnetic resonance *spectroscopy*
NP	Natural product
PDA *detector*	Photo-diode array *detector*
TCM	Traditional Chinese medicine
TEVC	Two-microelectrode voltage clamp
TOF	Time-of-flight
UV *spectrum*	Ultraviolet light *spectrum*
VIS *spectrum*	Visible light *spectrum*

SUMMARY

Gamma-aminobutyric acid type A (GABA$_A$) receptors are the major inhibitory neurotransmitter receptors in the central nervous system (CNS). These heteropentameric transmembrane proteins act as chloride ion channel upon activation by the endogenous ligand γ-amino butyric acid (GABA). Until now, 11 distinct GABA$_A$ receptor subtypes have been identified in the human brain. They differ in their subunit stoichiometry, tissue localization, functional characteristics, and pharmacological properties. Many CNS depressant drugs, such as the benzodiazepines exert their action via enhancement of the GABAergic neuronal inhibition. However, therapy may be accompanied by unwanted side-effects and specific clinical action is precluded due to the lack of GABA$_A$ receptor subtype selectivity.

In a preliminary screen the lipophilic extracts of *Piper nigrum* fruits, *Angelica pubescens* roots, *Acorus calamus* roots, *Biota orientalis* leaves and twigs, and *Kadsura longipedunculata* fruits had shown positive GABA$_A$ receptor modulating activity in an *in vitro* functional, automated two-microelectrode voltage clamp assay with *Xenopus laevis* oocytes, which transiently expressed $\alpha_1\beta_2\gamma_{2S}$ GABA$_A$ receptors.

Aiming at the discovery of new scaffolds which act at the GABA$_A$ receptor, the active constituents of these five plant extracts were identified by means of an HPLC-based activity profiling approach. In total, we discovered 28 secondary metabolites with positive GABA$_A$ receptor modulating properties belonging to the structural classes of coumarins, monoterpenes, sesquiterpenes, diterpenes, phenylpropanes, piperamides, and lignans. Their structures were elucidated by a combination of powerful analytical methods such as HPLC-PDA-TOF-MS, highly sensitive microprobe NMR, and for chiral compounds, polarimetry and ECD. Determination of relative and absolute configuration was supported by conformational analysis and quantum chemical calculations. Furthermore, three yet unknown natural products could be identified.

HPLC-based activity profiling with *P. nigrum* enabled the identification of 13 structurally related piperamides with minimum amount of extract. This allowed us to draw preliminary structure activity considerations for the scaffold of piperine, which was the main $\alpha_1\beta_2\gamma_{2S}$ GABA$_A$ receptor modulator in this plant (EC$_{50}$: 52.4 ± 9.4 μM, maximal stimulation of GABA induced chloride currents (I_{GABA}) by 302% ± 27%).

Sandaracopimaric acid and isopimaric acid from *B. orientalis* were tested for subtype selectivity at $\alpha_{1-3,5}\beta_{1-3}\gamma_{2S}$ subtypes which revealed a comparatively high efficiency of both compounds at $\alpha_{2/3}$-subunit containing receptors. Additionally, sandaracopimaric acid exerted superior efficiency at receptors comprising β_2-subunits. It showed EC_{50} values from 24.9 ± 6.3 µM to 82.2 ± 46.6 µM, and efficiencies ranging between $502\% \pm 56\%$ to $1101\% \pm 98\%$ potentiation of I_{GABA} at the subtypes of investigation. A decrease of locomotor activity in the Open Field behavioral model was observed after intraperitoneal injection of 3 to 30 mg sandaracopimaric acid per kg bodyweight in mice. A trend towards anxiolytic-like activity could be observed with 1 and 3 mg/kg.

Further "drug-like" GABA$_A$ receptor modulating scaffolds were discovered among the lignans from *K. longipedunculata* (potencies down to 12.8 ± 3.1 µM and efficiencies up to $886 \pm 291\%$ stimulation of I_{GABA}) and among the sesquiterpenes from *A. calamus* (potencies down to 34.0 ± 6.7 µM and efficiencies up to $886 \pm 105\%$ stimulation of I_{GABA}). These substances have potential for the further development as therapeutics acting at the GABA$_A$ receptor.

ZUSAMMENFASSUNG

Gamma-Aminobuttersäure Typ A (GABA$_A$) Rezeptoren sind die wichtigsten inhibitorischen Rezeptoren im zentralen Nervensystem. Neunzehn verschiedene GABA$_A$ Rezeptor Untereinheiten können in unterschiedlicher Stöchiometrie zu Heteropentameren (GABA$_A$ Rezeptor Subtypen) konglomerieren und so transmembranäre Chloridionenkanäle bilden, die durch den endogenen Liganden γ-Aminobuttersäure (GABA) aktiviert und dadurch geöffnet werden. Bisher konnten 11 verschiedene GABA$_A$-Rezeptor-Subtypen im menschlichen Gehirn identifiziert werden. Diese unterscheiden sich in ihrer Gewebe-Lokalisierung und ihren funktionellen und pharmakologischen Eigenschaften. Viele zentraldämpfende Medikamente, wie z.B. die Benzodiazepine üben ihre Wirkung über die Verstärkung der GABAergen Hemmung neuronaler Schaltkreise aus. Die Therapie mit diesen Wirkstoffen ist jedoch oft von unerwünschten Nebenwirkungen begleitet, und eine spezifische klinische Wirkung kann aufgrund der fehlenden Selektivität für einzelne GABA$_A$-Rezeptor-Subtypen nicht erreicht werden.

Im Rahmen eines vorausgehenden Screenings riefen lipophile Extrakte aus den Früchten von *Piper nigrum* und *Kadsura longipedunculata*, aus Wurzeln von *Angelica pubescens* und *Acorus calamus*, sowie aus Zweigen und Blättern von *Biota orientalis* eine Verstärkung des GABA-induzierten Chloridionen Stroms durch GABA$_A$ Rezeptoren des $\alpha_1\beta_2\gamma_{2S}$ Subtyps hervor. Als Testsystem diente ein automatisiertes Zwei-Mikroelektroden-Spannungsklemme Verfahren an *Xenopus* Oozyten. Die aktiven Inhaltsstoffe der fünf Pflanzenextrakte wurden mittels HPLC-basiertem Aktivitäts Profiling identifiziert, mit dem Ziel neuartige Verbindungen mit GABA$_A$ Rezeptoraktivität zu entdecken.

Insgesamt wurden 28 Naturstoffe aus verschiedenen Strukturklassen (Coumarine, Monoterpene, Sesquiterpene, Diterpene, Phenylpropane, Piperamide und Lignane) isoliert, welche alle positiv GABA$_A$-Rezeptor modulierende Eigenschaften aufwiesen. Für deren Strukturaufklärung wurden analytische Methoden wie HPLC-PDA-TOF-MS, 'Microprobe' NMR (Mikro-Probenkopf) und, für chirale Verbindungen, Polarimetrie und Zirkulardichroismus eingesetzt. Die Bestimmung der relativen und absoluten Konfiguration wurde dabei durch Konformationsanalysen und quantenchemische Berechnungen unterstützt. Darüber hinaus konnten drei bisher unbekannte Naturstoffe identifiziert werden.

Neben Piperin, das am $\alpha_1\beta_2\gamma_{2S}$-Subtyp eine Wirkstärke von 52.4 ± 9.4 μM (EC_{50}) und eine maximale Stimulation der GABA-induzierten Chloridströme von 302% ± 27% aufwies, konnten aus *Piper nigrum* mithilfe des HPLC-basierten Aktivitäts Profiling noch weitere strukturell verwandte, unterschiedlich stark aktive Piperamide identifiziert werden. Dadurch konnten erste Voraussagen bezüglich Struktur-Wirkungs Beziehungen dieser neuartigen $GABA_A$ Rezeptor Modulatoren zu getroffen werden.

Sandaracopimarsäure und Isopimarsäure aus *B. orientalis* wurden an $\alpha_{1-3,5}\beta_{1-3}\gamma_{2S}$ Subtypen auf mögliche Subtyp-Selektivität hin getestet. An Rezeptoren mit $\alpha_{2/3}$-Untereinheiten trat bei beiden Substanzen ein vergleichsweise hoher Maximaleffekt auf. Die Wirkstärken von Sandaracopimaric variierten zwischen 24.9 ± 6.3 μM und 82.2 ± 46.6 μM, die Maximaleffekte zwischen 502% ± 56% und 1101% ± 98% an den verschiedenen Subtypen. Zusätzlich konnte für diese Substanz ein vergleichsweise starker Maximaleffekt an Rezeptoren mit β_2-Untereinheiten gemessen werden.

Im Open-Field-Test mit Mäusen wurde nach intraperitonealer Injektion von 3 bis 30 mg Sandaracopimarsäure pro Kilogramm Körpergewicht eine Abnahme der lokomotorischen Aktivität beobachtet. Bei niedrigeren Dosierungen (1 und 3 mg/kg) war ein Trend hin zu anxiolytischer Aktivität festzustellen.

Weitere, aus pharmakologischer Sicht interessante, Naturstoffe mit vielversprechender $GABA_A$-Rezeptor Aktivität, konnten aus *K. longipedunculata* isoliert werden. Die Lignane wiesen EC_{50} Werte ≥ 12.8 ± 3.1 μM und Maximaleffekte ≤ 886% ± 291% auf. Auch unter den Sesquiterpenen aus *A. calamus* fanden sich einzelne interessante Verbindungen (EC_{50} ≥ 34.0 ± 6.7 μM, Maximaleffekte ≤ 886% ± 105%). Diese Substanzen sind geeignete Kandidaten für die Entwicklung neuer Wirkstoffe mit $GABA_A$-Rezeptor Aktivität.

1. AIM OF THE WORK

Therapy with drugs acting at the $GABA_A$ receptor has been hampered by serious unwanted side effects such as cognitive impairment, tolerance, and drug dependence. These are partly caused by insufficient $GABA_A$ receptor subtype selectivity. Current development of subtype-specific $GABA_A$ receptor modulators with a beneficial clinical profile largely focuses on exploring the benzodiazepine binding pocket using medicinal chemistry on known drugs. There is an urgent need for novel scaffolds acting at the $GABA_A$ receptor with potential for drug development. Moreover, such substances might enhance understanding of drug interaction with this complex target.

Nature provides a wealth of small molecules with huge structural diversity. Therefore a promising approach in lead discovery is to screen for new $GABA_A$ receptor ligands in biogenic material. Numerous studies have reported interaction of extracts or purified natural products with the $GABA_A$ receptor [1, 2]. However, many are limited to data from binding assays and hence only allow restricted estimation of a compound's potential as a lead candidate.

The starting point of this work was a screen of 982 plant and fungal extracts in an automated two-microelectrode voltage clamp *in vitro* assay using *Xenopus laevis* oocytes which transiently expressed $GABA_A$ receptors of the $\alpha_1\beta_2\gamma_{2S}$ subtype. A total of 101 extracts potentiated GABA induced chloride currents by more than 30% at 100 µg/ml, which was set as a threshold for sufficient activity.

As a first step, promising extracts had to be selected for isolation of their active principles. Selection criteria included sufficient positive $GABA_A$ receptor modulatory activity, expected chemical diversity based on taxonomic considerations, and contingently traditional usage.

In a next step, constituents responsible for the activity within active extracts had to be identified and evaluated according to their lead potential. The aim was to isolate the most interesting molecules with the aid of diverse chromatographic methods and to fully elucidate their structure by means of spectrometric and spectroscopic methods. The focus, however, had to be kept not solely on the isolation and characterization of the major bioactive compounds, but also on structurally related constituents occurring in the same plant to evaluate structure-activity relationships.

The activity of the compounds was to be reassessed in the *Xenopus* assay by complete pharmacological characterization at the $\alpha_1\beta_2\gamma_{2S}$ $GABA_A$ receptor subtype (that is the determination of potency by measuring EC_{50} values and efficiency by recording maximal potentiation of the GABA induced chloride current). Pronounced modulatory activity at the main

GABA$_A$ receptor subtype and structural "drug-likeness" were criteria for targeted selection of novel scaffolds that were to be tested for GABA$_A$ receptor subtype selectivity and, in a next step, for *in vivo* pharmacological effects.

References

1 *Johnston GAR, Hanrahan JR, Chebib M, Duke RK, Mewett KN*. Modulation of ionotropic GABA receptors by natural products of plant origin. Adv Pharmacol 2006; 54: 286-316
2 *Tsang S, Xue H*. Development of effective therapeutics targeting the GABAA receptor: naturally occurring alternatives. Curr Pharm Design 2004; 10: 1035

2. INTRODUCTION

2.1. Lead Finding from Nature

Nature has been a generous source for remedies for thousands of years. All over the world people have been treating their illnesses and diseases by using medicinal preparations from natural origin. While in western countries phytotherapeutics currently experience a renaissance as "soft medicine", nature has not ceased to be an important source for modern drug discovery [1]. Historically, many ground-breaking drugs were discovered from nature: penicillin from the fungus *Penicillium notatum*, morphine from the opium poppy (*Papaver somniferum*) or digoxin from the foxglove (*Digitalis purpurea*) to mention a few. These were, however, marketed in times when safety requirements for drug approval were at a much lower level than today. If Aspirin®, a derivative of salicylic acid from willow bark, had not been registered as a drug already in 1899 it would probably not cure billions of people's headaches today since it would have failed preclinical tests due to gastric toxicity in rats and dogs [2]. Despite constantly increasing regulatory requirements, nearly 30% of the new chemical entities (NCE) approved by the U.S. Food and Drug Administration (FDA) within more than two decades (1981-2006) were natural products or semi-synthetic derivatives thereof [3]. In March 2008, there were 37 new drug approvals (NDA) or close to NDA (late-stage clinical development) falling into this class [4]. Of these, 8 have been launched or are in registration with the (FDA) as at April 2011 (Table 1).

Table 1: Natural products and natural product derivatives which have been launched or are in registration with the FDA since March 2008 [4, 7].

Drug	Lead compound	Year introduced	Disease area	Classification
Launched				
Eribulin	Halichondrin B	2010	Oncology	NP-derived
Everolimus	Rapamycin	2009	Oncology	Semi-synthetic
	(Sirolimus)	2010	Immunosuppression	NP
Telavancin	Vancomycin	2009	Antibacterial	Semi-synthetic NP
Methylnaltrexone	Morphine	2008	Opioid-induced constipation and pain	NP-derived
Fingolimod	Myriocin	2010	Multiple sclerosis	NP-derived
Cabazitaxel	Paclitaxel	2010	Oncology	Semi-synthetic NP
NDAs				
Dapagiflozin	Phlorizin	2011	Type 2 diabetes	NP-derived
Fidaxomicin	Tiacumicin B	2010	Antibacterial	NP

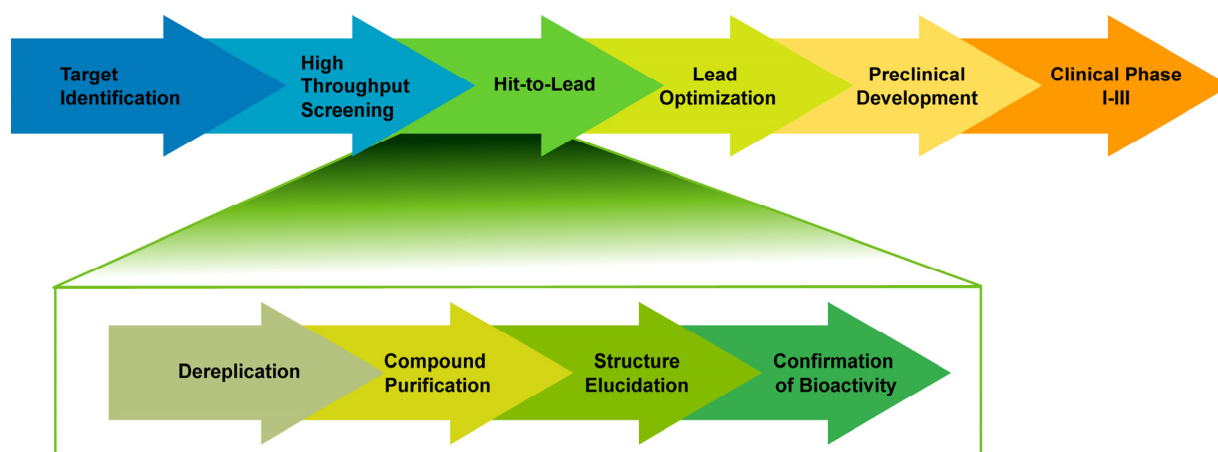NDA: New drug approval; NP: Natural Products

Figure 1: Drug discovery and development from natural origins. The upper bar shows the general steps in the drug discovery and development process. The lower bar highlights steps within the hit-to-lead process which need to be accomplished when screening is performed with crude extracts or fractions. On the basis of Koehn, F.E., 2008 [5]

Even though potent drugs recently have been developed from natural sources (for extensive reviews see Potterat and Hamburger, 2008 [1] and Newman and Cragg, 2007 [3]), drug discovery and development from natural sources seem to be less and less attractive for pharmaceutical companies [5]. Competitive marketing, laborious litigation, and the above mentioned increasing regulatory and public requirements concerning drug safety, have made drug discovery and development an extraordinarily cost-intensive business while pharmaceutical companies must calculate carefully cost-benefits ratios of each drug candidate to hold their ground [6].

Several "challenges facing drug discovery from natural sources" have been listed by Li and Vederas in 2009 [6]. They include disadvantages of high-throughput screening (HTS) of natural sources over HTS of synthetic compound libraries (poor solubility, complex mixtures, synergisms/antagonisms, poor compound stability). Moreover, traditional isolation strategies of bioactive natural products such as bioassay-guided isolation (see Chapter 2.2) are accompanied by a high probability of hit duplication [6, 8]. Further challenges in drug discovery from natural origin are characterization of the complex structures of natural products, cost-intensive development of synthesis strategies, difficulties in access and resupply of source material, and intellectual property issues [1, 6]. However, apart from various efforts undertaken in revolutionizing drug discovery from natural origin [6, 9], the traditional approach of lead discovery from nature is still pursued and therefore constantly being optimized [1, 8]. The most important steps in screening of biogenic material and hit-to-lead development with natural products (Figure 1) are described in Chapter 2.2.

References

1 *Potterat O, Hamburger M*. Drug discovery and development with plant-derived compounds. Prog Drug Res 2008; 65: 45, 7-118
2 *Lowe D*. Aspirin: Not Approvable. Spotlight Manhattan Institute for Policy Research, New York, 2005; http://www.medicalprogresstoday.com/spotlight/
3 *Newman DJ, Cragg GM*. Natural products as sources of new drugs over the last 25 years. J Nat Prod 2007; 70: 461-77
4 *Butler MS*. Natural products to drugs: natural product-derived compounds in clinical trials. Nat Prod Rep 2008; 25: 475-516
5 *Koehn FE*. High impact technologies for natural products screening. Prog Drug Res 2008; 65: 175, 7-210
6 *Li JW, Vederas JC*. Drug discovery and natural products: end of an era or an endless frontier? Science 2009; 325: 161-5
7 http://www.drugs.com/history/, Online Database, accessed: April 2011.
8 *Potterat O*. Targeted approaches in natural product lead discovery. Chimia 2006; 60: 19-22
9 *Potterat O, Hamburger M*. Natural products in drug discovery - concepts and approaches for tracking bioactivity. Curr Org Chem 2006; 10: 899-920

2.2. Identification and Structural Characterization of Bioactive Plant-derived Natural Products

Screening of Plant Extracts for Bioactivity

After target identification and establishment of a suitable bioassay, different approaches for lead discovery from plant material may be chosen. While prefractionated extracts or purified natural product libraries are preferred by pharmaceutical companies, a reasonable, less costly alternative is screening crude extracts. The latter provides a much greater structural diversity than a pure compound library and includes fewer samples to screen compared to prefractionated extracts [1]. Different strategies are pursued to assemble extract libraries. Source material may be collected randomly or in a targeted manner with a focus on chemotaxonomic relationships. Ethnomedicinal and traditional usage is another criterion for selection since traditional medicines are rich in pharmacologically active compounds [2], and phytotherapeutical resources like European folk medicine, traditional Chinese medicine (TCM), or Ayurvedic medicine are readily accessible.

Isolation of Bioactive Natural Products

Bioassay-guided isolation is the classical approach used to unravel the identity of bioactive natural products simultaneously with their exhaustive isolation from the source material. It usually begins with open column chromatography of an active extract followed by consecutive chromatographic steps with increasing separation performance. The isolation of the active principles is guided by intermediate testing of chromatographic fractions in the particular bioassay. Complete structure elucidation and compound identification is often done at the end of the process (Figure 2). Immediate large scale isolation without the possibility of linking the activity to single compounds makes this strategy extremely cost-intensive and time-consuming, especially if in the end known or otherwise uninteresting compounds are identified. Moreover, bioactivity is often lost during the purification process. These are the major drawbacks of this approach, often referred to as a "search for the needle in the haystack", making it little applicable for the high-throughput environment of modern drug discovery [3].
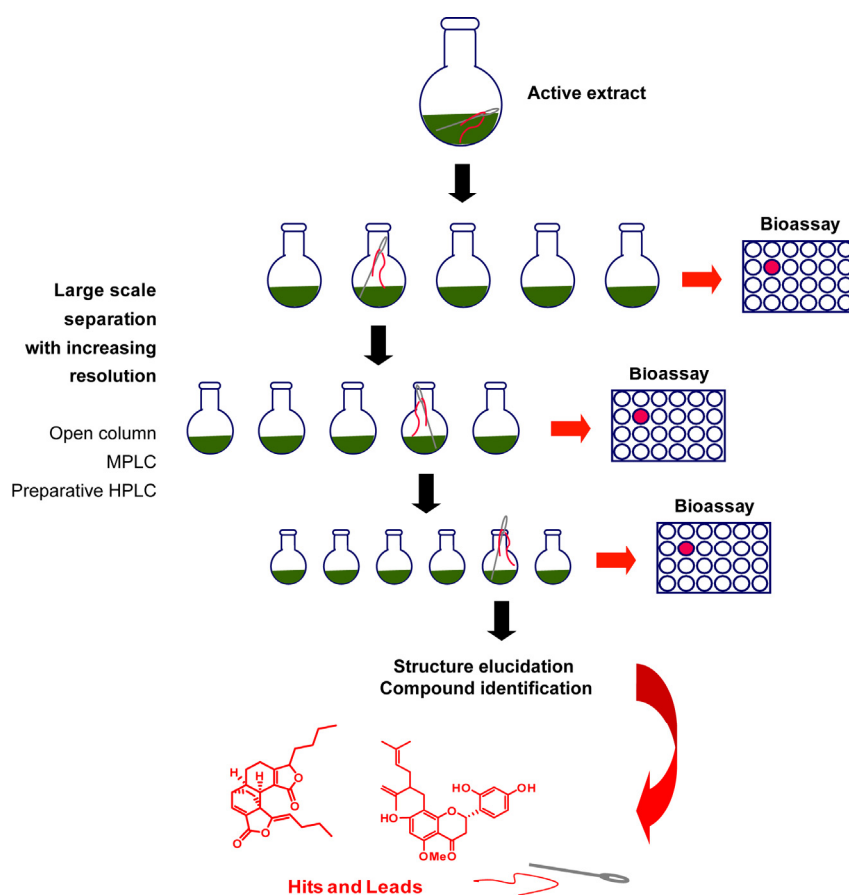
Figure 2: A search for the "needle in the haystack": the bioassay-guided approach. An active extract is separated in a large scale in a series of chromatographic steps starting with low resolution separation methods such as open column chromatography. Each fraction of every step is tested in the bioassay to track the active compound(s). Note that structure elucidation and hence compound identification is done at the end of the process.

The constant evolution of powerful analytical technologies like MS and NMR combined with the increasing performance of separation techniques has enabled a very elegant, miniaturized approach to accelerate dereplication[1] of bioactive compounds in crude extracts, namely HPLC-based activity profiling (Figure 3). Briefly, a minute amount of a bioactive extract is separated over analytical or semi-preparative HPLC and divided into microfractions which are to be tested in the particular bioassay. Simultaneously, on-line or off-line chemical analysis allows direct allocation of the activity to single constituents which is in contrast to the classical approach of bioassay-guided isolation [3, 4]. An on-line HPLC-MS system is the basic equipment for HPLC-

---

[1] Identification of known or otherwise uninteresting compounds early in the isolation process in order to avoid duplication.

based activity profiling since it provides UV-VIS absorbance spectrum, mass abundance, molecular mass, and even molecular formula in case of high accuracy mass detectors in a single run [5]. Simple quantitative information may also be obtained by hyphenated evaporative light scattering detection (ELSD) [3]. Detailed structural information is achieved by NMR measurements of peak-resolved HPLC-fractions containing the compounds of interest, and even determination of absolute configuration is possible by on-line HPLC-CD [6]. Comparison of combined spectral data with natural products databases allows rapid dereplication of interesting constituents. Hence, promising secondary metabolites can be distinguished from uninteresting ones. Based on these results, a project can be discontinued or further pursued by beginning large-scale isolation.
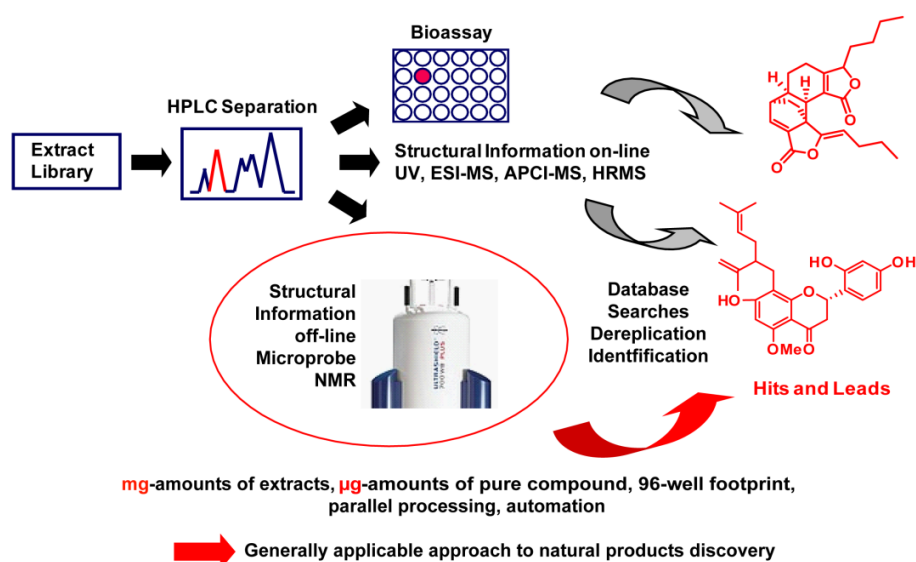

Figure 3: A schematic view of the miniaturized HPLC-based activity profiling approach. High performance chromatography allows early dereplication, and highly sensitive and accurate analytical instruments enable structure elucidation by using only minute amounts of an extract. Figure kindly provided by M. Hamburger.

Recently, a variety of innovative methodologies for tracking bioactivity within complex mixtures have been established, but they have not yet found broad application. These include diverse MS-based methods mostly detecting ligands binding to a specific immobilized target, NMR-based methods revealing ligand interaction with soluble proteins, and investigations on a microchip format such as *in vitro* or *in vivo* gene expression profiling on microarrays [3]. HPLC is the most widespread method for separation of extracts and it has been hyphenated to bioassays

(mostly receptor or enzymatic binding assays) to track bioactivity. However, such fully on-line strategies cannot be broadly applied since the number of bioassays compatible with HPLC separation conditions is limited. Moreover, post-column diffusion lowers peak resolution and every set-up using a different bioassay must be validated separately [3]. In principle, microfractionation such as in HPLC-based activity profiling and subsequent off-line sample testing allows combination with all cell-based and molecular assays which are usable in a microscale. This approach has been proven to be well suited to high throughput settings [7-10]. HPLC-based activity profiling is a cost-efficient and time-saving strategy to detect robust hits from natural origin. Early dereplication and complete structure elucidation using minimum amounts of extract is only possible due to a variety of high performance analytical methods which provide complementary data on the constitution and configuration of a compound. The most widely used methods combined with HPLC-based activity profiling are described briefly in the following section.

Structure Elucidation of Natural Products

A PDA detector is standard to modern HPLC equipment providing the spectral profile of a compound with a chromophore absorbing light from UV to near IR. The specific pattern of maximal absorptions, which for most natural products occurs between 200 and 550 nm, often allows relating them to classes of secondary metabolites with characteristic chromophores from the beginning [11]. Mass spectrometers with accuracy in the low ppm range provide accurate masses to calculate the molecular formula of a compound. Adequate equipment for the detection of accurate masses of non-volatile and thermally labile natural products consists of an ion source like electrospray ionization (ESI) or atmospheric-pressure chemical ionization (APCI), and a mass analyzer such as time-of-flight (TOF). Lower cost and lower accuracy ion trap analyzers are often coupled to HPLC and are suitable for MS^n experiments (repeated tandem mass spectrometry) which give insight into connectivity of atoms in a molecule [12]. Knowing the molecular formula is crucial for correct interpretation of NMR spectra, recorded in a next step for establishing a natural product's structure.

The technical advances made since the implementation of NMR into compound identification afforded the continuous generation of higher magnetic fields (currently, 23.5 Tesla can be reached with 1 GHz instruments), and high performance probes, such as capillary NMR flow probes and 1 mm microprobes with an active sample volume in the single-digit μL range, or

cryogenically cooled microprobes (down to 1.7 mm, active sample volume 30 µL). As a result, sensitivity and signal-to-noise ratio increased dramatically, allowing higher sample throughput and smaller sample quantities. This is very important for structure elucidation of natural products, since limited amount is one of the major issues [13]. The above mentioned technical preconditions enabled on-line interfacing NMR and chromatography. Sample application has been achieved by loop-transfer, on-flow, or stop-flow methods. In these cases, however, deuterated solvents are necessary for chromatography, and if undeuterated solvents are used, inevitable solvent suppression might interfere with analyte signals. Moreover, sample concentration is bound to natural abundance of the compound in the extract. At-line solid-phase extraction has been implemented to overcome these issues [11] but sample loss due to insufficient trapping/elution efficiency [14] remains a drawback. Off-line HPLC microfractionation and subsequent sample preparation by parallel drying and redissolving into an appropriate concentration for high sensitivity NMR, is a convenient, less costly alternative which is not hampered by concentration or passive diffusion issues, nor by sample loss.

A broad range of NMR experiments is available and the nature of the molecule dictates which ones are the most suitable for elucidation of constitution and configuration. One-dimensional ^{1}H-NMR and ^{13}C-NMR experiments, and two-dimensional homonuclear (^{1}H,^{1}H-COSY) and heteronuclear (^{1}H,^{13}C) correlation experiments such as HSQC and HMBC are standard in determining the covalent structure of a small molecule with limited signal overlap. For more complex structures with several overlapping spin systems, additional experiments like e.g. (^{1}H,^{1}H)-TOCSY or (^{1}H,^{13}C)-HSQC-TOCSY are recommended. While these experiments detect scalar couplings between two nuclei, NOESY and ROESY experiments provide stereochemical information by displaying through space correlations to determine the complete 3D-structure of a molecule. These experiments, however, only disclose the relative configuration [13].

The Challenge of the Absolute Configuration

The determination of the absolute configuration of a natural product is indispensable since bioactivity as a cause of ligand-protein interactions is stereoselective. Therefore, for chiral compounds, structure elucidation is only complete if the absolute configuration is assigned. In rare cases, it can be determined by NMR experiments after esterification of the compound with Mosher's acid or by application of chiral lanthanide shift reagents [13, 15, 16]. An alternative analytical method to determine the absolute configuration is X-ray diffraction, which requires the

natural product in crystallized form. Crystallization, however, depends on the compound's nature and is therefore not always possible [17]. In such cases, chiroptical methods such as optical rotation and circular dichroism (CD) may be essential to determine absolute configuration. CD provides information about conformation and absolute configuration but is restricted to compounds that have a chromophore in sufficient proximity to a stereocenter. Furthermore, its analysis relies largely on the comparison with reference spectra [18]. The emergence of high-performance computing allows prediction of CD spectra by quantum chemical calculations. This is especially valuable for the analysis of new molecular entities when chemical synthesis of the reference compound is not an alternative [19]. In 2008, Bringmann et al. suggested a solid approach (Boltzmann-approach) for *in silico* simulation of CD spectra (Figure 4).
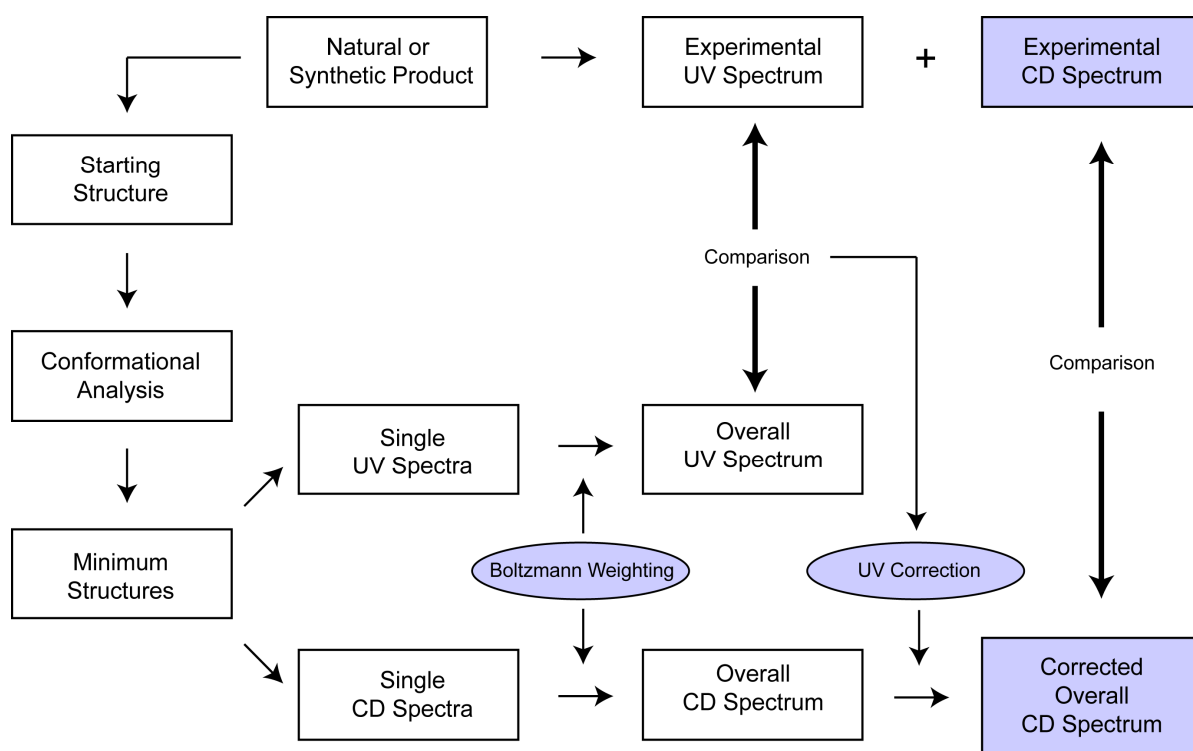

Figure 4: Overview of the Boltzmann-approach to determine the absolute configuration of a chiral compound by conformational analysis and CD calculations (adapted from Bringmann et al., 2008 [6]

Because flexible chromophores strongly influence the CD spectrum, a careful conformational analysis of an arbitrarily chosen enantiomer of the chiral compound is inevitable. This can be done by molecular mechanics. The most predominant conformers occurring within a specified energy window are then geometrically minimized by means of more sophisticated, quantum

chemical calculation methods, for example density function theory. Finally, time-dependent calculations of electronic transitions with each minimized conformer provide UV and CD spectra to be Boltzmann-weighted according to each conformer's energy. Superimposing these spectra results in an overall curve that can be compared with the experimental data. Computational errors sometimes make it necessary to slightly correct the calculated curve by adjusting it to the experimental spectrum based on the absorption maximum (UV-correction; Figure 4) [6].

Each of these calculation steps can be performed at different levels of accuracy and the best one depends on the nature of the investigated molecule [20]. An increase in accuracy usually corresponds to a longer calculation time and it is a challenge to find the right balance between sufficient accuracy and expenditure of time.

References

1   *Potterat O, Hamburger M*. Drug discovery and development with plant-derived compounds. Prog Drug Res 2008; 65: 45, 7-118

2   *Hamburger M, Marston A, Hostettmann K*. Search for new drugs of plant origin. Adv Drug Res 1991; 20: 167-215

3   *Potterat O, Hamburger M*. Natural products in drug discovery - concepts and approaches for tracking bioactivity. Curr Org Chem 2006; 10: 899-920

4   *Potterat O*. Targeted approaches in natural product lead discovery. Chimia 2006; 60: 19-22

5   *Koehn FE*. High impact technologies for natural products screening. Prog Drug Res 2008; 65: 175, 7-210

6   *Bringmann G, Gulder TAM, Reichert M, Gulder T*. The online assignment of the absolute configuration of natural products: HPLC-CD in combination with quantum chemical CD calculations. Chirality 2008; 20: 628-42

7   *Adams M, Christen M, Plitzko I, Zimmermann S, Brun R, Kaiser M, Hamburger M*. Antiplasmodial lanostanes from the *Ganoderma lucidum* mushroom. J Nat Prod 2010; 73: 897-900

8   *Danz H, Stoyanova S, Wippich P, Brattstroem A, Hamburger M*. Identification and isolation of the cyclooxygenase-2 inhibitory principle in *Isatis tinctoria*. Planta Med 2001; 67: 411-6

9   *Dittmann K, Gerhaeuser C, Klimo K, Hamburger M*. HPLC-based activity profiling of *Salvia miltiorrhiza* for MAO A and iNOS inhibitory activities. Planta Med 2004; 70: 909-13

10 *Potterat O, Wagner K, Gemmecker G, Mack J, Puder C, Vettermann R, Streicher R*. BI-32169, a bicyclic 19-peptide with strong glucagon receptor antagonist activity from *Streptomyces* sp. J Nat Prod 2004; 67: 1528-31

11 *Wolfender JL*. HPLC in natural product analysis: the detection issue. Planta Med 2009; 75: 719-34

12 *Glish GL, Vachet RW*. The basics of mass spectrometry in the twentyfirst century. Nat Rev Drug Discovery 2003; 2: 140-50

13 *Bross-Walch N, Kuehn T, Moskau D, Zerbe O*. Strategies and tools for structure determination of natural products using modern methods of NMR spectroscopy. Chem Biodivers 2005; 2: 147

14 *Jaroszewski JW*. Hyphenated NMR methods in natural products research, part 2: HPLC-SPE-NMR and other new trends in NMR hyphenation. Planta Med 2005; 71: 795-802

15 *Dale JA, Mosher HS*. Nuclear magnetic resonance nonequivalence of diastereomeric esters of alpha-substituted phenylacetic acids for determination of stereochemical purity. J Am Chem Soc 1968; 90: 3732-&

16 *Wenzel TJ, Morin CA, Brechting AA*. Lanthanide-chiral resolving agent mixtures as chiral NMR shift-reagents. J Org Chem 1992; 57: 3594-9

17 *Molinski TF*. Microscale methodology for structure elucidation of natural products. Curr Opin Biotechnol 2010; 21: 819-26

18 *Berova N, Di Bari L, Pescitelli G*. Application of electronic circular dichroism in configurational and conformational analysis of organic compounds. Chem Soc Rev 2007; 36: 914-31

19 *Li XC, Ferreira D, Ding YQ*. Determination of absolute configuration of natural products: theoretical calculation of electronic circular dichroism as a tool. Curr Org Chem 2010; 14: 1678-97

20 *Diederich C, Grimme S.* Systematic investigation of modern quantum chemical methods to predict electronic circular dichroism spectra. J Phys Chem A 2003; 107: 2524-39

2.3. The GABA$_A$ Receptor

Gamma-aminobutyric acid (GABA) is the major inhibitory neurotransmitter of the central nervous system (CNS). It is biosynthetically formed by simple decarboxylation of the major excitatory neurotransmitter, glutamate. GABA activates ionotropic GABA$_A$ receptors and metabotropic GABA$_B$ receptors. The GABA$_A$ receptors are the main inhibitory receptors in the CNS. They are primarily neuronal[2] transmembrane proteins of the cys-loop pentameric ligand-gated ion channel (LGIC) superfamily, with synaptic, extrasynaptic, and perisynaptic locations. Upon activation by GABA, the integral chloride channels of the GABA$_A$ receptors open. Resultant increase in membrane chloride permeability leads to an inhibitory postsynaptic potential (hyperpolarization of the neuronal membrane) that reduces triggering of further action potentials [1, 2].

The GABA$_A$ receptor is an assembly of five distinct subunits. Sequencing of the human genome revealed the existence of 19 different GABA$_A$ receptor subunits (Figure 5) [3]. They are classified according to their primary structure into α(1-6), β(1-3), γ(1-3, including splice variants γ_{2S} and γ_{2L}), δ, ϵ, π, θ, and ρ(1-3), the latter being able to form homopentamers formerly referred to as GABA$_C$ receptors [1]. The expression profile of the subunits varies depending on tissular and cellular region. This provides the basis for the putative existence of a huge variety of different heteropentameric GABA$_A$ receptor subtypes. So far, 11 functional GABA$_A$ receptor subtypes have been identified in the CNS. The exact physiological role of only a few is known. Moreover the number of native GABA$_A$ receptor subtypes will further rise as more information on subunit expression becomes available through, for example, *in situ* hybridization (on the mRNA level) in combination with coimmunoprecipitation methods (on the protein level). Furthermore, studying the coregulation of subunits in cells, and genetically engineered animals can help to enlarge the list of identified GABA$_A$ receptor subtypes [1, 4]. The α_1, β_2, and γ_2 subunits are chromosome partners and ubiquitously coexpressed [3, 5]. Accordingly, the most prominent GABA$_A$ receptor subtype, accounting for about 40% of all GABA$_A$ receptors, consists of 2 α_1, 2 β_2 and 1 γ_2 subunit [6]. The amounts of minor subtypes are still comparable with the

---

[2] GABA$_A$ receptors also have been detected in pancreatic tissue. However, their physiological role in this location is still under investigation. [1]*Olsen RW, Sieghart W*. International Union of Pharmacology. LXX. Subtypes of gamma-aminobutyric acid(A) receptors: classification on the basis of subunit composition, pharmacology, and function. Update. Pharmacol Rev 2008; 60: 243-60.

expression level of other CNS receptors, for example, for the biogenic amines or acetylcholine, reflecting the importance of the GABAergic system in neuronal circuits [1].
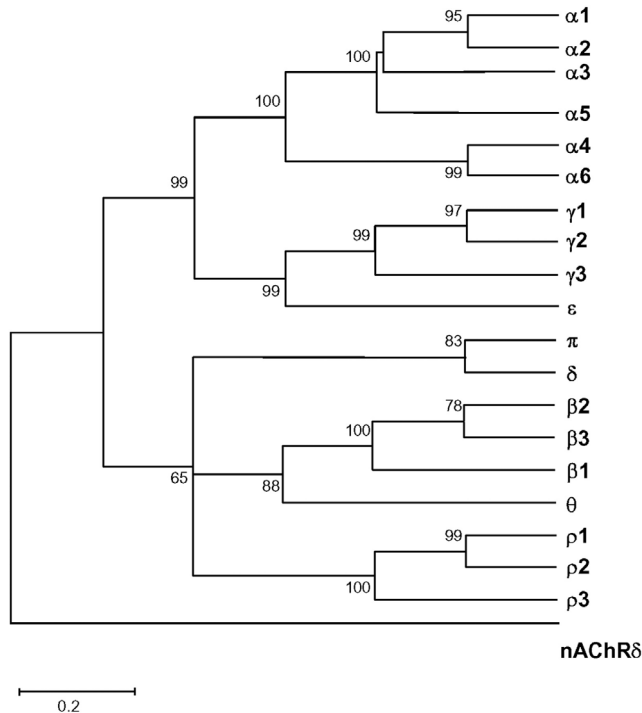

Figure 5: Dendrogram showing the sequence identity of the 19 genes encoding for human $GABA_A$ receptor subunits. The Greek letters (α, β, γ, ϵ, π, δ, ρ, θ) specify the 8 homologous subunit families which share high (>70%) sequence identity. The length of the horizontal branches connecting any two subunits reflects the partial divergence in their particular amino acid sequence. The scale bar indicates 20% sequence divergence (reproduced from Simon et al., 2004 [3])

Many clinically relevant drugs treating psychiatric diseases, but also various model drugs used in research, exert their action via the $GABA_A$ receptors (Figure 6) [2, 7-9].

The barbiturates were the tranquilizers of the first hour targeting the $GABA_A$ receptor. Barbital, introduced to the market by Bayer as Veronal® at the beginning of the twentieth century, was the first in a long series of barbituric acid derivatives. Probably due to their unrestricted prescription later on [11], they became notorious as "mother's little helpers" (The Rolling Stones, on their album "Aftermath", released 1966). In current clinical use, barbiturates have almost completely been substituted by the much safer benzodiazepines (BZD), which were launched first in the 1960's (Librium® in 1960 and Valium® 1962) [12]. Currently, BZD are probably the best studied $GABA_A$ receptor ligands. Their site of interaction with the $GABA_A$ receptor lies in the interface between the α and γ subunit [13].

Drugs acting at the BZD-binding site can be subdivided into three groups based on their mode of action: (i) positive allosteric modulators or BZD-site agonists, such as diazepam, (ii) negative allosteric modulators or BZD-site inverse agonists, such as methyl-6,7-dimethoxy-4-ethyl-β-carboline-3-carboxylate (DMCM; a β-carboline), and (iii) null modulators or BZD-site

antagonists like flumazenil. BZDs are not able to directly activate the target – a property which precludes lethal overdoses known from agonistic barbiturates. They have been prescribed to treat anxiety, panic and mood disorders, alcohol withdrawal symptoms, insomnia, and epilepsy [2]. Benzodiazepines modulate $GABA_A$ receptors comprising α_{1-3}, or α_5 subunits. Pharmacological
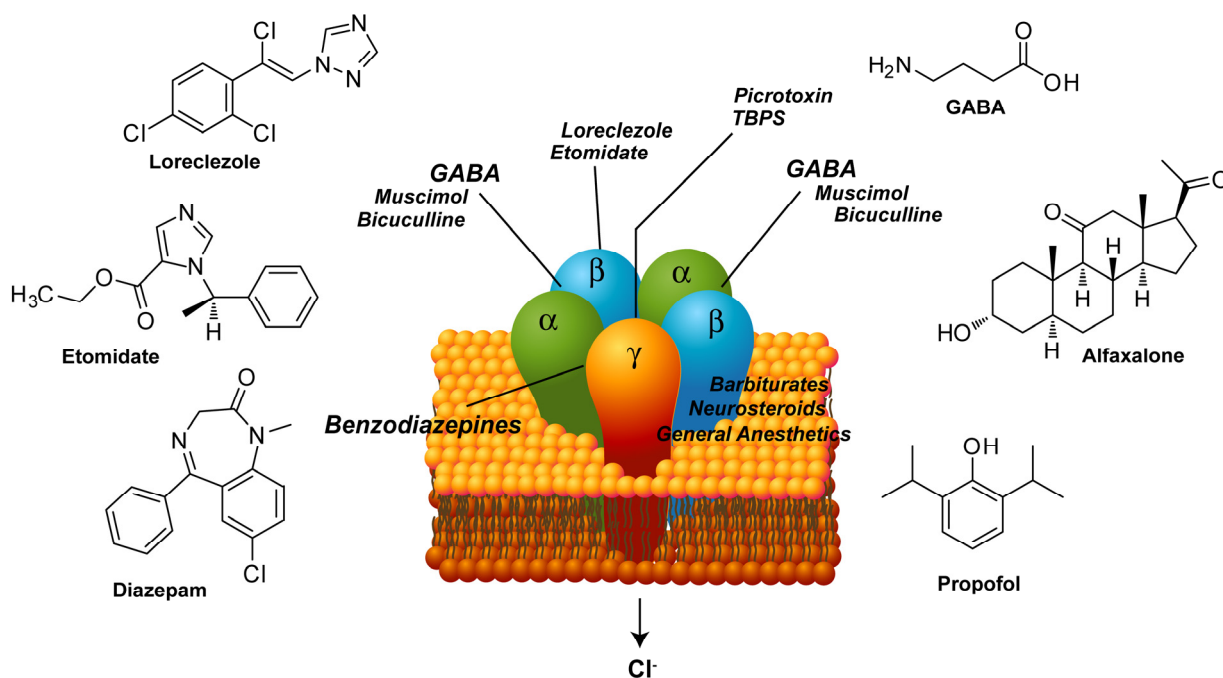

Figure 6: The $GABA_A$ receptor as a drug target. Various clinical and model drugs exert their activity via the $GABA_A$ receptor (list not complete): GABA (natural agonist), its competitive agonist muscimol and competitive antagonist bicuculline; benzodiazepines (allosteric modulators; e.g. diazepam); picrotoxin and t-butylbicyclophosphorothionate (TBPS) (allosteric antagonists); barbiturates, general anesthetics e.g. propofol and etomidate, and neurosteroids, e.g. alfaxalone (mixed allosteric modulators/agonists); loreclezole (allosteric modulator); miscellaneous substances binding to the $GABA_A$ receptor, not shown: furosemide (loop diuretic; inhibitor of GABA), Zn^{2+} (inhibitor of GABA), La^{3+} (stimulator of GABA), penicillin (antibiotic; open channel blocker in high concentrations), ethanol. The binding sites are able to interact with one another upon drug binding. Adapted from Belelli et al. [10].

functions evoked by the modulation of receptors comprising one of these subunits have been studied extensively ([1, 12] and citations therein). The α_1 containing receptors are responsible for the sedative action of diazepam [14-16], whereas anxiolytic-like and analgesic activity could be attributed to α_2 and α_3 containing subtypes by investigating $GABA_A$ receptor point mutated mice [17-20]. Moreover, drugs with preferential α_5 subunit efficiency positively influenced learning and memory in rodents [21-24] and humans [25]. Particular properties of other $GABA_A$ receptor subunits are still under investigation (their tentative physiological role has been listed by Korpi

and Sinkkonen, 2006 [5]). These and related findings on subtype-related pharmacological properties initiated the development of subtype-specific drugs with more selective pharmacological profiles and hence less unwanted side effects that arise due to insufficient GABA$_A$ receptor subtype selectivity [12]. The mechanism of long-term side effects of the BZDs, such as tolerance and dependence, is not yet fully understood but different subtypes seem to have different timescales for the onset and offset of these side-effects [26].

The complexity of the GABAergic system with its numerous distinct GABA$_A$ receptor subtypes varying in their tissular, cellular, and subcellular localization is an opportunity to develop highly subtype specific drugs with distinct pharmacological profiles. Most recent findings have shown that such drugs might not only be substitutes for the widely prescribed benzodiazepines but also help to further understand the physiological role of the diverse GABA$_A$ receptor subtypes [12]. The development of highly subtype–specific GABA$_A$ receptor ligands remains a challenge due to the lack of a crystal structure of the GABA$_A$ receptor. Comparative modelling (homology modelling) of the extracellular domain, mostly based on the X-ray crystallographic structure of a soluble acetylcholine binding protein and recently additionally on the electron microscopy structure of the n-Acetylcholine receptor and the X-ray structure of bacterial pentameric ion channels, has provided a certain insight into the quaternary structure of the GABA$_A$ receptor and the BZD binding site [4, 27, 28]. Most of the current subtype-selective drugs which are either on the market or still in clinical trials act via the BZD binding site [12]. Little is known about novel structural scaffolds binding to distinct binding sites, although these might provide yet unknown modes of action at the target and hence might bear a different clinical profile.

In vitro *Bioassays to Assess GABA$_A$ Receptor Activity*

Receptor binding assays using either native tissue, or human endothelian kidney cells (HEK293) or mouse fibroblast leukocyte tyrosine kinase cells (LTK- cells) that are transfected with specified GABA$_A$ receptor subunits, are used frequently in *in vitro* test methods to measure the GABA$_A$ receptor affinity of a compound by competitive or noncompetitive displacement of a radiolabelled or fluorescent reference ligand [4]. Such assays are site-specific, depending on the labelled ligand used, and can therefore not be used to detect scaffolds for unknown binding sites. The informative value is, moreover, limited, since intrinsic activity (chloride permeability) cannot be observed directly. Substances allosterically modulating GABA binding in a negative,

positive, or neutral manner, may be differentiated in experiments observing shifts of the concentration response curve for GABA binding [4]. Direct agonistic activity or antagonistic activity, however, is not revealed.

From the perspective of developing CNS depressant drugs acting via the GABA$_A$ receptor, it is crucial to know whether a compound acts as agonist, antagonist, or modulator at the GABA$_A$ receptor. Several functional high-throughput assays have been used to obtain such information. These include radioactivity-based ion flux assays (measuring intracellular ^{36}Cl concentration before and after drug application), fluorescence-based assays (either measuring chloride concentrations after quenching by fluorescent compounds or recording indirect changes in membrane potential), or microphysiometry studies (measuring extracellular or intracellular acidification rates, based on bicarbonate permeability of GABA$_A$ receptors). However, these techniques do not allow the membrane potential to be controlled: if electrochemical gradients are eliminated, electric transfer through ion channels is no longer driven which may lead to false negative responses. Furthermore, in the particular assays, artefacts may occur during fluorescence read-out, applied samples may themselves quench chloride ions impairing correct concentration measurements and cells cannot be continuously perfused which may lead to ligand accumulation in the cell. Hence, the gold-standard to study ion channel function, are electrophysiological techniques in which charge transfer is recorded directly and quantitatively [4, 29]. Automated patch-clamp instruments, demanding preferably stable cell lines and highly specialized consumables, are time-consuming, costly, and labor-intensive systems for electrophysiological measurements. The two-microelectrod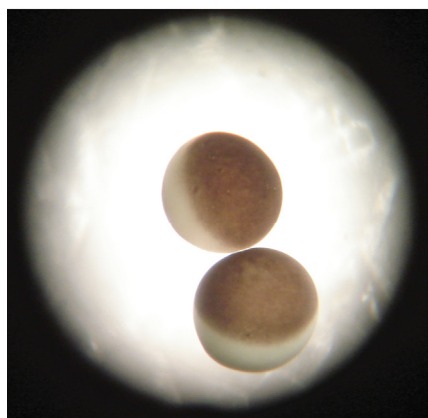e voltage clamp (TEVC) technique is a convenient, more flexible, robust method using *Xenopus* oocytes (Figure 7) to directly measure current changes through ion channels such as GABA$_A$ receptors. This is done under permanent control of the membrane potential by a feedback circuit (Figure 8) [4, 29, 30]. Although less suitable for high-throughput, it is a cost-effective technique and the data obtained are highly reproducible and accurate [29].

Other expression systems for functional studies on recombinant GABA$_A$ receptors of basically any adequate subtype include mouse fibroblast LTK-cells, Chinese Hamster Ovary cells (CHO), and human endothelial

Figure 7: Enzymatically defolliculated oocytes from Xenopus laevis. A diameter of about 1-1.2 mm makes these cells very easy to handle for electrophysiological measurements. (Picture J. Zaugg, Vienna)

kidney cells (HEK293) [4]. *Xenopus* oocytes, however, are able to transiently express various molecular targets in parallel (also antitargets such as hERG K$^+$-channels used to preliminarily evaluate potential for side effects and drug-drug interactions [31]) and are therefore more flexible than the above mentioned cell lines. Furthermore, they are favorable because they are well-documented, and advantageous due to high expression, low endogenous expression of membrane proteins, and easy maintenance (Figure 7 and Figure 8).
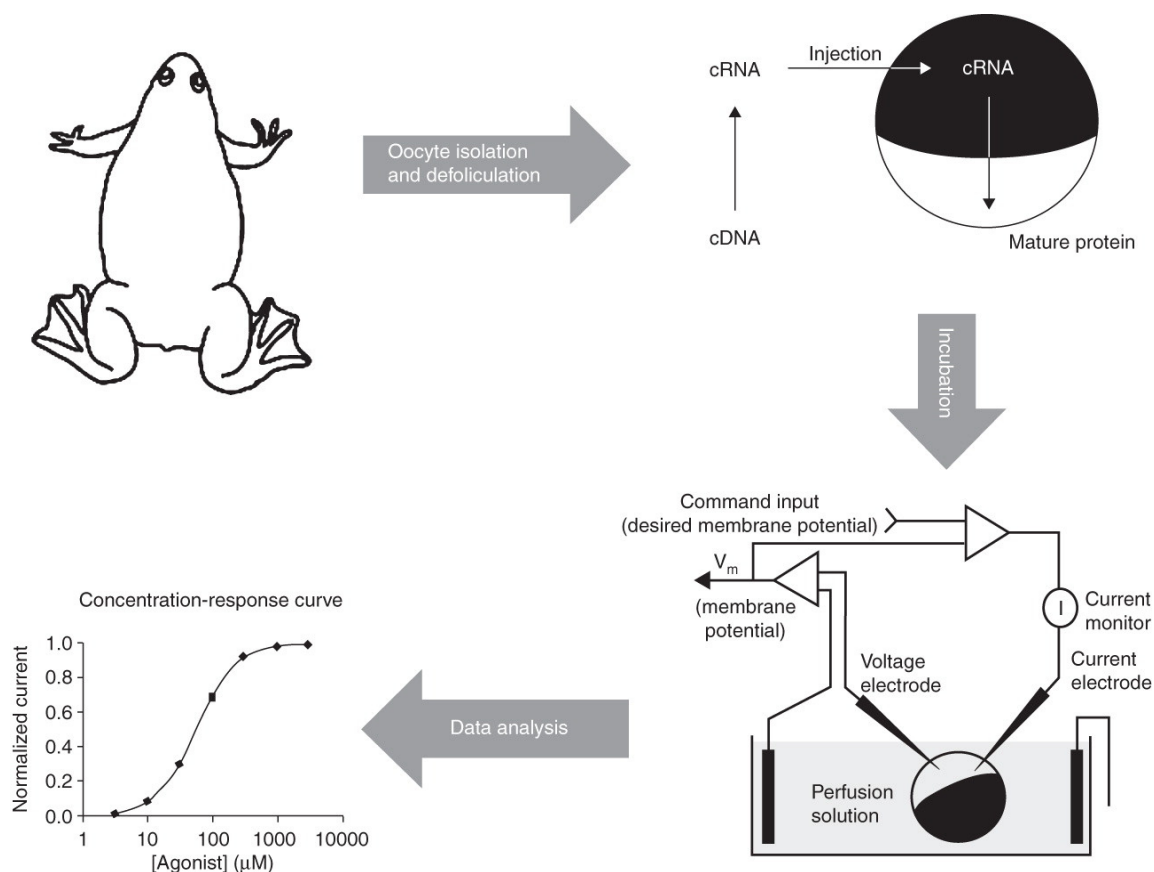
Figure 8: Schematic workflow of two-microelectrode voltage clamp studies using *Xenopus* oocytes for measuring GABA$_A$ receptor activity. The oocytes are surgically removed from female *Xenopus laevis*. After enzymatic defolliculation of the oocyte, cRNAs, transcripted from cDNA of adequate GABA$_A$ receptor subunits, are injected in a proper ratio to ensure subtype expression (e.g. 1:1:10 for $\alpha_1\beta_2\gamma_{2S}$ subtypes). After 24 to 48 hrs of incubation, the oocytes can be used for voltage clamp measurements (Figure by Kvist et al., 2011 [29]).

GABA$_A$ receptor activation, and opening and closure of the chloride channel is characterized by complex kinetics including receptor desensitization after activation [2]. Therefore, fast and timed sample application as well as fast perfusion of the oocyte are essential for assessing reproducible data with the TEVC technique [30]. Moreover, slow false-positive currents, likely resulting from detergent-like compounds that have a tendency to disrupt the membrane and are

quite common among natural products (saponins, fatty acids) [32], can be better distinguished from fast GABA or drug-induced currents. These conditions are ensured by the use of a medium-throughput automated fast perfusion system and a sampling robot such as implemented by the Hering group in Vienna (Figure 9) [30].
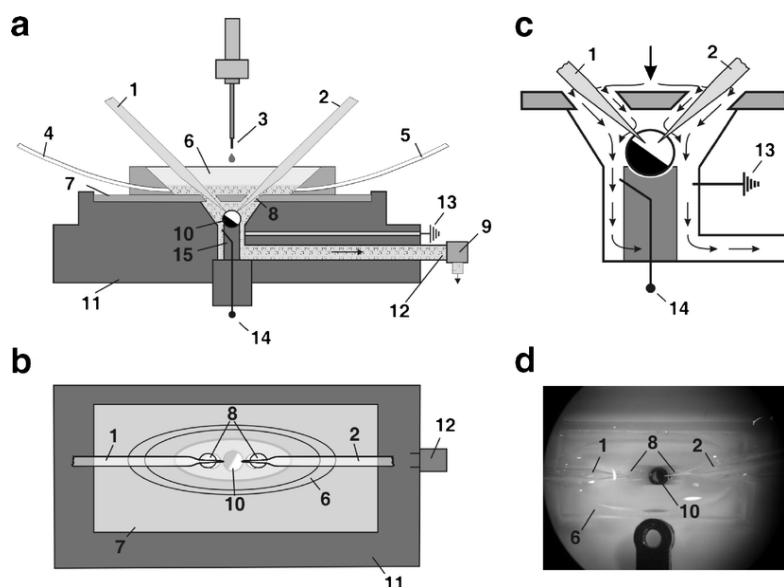

Figure 9: Cross-section view (**a**) and top view (**b**) of the oocyte perfusion chamber of the automated two-microelectrode voltage clamp assay as implemented by the Hering group in Vienna [30]. Two microelectrodes (*1* and *2*) are inserted via the sloping access inlets (*8*) through a glass cover plate (*7*) into the small ($\sim$15 μL) oocyte chamber (**c**). Samples are applied by the tip of the liquid handling arm (*3*) of a TECAN Miniprep 60 to a funnel reservoir made of quartz (*6*) surrounding the microelectrode access holes. Perfusion of the oocyte (*10*, **c**) that is placed on a cylindrical holding device (*15*) is enabled by means of the syringe pump (*9*) of the Miniprep 60 connected to the chamber body (*11*) via the outlet (*12*). Residual solution is removed from the funnel before drug application via the funnel outlets (*4* and *5*). In addition to the ground reference electrode (*13*), the cylindrical holder for the oocyte contains a reference electrode (*14*) that serves as an extracellular reference for the potential electrode. Salt bridges can be inserted into the side outlet for the ground electrode (*13*). **c** Schematic drawing of the solution flow inside the perfusion chamber and in the annular gap around the cylinder with oocyte. **d** Photo of the oocyte perfusion chamber. An oocyte (*10*) is placed on a cylinder and impaled with two microelectrodes (*1,2*) surrounded by the funnel (*6*). Figure and figure caption kindly provided by I. Baburin [30]

Behavioral Models for GABA_A Receptor Related Pharmacological Effects

Animal models provide preliminary ideas of how a drug might act in humans. They are standard to preliminary assessments of the pharmacological effect of a drug *in vivo* that has been previously identified as active at a specific target in an appropriate *in vitro* assay. Inclusively, animal tests can give insight into pharmacokinetic and toxicological properties of a drug. Various behavioral models are used to study anxiolytic-like[3] properties of a drug. The predictive value of most of them has been validated with BZDs [33]. Animal models of anxiety are grouped into two main classes (i) involving conditioned responses to stress (often painful events such as electric shocks used in the four-plates test or in the Vogel drinking conflict test [33] or (ii) ethology-

---

[3] 'Anxiolytic-like', 'sedative-like', and 'anticonvulsant-like' are terms for pharmacological effects of a drug in animals. The terms 'sedative', 'anxiolytic', and 'anticonvulsant' refer to pharmacological effects in humans.

based models exploring spontaneous and natural reactions such as flight, avoidance, and freezing as a cause of stressful challenges [33]. In natural product research the most popular anxiety models investigating unconditioned responses have been the Elevated plus maze (measuring conflict between exploration and aversion to elevated open places [33, 34]), followed by the hole-board test (measuring the response of the animal to an unfamiliar setting such as holes in the ground) [34], and the open field test [35]. The open field test, sensitive to BZDs and 5-HT$_{1A}$ receptor agonists [36], is based on the natural agoraphobia of rodents. The ratio of time spent in the periphery of an illuminated open field over time spent in the centre is measured to evaluate the influence of potentially anxiolytic drugs on stress-induced inhibition of exploration behavior [33]. Other *in vivo* paradigms used in relation to GABAergic activity include the accelerating rotating rod (rotarod) measuring motor incoordination [37], and the horizontal wire test to assess neuromuscular strength [37]. Both tests have been applied to detect substance induced myorelaxation [38]. The actimeter test independently evaluates locomotor activity and has been used as a control for anxiety paradigms where locomotion could influence explorative behavior [39]. Studies evaluating antiepileptic potential of a drug have been performed by induction of seizures either by convulsant drugs such as the GABA$_A$ receptor antagonists picrotoxin, bicuculline, and pentylenetetrazole [40-42], or by electroshocks [43]. Other experiments evaluate influence on hypnotic-induced sleeping time [44, 45]. Seizure activity is directly recorded during electroencephalographic (EEG) measurements [46], which are as well beneficial to observe electrical activity in the animal's brain during experiments investigating the anxiolytic-like and sedative-like effect of a drug [47].

References

1 *Olsen RW, Sieghart W*. International Union of Pharmacology. LXX. Subtypes of gamma-aminobutyric acid(A) receptors: classification on the basis of subunit composition, pharmacology, and function. Update. Pharmacol Rev 2008; 60: 243-60

2 *Hevers W, Luddens H*. The diversity of GABA(A) receptors - Pharmacological and electrophysiological properties of GABA(A) channel subtypes. Mol Neurobiol 1998; 18: 35-86

3 *Simon J, Wakimoto H, Fujita N, Lalande M, Barnard EA*. Analysis of the set of GABA(A) receptor genes in the human genome. J Biol Chem 2004; 279: 41422-35

4 *Smith AJ, Simpson PB*. Methodological approaches for the study of GABA(A) receptor pharmacology and functional responses. Anal Bioanal Chem 2003; 377: 843-51

5 *Korpi ER, Sinkkonen ST*. GABA(A) receptor subtypes as targets for neuropsychiatric drug development. Pharmacol Ther 2006; 109: 12-32

6 *McKernan RM, Whiting PJ*. Which GABAA-receptor subtypes really occur in the brain? Trends Neurosci 1996; 19: 139

7 *Johnston GAR*. GABA(A) receptor channel pharmacology. Curr Pharm Design 2005; 11: 1867-85

8 *Foster AC, Kemp JA*. Glutamate- and GABA-based CNS therapeutics. Curr Opin Pharmacol 2006; 6: 7-17

9 *Johnston GAR*. GABAA receptor pharmacology. Pharmacol Ther 1996; 69: 173

10 *Belelli D, Lambert JJ*. Neurosteroids: endogenous regulators of the GABA(A) receptor. Nat Rev Neurosci 2005; 6: 565-75

11 *Emerson H, Aranow H, Baehr G, Cattel M, Howe HS, Kolb LC, Laidlaw RW, Steele JM, Kruse HD, Donovan EJ*. Report on barbiturates. Public Health Reports 1956; 71:

12 *Mohler H*. The rise of a new GABA pharmacology. Neuropharmacology 2010; doi: 10.1016/j.neuropharm.2010.10.020:

13 *Hadingham KL, Wingrove PB, Wafford KA, Bain C, Kemp JA, Palmer KJ, Wilson AW, Wilcox AS, Sikela JM, Ragan CI, et al*. Role of the beta subunit in determining the pharmacology of human gamma-aminobutyric acid type A receptors. Mol Pharmacol 1993; 44: 1211-8

14 *Rudolph U, Crestani F, Benke D, Brunig I, Benson JA, Fritschy JM, Martin JR, Bluethmann H, Mohler H*. Benzodiazepine actions mediated by specific gamma-aminobutyric acid(A) receptor subtypes. Nature 1999; 401: 796-800

15 *McKernan RM, Rosahl TW, Reynolds DS, Sur C, Wafford KA, Atack JR, Farrar S, Myers J, Cook G, Ferris P, Garrett L, Bristow L, Marshall G, Macaulay A, Brown N, Howell O, Moore KW, Carling RW, Street LJ, Castro JL, Ragan CI, Dawson GR, Whiting PJ*. Sedative but not anxiolytic properties of benzodiazepines are mediated by the GABAA receptor α1 subtype. Nat Neurosci 2000; 3: 587

16 *Crestani F, Martin JR, Mohler H, Rudolph U*. Resolving differences in GABAA receptor mutant mouse studies. Nat Neurosci 2000; 3: 1059

17 *Low K, Crestani F, Keist R, Benke D, Brunig I, Benson JA, Fritschy JM, Rulicke T, Bluethmann H, Mohler H, Rudolph U*. Molecular and neuronal substrate for the selective attenuation of anxiety. Science 2000; 290: 131-4

18 *Crestani F, Keist R, Fritschy JM, Benke D, Vogt K, Prut L, Bluthmann H, Mohler H, Rudolph U*. Trace fear conditioning involves hippocampal alpha(5) GABA(A) receptors. Proc Natl Acad Sci U S A 2002; 99: 8980-5

19 *Dias R, Sheppard WF, Fradley RL, Garrett EM, Stanley JL, Tye SJ, Goodacre S, Lincoln RJ, Cook SM, Conley R, Hallett D, Humphries AC, Thompson SA, Wafford KA, Street LJ, Castro JL, Whiting PJ, Rosahl TW, Atack JR, McKernan RM, Dawson GR, Reynolds DS*. Evidence for a significant role of alpha 3-containing GABAA receptors in mediating the anxiolytic effects of benzodiazepines. J Neurosci 2005; 25: 10682-8

20 *Knabl J, Witschi R, Hosl K, Reinold H, Zeilhofer UB, Ahmadi S, Brockhaus J, Sergejeva M, Hess A, Brune K, Fritschy JM, Rudolph U, Mohler H, Zeilhofer HU*. Reversal of pathological pain through specific spinal GABAA receptor subtypes. Nature 2008; 451: 330-4

21 *Chambers MS, Atack JR, Carling RW, Collinson N, Cook SM, Dawson GR, Ferris P, Hobbs SC, O'Connor D, Marshall G, Rycroft W, Macleod AM*. An orally bioavailable, functionally selective inverse agonist at the benzodiazepine site of GABAA alpha5 receptors with cognition enhancing properties. J Med Chem 2004; 47: 5829-32

22 *Navarro JF, Ibanez M, Luna G*. Behavioral profile of SB 269970, a selective 5-HT(7) serotonin receptor antagonist, in social encounters between male mice. Methods Find Exp Clin Pharmacol 2004; 26: 515-8

23 *Dawson GR, Maubach KA, Collinson N, Cobain M, Everitt BJ, MacLeod AM, Choudhury HI, McDonald LM, Pillai G, Rycroft W, Smith AJ, Sternfeld F, Tattersall FD, Wafford KA, Reynolds DS, Seabrook GR, Atack JR*. An inverse agonist selective for alpha5 subunit-containing GABAA receptors enhances cognition. J Pharmacol Exp Ther 2006; 316: 1335-45

24 *Ballard TM, Knoflach F, Prinssen E, Borroni E, Vivian JA, Basile J, Gasser R, Moreau JL, Wettstein JG, Buettelmann B, Knust H, Thomas AW, Trube G, Hernandez MC*. RO4938581, a novel cognitive enhancer acting at GABAA alpha5 subunit-containing receptors. Psychopharmacology 2009; 202: 207-23

25 *Nutt DJ, Besson M, Wilson SJ, Dawson GR, Lingford-Hughes AR*. Blockade of alcohol's amnestic activity in humans by an alpha5 subtype benzodiazepine receptor inverse agonist. Neuropharmacology 2007; 53: 810-20

26 *Bateson AN*. Basic pharmacologic mechanisms involved in benzodiazepine tolerance and withdrawal. Curr Pharm Design 2002; 8: 5-21

27 *Ernst M, Brauchart D, Boresch S, Sieghart W*. Comparative modeling of GABA(A) receptors: limits, insights, future developments. Neuroscience 2003; 119: 933-43

28 *Sander T, Frolund B, Bruun AT, Ivanov I, McCammon JA, Balle T*. New insights into the GABA(A) receptor structure and orthosteric ligand binding: Receptor modeling guided by experimental data. Proteins 2011; 79: 1458-77

29 *Kvist T, Hansen KB, Brauner-Osborne H*. The use of *Xenopus* oocytes in drug screening. Expert Opin Drug Dis 2011; 6: 141-53

30 *Baburin I, Beyl S, Hering S*. Automated fast perfusion of *Xenopus* oocytes for drug screening. Pflug Arch Eur J Phy 2006; 453: 117

31 *Schramm A, Baburin I, Hering S, Hamburger M*. hERG channel inhibitors in extracts of *Coptidis* rhizoma. Planta Med 2011; 77: 692-7

32 *Potterat O, Hamburger M*. Drug discovery and development with plant-derived compounds. Prog Drug Res 2008; 65: 45, 7-118

33 *Bourin M, Petit-Demouliere B, Dhonnchadha BN, Hascoet M*. Animal models of anxiety in mice. Fundam Clin Pharmacol 2007; 21: 567-74

34 *Calabrese EJ*. An assessment of anxiolytic drug screening tests: Hormetic dose responses predominate. Crit Rev Toxicol 2008; 38: 489-542

35 *Moser AD*. Naturstoffe mit GABAA-Rezeptor-Aktivität. Division of Pharmaceutical Biology, University of Basel, Basel, 2009. Master's thesis

36 *Prut L, Belzung C*. The open field as a paradigm to measure the effects of drugs on anxiety-like behaviors: a review. Eur J Pharmacol 2003; 463: 3-33

37 *Crawley JN*. Behavioral phenotyping of transgenic and knockout mice: experimental design and evaluation of general health, sensory functions, motor abilities, and specific behavioral tests. Brain Res 1999; 835: 18-26

38 *Steiner MA, Lecourt H, Strasser DS, Brisbare-Roch C, Jenck F*. Differential effects of the dual orexin receptor antagonist almorexant and the GABA(A)-alpha 1 receptor modulator zolpidem, alone or combined with ethanol, on motor performance in the rat. Neuropsychopharmacol 2011; 36: 848-56

39 *Hascoet M, Bourin M*. A new approach to the light/dark test procedure in mice. Pharmacol Biochem Behav 1998; 60: 645-53

40 *Avallone R, Zanoli P, Puia G, Kleinschnitz M, Schreier P, Baraldi M*. Pharmacological profile of apigenin, a flavonoid isolated from *Matricaria chamomilla*. Biochem Pharmacol 2000; 59: 1387-94

41 *Muceniece R, Saleniece K, Rumaks J, Krigere L, Dzirkale Z, Mezhapuke R, Zharkova O, Klusa V*. Betulin binds to gamma-aminobutyric acid receptors and exerts anticonvulsant action in mice. Pharmacol Biochem Behav 2008; 90: 712-6

42 *Viola H, Wasowski C, Levi de Stein M, Wolfman C, Silveira R, Dajas F, Medina JH, Paladini AC*. Apigenin, a component of *Matricaria recutita* flowers, is a central benzodiazepine receptors-ligand with anxiolytic effects. Planta Med 1995; 61: 213-6

43 *Park HG, Yoon SY, Choi JY, Lee GS, Choi JH, Shin CY, Son KH, Lee YS, Kim WK, Ryu JH, Ko KH, Cheong JH*. Anticonvulsant effect of wogonin isolated from *Scutellaria baicalensis*. Eur J Pharmacol 2007; 574: 112-9

44 *Fernandez SP, Wasowski C, Paladini AC, Marder M*. Synergistic interaction between hesperidin, a natural flavonoid, and diazepam. Eur J Pharmacol 2005; 512: 189-98

45 *Marder M, Viola H, Wasowski C, Fernandez S, Medina JH, Paladini AC*. 6-Methylapigenin and hesperidin: new valeriana flavonoids with activity on the CNS. Pharmacol Biochem Behav 2003; 75: 537-45

46 *Etholm L, Linden H, Eken T, Heggelund P*. Electroencephalographic characterization of seizure activity in the synapsin I/II double knockout mouse. Brain Res 2011; 1383: 270-88

47 *van Lier H, Drinkenburg WHIM, van Eeten YJW, Coenen AML*. Effects of diazepam and zolpidem on EEG beta frequencies are behavior-specific in rats. Neuropharmacology 2004; 47: 163-74

2.4. Natural Products as GABA$_A$ Receptor Modulators

In Switzerland, one of the first choices to treat weak forms of insomnia, panic attacks, and mood disorders is an over-the-counter sedative or tranquillizing phytotherapeutical preparation. These comprise medicinal plants such as valerian roots (*Valeriana officinalis*) or passionflower (*Passiflora incarnata*) [1]; one possible mechanism of action has been related to the GABA$_A$ receptor [2, 3]. Also in other health systems, such as in traditional Chinese medicine (TCM) and Ayurveda, one can find herbal preparations with reports of *in vitro* GABA$_A$ergic activity (*Ziziphus jujuba* or *Withania somnifera*) [4]. Regarding prescription drugs against severe CNS related pathologies, only 1 natural product and 6 natural product derivatives of a total of 85 drugs were approved by the FDA between 1981 and 2006 [5]. Those having a specific indication related to the GABA$_A$ receptor were synthetic compounds mostly deriving from the BZD scaffold. This situation has not changed much recently, as mentioned in the previous chapter. In contrast, there is a multitude of scientific publications that report on structurally diverse natural products from plant origin that act at GABA$_A$ receptors [4, 6-8]. The quality of the data, however, largely relies on the type of bioassay which is applied for gathering *in vitro* data and of the animal model which is chosen to confirm these data *in vivo* (Chapter 2.3).

A selection of important natural products acting at the GABA$_A$ receptor as control drugs or compounds which qualify as lead structures and are currently being investigated for the development of novel therapeutic agents is provided in the following section.

Flavonoids with GABA$_A$ Receptor Activity

Flavonoids are a class of ubiquitously occurring polyphenols of plant origin. Many biological functions have been attributed to them, both *in vitro* and *in vivo* [9-11]. Some 20 years ago GABA$_A$ receptor activity was discovered for chrysin (**1**) and for the biflavone amentoflavone (**2**) [12, 13]. Flavonoids have demonstrated *inter alia* anxiolytic-like, sedative-like, and anticonvulsant-like properties and it is now known, that they exert their action via diverse mechanisms in the CNS [14]. Today, they are the most extensively studied GABA$_A$ receptor modulators from plant origin. Pharmacophore models have been generated to investigate their binding site [15-17] and they have served as a scaffold for medicinal chemistry [14, 18, 19].

6,3'-Dinitroflavone (**3**) is a flavonoid derivative with similarly high affinity to the GABA$_A$ receptor as diazepam in a [^{3}H]-flunitrazepam binding assay. At a 30-100 times lower

concentration than diazepam it had highly selective anxiolytic-like effects in mice [19, 20]. However, a recent study with **3** on GABA$_A$ receptor subtype selectivity proved controversial for the current understanding of $\alpha_{2/3}$-subunit-mediated anxiolytic-like effects. This raised the theory of active flavonoid metabolites [21] which is in accordance with the yet limited information about brain bioavailability of most flavonoids [22]. Furthermore, discussions on the bioavailability of flavonoids in humans are controversial [14, 23].

The mode of action of flavonoids at the GABA$_A$ receptor varies strongly with the substitution pattern which originates from different hydroxylation, *C*-prenylation, *O*-methylation, *C*- and *O*-glycosidation, and/or polymerization [14, 18, 24]. Currently, two proposed distinct flavonoid binding sites are under discussion: a high affinity site identical with the BZD-binding site and an alternative low-affinity site [14]. Very recently, a second-order positive modulation (metamodulation) of diazepam action was observed for apigenin (**4**) and hesperidin (**5**) at concentrations too low for the flavonoids to show their own modulatory effects. [14, 25, 26]. These findings revealed an interesting, new aspect of GABA$_A$ receptor modulation by natural products, namely the interaction with established therapeutics. In conclusion, flavonoids are a very interesting class of natural products with high potential as lead compounds for developing drugs with GABA$_A$ receptor activity.

1	R$_{1,3}$ = OH	R$_{2,4,5}$ = H
3	R$_{1,3,4}$ = H	R$_{2,5}$ = NO2
4	R$_{1,3,4}$ = OH	R$_{2,5}$ = H
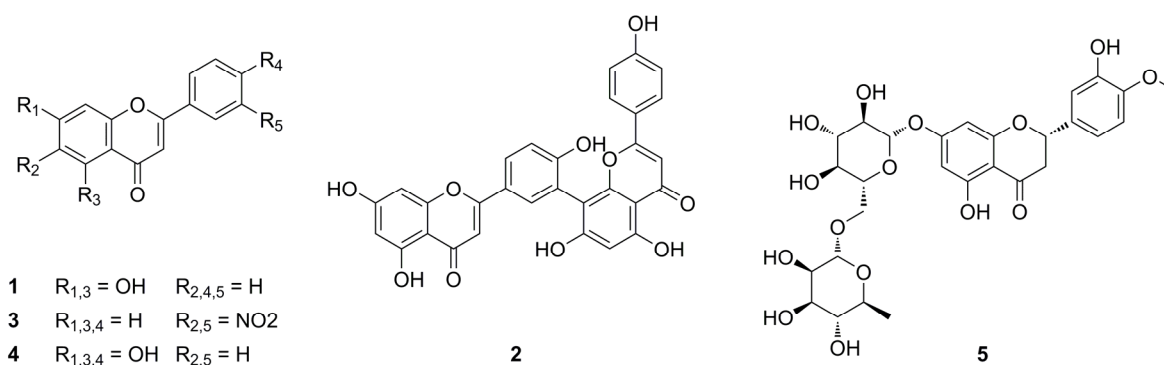
Chart 1: Flavonoids with GABA$_A$ receptor activity

Terpenoids with GABA$_A$ Receptor Activity

Probably the most important terpenoid with GABA$_A$ receptor activity is picrotoxin. It is an equimolar mixture of two convulsant sesquiterpene lactones, picrotoxinin (**6**) and picrotin (**7**). Picrotoxin and pure picrotoxinin (**6**), which is the stronger convulsant of the two compounds [CD$_{50}$ 1.5 mg/kg BW (**6**) vs. 80 mg/kg BW (**7**)] [27], are used as controls as potent GABA$_A$ receptor channel blockers *in vitro*, and in animal convulsion studies.

From the perspective of lead discovery for novel therapeutic agents, valerenic acid (**8**) (a sesquiterpene with a structure reminiscent of etomidate or loreclezole; Figure 6) must be mentioned. In thorough investigations of GABA$_A$ receptor subtype selectivity, Khom et al. found that **8** specifically modulates GABA$_A$ receptors comprising $\beta_{2/3}$ but not β_1 subunits in concentrations between 0.1 and 30 μM. No pronounced selectivity was found for the different α-subunits tested [28]. Later on, behavioral studies confirmed the *in vitro* data of **8** by showing anxiolytic-like activity in mice at a concentration range of 1-6 mg/kg BW [29, 30]. This effect was mediated by β_3-subunit containing GABA$_A$ receptors as studies with point-mutated mice revealed [29]. Valerenic acid (**8**) served as a scaffold for medicinal chemistry to develop derivatives with higher GABA$_A$ receptor efficiency and potency [30, 31]. Although **8** was shown to likely be able to cross the blood-brain barrier in an *in vitro* cell culture model [32], it needs to be clarified to what extent **8** and its synthetic derivatives are bioavailable and whether metabolites might be responsible for GABA$_A$ergic activity *in vivo*.

1S2R5S-(+)-Menthol (**9**), a monoterpene found in many essential oils, was shown to be a superior positive GABA$_A$ receptor modulator *in vitro* than its enantiomer (-)-menthol. This study on stereoselective activity at the GABA$_A$ receptor nicely shows the importance of correctly determining the absolute configurations of natural products.

Miltiron (**10**) is a promising diterpene from the Chinese medicinal herb *Salvia miltiorrhiza* exerting anxiolytic-like behavior but not sedative-like behavior or addictive effects in mice [33]. Whether the mechanism of action is via direct activity at the GABA$_A$ receptor is, however, unclear [34].
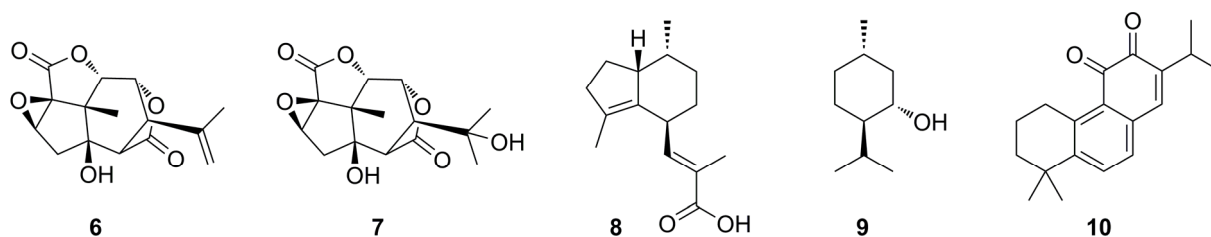
Chart 2: Terpenoids with GABA$_A$ receptor activity

Alkaloids with GABA$_A$ Receptor Activity

Bicuculline (**11**), a phtalide isoquinoline and muscimol (**12**), an isoxazole from fly agaric (*Amanita muscaria*), are alkaloids that bind to the GABA binding site with antagonistic (**11**) and agonistic (**12**) intrinsic activity. Accordingly, they exhibit convulsant (**11**) and anticonvulsant-like

(**12**) activity *in vivo* [35, 36]. These two natural products have served for many years as reference compounds for GABA$_A$ receptor research. Synthetic but also natural β-carboline alkaloids such as harmane (**13**) are full, partial or mixed agonists, antagonists, or inverse antagonists at the GABA$_A$ receptor. This is concurrent with their either CNS depressant or CNS stimulating effects *in vivo* [37]. The β-carboline scaffold has served for the development of the anxiolytic compound abecarnil which, however, failed to show superiority over placebo in clinical trials phase II and III [38]. In contrast to the nitrogen-bearing BZD or nonbenzodiazepines, most natural alkaloids with identified GABA$_A$ receptor activity are inhibitors of the chloride current and convulsant in animal models and therefore less interesting for drug development [4].
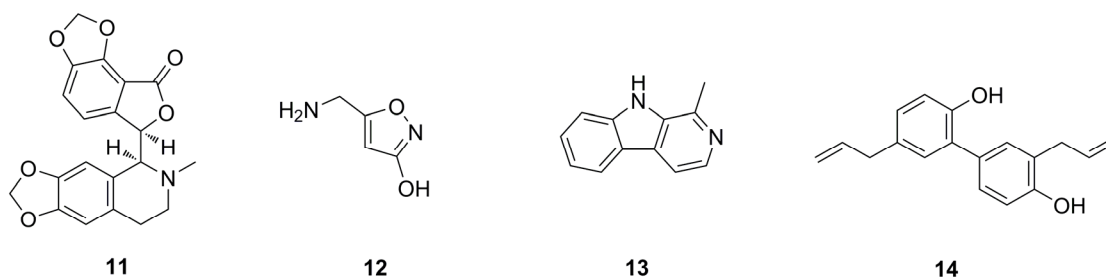
Chart 3: Alkaloids and other miscellaneous natural products with GABAA receptor activity

Miscellanous Structural Classes with GABA$_A$ Receptor Activity

Honokiol (**14**), a neolignan from *Magnolia officinalis* showed an anxio-selective effect in mice [39, 40] and has already served for medicinal chemistry efforts [41]. It has been shown to interact with the GABA$_A$ receptor in binding studies [42] and recent investigations using a functional assay revealed its β$_{2/3}$ subunit selectivity for positive allosteric modulation efficiency [43].

The comprehensive list of nearly 200 natural products with *in vitro* and/or *in vivo* GABA$_A$ergic activity composed by Moser in 2009 include the structural classes of flavonoids, terpenoids, alkaloids, coumarins, neolignans, diverse phenolics, polyacetylenes, pyrones, naphtodianthrones, and phtalides [4]. This review revealed that most studies are restricted to *in vitro* binding assays. These provide information on affinity at the GABA$_A$ receptor; however, as mentioned earlier, this is insufficient for a proper evaluation of the compound's lead potential, since intrinsic activity is not detected in functional assays.

References

1 Arzneimittel-Kompendium der Schweiz, Documed AG, Basel, 2011

2 *Trauner G, Khom S, Baburin I, Benedek B, Hering S, Kopp B*. Modulation of GABAA receptors by valerian extracts is related to the content of valerenic acid. Planta Med 2008; 74: 19-24

3 *Grundmann O, Wang J, McGregor GP, Butterweck V*. Anxiolytic activity of a phytochemically characterized *Passiflora incarnata* extract is mediated via the GABAergic system. Planta Med 2008; 74: 1769-73

4 *Moser AD*. Naturstoffe mit GABAA-Rezeptor-Aktivität. Division of Pharmaceutical Biology, University of Basel, Basel, 2009. Master's thesis

5 *Newman DJ, Cragg GM*. Natural products as sources of new drugs over the last 25 years. J Nat Prod 2007; 70: 461-77

6 *Johnston GAR*. GABA(A) receptor channel pharmacology. Curr Pharm Design 2005; 11: 1867-85

7 *Tsang S, Xue H*. Development of effective therapeutics targeting the GABAA receptor: naturally occurring alternatives. Curr Pharm Design 2004; 10: 1035

8 *Johnston GAR, Hanrahan JR, Chebib M, Duke RK, Mewett KN*. Modulation of ionotropic GABA receptors by natural products of plant origin. Adv Pharmacol 2006; 54: 286-316

9 *Havsteen BH*. The biochemistry and medical significance of the flavonoids. Pharmacol Ther 2002; 96: 67-202

10 *Middleton E, Jr., Kandaswami C, Theoharides TC*. The effects of plant flavonoids on mammalian cells: implications for inflammation, heart disease, and cancer. Pharmacol Rev 2000; 52: 673-751

11 *Pietta PG*. Flavonoids as antioxidants. J Nat Prod 2000; 63: 1035-42

12 *Medina JH, Paladini AC, Wolfman C, Destein ML, Calvo D, Diaz LE, Pena C*. Chrysin (5,7-Di-OH-Flavone), a naturally-occurring ligand for benzodiazepine receptors, with anticonvulsant properties. Biochem Pharmacol 1990; 40: 2227-31

13 *Nielsen M, Frokjaer S, Braestrup C*. High-affinity of the naturally-occurring biflavonoid, amentoflavon, to brain benzodiazepine receptors *in vitro*. Biochem Pharmacol 1988; 37: 3285-7

14 *Hanrahan JR, Chebib M, Johnston GA*. Flavonoid modulation of GABA(A) receptors. Br J Pharmacol 2011; 163: 234-45

15 *Huang X, Liu T, Gu J, Luo X, Ji R, Cao Y, Xue H, Wong JT, Wong BL, Pei G, Jiang H, Chen K*. 3D-QSAR model of flavonoids binding at the benzodiazepine site in GABA(A) receptors. J Med Chem 2001; 44: 1883-91

16 *Kahnberg P, Lager E, Rosenberg C, Schougaard J, Camet L, Sterner O, Nielsen EO, Nielsen M, Liljefors T*. Refinement and evaluation of a pharmacophore model for flavone derivatives binding to the benzodiazepine site of the GABA(A) receptor. J Med Chem 2002; 45: 4188-201

17 *Marder M, Estiu G, Blanch LB, Viola H, Wasowski C, Medina JH*. Molecular Modeling and QSAR analysis of the interaction of flavone derivatives with the benzodiazepine binding site of the GABAA receptor complex. Bioorg Med Chem 2001; 9: 323-35

18 *Marder M, Viola H, Bacigaluppo JA, Colombo MI, Wasowski C, Wolfman C*. Detection of benzodiazepine receptor ligands in small libraries of flavone derivatives synthetized by solution phase combinatorial chemistry. Biochem Biophys Res Commun 1988; 249: 481-5

19 *Marder M, Viola H, Wasowski C, Wolfman C, Waterman PG, Medina JH, Paladini AC*. 6,3'-Dinitroflavone, a novel high-affinity ligand for the benzodiazepine receptor with potent anxiolytic properties. Bioorg Med Chem Lett 1995; 5: 2717-20

20 *Wolfman C, Viola H, Marder M, Wasowski C, Ardenghi P, Izquierdo I, Paladini AC, Medina JH*. Anxioselective properties of 6,3'-dinitroflavone, a high-affinity benzodiazepine receptor ligand. Eur J Pharmacol 1996; 318: 23-30

21 *Furtmueller R, Furtmueller B, Ramerstorfer J, Paladini AC, Wasowski C, Marder M, Huck S, Sieghart W*. 6,3'-Dinitroflavone is a low efficacy modulator of GABA(A) receptors. Eur J Pharmacol 2008; 591: 142-6

22 *Youdim KA, Dobbie MS, Kuhnle G, Proteggente AR, Abbott NJ, Rice-Evans C*. Interaction between flavonoids and the blood-brain barrier: *in vitro* studies. J Neurochem 2003; 85: 180-92

23 *Manach C, Donovan JL*. Pharmacokinetics and metabolism of dietary flavonoids in humans. Free Radical Res 2004; 38: 771-85

24 *Yang X, Baburin I, Plitzko I, Hering S, Hamburger M*. HPLC-based activity profiling for GABA(A) receptor modulators from the traditional Chinese herbal drug Kushen (*Sophora flavescens* root). Mol Divers 2011; 15: 361-72

25 *Campbell EL, Chebib M, Johnston GAR*. The dietary flavonoids apigenin and (-)-epigallocatechin gallate enhance the positive modulation by diazepam of the activation by GABA of recombinant GABA(A) receptors. Biochem Pharmacol 2004; 68: 1631-8

26 *Fernandez SP, Wasowski C, Paladini AC, Marder M*. Synergistic interaction between hesperidin, a natural flavonoid, and diazepam. Eur J Pharmacol 2005; 512: 189-98

27 *Jarboe CH, Poerter LA, Buckler RT*. Structural aspects of picrotoxinin action. J Med Chem 1968; 11: 729-31

28 *Khom S, Baburin I, Timin E, Hohaus A, Trauner G, Kopp B, Hering S*. Valerenic acid potentiates and inhibits GABA(A) receptors: molecular mechanism and subunit specificity. Neuropharmacology 2007; 53: 178-87

29 *Benke D, Barberis A, Kopp S, Altmann KH, Schubiger M, Vogt KE, Rudolph U, Mohler H*. GABA(A) receptors as in vivo substrate for the anxiolytic action of valerenic acid, a major constituent of valerian root extracts. Neuropharmacology 2009; 56: 174-81

30 *Khom S, Strommer B, Ramharter J, Schwarz T, Schwarzer C, Erker T, Ecker GF, Mulzer J, Hering S*. Valerenic acid derivatives as novel subunit-selective GABAA receptor ligands - in vitro and in vivo characterization. Br J Pharmacol 2010; 161: 65-78

31 *Kopp S, Baur R, Sigel E, Mohler H, Altmann KH*. Highly potent modulation of GABA(A) receptors by valerenic acid derivatives. Chem Med Chem 2010; 5: 678-81

32 *Neuhaus W, Trauner G, Gruber D, Oelzant S, Klepal W, Kopp B, Noe CR*. Transport of a GABA(A) receptor modulator and its derivatives from *Valeriana officinalis* L. s. l. across an *in vitro* cell culture model of the blood-brain barrier. Planta Med 2008; 74: 1338-44

33 *Lee CM, Wong HNC, Chui K-Y, Choang TF, Hon P-M, Chang H-M*. Miltirone, a central benzodiazepine receptor partial agonist from Chinese medicinal herb *Salvia miltiorrhiza*. Neurosci Lett 1991; 127: 237-41

34 *Mostallino MC, Mascia MP, Pisu MG, Busonero F, Talani G, Biggio G*. Inhibition by miltirone of up-regulation of GABAA receptor alpha4 subunit mRNA by ethanol withdrawal in hippocampal neurons. Eur J Pharmacol 2004; 494: 83-90

35 *Johnston GAR*. GABAA receptor pharmacology. Pharmacol Ther 1996; 69: 173

36 *Matthews WD, Intoccia AP, Osborne VL, McCafferty GP*. Correlation of [14C]muscimol concentration in rat brain with anticonvulsant activity. Eur J Pharmacol 1981; 69: 249-54

37 *Cao R, Peng W, Wang Z, Xu A*. b-Carboline alkaloids. Biochemical and pharmacological functions. Curr Med Chem 2007; 14: 479-500

38 *Atack JR*. The benzodiazepine binding site of GABA(A) receptors as a target for the development of novel anxiolytics. Expert Opin Investig Drugs 2005; 14: 601-18

39 *Kuribara H, Stavinoha WB, Maruyama Y*. Honokiol, a putative anxiolytic agent extracted from magnolia bark, has no diazepam-like side-effects in mice. J Pharm Pharmacol 1999; 51: 97-103

40 *Maruyama Y, Kuribara H, Morita M, Yuzurihara M, Weintraub ST*. Identification of magnolol and honokiol as anxiolytic agents in extracts of saiboku-to, an oriental herbal medicine. J Nat Prod 1998; 61: 135-8

41 *Kuribara H, Kishi E, Kimura M, Weintraub ST, Maruyama Y*. Comparative assessment of the anxiolytic-like activities of honokiol and derivatives. Pharmacol Biochem Behav 2000; 67: 597-601

42 *Ai J, Wang X, Nielsen M*. Honokiol and magnolol selectively interact with GABAA receptor subtypes in vitro. Pharmacology 2001; 63: 34-41

43 *Baburin I, Taferner B, Wiesner K, Hamburger M, Schühly W, Hering S*. Honokiol modulates GABA(A) receptors subunit specifically. Sci Pharm 2009; 77: 225

3. RESULTS AND DISCUSSION

3.1. HPLC-BASED ACTIVITY PROFILING: DISCOVERY OF PIPERINE AS A POSITIVE GABA$_A$ RECEPTOR MODULATOR TARGETING A BENZODIAZEPINE-INDEPENDENT BINDING SITE

4
115.71 % I$_{GABA}$

5
225.76 % I$_{GABA}$
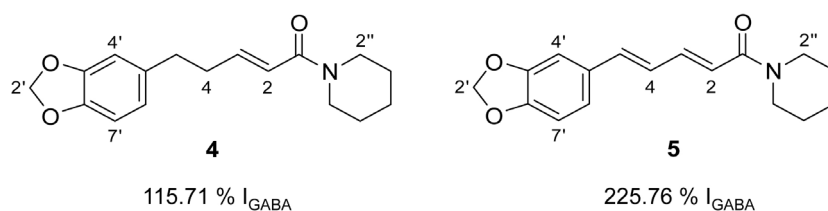
Piperine was identified as main positive $\alpha_1\beta_2\gamma_{2S}$ GABA$_A$ receptor modulatory constituent of *Piper nigrum* fruits by HPLC-based activity profiling. On-line high-resolution mass spectrometry and off-line microprobe NMR provided the analytical basis for the identification of another 12 structurally related piperamides with less or no activity in the functional assay with *Xenopus* oocytes. Preliminary structure-activity relationships could be observed using minute amounts of extract.

Extraction of plant material for isolation, isolation of the piperamides, recording and interpretation of analytical data for structure elucidation (HPLC-PDA-ESI-TOF-MS and semipreparative HPLC – off-line microprobe NMR), writing of the manuscript, and preparation of figures (except for Fig. 3 and 4) were my contributions to this publication.

Janine Zaugg

HPLC-Based Activity Profiling: Discovery of Piperine as a Positive GABA_A Receptor Modulator Targeting a Benzodiazepine-Independent Binding Site

Janine Zaugg,[†,§] Igor Baburin,[‡,§] Barbara Strommer,[‡] Hyun-Jung Kim,[†] Steffen Hering,[‡] and Matthias Hamburger*,[†]

Institute of Pharmaceutical Biology, University of Basel, Klingelbergstrasse 50, 4056 Basel, Switzerland, and Departement of Pharmacology and Toxicology, University of Vienna, Althanstrasse 14, 1090 Vienna, Austria

A plant extract library was screened for GABA_A receptor activity making use of a two-microelectrode voltage clamp assay on *Xenopus laevis* oocytes. An ethyl acetate extract of black pepper fruits [*Piper nigrum* L. (Piperaceae) 100 μg/mL] potentiated GABA-induced chloride currents through GABA_A receptors (composed of α_1, β_2, and γ_{2S} subunits) by 169.1 ± 2.4%. With the aid of an HPLC-based activity profiling approach, piperine (**5**) was identified as the main active compound, together with 12 structurally related less active or inactive piperamides (**1−4**, **6−13**). Identification was achieved by on-line high-resolution mass spectrometry and off-line microprobe 1D and 2D NMR spectroscopy, using only milligram amounts of extract. Compound **5** induced a maximum potentiation of the chloride currents by 301.9 ± 26.5% with an EC_{50} of 52.4 ± 9.4 μM. A comparison of the modulatory activity of **5** and other naturally occurring piperamides enabled insights into structural features critical for GABA_A receptor modulation. The stimulation of chloride currents through GABA_A receptors by compound **5** was not antagonized by flumazenil (10 μM). These data show that piperine (**5**) represents a new scaffold of positive allosteric GABA_A receptor modulators targeting a benzodiazepine-independent binding site.

Gamma-aminobutyric acid type A (GABA_A) receptors are the major inhibitory neurotransmitter receptors in the brain. The assembly of five subunits forms a central pore that is permeable for chloride ions upon activation by the endogenous ligand γ-aminobutyric acid (GABA). A total of 19 different subunit isoforms have been identified in the human genome, which form GABA_A receptors in numerous combinations.[1] The most abundant GABA_A receptor subtype consists of 2 α_1, 2 β_2, and 1 γ_2 subunits, and more than 10 subtypes composed of other subunit combinations have been identified.[2] GABA_A receptor subtypes differ in tissue localization, functional characteristics, and their pharmacological properties.[3,4]

The therapeutic action of the benzodiazepines and other pharmacological compounds used to treat anxiety, panic, insomnia, and epilepsy is mediated by an enhancement of GABAergic neuronal inhibition through GABA_A receptors.[5,6] Various natural products modulating GABA_A receptors (e.g., flavonoids, monoterpenes, diterpenes, neolignans, and β-carbolines) have been identified.[7,8] Little is known in most cases, however, about their subunit selectivity, and presently no natural product derived compound is in clinical development.

We recently embarked on a project aimed at the discovery of GABA_A receptor modulating compounds with scaffolds new for the target. In a screening of 880 plant and fungal extracts with an automated functional assay using *Xenopus* oocytes expressing GABA_A ($\alpha_1\beta_2\gamma_{2S}$) receptors, an ethyl acetate extract of *Piper nigrum* showed promising activity. This observation was intriguing insofar as it somehow seemed to corroborate traditional use of pepper in Asian folk medicine as antiepileptic, antianxiety, sedative, and sleep-inducing herbal preparations.[9−11] Therefore, we deemed this extract sufficiently interesting to identify the constituent(s) responsible for the GABA_A receptor modulating activity with the aid of HPLC-based activity profiling. HPLC-based activity profiling is a rapid and miniaturized approach for localization, dereplication, and characterization of bioactive natural products in extracts.[12] We have

successfully used it with various cell-based and biochemical assays[13−15] and recently developed and validated a profiling protocol for the discovery of new GABA_A receptor ligands.[16] Here, we describe the identification of piperine (**5**) as a new scaffold of positive allosteric modulators of the GABA_A receptor targeting a benzodiazepine-independent binding site.

Results and Discussion

Extracts were screened by means of an automated, fast perfusion system during two-microelectrode voltage clamp measurements in *Xenopus* oocytes expressing functional GABA_A receptors with defined subunit composition ($\alpha_1\beta_2\gamma_{2S}$).[17] When tested at 100 μg/mL, the *P. nigrum* ethyl acetate extract enhanced GABA-induced chloride ion current (I_{GABA}) by 169.1 ± 2.4%. The extract was submitted to HPLC-based activity profiling using a validated protocol.[16] The chromatogram of a semipreparative separation of extract (5 mg) and the corresponding activity profile of the time-based fractionation (22 microfractions of 90 s each) are shown in Figure 1.

A prominent peak of activity was found in fractions 7 and 8 (potentiation of I_{GABA} by 316.1 ± 7.0% and 248.1 ± 10.6%, respectively), which contained the major compound of the extract. Fraction 9 showed moderate activity (35.5 ± 1.1%), while fractions 6, 10, and 13 were only marginally active. However, nonresolved peaks occurred in the chromatogram, in particular in the time window of the activity peak. Therefore, separation conditions were optimized for full resolution of the critical HPLC peaks. These conditions were then used to measure high-resolution LC-MS data and for peak-based microfractionation by semipreparative HPLC for subsequent off-line microprobe NMR.

The semipreparative HPLC chromatogram obtained with 10 mg of extract is shown in Figure 2A. A total of 30 peaks were collected and submitted to parallel evaporation. For each peak a ^{1}H NMR spectrum (128 scans) was recorded with a 1 mm TXI probe. For 13 peaks, the spectra were of sufficient quality for reliable structure identification. Molecular formulas were calculated for compounds **1−13** using accurate mass data obtained by HPLC-PDA-ESI-TOFMS analysis of the extract. Since *P. nigrum* is phytochemically well studied (95 compound entries in the Chapman and Hall Dictionary of Natural Products[18]), 1−4 entries were found for each

* To whom correspondence should be addressed. Tel: ++41-61-267-1425. Fax: ++41-61-267-1474. E-mail: matthias.hamburger@unibas.ch.
† University of Basel.
‡ University of Vienna.
§ These authors contributed equally to this work.

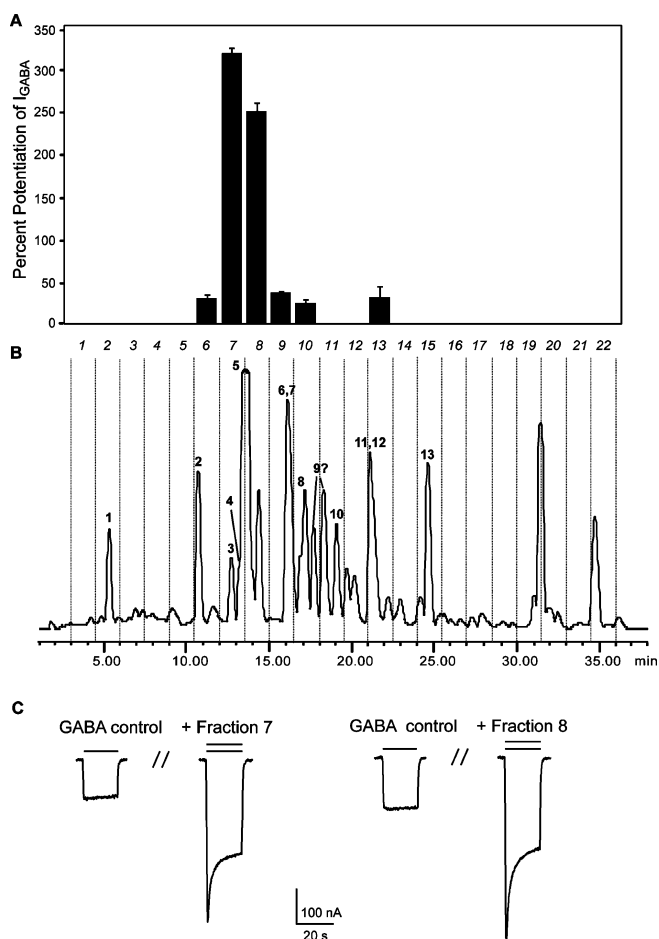**Figure 1.** HPLC-based activity profiling of the black pepper extract for GABA$_A$ receptor modulating properties. The HPLC chromatogram (254 nm) of a semipreparative separation of 5 mg of extract is shown in B. Peak numbering corresponds to compounds **1**−**13**. The 22 collected time-based fractions, 90 s each, are indicated with dashed lines. The potentiation of the GABA-induced chloride current in *Xenopus* oocytes (I_{GABA}) by each fraction is shown in A. Part C shows typical traces for the modulation of GABA-induced chloride currents through GABA$_A$ ($\alpha_1\beta_2\gamma_{2S}$) receptors by fractions 7 and 8 of the *P. nigrum* EtOAc extract.

of the 13 molecular formulas. Results of the HPLC-PDA-ESI-TOFMS analysis and database search are summarized in Table 1.

Compounds **1**−**13** were unambiguously identified with the aid of ^{1}H NMR data and comparison with published reference data.[19−29] The major peak was piperine (**5**), the main pungent piperamide in *P. nigrum*,[30] and the remaining compounds were all structurally related amides (Chart 1). Data for **1**−**13** are provided as Supporting Information. Figure 2B shows ^{1}H NMR spectra of minor amides **3** and **4**, and **5** collected from the peak-based microfractionation. Representative HSQC and HMBC spectra of compounds **4** and **5**, respectively, are shown in Figure 2C to provide an impression of the quality of spectra that can be obtained with this off-line HPLC-microprobe NMR approach.

For a quantitative determination of GABA$_A$ receptor activity of compounds in the active time window, piperlonguminine (**3**), piperanine (**4**), and piperine (**5**) were purified at preparative scale, along with structurally related trichostachine (**2**) and piperettine (**7**). These compounds were tested at a concentration of 100 μM in the oocyte assay. Piperine (**5**) was most efficient, as it potentiated I_{GABA} by 226 ± 26%, while piperanine (**4**) at the same concentration was less efficient (potentiation of I_{GABA} by 138 ± 20%). Weak enhancement of I_{GABA} (32 ± 24%) was observed for **7**, and compounds **2** and **3** slightly inhibited I_{GABA} (−29 ± 13% and −10

± 3%, respectively) (Chart 1). Given the lack of I_{GABA} potentiation in other fractions of the activity profile (Figure 1A), the other amides must be considered inactive.

As shown in Figure 3, both piperanine (**4**) and piperine (**5**) enhanced I_{GABA} at a GABA EC$_{5−10}$ in a dose-dependent manner. The currents were stimulated at concentrations ≥ 1 μM. Maximum I_{GABA} enhancement by **4** and **5** (187 ± 10%, $n = 3$, and 302 ± 26%, $n = 3$, respectively) occurred at ∼300 μM with EC$_{50}$ values of 56 ± 19 and 52 ± 9 μM, respectively. The application of **5** prior to GABA showed no activity, indicating an allosteric modulation of the receptor (response to application of 100 μM **5** in the absence of GABA is shown in Figure 3C). Furthermore, the application of 100 μM trichostachine (**2**), piperlonguminine (**3**), piperanine (**4**), and piperettine (**7**) in the absence of GABA displayed as well no activity on GABA$_A$ receptors composed of $\alpha_1\beta_2\gamma_{2S}$ subunits (see Figure 3C).

To investigate a possible interaction of **5** with the benzodiazepine binding site, we analyzed its effect on I_{GABA} in the presence of the benzodiazepine receptor antagonist flumazenil (10 μM). Potentiation of I_{GABA} by 300 μM piperine (**5**) was not significantly affected by flumazenil (304 ± 40%, $n = 3$ control vs 334 ± 108% in the presence of flumazenil, $n = 3$) (Figure 4A and B). Figure 4C illustrates the additive effects of 100 μM **5** (180 ± 69%, $n = 3$) and diazepam (1 μM) (204 ± 48%, $n = 3$) on I_{GABA} when coapplied (391 ± 104%, $n = 3$) (Figure 4C and D).

The example of piperamides highlights the advantages of an HPLC-based approach and, in particular, the possibility of obtaining valuable preliminary structure−activity information via the characterization of focused compound subsets without a need for preparative purification. Activity can be easily localized in the extract, and all peaks in the critical time window rapidly separated by semipreparative HPLC under optimized conditions (Figures 1 and 2). A series of compounds structurally related to **5** could be identified by a combination of on-line (HPLC-PDA-HRMS) and off-line (microprobe NMR) requiring only milligram amounts of extract. Off-line NMR with disposable 1 mm tubes has several attractive features for profiling. Collected HPLC peaks can be processed in parallel (evaporation, sample preparation for NMR). An NMR autosampler permits unattended measurement of 1D ^{1}H NMR spectra, on the basis of which the need for more advanced NMR experiments can be checked. The microtubes can be stored for a certain time similar to classical NMR tubes, and time-consuming experiments can be performed at a later moment. By extending the profiling beyond the active compounds toward inactive but structurally related molecules, small focused "virtual" libraries are generated that provide valuable information for preliminary structure−activity considerations. In the present case it was clear that the nature of the amide moiety and the chain length between the aromatic ring and the amide were critical for the observed allosteric modulation of GABA$_A$ receptors. Rigidity of the chain might also be important for the efficiency, as the 4,5-dihydro derivative **4** was significantly less efficient in stimulating I_{GABA} compared to **5** (Figure 3).

Very recently, Pedersen et al. reported **5** as a GABA$_A$ receptor ligand presumed to bind to the benzodiazepine binding site.[31] However, only low affinity (IC$_{50}$ of 1.2 mM in a [^{3}H]-flumazenil binding assay) was reported. We assume that the activity observed by Pedersen et al.[31] was due to low-affinity binding to the benzodiazepine binding site at very high compound concentrations. Besides the fact that the affinity was extremely low, a binding assay provides neither information on the intrinsic activity of a compound nor insights into the molecular mechanism of its action.

In contrast, our functional assay clearly demonstrated a positive allosteric modulation of the GABA$_A$ receptor by **5** and **4** with comparable potencies and revealed a higher efficiency of **5** in stimulating I_{GABA} (Figure 3). Studies with the benzodiazepine receptor antagonist flumazenil (Figure 4A and B) and the additive
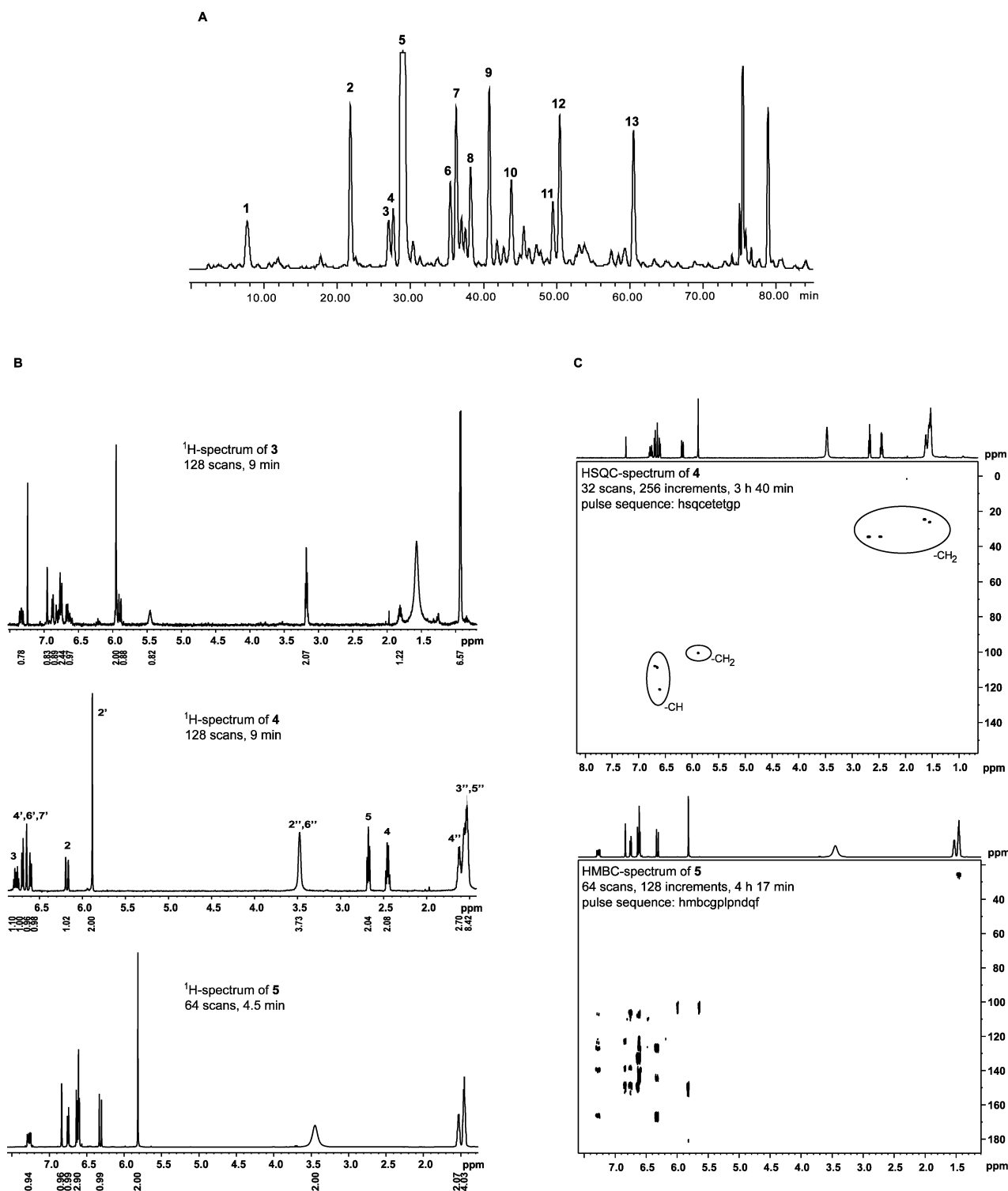
Figure 2. Part A shows the chromatogram (254 nm) of the optimized, semipreparative HPLC separation of the active *P. nigrum* extract (10 mg in 100 μL of DMSO). A total of 30 peaks were collected for off-line microprobe NMR. Peak labeling corresponds to compounds **1−13**. Part B shows ¹H NMR spectra of selected compounds obtained by the separation mentioned above, whereas part C shows the spectra of two representative 2D NMR experiments.

effects of **5** and diazepam (Figure 4C and D) clearly demonstrate that **5** does not interact with the benzodiazepine binding site.

Benzodiazepines may cause undesirable effects including reduced coordination, cognitive impairment, increased accident proneness, physiological dependence, and withdrawal symptoms.[5,32] GABA$_A$ receptor ligands with fewer side effects are, therefore, an unmet medical need.[5,33]

Our data show that **5** represents a new scaffold for positive allosteric GABA$_A$ receptor modulators interaction with a benzo-diazepine-independent binding site. Our study provides a molecular basis for earlier reports on the antidepressant[34,35] and anticonvulsant activity of piperine (**5**)[9,36,37] in rodents and corroborates traditional uses of *Piper nigrum* and other *Piper* species.[9−11,38] Even though a number of other pharmacological properties have been reported,[39−42] **5** may represent an interesting lead structure. It complies in all respects with Lipinski's "rule of five" (MW: 285 g/mol, ClogP: 3.31, H-bond-donor/acceptor sites: 0/4.),[43] is orally bioavailable, and is readily accessible. Piperine (**5**) is, however, known

Table 1. Data of HPLC-PDA-TOFMS Analysis and Associated Database Findings of Compounds **1−13**, Which Were Purified from the Active Ethyl Acetate Extract by Semipreparative HPLC

cpd	t_{R1} (min)[a]	t_{R2} (min)[b]	λ_{max} (nm)	acc. mass found	acc. mass calcd	calcd formula	DNP hits[c]
1	6.1	6.6	221, 294, 316	313.1295	313.1308	$C_{18}H_{19}NO_3$	2
2	21.5	20.6	241, 309, 342	271.1195	271.1202	$C_{16}H_{17}NO_3$	1
3	26.8	25.4	243, 309, 338	273.1346	273.1359	$C_{16}H_{19}NO_3$	2
4	27.9	26.2	232, 285	287.1513	287.1515	$C_{17}H_{21}NO_3$	2
5	29.0	27.1	255, 310, 338	285.1361	285.1359	$C_{17}H_{19}NO_3$	4
6	36.3	33.7	213, 263, 305	313.1673	313.1672	$C_{19}H_{23}NO_3$	2
7	36.9	34.5	348	311.1512	311.1515	$C_{19}H_{21}NO_3$	1
8	39.2	36.4	210, 263, 310, 358	315.1826	315.1828	$C_{19}H_{25}NO_3$	2
9	41.7	38.7	261	327.1816	327.1828	$C_{20}H_{25}NO_3$	2
10	44.9	41.6	268, 305	339.1837	339.1828	$C_{21}H_{25}NO_3$	2
11	50.4	47.3	261, 307	343.2145	343.2141	$C_{21}H_{29}NO_3$	2
12	51.4	48.0	213, 263, 303	355.2141	355.2141	$C_{22}H_{29}NO_3$	3
13	61.1	58.5	261, 303	383.2460	383.2454	$C_{24}H_{33}NO_3$	3

[a] Retention time in the HPLC-PDA-ESITOFMS analysis. [b] Retention time in the semipreparative HPLC separation (Figure 2A). [c] Hits in the natural products database (Chapman and Hall Dictionary of Natural Products); search query limited by the term "*piper*".

Chart 1. Structures of Piperamides **1−13** and Potentiation of GABA-Induced Chloride Current (I_{GABA}) in *Xenopus* Oocytes by 100 μM **2−5** and **7**

1

2   -28.8 % I_{GABA}

3   -10.1 % I_{GABA}

4 -   137.9 % I_{GABA}

5 $\Delta^{4,5}$ 225.8 % I_{GABA}

6 $\Delta^{2,3}$

7 $\Delta^{2,3},\Delta^{4,5}$ 31.6 % I_{GABA}

8 -

10 $\Delta^{2,3}, \Delta^{4,5}$

11 -

9 n = 1, -

12 n = 2, $\Delta^{2,3}$

13 n = 3, $\Delta^{2,3}$
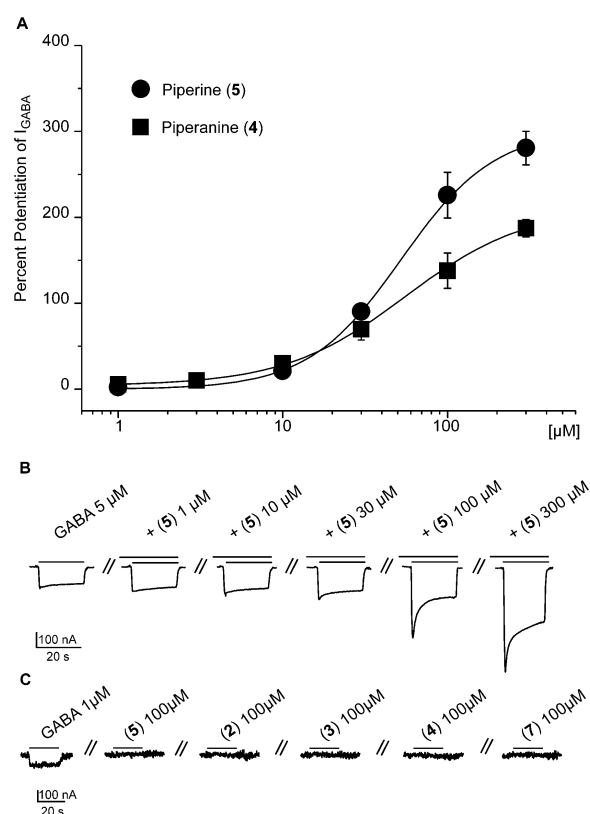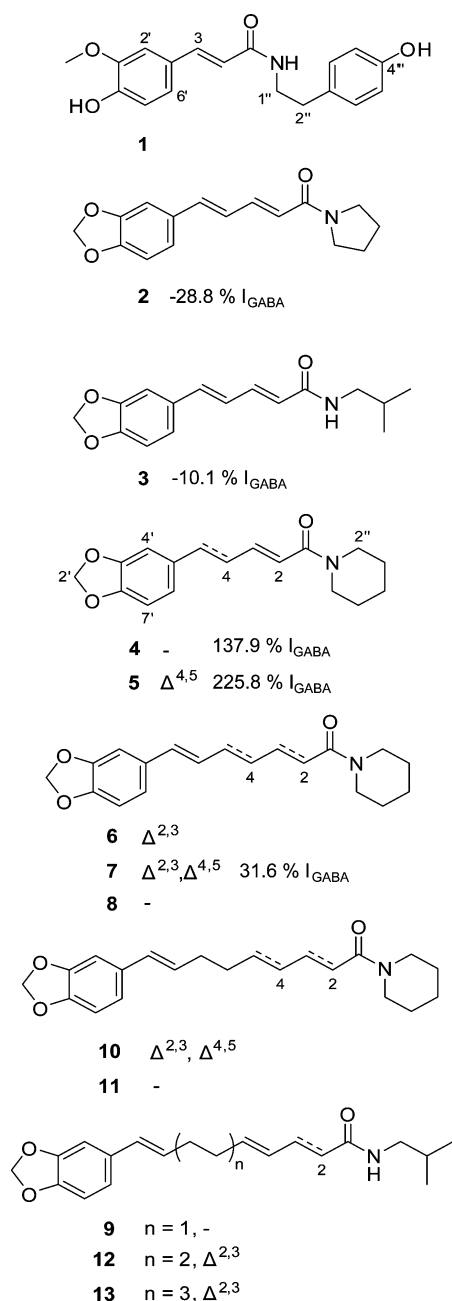
Figure 3. Part A shows the concentration−response curves for compounds **4** and **5** on GABA$_A$ receptors composed of α_1, β_2, and γ_{2S} subunits using a GABA EC$_{5-10}$. Part B displays typical traces for modulation of chloride currents through $\alpha_1\beta_2\gamma_{2S}$ GABA$_A$ receptors by piperine (**5**). In part C representative currents illustrate the absence of direct activation of GABA$_A$ receptors ($\alpha_1\beta_2\gamma_{2S}$) by piperine (**5**), trichostachine (**2**), piperlonguminine (**3**), piperanine (**4**), and piperettine (**7**) at 100 μM in comparison to a GABA-induced current at 1 μM.

to activate TRPV1 receptors[40] and is a general inhibitor of both phase I and phase II metabolism,[44] which might cause side effects and drug interactions. It should be explored to what extent pharmacological promiscuity of piperamides can be reduced through structural modifications.

Experimental Section

General Experimental Procedures. NMR spectra were recorded at room temperature with a Bruker Avance III spectrometer operating at 500.13 MHz. Proton NMR experiments and 1D and 2D homonuclear and heteronuclear NMR spectra were measured with a 1 mm TXI probe.
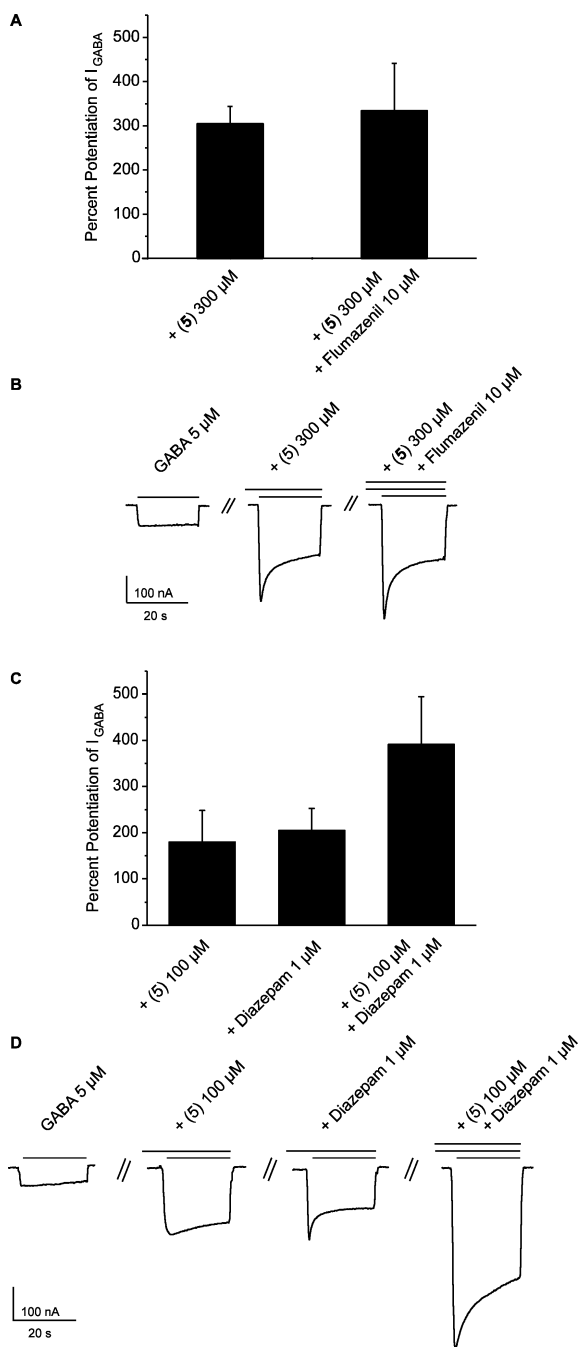
Figure 4. Effect of (**5**) on I_{GABA} in the presence of flumazenil and diazepam. (A) Stimulation of I_{GABA} by **5** in the presence of flumazenil (10 μM). The left bar shows the positive allosteric modulation of the GABA (EC_{5-10})-induced chloride current by 300 μM piperine (**5**). The right bar illustrates that flumazenil does not antagonize the **5**-induced enhancement of I_{GABA}. (B) Typical GABA-induced chloride currents in the absence and presence of the indicated concentrations of **5**, or **5** and flumazenil, respectively. (C) Additive effects of **5** and diazepam on I_{GABA}. The left bar illustrates the enhancement of I_{GABA} by 100 μM (**5**); the bar in the middle, by 1 μM diazepam, and the right bar illustrates enhancement of I_{GABA} when both compounds were coapplied. (D) Representative chloride currents induced by 5 μM GABA (corresponding to EC_{5-10}), current enhancement by **5** (100 μM) and diazepam (1 μM), and I_{GABA} during coapplication of both compounds.

Spectra were analyzed using Bruker TopSpin 2.1 software. High-resolution mass spectra (HPLC-PDA-ESITOFMS) were obtained on a micrOTOF ESI-MS system (Bruker Daltonics) connected via a T-splitter (1:10) to an HP 1100 series system (Agilent) consisting of a binary pump, autosampler, column oven, and diode array detector (G1315B).

Data acquisition and processing was performed using HyStar 3.0 software (Bruker Daltonics). Semipreparative HPLC separations for activity profiling and off-line microprobe NMR was performed with an HP 1100 series system (Agilent) consisting of a quaternary pump, autosampler, column oven, and diode array detector (G1315B). Parallel evaporation of microfractions and semipreparative HPLC fractions was performed with a Genevac EZ-2 plus vacuum centrifuge (Avantec). SunFire C18 (3.5 μm, 3.0 × 150 mm) and SunFire Prep C18 (5 μm, 10 × 150 mm) columns (Waters) were used for HPLC-PDA-ESITOFMS and semipreparative HPLC, respectively. HPLC-grade acetonitrile (Scharlau Chemie S.A.) and water were used for HPLC separations. Solvents used for extraction and column chromatography were of analytical grade. Petroleum ether of technical grade was purified by distillation for extraction and column chromatography. Silica gel (63−200 μm, Merck) was used for column chromatography.

Plant Material. Dried fruits of *P. nigrum* L. were purchased from the Juhuayuan Herbal Market in Kunming (Yunnan Province, China). A voucher specimen (00 286) is deposited at the Institute of Pharmaceutical Biology, University of Basel.

Extraction. The plant material was frozen with liquid nitrogen and ground with a ZM1 ultracentrifugal mill (Retsch). The extract for the screening and HPLC-based activity profiling was prepared with an ASE 200 extraction system with solvent module (Dionex) by extraction with ethyl acetate. Extraction pressure was 120 bar, and the temperature was set at 70 °C. For isolation of the piperamides, 343 g of ground fruits was extracted by maceration at room temperature with petroleum ether (4 × 2.5 L, 2 h each), followed by ethyl acetate (4 × 2.5 L, 2 h each). The solvents were evaporated at reduced pressure to yield 14.22 and 18.84 g of petroleum ether and ethyl acetate extract, respectively. The extracts were stored at −20 °C until use.

Microfractionation for Activity Profiling. Microfractionation for $GABA_A$ receptor activity profiling was performed as previously described,[16] with minor modifications: separation was carried out on a semipreparative HPLC column with acetonitrile (solvent A) and water (solvent B) using the following gradient: 30% A to 100% A for 30 min, hold for 10 min. The flow rate was 4 mL/min, and 50 μL of extract (100 mg/mL in DMSO) was injected. A total of 22 time-based microfractions of 90 s each were collected. Microfractions were evaporated in parallel and submitted to activity testing.

HPLC-PDA-ESITOFMS. The ethyl acetate extract of *P. nigrum* was analyzed with acetonitrile (solvent A) and water containing 0.1% formic acid (solvent B) using an optimized gradient profile: 30% A isocratic for 5 min, 30% to 80% A in 65 min, 80% to 100% A in 1 min, hold for 9 min. The flow rate was 0.5 mL/min. The sample was dissolved in DMSO at a concentration of 10 mg/mL, and the injection volume was 200 μL. Conditions for ESITOFMS were as follows: spectra were recorded in the range m/z 100−600 in positive mode. Nitrogen was used as a nebulizing gas at a pressure of 2.0 bar and as a drying gas at a flow rate of 9.0 L/min (dry gas temperature 240 °C). Capillary voltage was set at 4500 V, hexapole at 230.0 Vpp. Instrument calibration was performed using a reference solution of sodium formiate 0.1% in 2-propanol/water (1:1) containing 5 mM NaOH.

Semipreparative HPLC and Off-Line Microprobe NMR. Separation of *P. nigrum* ethyl acetate extract was carried out with the same solvent system and gradient elution as for HPLC-PDA-ESITOFMS. The flow rate was set at 4 mL/min, and the injected volume of extract was 100 μL at a concentration of 100 mg/mL in DMSO. A total of 30 peak-based fractions were collected manually, evaporated in parallel, and redissolved in d_4-methanol, d_1-chloroform, or d_6-DMSO. For NMR experiments of the collected fractions, the following settings were used: 64 or 128 scans to record ^{1}H spectra; 8 scans for [1]H[1]H-COSY spectra using the *cosygpqf* pulse program; 32 scans and 256 increments to record HSQC experiments using the *hsqcedetgp* or *hsqcetgpsi2* pulse program, and for HMBC-NMR, 64 scans, 128 increments, and the *hmbcgplpndqf* pulse program.

Isolation of Piperamides. A portion (16.6 g) of the ethyl acetate extract was separated by chromatography on a silica gel column (70 × 6.5 cm i.d.) using a step gradient of petroleum ether (solvent A) and ethyl acetate (solvent B) in ratios of 10:0, 8:2, 6:4, 4:6, 2:8, and 10:0 (2 L each), respectively, to yield 20 fractions (1−20). Fractions 10 and 11 (2.02 and 9.02 g, respectively) were used for crystallization of **5** (7.16 g). The residue of the mother liquor of fraction 10 (830 mg) was separated into 18 fractions (10A−10R) by medium-pressure liquid chromatography on a silica gel cartridge (40−63 μm, 150 × 40 mm i.d.). A gradient of 10% B to 50% B in 95 min and 50% B to 100% B

in 60 min was applied at a flow rate of 20 mL/min. From fraction 10L (140 mg), a total of 65.3 mg was separated by injecting different volumes of a concentration of 10 mg/mL DMSO onto the semipreparative HPLC column in order to isolate **4** (1.5 mg) and **7** (13.4 mg). The gradient profile using acetonitrile (solvent C) and water containing 0.1% formic acid (solvent D) was 40% C to 55% C in 25 min. The flow rate was set at 4 mL/min. Further on, a total of 68.3 mg of fraction 19 (1.2 g) and 56.2 mg of fraction 9 (60 mg) were separated using the semipreparative HPLC system by repeated injection of different volumes of 10 mg/mL DMSO dilutions. Separation of fraction 19 yielded compound **2** (10.5 mg) using the following gradient system: 40% isocratic C for 2 min, followed by 40% C to 45% C in 18 min. Fraction 9 was separated isocratically at 50% C to yield compound **3** (6.5 mg). The flow rate for both separations was 4 mL/min. Compounds **2**–**4** and **7** were identified by comparison of physicochemical data (^{1}H NMR and UV–vis) with published values[20,23,24,27] and recorded data for the peaks in the off-line HPLC microprobe NMR approach. The purity of the compounds was >95% (^{1}H NMR).

Expression of GABA$_A$ Receptors. Stage V–VI oocytes from *Xenopus laevis* were prepared, and cRNA was injected as previously described by Khom et al. (2006).[45] Female *Xenopus laevis* (NASCO, Fort Atkinson, WI) were anesthetized by exposing them for 15 min to a 0.2% MS-222 (methanesulfonate salt of 3-aminobenzoic acid ethyl, Sigma) solution before surgically removing parts of the ovaries. Follicle membranes from isolated oocytes were enzymatically digested with 2 mg/mL collagenase (Type 1A, Sigma). Synthesis of capped runoff poly(A+) cRNA transcripts was obtained from linearized cDNA templates (pCMV vector). One day after enzymatic isolation, the oocytes were injected with 50 nL of DEPC-treated water (Sigma) containing different cRNAs at a concentration of approximately 300–3000 pg/nL per subunit. The amount of injected cRNA mixture was determined by means of a NanoDrop ND-1000 (Kisker Biotech). To ensure expression of the gamma subunit in $\alpha_1\beta_2\gamma_{2S}$ receptors, rat cRNAs were mixed in a 1:1:10 ratio. Oocytes were then stored at 18 °C in ND96 solution.[46] Voltage clamp measurements were performed between days 1 and 5 after cRNA injection.

Two-Microelectrode Voltage Clamp Studies. Electrophysiological experiments were performed by the two-microelectrode voltage clamp method making use of a TURBO TEC 03X amplifier (npi electronic GmbH) at a holding potential of −70 mV and pCLAMP 10 data acquisition software (Molecular Devices). Currents were low-pass-filtered at 1 kHz and sampled at 3 kHz. The bath solution contained 90 mM NaCl, 1 mM KCl, 1 mM MgCl$_2$, 1 mM CaCl$_2$, and 5 mM HEPES (pH 7.4). Electrode filling solution contained 2 M KCl. Oocytes with maximal current amplitudes > 3 μA were discarded to exclude voltage clamp errors.

Fast Solution Exchange during I_{GABA} Recordings. Test solutions (100 μL) were applied to the oocytes at a speed of 300 μL/s by means of an automated fast perfusion system.[17] In order to determine GABA EC$_{5-10}$ (typically between 3 and 8 μM), a dose–response experiment with GABA concentrations ranging from 0.1 μM to 1 mM was performed. Stock solution of *P. nigrum* (10 mg/mL in DMSO) was diluted to a concentration of 100 μg/mL with bath solution and then mixed with GABA EC$_{5-10}$. As previously described, microfractions collected from the semipreparative HPLC separations were dissolved in 30 μL of DMSO and subsequently mixed with 2.97 mL of bath solution containing GABA EC$_{5-10}$.[16] Stock solutions of compounds **2**–**5** and **7** (10 mM in DMSO) were diluted to a concentration of 100 μM with bath solution and then mixed with GABA EC$_{5-10}$ or applied alone. For dose–response experiments, bath solution containing compound **4** or **5** in concentrations ranging from 1 to 300 μM was applied to the oocyte 90 s prior to application of the corresponding compound solution containing GABA EC$_{5-10}$. Diazepam and flumazenil (Sigma) were dissolved in DMSO (10 mM) and subsequently diluted in bath solution or bath solution containing GABA EC$_{5-10}$. Oocytes were preincubated for 90 s with flumazenil or diazepam before the corresponding GABA EC$_{5-10}$ containing test solution was applied.[45]

Data Analysis. Enhancement of the chloride current (I_{GABA}) was defined as $I_{(GABA+Comp)}/I_{GABA} - 1$, where $I_{(GABA+Comp)}$ is the current response in the presence of a given compound, and I_{GABA} is the control GABA-induced chloride current. Data are given as mean ± SE of at least two oocytes and ≥2 oocyte batches.

Supporting Information Available: Spectral characterization data of compounds **1**–**13**, including ^{1}H and ^{13}C chemical shifts from 1D-^{1}H NMR- and 2D-heteronuclear NMR spectra. This material is available free of charge via the Internet at http://pubs.acs.org.

References and Notes

(1) Simon, J.; Wakimoto, H.; Fujita, N.; Lalande, M.; Barnard, E. A. *J. Biol. Chem.* **2004**, *279*, 41422–41435.
(2) Olsen, R. W.; Sieghart, W. *Pharmacol. Rev.* **2008**, *60*, 243–260.
(3) Barrera, N. P.; Edwardson, J. M. *Trends Neurosci.* **2008**, *31*, 569–576.
(4) Sieghart, W.; Sperk, G. *Curr. Top. Med. Chem.* **2002**, *2*, 795–616.
(5) Whiting, P. J. *Curr. Opin. Pharmacol.* **2006**, *6*, 24–29.
(6) Riss, J.; Cloyd, J.; Gates, J.; Collins, S. *Acta Neurol. Scand.* **2008**, *118*, 69–86.
(7) Johnston, G. A. R.; Hanrahan, J. R.; Chebib, M.; Duke, R. K.; Mewett, K. N. *Adv. Pharmacol.* **2006**, *54*, 286–316.
(8) Tsang, S. Y.; Xue, H. *Curr. Pharm. Des.* **2004**, *10*, 1035–1044.
(9) Pei, Y. Q. *Epilepsia* **1983**, *24*, 177–182.
(10) Szallasi, A. *Trends Pharmacol. Sci.* **2005**, *26*, 437–439.
(11) Sunila, E.; Kuttan, G. *J. Ethnopharmacol.* **2004**, *90*, 339–346.
(12) Potterat, O.; Hamburger, M. *Curr. Org. Chem.* **2006**, *10*, 899–920.
(13) Potterat, O.; Wagner, K.; Gemmecker, G.; Mack, J.; Puder, C.; Vettermann, R.; Streicher, R. *J. Nat. Prod.* **2004**, *67*, 1528–1531.
(14) Danz, H.; Stoyanova, S.; Wippich, P.; Brattstroem, A.; Hamburger, M. *Planta Med.* **2001**, *67*, 411–416.
(15) Dittmann, K.; Gerhaeuser, C.; Klimo, K.; Hamburger, M. *Planta Med.* **2004**, *70*, 909–913.
(16) Kim, H. J.; Baburin, I.; Khom, S.; Hering, S.; Hamburger, M. *Planta Med.* **2008**, *74*, 521–526.
(17) Baburin, I.; Beyl, S.; Hering, S. *Pflug. Arch. Eur. J. Phys.* **2006**, *453*, 117–123.
(18) Chapman, J. *Chapman and Hall Dictionary of Natural Products*; CRC Press, Hampden Data Services Ltd., 2008.
(19) Chen, J.-J.; Huang, Y.-C.; Chen, Y.-C.; Huang, S.-W.; Wang, S.-W.; Peng, C.-Y.; Teng, C.-M.; Chen, I.-S. *Planta Med.* **2002**, *68*, 980–985.
(20) De Araujo-Junior, J. X.; Da-Cunha, E. V. L.; De O. Chaves, M. C.; Gray, A. I. *Phytochemistry* **1997**, *44*, 559–561.
(21) Hussain, S. F.; Goezler, B.; Shamma, M.; Goezler, T. *Phytochemistry* **1982**, *21*, 2979–2980.
(22) Lee, S. W.; Rho, M.-C.; Park, H. R.; Choi, J.-H.; Kang, J. Y.; Lee, J. W.; Kim, K.; Lee, H. S.; Kim, Y. K. *J. Agric. Food Chem.* **2006**, *54*, 9759–9763.
(23) Min, K. R.; Kim, K.-S.; Ro, J. S.; Lee, S. H.; Kim, J. A.; Son, J. K.; Kim, Y. *Planta Med.* **2004**, *70*, 1115–1118.
(24) Olsen, R. A.; Spessard, G. O. *J. Agric. Food Chem.* **1981**, *29*, 942–944.
(25) Park, I.-K.; Lee, S.-G.; Shin, S.-C.; Park, J.-D.; Ahn, Y.-J. *J. Agric. Food Chem.* **2002**, *50*, 1866–1870.
(26) Strunz, G. M.; Finlay, H. *Tetrahedron* **1994**, *50*, 11113.
(27) Traxler, J. T. *J. Agric. Food Chem.* **1971**, *19*, 1135–1138.
(28) Wu, S.; Sun, C.; Pei, S.; Lu, Y.; Pan, Y. *J. Chromatogr.* **2004**, *1040*, 193.
(29) Wei, K.; Li, W.; Koike, K.; Pei, Y.; Chen, Y.; Nikaido, T. *J. Nat. Prod.* **2004**, *67*, 1005–1009.
(30) Friedman, M.; Levin, C. E.; Lee, S. U.; Lee, J. S.; Ohnisi-Kameyama, M.; Kozukue, N. *J. Agric. Food Chem.* **2008**, *56*, 3028–3036.
(31) Pedersen, M. E.; Metzler, B.; Stafford, G. I.; van Staden, J.; Jaeger, A. K.; Rasmussen, H. B. *Molecules* **2009**, *14*, 3833–3843.
(32) Kaplan, E. M.; DuPont, R. L. *Curr. Med. Res. Opin.* **2005**, *21*, 941–950.
(33) Rupprecht, R.; Eser, D.; Zwanzger, P.; Moeller, H.-J. *World J. Biol. Psychiatry* **2006**, *7*, 231–237.
(34) Li, S.; Wang, C.; Li, W.; Koike, K.; Nikaido, T.; Wang, M.-W. *J. Asian Nat. Prod. Res.* **2007**, *9*, 421.
(35) Wattanathorn, J.; Chonpathompikunlert, P.; Muchimapura, S.; Priprem, A.; Tankamnerdthai, O. *Food Chem. Toxicol.* **2008**, *46*, 3106–3110.
(36) Hou, T. J.; Li, Y. Y.; Liao, N.; Xu, X. J. *J. Mol. Model.* **2000**, *6*, 438–445.

(37) D'Hooge, R.; Pei, Y. Q.; Raes, A.; Lebrun, P.; Van Bogaert, P. P.; De Deyn, P. P. *Arzneim.-Forsch.* **1996**, *46*, 557–560.

(38) Awad, R.; Ahmed, F.; Bourbonnais-Spear, N.; Mullally, M.; Ta, C. A.; Tang, A.; Merali, Z.; Maquin, P.; Caal, F.; Cal, V.; Poveda, L.; Vindas, P. S.; Trudeau, V. L.; Arnason, J. T. *J. Ethnopharmacol.* **2009**, *125*, 257–264.

(39) Bajad, S.; Bedi, K. L.; Singla, A. K.; Johri, R. K. *Planta Med.* **2001**, *67*, 176–179.

(40) McNamara, F. N.; Randall, A.; Gunthorpe, M. J. *Br. J. Pharmacol.* **2005**, *144*, 781–790.

(41) Bhardwaj, R. K.; Glaeser, H.; Becquemont, L.; Klotz, U.; Gupta, S. K.; Fromm, M. F. *J. Pharmacol. Exp. Ther.* **2002**, *302*, 645–650.

(42) Volak, L. P.; Ghirmai, S.; Cashman, J. R.; Court, M. H. *Drug Metab. Dispos.* **2008**, *36*, 1594–1605.

(43) Lipinski, C. A.; Lombardo, F.; Dominy, B. W.; Feeney, P. J. *Adv. Drug Delivery Rev.* **1997**, *23*, 3–25.

(44) Anand, P.; Kunnumakkara, A. B.; Newman, R. A.; Aggarwal, B. B. *Mol. Pharmacol.* **2007**, *4*, 807–818.

(45) Khom, S.; Baburin, I.; Timin, E. N.; Hohaus, A.; Sieghart, W.; Hering, S. *Mol. Pharmacol.* **2006**, *69*, 640–649.

(46) Methfessel, C.; Witzemann, V.; Takahashi, T.; Mishina, M.; Numa, S.; Sakmann, B. *Pflug. Arch. Eur. J. Phys.* **1986**, *407*, 577–588.

SUPPORTING INFORMATION

HPLC-based activity profiling – Discovery of piperine as a positive GABA$_A$ receptor modulator targeting a benzodiazepine-independent binding site

Janine Zaugg[†,§], Igor Baburin[‡,§], Barbara Strommer[‡], Hyun-Jung Kim[†], Steffen Hering[‡], and Matthias Hamburger*[†]

[†]Institute of Pharmaceutical Biology, University of Basel, Klingelbergstrasse 50, 4056 Basel, Switzerland

[‡]Departement of Pharmacology and Toxicology, University of Vienna, Althanstrasse 14, 1090 Vienna, Austria

*To whom correspondence should be addressed. Tel: ++41-61-267-1425. Fax: ++41-61-267-1474. E-mail: matthias.hamburger@unibas.ch

[§]Janine Zaugg and Igor Baburin contributed equally to this work.

Table S1. NMR spectroscopic data (500 MHz, MeOD) for (**1**)

(E)-3-(4-hydroxy-3-methoxyphenyl)-N-(4-hydroxyphenethyl)acrylamide (syn.: moupinamide) (1) [b]

CAS Nr. 66648-43-9
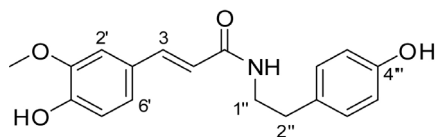
position	δ_C [a]	δ_H (J in Hz)
2	140.42	7.43, d (15.7)
3	117.52	6.40, d (15.7)
2'	110.46	7.11, d (1.8)
3'-MeO	54.97	3.89, s
5'	115.09	6.80, d (8.2)
6'	121.82	7.02, dd (8.2, 1.8)
1''	40.94	3.47, t (7.3)
2''	34.31	2.76, t (7.3)
2'''	129.21	7.05, d (8.5)
3'''	114.95	6.72, d (8.5)
5'''	114.95	6.72, d (8.5)
6'''	129.21	7.05, d (8.5)

[a] ^{13}C chemical shifts deduced from HSQC-NMR spectrum

[b] δ_C and δ_H reference data can be found in Hussain, S. F.; Goezler, B.; Shamma, M.; Goezler, T. *Phytochemistry* **1982**, *21*, 2979-2980

Table S2. NMR spectroscopic data (500 MHz, CDCl$_3$) for (**2**)

(2E,4E)-5-(benzo[d][1,3]dioxol-5-yl)-1-(pyrrolidin-1-yl)penta-2,4-dien-1-one (syn.: trichostachine) (2) [b]

CAS Nr. 25924-78-1
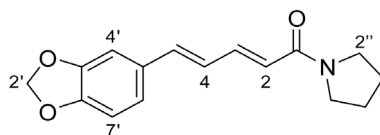
position	δ_C [a]	δ_H (_J_ in Hz)
2	-	6.23, d (14.7)
3	-	7.42, dd (14.7, 10.4)
4	-	6.71, dd (14.7, 10.4)
5	-	6.73, d (14.7)
2'	-	5.95, s
4'	-	6.96, d (1.3)
6'	-	6.88, dd (8.0,1.3)
7'	-	6.75, d (8.0)
2''	-	1.91, m
3''	-	3.54, t (6.6)
4''	-	3.54, t (6.6)
5''	-	1.91, m

[a] no heteronuclear 2D-NMR spectra were recorded
[b] δ_H reference data can be found in Olsen, R. A.; Spessard, G. O. _J. Agric. Food Chem._ **1981**, _29_, 942-944

Table S3. NMR spectroscopic data (500 MHz, CDCl$_3$) for (**3**)

(2E,4E)-5-(benzo[d][1,3]dioxol-5-yl)-N-isobutylpenta-2,4-dienamide (syn.: piperlonguminine) (3) [b]

CAS Nr. 5950-12-9
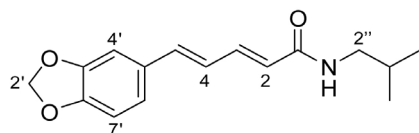
position	δ_C[a]	δ_H (*J* in Hz)
2	-	5.89, d (14.5)
3	-	7.33, dd (14.5,11.0)
4	-	6.65, dd (15.2, 11.0)
5	-	6.76, d (15.2)
2'	-	6.95, s
4'	-	6.88, d (1.5)
6'	-	6.88, dd (8.0, 1.5)
7'	-	6.76, d (8.0)
2''	-	3.17, t (6.5)
3''	-	1.81, m (6.5)
4''	-	0.93, d (6.5)
5''	-	0.93, d (6.5)

[a] no heteronuclear 2D-NMR spectra were recorded
[b] δ_H reference data can be found in Olsen, R. A.; Spessard, G. O. *J. Agric. Food Chem.* **1981**, *29*, 942-944

Table S4. NMR spectroscopic data (500 MHz, CDCl$_3$) for (**4**)

(E)-5-(benzo[d][1,3]dioxol-5-yl)-1-(piperidin-1-yl)pent-2-en-1-one (syn.: piperanine) (4) [b]
CAS Nr. 23512-46-1
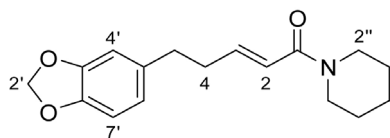
position	δ_C[a]	δ_H (*J* in Hz)
2	121.45	6.18, d (15.0)
3	143.61	6.77, dt (15.0, 7.0)
4	34.36	2.45, dt (15.0, 7.5)
5	34.42	2.68, t (7.5)
2'	100.58	5.89, s
4'	108.76	6.65, d (1.5)
6'	121.13	6.60, dd (8.0, 1.5)
7'	108.00	6.70, d (8.0)
2''	n.d.	3.48, broad
3''	26.02	1.54, m
4''	24.51	1.62, m
5''	26.02	1.54, m
6''	n.d.	3.48, broad

[a] ^{13}C chemical shifts deduced from HSQC-NMR spectrum

[b] δ_H reference data can be found in Traxler, J.T. *J. Agr. Food Chem.*, **1971**, *19*, 1135-1138

Table S5. NMR spectroscopic data (500 MHz, CDCl$_3$) for (**5**)

(2E,4E)-5-(benzo[d][1,3]dioxol-5-yl)-1-(piperidin-1-yl)penta-2,4-dien-1-one (syn.: piperine) (5) [b]

CAS Nr. 94-62-2
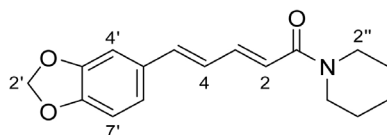
position	δ_C [a]	δ_H (*J* in Hz)
1	166.01	-
2	120.12	6.32, d (15.0)
3	142.16	7.27, dd (15.0, 10.0)
4	125.25	6.72, dd (15.0, 10.0
5	137.92	6.69, d (15.0)
1'	148.38	-
2'	101.14	5.95, s
3'	148.38	-
4'	105.59	6.84, d, (1.5)
5'	132.40	-
6'	122.21	6.75, d (8.0, 1.5)
7'	108.15	6.63, d (8.0)
2''	43.01	3.45, broad
3''	24.54	1.45, m
4''	24.48	1.53, m
5''	25.97	1.45, m
6''	46.74	3.45, broad

[a] ^{13}C chemical shifts deduced from HSQC- and HMBC-NMR spectra

[b] δ_H and δ_C reference data can be found in De Araujo-Junior, J.X.; Da-Cunha, E.V.L.; Chaves, M.C.; Gray, A.I. *Phytochemistry* **1997**, *44*, 559-561

Table S6. NMR spectroscopic data (500 MHz, CDCl$_3$) for (**6**)

(2E,6E)-7-(benzo[d][1,3]dioxol-5-yl)-1-(piperidin-1-yl)hepta-2,6-dien-1-one (syn.: 4,5-dihydropiperettine; pipersintenamide) (6) [b]

CAS Nr. -
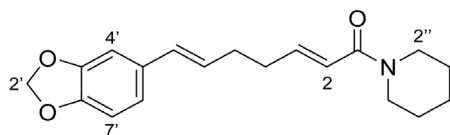
position	δ$_C$[a]	δ$_H$ (*J* in Hz)
2	121.29	6.25, d (15.0)
3	n.d.	6.81, dt (15.0, 6.9)
4	31.98	2.34, m
5	31.98	2.34, m
6	n.d.	6.01, dt (15.7, 7.0)
7	130.28	6.31, d (15.7)
2'	100.87	5.91, s
4'	105.41	6.85, d (1.5)
6'	120.31	6.73, dd (7.9, 1.5)
7'	108.10	6.70, d (7.9)
2''	n.d.	3.51, broad
3''	25.96	1.52, m
4''	24.53	1.63, m
5''	25.96	1.52, m
6''	n.d.	3.51, broad

[a] ^{13}C chemical shifts deduced from HSQC-NMR spectrum
[b] δ$_H$ and δ$_C$ reference data can be found in Chen, J.J; Huang, Y.C.; Chen, Y.C.; Huang, Y.T.; Wang, S.W.; Peng, C.Y.; Teng, C.M.; Chen, I.S. *Planta Med.* **2002**, *68*, 980-985

Table S7. NMR spectroscopic data (500 MHz, CDCl$_3$) for (**7**)

(2E,4E,6E)-7-(benzo[d][1,3]dioxol-5-yl)-1-(piperidin-1-yl)hepta-2,4,6-trien-1-one (syn.: piperettine) (7) [b]

CAS Nr. 583-34-6
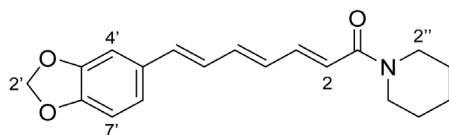
position	δ_C [a]	δ_H (*J* in Hz)
2	-	6.34, d (14.5)
3	-	7.33, dd (14.5, 11.3)
4	-	6.41, dt (11.3, 13.4)
5	-	6.62, dt (10.5, 13.4)
6	-	6.66, dd (15.0, 10.5)
7	-	6.58, d (15.0)
2'	-	5.94, s
4'	-	6.93, d (1.5)
6'	-	6.84, dd (8.0, 1.5)
7'	-	6.74, d (8.0)
2''	-	3.55, m
3''	-	1.57, m
4''	-	1.64, m
5''	-	1.57, m
6''	-	3.55, m

[a] no heteronuclear 2D-NMR spectra were recorded

[b] δ_H reference data can be found in De Araujo-Junior, J.X.; Da-Cunha, E.V.L.; Chaves, M.C.; Gray, A.I. *Phytochemistry* **1997**, *44*, 559-561

Table S8. NMR spectroscopic data (500 MHz, CDCl$_3$) for (**8**)

(E)-7-(benzo[d][1,3]dioxol-5-yl)-1-(piperidin-1-yl)hept-6-en-1-one (syn.: piperolein A) (8) [b]

CAS Nr. 30505-92-1
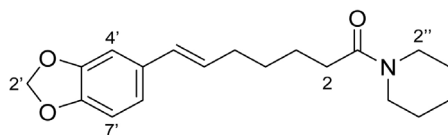
position	δ_C [a]	δ_H (J in Hz)
2	-	2.32, t (8.0)
3	-	1.67, m
4	-	1.50, m
5	-	2.20, dt (7.3, 7.1)
6	-	6.02, dt (7.3, 15.8)
7	-	6.28, d (15.8)
2'	-	5.90, s
4'	-	6.85, d (1.5)
6'	-	6.73, dd (8.1, 1.5)
7'	-	6.70, d (8.1)
2''	-	3.46, m
3''	-	1.53, m
4''	-	1.65, m
5''	-	1.53, m
6''	-	3.46, m

[a] no heteronuclear 2D-NMR spectra were recorded

[b] δ_H reference data can be found in Strunz, G.M.; Finlay, H. *Tetrahedron*, **1994**, *50*, 11113-11122

Table S9. NMR spectroscopic data (500 MHz, CDCl$_3$) for (**9**)

(2E,4E,8E)-9-(benzo[d][1,3]dioxol-5-yl)-N-isobutylnona-2,4,8-trienamide (syn.: retrofractamide A) (9) [b]

CAS Nr 94079-67-1
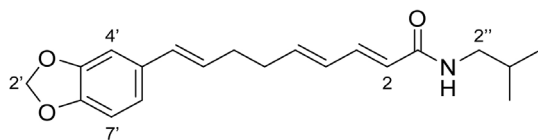
position	δ$_C$ [a]	δ$_H$ (*J* in Hz)
2	-	5.72, d (15.0)
3	-	7.16, dd (15.0, 10.5)
4	-	6.15, dd (15.0, 10.5)
5	-	6.07, m
6	-	2.30, m
7	-	2.30, m
8	-	6.01, m
9	-	6.30, d (15.4)
2'	-	5.92, s
4'	-	6.86, d (1.4)
6'	-	6.73, m
7'	-	6.73, m
2''	-	3.15, t (6.3)
3''	-	1.79, m
4''	-	0.91, d (6.5)
5''	-	0.91, d (6.5)

[a] no heteronuclear 2D-NMR spectra were recorded
[b] δ$_H$ reference data can be found in Park, I.K.; Lee, S.G.; Shin, S.C.; Park, J.D.; Ahn, Y.J. *J. Agric. Food Chem.* **2002**, *50*, 1866-1870

Table S10. NMR spectroscopic data (500 MHz, CDCl$_3$) for (**10**)

(2E,4E,8E)-9-(benzo[d][1,3]dioxol-5-yl)-1-(piperidin-1-yl)nona-2,4,8-trien-1-one (syn.: dehydropipernonaline) (10)[b]

CAS Nr 107584-38-3
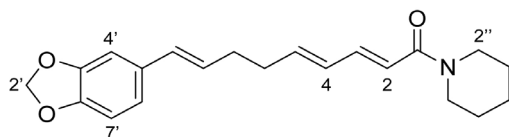
position	δ_C[a]	δ_H (J in Hz)
2	-	6.24, d (15.3)
3	-	7.21, dd (15.3, 11.7)
4	-	6.20, dd (15.0, 11.0)
5	-	6.07, m
6	-	2.30, m
7	-	2.30, m
8	-	5.99, m
9	-	6.29, d (15.2)
2'	-	5.90, s
4'	-	6.85, m
6'	-	6.73, dd (7.8, 1.5)
7'	-	6.71, d (7.8)
2''	-	3.53, m
3''	-	1.56, m
4''	-	1.63, m
5''	-	1.56, m
6''	-	3.53, m

[a] no heteronuclear 2D-NMR spectra were recorded

[b] δ_H reference data can be found in Lee, S.W.; Rho, M.C.; Parl, H.R.; Choi, J.H.; Kang, J.Y.; Lee, J.W.; Kim, K.; Lee, H.S.; Kim, Y.K. *J. Agric. Food Chem.* **2006**, *54*, 9759-9763

Table S11. NMR spectroscopic data (500 MHz, CDCl$_3$) for (**11**)

(E)-9-(benzo[d][1,3]dioxol-5-yl)-1-(piperidin-1-yl)non-8-en-1-one
(syn.: piperolein B) (11)[b]
CAS Nr 30505-89-6
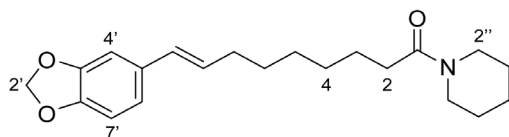
position	δ$_C$[a]	δ$_H$ (J in Hz)
2	-	2.30, t (7.4)
3	-	1.62, m
4	-	1.35, m
5	-	1.35, m
6	-	1.45, m
7	-	2.16, dt (7.5, 7.5)
8	-	6.02, dt (15.8, 7.4)
9	-	6.27, d (15.8)
2'	-	5.90, s
4'	-	6.86, d (1.5)
6'	-	6.73, dd (8.1, 1.5)
7'	-	6.71, d (8.1)
2''	-	3.45, m
3''	-	1.53, m
4''	-	1.62, m
5''	-	1.53, m
6''	-	3.45, m

[a] no heteronuclear 2D-NMR spectra were recorded
[b] δ$_H$ reference data can be found in Wei, K.; Li, W.; Koike, K.; Pei, Y.; Chen, Y.; Nikaido, T. *J. Nat. Prod.* **2004**, *67*, 1005-1009, supporting information

Table S12. NMR spectroscopic data (500 MHz, CDCl$_3$) for (**12**)

(2E,4E,10E)-11-(benzo[d][1,3]dioxol-5-yl)-N-isobutylundeca-2,4,10-trienamide (syn.: pipercide) (12)[b]
CAS Nr 54794-74-0
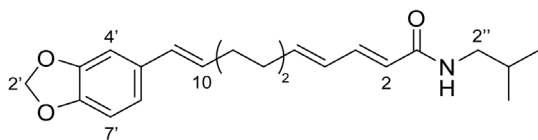
position	δ_C[a]	δ_H (*J* in Hz)
2	-	5.72, d (15.0)
3	-	7.16, dd (15.1, 10.4)
4	-	6.11, m
5	-	6.13, m
6	-	2.16, m
7	-	1.46, m
8	-	1.46, m
9	-	2.18, m
10	-	6.00, dt (15.7, 6.7)
11	-	6.27, d (15.6)
2'	-	5.90, s
4'	-	6.86, d (1.5)
6'	-	6.73, dd (7.4, 1.5)
7'	-	6.71, d (7.4)
2''	-	3.15, t (6.3)
3''	-	1.79, m
4''	-	0.91, d (6.7)
5''	-	0.91, d (6.7)

[a] no heteronuclear 2D-NMR spectra were recorded
[b] δ_H reference data can be found in Park, I.K.; Lee, S.G.; Shin, S.C.; Park, J.D.; Ahn, Y.J. *J. Agric. Food Chem.* **2002**, *50*, 1866-1870

Table S13. NMR spectroscopic data (500 MHz, CDCl$_3$) for (**13**)

(2E,4E,12E)-13-(benzo[d][1,3]dioxol-5-yl)-N-isobutyltrideca-2,4,12-trienamide (syn.: guineensine) (13)[b]

CAS Nr. 55038-30-7
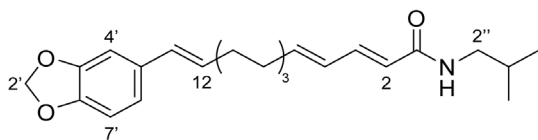
position	δ_C [a]	δ_H (J in Hz)
2	-	5.72, d (15.0)
3	-	7.16, dd (15.3, 10.8)
4	-	6.10, m
5	-	6.07, m
6	-	2.14, m
7	-	1.43, m
8	-	1.32, m
9	-	1.32, m
10	-	1.43, m
11	-	2.14, m
12	-	6.02, dt (15.7, 7.3)
13	-	6.26, d (15.7)
2'	-	5.90, s
4'	-	6.86, d (1.5)
6'	-	6.73, dd (7.4, 1.5)
7'	-	6.71, d (7.4)
2''	-	3.15, t (6.3)
3''	-	1.79, m
4''	-	0.91, d (6.7)
5''	-	0.91, d (6.7)

[a] no heteronuclear 2D-NMR spectra were recorded

[b] δ_H reference data can be found in Park, I.K.; Lee, S.G.; Shin, S.C.; Park, J.D.; Ahn, Y.J. *J. Agric. Food Chem*. **2002**, *50*, 1866-1870

3.2. HPLC-BASED ACTIVITY PROFILING OF *ANGELICA PUBESCENS* ROOTS FOR NEW POSITIVE GABA$_A$ RECEPTOR MODULATORS IN *XENOPUS* OOCYTES

Cnidilin (**4**) (300 μM)
204.5% ± 33.2% Potentiation of I$_{GABA}$

Osthol (**5**) (300 μM)
273.6% ± 39.4% Potentiation of I$_{GABA}$
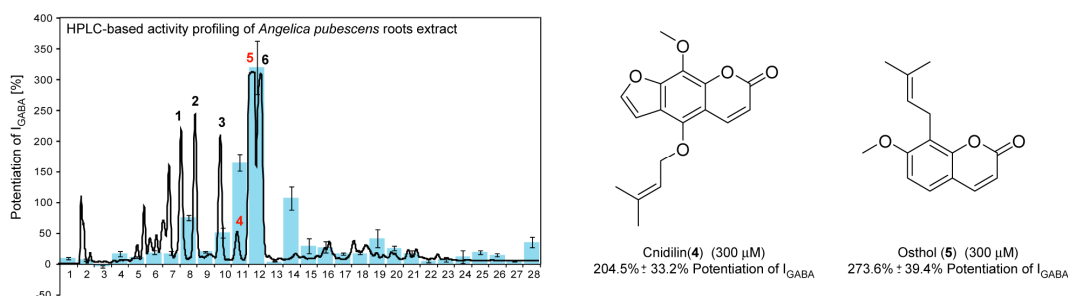
Five coumarins and bisabolangelone were identified as positive α$_1$β$_2$γ$_{2S}$ GABA$_A$ receptor modulating constituents of *Angelica pubescens* roots by HPLC based activity profiling. Structures were elucidated by high resolution mass spectrometry and microprobe NMR. Osthol and cnidilin were identified as main active compounds in the functional assay with *Xenopus* oocytes.

Eva Eickmeier did upscaled extraction of plant material, isolation of compounds, recording and interpretation of analytical data for structure elucidation (HPLC-PDA-ESI-TOF-MS, microprobe NMR, optical rotation) as part of her master's thesis under my direct supervision. HPLC microfractionation, Xenopus surgery, preparation of oocytes for electrophysiological measurements, two-microelectrode voltage clamp studies on fractions and pure compounds (except for direct activation studies), data analysis, writing of the manuscript, and preparation of figures were my contribution to this publication.

Janine Zaugg

ELSEVIER

HPLC-based activity profiling of *Angelica pubescens* roots for new positive GABA_A receptor modulators in *Xenopus* oocytes

Janine Zaugg [a], Eva Eickmeier [a], Diana C. Rueda [a], Steffen Hering [b], Matthias Hamburger [a],*

[a] *Institute of Pharmaceutical Biology, University of Basel, Klingelbergstrasse 50, 4056 Basel, Switzerland*
[b] *Institute of Pharmacology and Toxicology, University of Vienna, Althanstrasse 14, 1090 Vienna, Austria*

ARTICLE INFO

ABSTRACT

A petroleum ether extract of the traditional Chinese herbal drug *Duhuo* (roots of *Angelica pubescens* Maxim. f. *biserrata* Shan et Yuan), showed significant activity in a functional two-microelectrode voltage clamp assay with *Xenopus* oocytes which expressed recombinant γ-aminobutyric acid type A (GABA_A) receptors of the subtype $\alpha_1\beta_2\gamma_{2S}$. HPLC-based activity profiling of the active extract revealed six compounds responsible for the GABA_A receptor modulating activity. They were identified by microprobe NMR and high resolution mass spectrometry as columbianetin acetate (**1**), imperatorin (**3**), cnidilin (**4**), osthol (**5**), and columbianedin (**6**). In concentration-dependent experiments, osthol and cnidilin showed the highest potentiation of the GABA induced chloride current ($273.6\% \pm 39.4\%$ and $204.5\% \pm 33.2\%$, respectively at 300 μM). Bisabolangelone (**2**) only showed minor activity at the GABA_A receptor. The example demonstrates that HPLC-based activity profiling is a simple and efficient method to rapidly identify GABA_A receptor modulators in a bioactive plant extract.

© 2011 Elsevier B.V. All rights reserved.

1. Introduction

Angelica pubescens Maxim. f. *biserrata* Shan et Yuan belongs to the *Apiaceae* family and mainly grows in Chinese provinces such as Hubei and Sichuan [1]. Roots of the species are used in Traditional Chinese Medicine (TCM) as herbal drug *Duhuo*. Coumarins and furanocoumarins are the main constituents of this drug [2–4]. In TCM, *Duhuo* is used to treat pain, fever, rheumatism, heaviness of the low-back and knees, and contracture of the limbs [4,5]. *In vivo* studies also reported sedative and hypnotic activities of the fluid extract and decoction of *A. pubescens* in mice or rats [5,6]. In a screening of herbal drugs, a petroleum ether extract of *Duhuo* positively

modulated GABA_A receptors. For assessment of activity we used an established functional two-microelectrode voltage clamp assay with *Xenopus* oocytes which transiently express GABA_A receptors of the subunit combination $\alpha1\beta2\gamma2s$ [7].

GABA_A receptors are the most important inhibitory ion channels in the central nervous system. A total of 19 different GABA_A receptor subunits have been identified in the human genome which may form pentameric assemblies in numerous combinations resulting in functional chloride channels [8,9]. These differ in tissue localization, functional characteristics, and their pharmacological properties [10,11]. GABA_A receptors are targeted by many clinically used drugs to treat insomnia, panic disorders, epilepsy, and also to induce anesthesia. The benzodiazepines which are widely prescribed GABA_A receptor modulators are clinically used as sedative-hypnotics, anxiolytics and anticonvulsants. However, their long-term-use leads to development of tolerance and physical dependence [12]. Thus, there is a need for the development of novel GABA_A receptor modulators which are devoid of these adverse effects. Natural compounds from plant extracts may represent interesting scaffolds for

---

development of new subunit selective GABA_A receptor modulators [13]. In the present study we have identified the compounds in the *Duhuo* extract responsible for GABA_A receptor modulation.

Activity in the *Duhuo* extract was tracked with the aid of HPLC-based activity profiling. HPLC-based activity profiling is a miniaturized and rapid approach for the localization, dereplication and characterization of bioactive natural products in crude extracts [14], which has been successfully used with various cell-based and biochemical assays [15–20]. Subsequent preparative separation of the active extract yielded the sesquiterpene bisabolangelone (**2**), two linear furanocoumarins, imperatorin (**3**) and cnidilin (**4**), two angular furanocoumarins, columbianetin acetate (**1**) and columbianedin (**6**), and the isoprenylated coumarin osthol (**5**). The compounds were fully characterized by high resolution mass spectrometry, 1D and 2D microprobe NMR experiments, polarimetry, and by comparison with literature data [21–28]. Compounds **1–6** were tested at three different concentrations in the oocyte assay to investigate their individual GABA_A receptor modulatory activities.

2. Experimental

2.1. General experimental procedures

NMR spectra were recorded at room temperature with a Bruker Avance III spectrometer operating at 500.13 MHz. ^1H NMR, COSY, DEPT-edited HSQC, and HMBC spectra were measured with a 1 mm TXI probe. Spectra were analyzed using Bruker TopSpin 2.1 software. HPLC-PDA-ESI-TOF-MS spectra were obtained on a micrOTOF ESI–MS system (Bruker Daltonics) connected via T-splitter (1:10) to an HP 1100 series system (Agilent) consisting of a binary pump, autosampler, column oven and diode array detector (G1315B). The petroleum ether extract was analyzed with methanol (solvent A) and water (solvent B), both containing 0.1% formic acid with gradient elution of 50% A to 100% A in 30 min, hold for 10 min at a flow rate of 0.4 mL/min. The sample concentration was 10 mg/mL in DMSO, and the injection volume was 5 μL. Spectra were recorded in the range of *m/z* 100–700 in positive mode. Nitrogen was used as a nebulizing gas at a pressure of 2.0 bar and as a drying gas at a flow rate of 9.0 L/min (dry gas temperature 240 °C). Capillary voltage was set at 4500 V, hexapole at 230.0 Vpp. Instrument calibration was performed using a reference solution of sodium formiate 0.1% in isopropanol/water (1:1) containing 5 mM sodium hydroxide. Data acquisition and processing was performed using HyStar 3.0 software (Bruker Daltonics). Optical rotation was measured on a Perkin Elmer polarimeter (model 341) equipped with a 10 cm microcell. The optical rotation for the Na-D-line (589) was extrapolated from the lines of a mercury lamp using the Drude equation [29]. Semi-preparative HPLC separation for activity profiling was performed with an HP 1100 series system (Agilent) consisting of a quaternary pump, autosampler, column oven, and diode array detector (G1315B). SunFire C18 (3.5 μm, 3.0×150 mm) and SunFire Prep C18 (5 μm, 10×150 mm) columns (Waters) were used for HPLC-PDA-ESI-TOF-MS and semi-preparative HPLC, respectively. Medium pressure liquid chromatography (MPLC) was done on a pre-packed normal phase cartridge (40–63 μm, 40×150 mm) using a Sepacore system (Buchi) consisting of a control unit C-620, two pump

modules C-605, and a fraction collector C-660. The MPLC unit was controlled with the SepacoreControl software (version 1.0.3000.1). Preparative HPLC separation was performed with a SunFire Prep C18 OBD (5 μm, 30×150 mm) column using a Shimadzu LC-8A preparative separation chromatograph equipped with a SPD-M10A VP diode array detector. HPLC-grade methanol (Scharlau Chemie S.A.) and water were used for HPLC separations. Deuterated chloroform was purchased from Armar Chemicals. Solvents used for extraction, open column chromatography, and MPLC were of technical grade and purified by distillation. Silica gel (63–200 μm, Merck) was used for open column chromatography.

2.2. Plant material

Duhuo (dried roots of *A. pubescens* Maxim. f. *biserrata* Shan et Yuan) was purchased from sinoMed GmbH & Co. (Bad Kötzting, Germany) for screening and HPLC-based activity profiling (batch K26.04.2004), and from Complemedis AG (Schönenwerd, Switzerland) for compound isolation (batch 051459). Voucher specimens (00 378 and 00 596, respectively) are deposited at the Institute of Pharmaceutical Biology, University of Basel.

2.3. HPLC microfractionation

An aliquot (ca. 20 g) of ground roots was macerated at room temperature with petroleum ether (3×0.5 L, 1 h each). Microfractionation for GABA_A receptor activity profiling was performed as previously described [18,30,31], with minor modifications: separation was carried out on a semi-preparative HPLC column with methanol (solvent A) and water (solvent B) using the following gradient: 50% A to 100% A in 30 min, hold for 10 min. The flow rate was 4 mL/min, and 100 μL of the extract (100 mg/mL in DMSO) were injected. A total of 28 time-based microfractions of each 90 s were collected. Microfractions were evaporated in parallel with a Genevac EZ-2 plus vacuum centrifuge (Avantec). The dry films were redissolved in 1 mL of methanol; aliquots of 0.5 mL were dispensed in two vials, dried under N_2 gas, and submitted to bioassay.

2.4. Extraction and isolation

The plant material was ground with a ZM1 ultracentrifugal mill (Retsch). For compound isolation, 884 g of ground roots were extracted by maceration at room temperature with petroleum ether (4×2.5 L, 1 h each). The solvent was evaporated at reduced pressure to yield 21.8 g of petroleum ether extract. A part of the extract (19.3 g) was separated by open column chromatography (9×80 cm, 1.2 kg silica gel) using a step gradient of hexane–chloroform–methanol (20:80:0, 3 L; 15:85:0, 2 L; 10:90:0, 2 L; 5:95:0, 2 L; 0:100:0, 2 L; 0:99:1, 4 L; 0:90:10, 1 L; 50:50, 1 L). The flow rate was approximately 15 mL/min. The effluent was combined to 15 fractions (1–15) according to TLC patterns (detection at 254 nm and at daylight after staining with anisaldehyde-sulphuric acid reagent). Recrystallization of fraction 10 (3.80 g) afforded **5** (2.32 g). A portion of the mother liquor of fraction 10 (0.9 g) was separated by MPLC using a toluene–ethyl acetate gradient (100:0 to 70:30 in 2 h) with a flow rate of 30 mL/min. A total of 16 fractions (10A–10P) were collected based on TLC analysis. Fractions 10E (57.1 mg), 10 L

(48.2 mg), 10 N (33.6 mg), and a portion of fraction 10 G (50 mg) were each dissolved in 800 μL DMSO–methanol (1:1) and separated by preparative HPLC using a gradient of methanol–water (50:50 to 100:0 in 30 min, flow rate 20 mL/ min). Columbianetin acetate (**1**) (11.1 mg) was obtained from fraction 10 L, bisabolangelone (**2**) (2.6 mg) from fraction 10 N, imperatorin (**3**) (0.61 mg) and cnidilin (**4**) (0.48 mg) from fraction 10E, and columbianedin (**6**) (22.8 mg) from fraction 10E (18.3 mg) and 10 G (4.5 mg). Compounds **1–6** were identified by comparison of 1D and 2D NMR, HPLC-PDA-ESI-TOF-MS and polarimetry data with published values [21–28]. For complete data see the supporting information in the Appendix.

2.5. Expression of GABA$_A$ receptors

Stages V–VI oocytes from *Xenopus laevis* were prepared and cRNA was injected as previously described by Khom et al. [32]. Female *X. laevis* (NASCO) were anesthetized by exposing them for 15 min to a 0.2% MS-222 (3-aminobenzoic acid ethyl ester methanesulfonate, Sigma) solution before surgically removing parts of the ovaries. Follicle membranes from isolated oocytes were enzymatically digested with 2 mg/mL collagenase from *Clostridium histolyticum* (Type 1A, Sigma). Synthesis of capped run-off poly(A+) cRNA transcripts was obtained from linearized cDNA templates (pCMV vector). One

day after enzymatic isolation, the oocytes were injected with 50 nL of DEPC-treated water (Sigma) containing different cRNAs at a concentration of approximately 300–3000 pg/nL per subunit. The amount of injected cRNA mixture was determined by means of a NanoDrop ND-1000 (Kisker Biotech). Rat cRNAs were mixed in a 1:1:10 ratio to ensure expression of the gamma subunit in $\alpha_1\beta_2\gamma_{2S}$ receptors. Oocytes were then stored at 18 °C in an aqueous solution of 90 mM NaCl, 1 mM KCl, 1 mM MgCl$_2$, 1 mM CaCl$_2$ and 5 mM HEPES (pH 7.4), containing 1% of Penicillin–Streptomycin solution (Sigma) [33]. Voltage clamp measurements were performed between days 1 and 5 after cRNA injection.

2.6. Two-microelectrode voltage clamp studies

Electrophysiological experiments were performed by the two-microelectrode voltage clamp method making use of a TURBO TEC 03X amplifier (npi electronic, Tamm, Germany) at a holding potential of −70 mV and pCLAMP 10 data acquisition software (Molecular Devices, USA). Currents were low-pass-filtered at 1 kHz and sampled at 3 kHz. The bath solution contained 90 mM NaCl, 1 mM KCl, 1 mM MgCl$_2$, 1 mM CaCl$_2$ and 5 mM HEPES (pH 7.4). Electrode filling solution contained 2 M KCl.
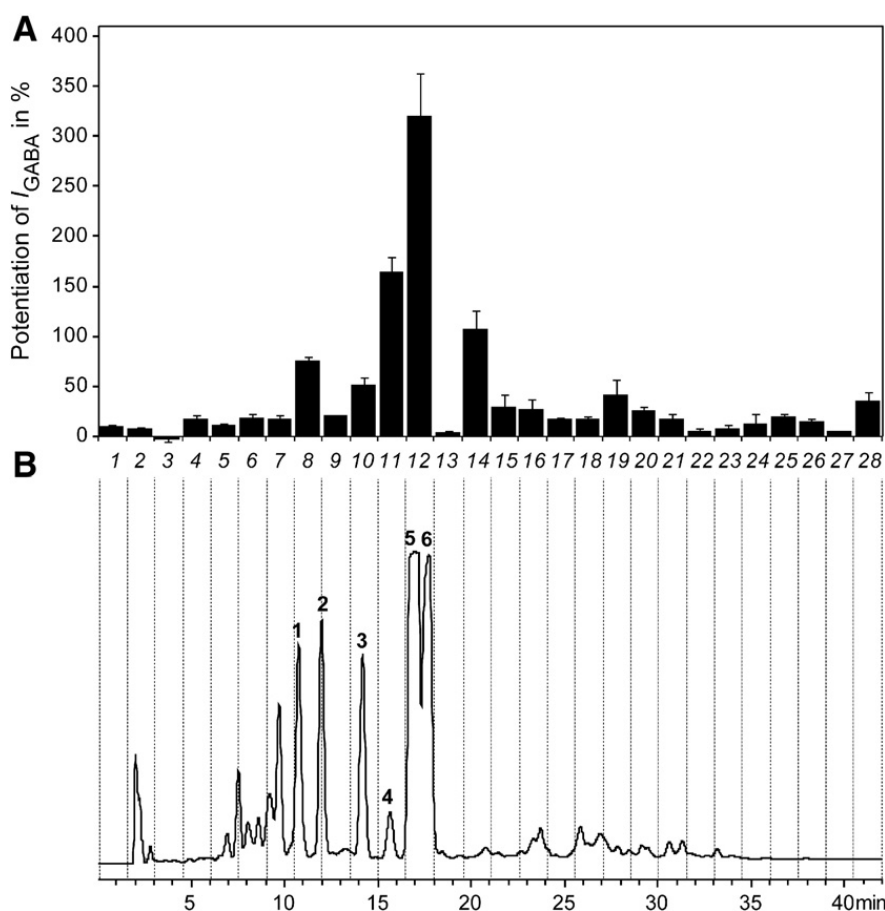
Fig. 1. HPLC-based activity profiling of *A. pubescens* petroleum ether extract for GABA$_A$ receptor modulating properties. B: HPLC chromatogram (240 nm) of a semipreparative separation of 10 mg of extract. Peak numbering corresponds to compounds **1–6**. The 28 collected time-based microfractions, 90 s each, are indicated with dashed lines. A: The potentiation of the GABA-induced chloride current in *Xenopus* oocytes (I_{GABA}) by each fraction. A current elicited by a GABA EC$_{5–10}$ was used as control current.

2.7. Fast solution exchange during I_{GABA} recordings

Test solutions (100 μL) of extracts, fractions and pure compounds were applied to the oocytes at a speed of 300 μL/s by means of the ScreeningTool automated fast perfusion system [7]. In order to determine GABA EC$_{5-10}$ (typically between 3 and 10 μM for receptors of the subunit combination $\alpha_1\beta_2\gamma_{2S}$), a concentration–response experiment with GABA concentrations ranging from 0.1 μM to 1 mM was performed. Stock solution of *A. pubescens* extract (10 mg/mL in DMSO) was diluted to a concentration of 100 μg/mL with bath solution containing GABA EC$_{5-10}$ according to a validated protocol [18]. As previously described, microfractions collected from the semi-preparative HPLC separations were dissolved in 30 μL DMSO and subsequently mixed with 2.97 mL of bath solution containing GABA EC$_{5-10}$ [18]. Stock solutions of compounds 1–6 (100 mM in DMSO) were diluted to a concentration of 30, 100, and 300 μM with bath solution for measuring direct activation, or with bath solution containing GABA EC$_{5-10}$ for measuring modulation of the GABA$_A$ receptors. The final DMSO concentration in all samples including the GABA control samples was adjusted 1% to avoid solvent effects at the GABA$_A$ receptor. Enhancement of the GABA induced chloride current (I_{GABA}) was defined as $I_{(GABA + Comp)}/I_{GABA} - 1$, where $I_{(GABA + Comp)}$ is the current response in the presence of a given compound, and I_{GABA} is the control GABA-induced chloride current. Data were analyzed using the ORIGIN 7.0 SR0 software (OriginLab Corporation) and are given as mean ± S.E. of at least 2 oocytes and ≥2 oocyte batches.

3. Results and discussion

Pharmacological studies were performed on *Xenopus* oocytes expressing the most abundant GABA$_A$ receptor subtype of the human brain composed of two α_1, two β_2, and one γ_2 subunit [8]. In our two-microelectrode assay [7] the petroleum ether extract of *A. pubescens* enhanced the GABA-induced chloride ion current (I_{GABA}) through $\alpha_1\beta_2\gamma_{2S}$ receptors by 197.0% ± 56.8%. The active extract was submitted to HPLC-based activity profiling using a validated protocol [18]. The chromatogram of a semipreparative separation of 10 mg extract and the corresponding activity profile of the time-based fractionation (28 microfractions of 90 s each) are shown in Fig. 1. Moderate GABA$_A$ receptor modulating activity was found in microfractions 8, 10, and 14 (75.3% ± 4.2%, 50.7% ± 8.1%, and 107.1% ± 19.1%, respectively), while high activity could be detected in microfractions 11 and 12 (164.8% ± 13.9% and 320.3% ± 43.0%, respectively). The major peak (eluting in microfraction 12) was then collected for structure elucidation with semipreparative HPLC using the same separation conditions as for microfractionation. The molecular formula of the compound was extracted from an HPLC-PDA-ESI-TOF-MS analysis of the extract, and the ^{1}H NMR of the collected peak yielded a spectrum reminiscent of 7,8-substituted coumarins, showing two pairs of doublets at 6.19 and 7.57 ppm, and 7.25 and 6.81 ppm with coupling constants of 9.5 Hz and 8.5 Hz, respectively. The compound could be identified as osthol (5) by comparing the data to published values [26]. For determination of concentration-dependent GABA$_A$ receptor modulation, the compounds of the active time-windows were purified at preparative scale and

identified as columbianetin acetate (1), bisabolangelone (2), imperatorin (3), cnidilin (4), and columbianedin (6) (Fig. 2) by comparing ^{1}H NMR shifts and ^{13}C shifts deduced from heteronuclear 2D NMR spectra, molecular formula derived from high resolution mass spectra, and optical rotation (compounds 1, 2, and 6) with published values [21–28]. Spectroscopic data of 1–6 are available as supporting information in the Appendix. All compounds were tested at concentrations of 10, 100, and 300 μM in the oocyte assay (Fig. 3). At 300 and 100 μM concentrations, osthol (5) potentiated I_{GABA} by 273.6% ± 39.4% and 108.3% ± 29.9%, respectively. Compound 6, in contrast, was only marginally active (61.2% ± 20.2% at 300 μM and 42.2% ± 4.9% at 100 μM). Cnidilin (4), which had been previously reported from a different *Angelica* species [34], showed comparable activity as 5 (204.5% ± 33.2% at 300 μM and 71.6% ± 8.7% at 100 μM). Compound 3 was responsible for the moderate activity of microfraction 10, and potentiated I_{GABA} at 100 μM by 50.5% ± 16.3% and at 300 μM by 109.8% ± 37.7%. Compounds 1 and 2 were weakly effective as pure compounds (potentiation of I_{GABA} of 33.0% ± 9.3% and 1.1% ± 4.7%, respectively at 100 μM, and of 38.0% ± 21.3% and 25.8% ± 12.7%, respectively at 300 μM). Compounds 1–6 modulated GABA$_A$ receptors of the subunit combination $\alpha_1\beta_2\gamma_{2S}$ with low potency, since no significant potentiation of I_{GABA} could be detected at 10 μM concentration (1: 3.4% ± 1.8%, 2: 3.4% ± 8.3%, 3: 9.8% ± 11.4%, 4: 5.7% ± 11.1%, 5: 19.4% ± 7.4%, 6: 6.3% ± 5.6%). None of the compounds showed significant direct activation on GABA$_A$ receptors when applied at a test concentration of 300 μM (Fig. 3C).

There have been previous reports on coumarins as GABA$_A$ receptor ligands. Li et al. isolated a new dihydroisocoumarin
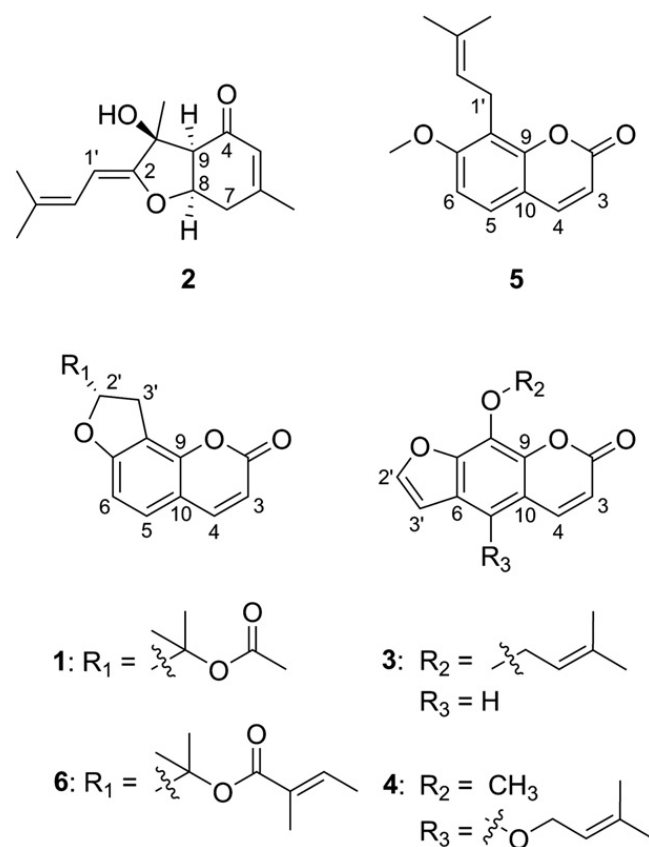
Fig. 2. The chemical structures of compounds 1–6.
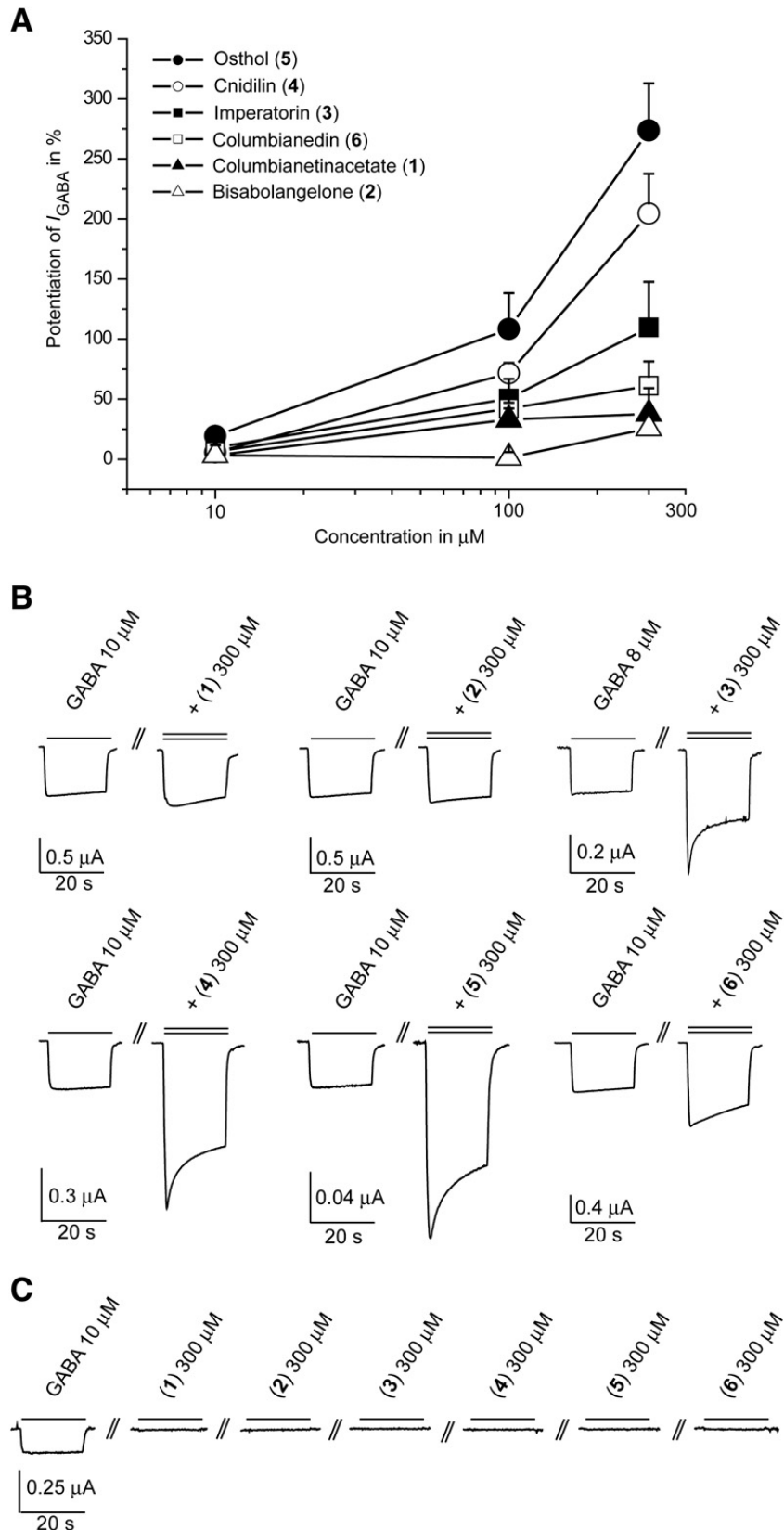
Fig. 3. A: Concentration-dependent potentiation of the GABA-induced chloride current (I_{GABA}) by compounds **1–6** on GABA$_A$ receptors composed of α_1, β_2, and γ_{2S} subunits using a GABA EC$_{5–10}$. Potencies (EC$_{50}$) of compounds **3**, **4**, and **5** can be estimated to lie beyond 100 μM. B: Typical traces for modulation of chloride currents through $\alpha_1\beta_2\gamma_{2S}$ GABA$_A$ receptors by compounds **1–6** at a concentration of 300 μM. C: Representative currents illustrate the absence of direct activation of GABA$_A$ receptors ($\alpha_1\beta_2\gamma_{2S}$) by compounds **1–6**.

from *Haloxylon scoparium*, which acts as a positive modulator at GABA$_A$ receptors of the subtype $\alpha_1\beta_2\gamma_{2S}$ [31]. Dekermendjian et al. tested imperatorin (**3**) and phellopterin, another linear furanocoumarin, in a radioreceptor binding assay and found that phellopterin and imperatorin inhibited [^{3}H]diazepam (2 nM) binding to rat cortical brain GABA$_A$ receptors with IC$_{50}$ values of 12.3 µM and 0.4 µM, respectively [35]. From the functional assay data shown in Fig. 3, it can be estimated that the EC$_{50}$ values of **3, 4** and **5** have to be >100 µM. However, the binding affinity (determined as IC$_{50}$) calculated from a binding assay cannot be directly related to the potency (EC$_{50}$) in a functional assay due to fundamental differences of the test systems (for a general review on this topic, see [36]).

To our knowledge, angular furanocoumarins such as columbianetin acetate (**1**) and columbianedin (**6**), which marginally modulated GABA$_A$ receptors ($\alpha_1\beta_2\gamma_{2S}$), have not been reported previously for any GABA$_A$ receptor activity. Given the structural diversity of a relatively small number of coumarins isolated in this profiling, structural features critical for activity could not be identified. A study on structure–activity-relationship of (furano)coumarins at $\alpha_1\beta_2\gamma_{2S}$ GABA$_A$ receptors will be published elsewhere [37].

With estimated EC$_{50}$ values of >100 µM, the potencies of **3**, **4**, and **5** were >500 fold lower than the potency of benzodiazepines (e.g. such as clotiazepam, EC$_{50}$: 0.184 µM ± 0.088 µM) [32], indicating that the identified active coumarins **3–5** represent low affinity GABA$_A$ receptor ligands *in vitro*. There is limited data available on the bioavailability of these coumarins and their CNS penetration. In a Caco-2 cell model, Galkin et al. demonstrated that imperatorin rapidly permeates across the membrane without being limited by efflux [38]. In a Caco-2 model modified with a phase I reaction system on the basolateral side, osthol passively permeated the membrane but was immediately metabolized thereafter [39]. This finding was consistent with a rather short half-life (t$_{1/2}$ = 41.13 ± 5.73 min) of osthol found in rats after i.v. application [40]. To our knowledge, a quantitative study on blood–brain barrier penetration of naturally occurring coumarins and their metabolites is still lacking. Interestingly, an earlier *in vivo* study using the maximal electroshock seizure test and the chimney test with mice revealed some degree of anticonvulsant[1] but also neurotoxic activity of imperatorin (**3**) and osthol (**5**) [41,42]. As possible mechanism of the anticonvulsive action the authors discussed an inactivation of the GABA-transaminase which would lead to a higher GABA concentration in the synaptic cleft and, therefore, to an elevated inhibitory neurotransmitter level in the brain [43]. Considering our results, an enhancement of the GABA-induced chloride current by **3** and **5** (or their metabolites), could have been partly responsible for their anticonvulsant activity *in vivo* [41,42]. In summary, the investigated coumarins act on several CNS targets *in vitro* [43–45], but have limited potential for further development considering the reported neurotoxicity of osthol and imperatorin [41], and the known phototoxicity of linear furanocoumarins [46].

The investigation of compounds **1**, and **3–6** provides additional data on GABA$_A$ receptor activity of the coumarin

scaffold [31]. The example of *A. pubescens* corroborates the usefulness of an HPLC-based activity profiling approach in the search for bioactive molecules of natural origin [18,30,31].

Appendix A. Supplementary data

Supplementary data to this article can be found online at doi:10.1016/j.fitote.2010.12.001.

References

[1] Zhongzhen Z. An illustrated Chinese Materia Medica in Hong Kong. First ed. Hong Kong Baptist University, Hong Kong: School of Chinese Medicine; 2004.
[2] Pan JX, Lam YK, Arison B, Smith J, Han GQ. Isolation and identification of isoangelol, anpubesol and other coumarins from *Angelica pubescens* Maxim. Yao Xue Xue Bao (Acta Pharm. Sin.) 1987;22:380–4.
[3] Li RZ, He YQ, Chiao M, Xu Y, Zhang QB, Meng JR, et al. Studies of the active constituents of the Chinese drug duhuo *Angelica pubescentis*. Yao Xue Xue Bao (Acta Pharm. Sin.) 1989;24:546–51.
[4] Tang W, Eisenbrand G. Chinese drugs of plant origin. Berlin Heidelberg New York: Springer Verlag; 1992.
[5] Chang H-M, But PP-H. Pharmacology and applications of Chinese Materia Medica, Vol. 2. Singapore: World Scientific Publishing Co. Pte. Ltd; 1987.
[6] Huang KC. The pharmacology of Chinese herbs. Second ed. Boca Raton, Florida: CRC Press; 1999.
[7] Baburin I, Beyl S, Hering S. Automated fast perfusion of *Xenopus* oocytes for drug screening. Pfluegers Arch Eur J Phys 2006;453:117–23.
[8] Simon J, Wakimoto H, Fujita N, Lalande M, Barnard EA. Analysis of the set of GABA(A) receptor genes in the human genome. J Biol Chem 2004;279:41,422–35.
[9] Olsen RW, Sieghart W. International Union of Pharmacology. LXX. Subtypes of gamma-aminobutyric acid(A) receptors: classification on the basis of subunit composition, pharmacology, and function. Update. Pharmacol Rev 2008;60:243–60.
[10] Barrera NP, Edwardson JM. The subunit arrangement and assembly of ionotropic receptors. Trends Neurosci 2008;31:569–76.
[11] Olsen RW, Sieghart W. GABA(A) receptors: subtypes provide diversity of function and pharmacology. Neuropharmacology 2009;56:141–8.
[12] D'Hulst C, Atack JR, Kooy RF. The complexity of the GABA(A) receptor shapes unique pharmacological profiles. Drug Discovery Today 2009;14:866–75.
[13] Khom S, Strommer B, Ramharter J, Schwarz T, Schwarzer C, Erker T, et al. Valerenic acid derivatives as novel subunit-selective GABA(A) receptor ligands — *in vitro* and *in vivo* characterization. Br J Pharmacol 2010;161:65–78.
[14] Potterat O, Hamburger M. Natural products in drug discovery — concepts and approaches for tracking bioactivity. Curr Org Chem 2006;10:899–920.
[15] Potterat O, Wagner K, Gemmecker G, Mack J, Puder C, Vettermann R, et al. BI-32169, a bicyclic 19-peptide with strong glucagon receptor antagonist activity from *Streptomyces sp.* J Nat Prod 2004;67:1528–31.
[16] Danz H, Stoyanova S, Wippich P, Brattstroem A, Hamburger M. Identification and isolation of the cyclooxygenase-2 inhibitory principle in *Isatis tinctoria*. Planta Med 2001;67:411–6.
[17] Dittmann K, Gerhaeuser C, Klimo K, Hamburger M. HPLC-based activity profiling of *Salvia miltiorrhiza* for MAO A and iNOS inhibitory activities. Planta Med 2004;70:909–13.
[18] Kim HJ, Baburin I, Khom S, Hering S, Hamburger M. HPLC-based activity profiling approach for the discovery of GABA(A) receptor ligands using an automated two microelectrode voltage clamp assay on *Xenopus* oocytes. Planta Med 2008;74:521–6.

---

[1] Male Swiss albino mice, i.p. administration, 30 min pretreatment time. ED$_{50}$ per kg body weight of imperatorin, osthol, valproate [41], and clonazepam [42]: 167 mg, 253 mg, 217 mg, 29.14 mg.

[19] Adams M, Zimmermann S, Kaiser M, Brun R, Hamburger M. A protocol for HPLC-based activity profiling for natural products with activities against tropical parasites. Nat Prod Commun 2009;4:1377–81.

[20] Adams M, Christen M, Plitzko I, Zimmermann S, Brun R, Kaiser M, et al. Antiplasmodial lanostanes from the *Ganoderma lucidum* mushroom. J Nat Prod 2010;73:897–900.

[21] Hata K, Kozawa M, Baba K, Yen K-Y. Coumarins from the roots of *Angelica laxiflora*. Chem Pharm Bull 1971;19:640–2.

[22] Liu R, Feng L, Sun A, Kong L. Preparative isolation and purification of coumarins from *Cnidium monnieri* (L.) Cusson by high-speed counter-current chromatography. J Chromatogr 2004;1055:71–6.

[23] Hata K, Kozawa M, Baba K, Chi H-J, Konoshima M. Coumarins and a sesquiterpene from the crude drug Korean qianghuo the roots of *Angelica spp.* Chem Pharm Bull 1971;19:1963–7.

[24] Bergendorff O, Dekermendjian K, Nielsen M, Shan R, Witt R, Ai J, et al. Furanocoumarins with affinity to brain benzodiazepine receptors in vitro. Phytochemistry 1997;44:1121–4.

[25] Franke K, Porzel A, Masaoud M, Adam G, Schmidt J. Furanocoumarins from *Dorstenia gigas*. Phytochemistry 2001;56:611–21.

[26] Basile A, Sorbo S, Spadaro V, Bruno M, Maggio A, Faraone N, et al. Antimicrobial and antioxidant activities of coumarins from the roots of *Ferulago campestris* (*Apiaceae*). Molecules 2009;14:939–52.

[27] Khetwal KS, Pathak RP. Columbianadin: a novel coumarin from *Heracleum brunonis*. Planta Med 1987;53:581.

[28] Vuorela H, Erdelmeier CA, Nyiredy S, Dallenbach-Tolke K, Anklin C, Hiltunen R, et al. Isobyakangelicin angelate; a novel furanocoumarin from *Peucedanum palustre*. Planta Med 1988;54:538–42.

[29] Fluegge J. Grundlagen der Polarimetrie. Berlin: De Gruyter-Verlag; 1970.

[30] Zaugg J, Baburin I, Strommer B, Kim HJ, Hering S, Hamburger M. HPLC-based activity profiling: discovery of piperine as a positive GABA(A) receptor modulator targeting a benzodiazepine-independent binding site. J Nat Prod 2010;73:185–91.

[31] Li Y, Plitzko I, Zaugg J, Hering S, Hamburger M. HPLC-based activity profiling for GABA(A) receptor modulators: a new dihydroisocoumarin from *Haloxylon scoparium*. J Nat Prod 2010;73:768–70.

[32] Khom S, Baburin I, Timin EN, Hohaus A, Sieghart W, Hering S. Pharmacological properties of GABA(A) receptors containing gamma1 subunits. Mol Pharmacol 2006;69:640–9.

[33] Methfessel C, Witzemann V, Takahashi T, Mishina M, Numa S, Sakmann B. Patch clamp measurements on *Xenopus laevis* oocytes: currents through endogenous channels and implanted acetylcholine receptor and sodium channels. Pfluegers Arch Eur J Phys 1986;407:577–88.

[34] Baek NI, Ahn EM, Kim HY, Park YD. Furanocoumarins from the root of *Angelica dahurica*. Arch Pharm Res 2000;23:467–70.

[35] Dekermendjian K, Ai J, Nielsen M, Sterner O, Shan R, Witt MR. Characterisation of the furanocoumarin phellopterin as a rat brain benzodiazepine receptor partial agonist in vitro. Neurosci Lett 1996;219:151–4.

[36] Kenakin T. Quantifying biological activity in chemical terms: a pharmacology primer to describe drug effect. ACS Chem Biol 2009;4:249–60.

[37] J. Singhuber, I. Baburin, M. Zehl, S. Hering, B. Kopp, in preparation.

[38] Galkin A, Fallarero A, Vuorela PM. Coumarins permeability in Caco-2 cell model. J Pharm Pharmacol 2009;61:177–84.

[39] Yuan Z, Xu H, Wang K, Zhao Z, Hu M. Determination of osthol and its metabolites in a phase I reaction system and the Caco-2 cell model by HPLC-UV and LC-MS/MS. J Pharm Biomed Anal 2009;49:1226–32.

[40] Tsai TH, Tsai TR, Chen CC, Chen CF. Pharmacokinetics of osthole in rat plasma using high-performance liquid chromatography. J Pharm Biomed Anal 1996;14:749–53.

[41] Luszczki JJ, Wojda E, Andres-Mach M, Cisowski W, Glensk M, Glowniak K, et al. Anticonvulsant and acute neurotoxic effects of imperatorin, osthole and valproate in the maximal electroshock seizure and chimney tests in mice: a comparative study. Epilepsy Res 2009;85:293–9.

[42] Luszczki JJ, Czuczwar SJ. Three-dimensional isobolographic analysis of interactions between lamotrigine and clonazepam in maximal electroshock-induced seizures in mice. Naunyn-Schmiedeberg's Arch Pharmacol 2004;370:369–80.

[43] Choi SY, Ahn EM, Song MC, Kim DW, Kang JH, Kwon OS, et al. In vitro GABA-transaminase inhibitory compounds from the root of *Angelica dahurica*. Phytother Res 2005;19:839–45.

[44] Wang SJ, Lin TY, Lu CW, Huang WJ. Osthole and imperatorin, the active constituents of *Cnidium monnieri* (L.) Cusson, facilitate glutamate release from rat hippocampal nerve terminals. Neurochem Int 2008;53:416–23.

[45] Lin TY, Lu CW, Huang WJ, Wang SJ. Osthole or imperatorin-mediated facilitation of glutamate release is associated with a synaptic vesicle mobilization in rat hippocampal glutamatergic nerve endings. Synapse 2010;64:390–6.

[46] Kitamura N, Kohtani S, Nakagaki R. Molecular aspects of furocoumarin reactions: photophysics, photochemistry, photobiology, and structural analysis. J Photochem Rev 2005;6:168–85.

SUPPORTING INFORMATION

HPLC-based activity profiling of *Angelica pubescens* roots for new positive GABA_A receptor modulators in *Xenopus* oocytes

Janine Zaugg[a], Eva Eickmeier[a], Diana Rueda[a], Steffen Hering[b], Matthias Hamburger[a,*]

[a] *Institute of Pharmaceutical Biology, University of Basel, Klingelbergstrasse 50, 4056 Basel, Switzerland*

[b] *Institute of Pharmacology and Toxicology, University of Vienna, Althanstrasse 14, 1090 Vienna, Austria*

*Corresponding author. Tel.: +41 612671425; fax: +41 612671474.

E-mail addresses: steffen.hering@univie.ac.at (S. Hering) matthias.hamburger@unibas.ch (M. Hamburger)

Table S1. NMR spectroscopic data (500 MHz, CDCl$_3$) for (**1**)

(+)-Columbianetin acetate
CAS Nr.: 23180-65-6
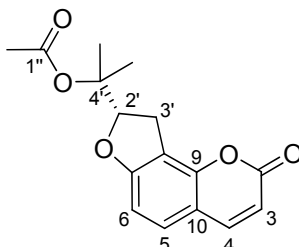
m/z (ESITOFMS)	289.1065 [M+H$^+$]	(Calc.: 289.1071)

[α]$_D$ (20.2°C)   +213° (*c* = 0.72, CHCl$_3$)[a]

position	δ$_C$[b]	δ$_H$ (I, m, *J* in Hz)[b]
2	160.8	-
3	112.2	6.19 (CH, d, *9.4*)
4	143.8	7.60 (CH, d, *9.4*)
5	128.7	7.25 (CH, d, *8.5*)
6	106.5	6.72 (CH, d, *8.5*)
7	163.8	-
8	113.0	-
9	151.2	-
10	113.0	-
2'	88.7	5.12 (CH, dd, *9.8, 7.9*)
3'	27.6	3.26 (CH$_2$, dd, *16.5, 7.9*) 3.35 (CH$_2$, dd, *16.5, 9.8*)
4'	81.9	-
4'-Me[a]	21.9	1.55 (CH$_3$, s)
4'-Me[b]	20.8	1.49 (CH$_3$, s)
1"	170.3	-
2"	22.1	1.96 (CH$_3$, s)

[a]Reference value can be found in K. Hata, Chem. Pharm. Bull. 1971, 19, 640-642
[b] ^{13}C-NMR shifts obtained from HSQC- and HMBC-NMR experiments. Spin systems evaluated by HSQC- NMR experiment
[c]Reference data can be found in H. Vuorela et al., Planta Med. 1988, 54, 538-542 (except for 1" and 2")
[d]Reference data can be found in K.S. Khetwal et al., Planta Med. 1987, 53, 581 (except for 1" and 2")

Table S2. NMR spectroscopic data (500 MHz, CDCl$_3$) for (**2**)

(+)-Bisabolangelone
CAS Nr.: 30557-81-4
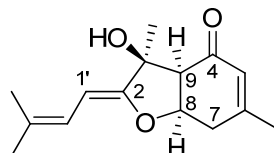
m/z (ESITOFMS)   271.1298 [M+H$^+$]   (Calc.: 271.1305)

$[\alpha]_D$ (20.5°C)   +128° (*c* = 0.016, CHCl$_3$)^a

position	δ_C ^{b,c}	δ_H (I, m, *J* in Hz)^c
2	160.2	-
3	78.6	-
4	196.8	-
5	123.3	5.98 (CH, m)
6	158.3	-
7	34.9	2.66 (CH, dd, *18.6, 6.0*)
		2.75 (CH, dd, *18.6, 6.0*)
8	75.9	4.84 (CH, ddd, *6.5, 6.0, 6.0*)
9	53.7	2.62 (CH, d, *6.5*)
1'	94.6	5.34 (CH, d, *11.4*)
2'	117.3	5.98 (CH, m, *11.4*)
3'	132.6	-
4'	26.1	1.76 (CH$_3$, s)
5'	18.2	1.69 (CH$_3$, s)
3-Me	27.4	1.59 (CH$_3$, s)
6-Me	24.6	1.98 (CH$_3$, s)

^{a}Reference data can be found in K. Hata, Chem. Pharm. Bull. 1971, 19, 1963-1967.
^{b} ^{13}C-NMR shifts obtained from HSQC- and HMBC-NMR experiments. Spin systems evaluated by HSQC- NMR experiment
^{c}Reference data can be found in J.-H. Liu, Phytochemistry 1998, 49, 211-213.

Table S3. NMR spectroscopic data (500 MHz, CDCl$_3$) for (**3**)

Imperatorin
CAS Nr.: 482-44-0
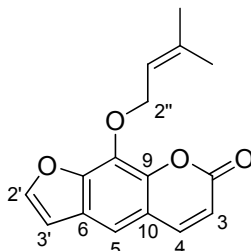
| *m/z* (ESITOFMS) | 293.0771 [M+Na$^+$] | (Calc.: 293.0784) |

position	$\delta_C{}^{a,\,b}$	δ_H (I, m, *J* in Hz)^b
2	160.5	-
3	114.3	6.34 (CH, d, *9.5*)
4	144.8	7.73 (CH, d, *9.5*)
5	113.0	7.33 (CH, s)
6	125.8	-
7	148.6	-
8	131.4	-
9	143.9	-
10	116.3	-
2'	146.4	7.66 (CH, d, *2.5*)
3'	106.7	6.78 (CH, d, *2.5*)
2"	70.3	4.98 (CH$_2$, d, *7.4*)
3"	119.7	5.58 (CH, t, *7.4*)
4"	139.9	-
5"	25.7	1.71 (CH$_3$, s)
6"	18.2	1.68 (CH$_3$, s)

^{a} ^{13}C-NMR shifts obtained from HSQC- and HMBC-NMR experiments. Spin systems evaluated by HSQC- NMR experiment
^{b}Reference data can be found in O. Bergendorff et al. Phytochemistry, 1997, 44, 1121-1124

Table S4. NMR spectroscopic data (500 MHz, CDCl$_3$) for (**4**)

Cnidilin
CAS Nr.: 14348-22-2
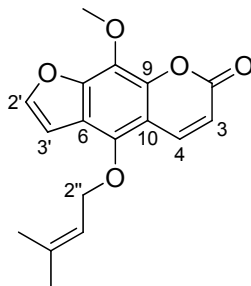
m/z (ESITOFMS)   301.1070 [M+H$^+$]   (Calc.: 301.1071)

position	δ$_C$$^{a, b}$	δ$_H$ (I, m, *J* in Hz)
2	161.0	-
3	112.4	6.26 (CH, d, *9.7*)
4	139.7	8.09 (CH, d, *9.7*)
5	143.2	-
6	116.9	-
7	150.3	-
8	127.8	-
9	143.4	-
10	108.9	-
2'	145.5	7.60 (CH, d, *2.5*)
3'	104.9	6.92 (CH, d, *2.5*)
2"	70.8	4.77 (CH$_2$, d, *7.2*)
3"	119.2	5.50 (CH, tm, *7.2*)
4"	139.9	-
5"	26.0	1.76 (CH$_3$, s)
6"	18.4	1.63 (CH$_3$, s)
5-OMe	61.5	4.16 (CH$_3$, s)

^{a} ^{13}C-NMR shifts obtained from HSQC- and HMBC-NMR experiments. Spin systems evaluated by HSQC- NMR experiment
^{b}Reference data can be found in K. Franke et al. Phytochemistry 2001, 56, 611-621

Table S5. NMR spectroscopic data (500 MHz, CDCl$_3$) for (**5**)

Osthole
CAS Nr. 484-12-8
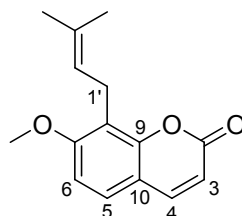
m/z (ESITOFMS)   245.1180 [M+H$^+$]   (Calc.: 245.1172)

position	$\delta_C^{a, b}$	δ_H (I, m, *J* in Hz)^b
2	161.0	-
3	112.8	6.19 (CH, d, *9.5*)
4	143.7	7.57 (CH, d, *9.5*)
5	126.3	7.25 (CH, d, *8.5*)
6	107.5	6.81 (CH, d, *8.5*)
7	160.4	-
8	118.3	-
9	152.4	-
10	112.9	-
1'	22.1	3.52 (CH$_2$, d, *7.3*)
2'	121.2	5.21 (CH, t, *7.3*)
3'	132.5	-
4'	17.8	1.82 (CH$_3$, s)
5'	25.8	1.65 (CH$_3$, s)
7 -OMe	56.3	3.89 (CH$_3$, s)

^{a} ^{13}C-NMR shifts obtained from HSQC- and HMBC-NMR experiments. Spin systems evaluated by HSQC- NMR experiment
^{b}Reference data can be found in A. Basile et al., Molecules 2009, 14, 939-952

Table S6. NMR spectroscopic data (500 MHz, CDCl$_3$) for (**6**)

(+)-Columbianedin
CAS Nr.: 5058-13-9
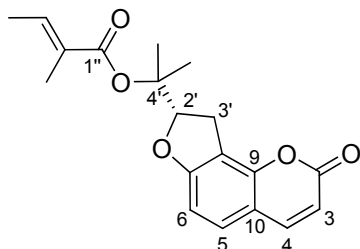
| *m/z* (ESITOFMS) | 329.1382 [M+H$^+$] | (Calc.: 329.1384) |

$[\alpha]_D$ (20.8°C)   +249° (*c* = 1.42, CHCl$_3$)[a]

position	δ_C [b,c]	δ_H (I, m, *J* in Hz)[d]
2	160.7	-
3	112.0	6.16 (CH, d, *9.7*)
4	143.8	7.59 (CH, d, *9.7*)
5	128.7	7.22 (CH, d, *8.5*)
6	106.5	6.70 (CH, d, *8.5*)
7	163.3	-
8	113.2	-
9	150.6	-
10	112.7	-
2'	88.9	5.13 (CH, dd, *7.8, 9.6*)
3'	27.6	3.31 (CH$_2$, dd *7.8, 16.3*)
		3.35 (CH$_2$, dd, *9.6, 16.3*)
4'	81.3	-
4'-Me[a]	21.2	1.55 (CH$_3$, s)
4'-Me[b]	22.2	1.60 (CH$_3$, s)
1"	166.9	-
2"	128.2	-
2"-Me	20.5	1.63 (CH$_3$, m)
3"	137.7	5.93 (CH, q, *7.1*)
4"	15.6	1.84 (CH$_3$, d, *7.1*)

[a] Reference value can be found in K. Hata, Chem. Pharm. Bull. 1971, 19, 640-642.
[b] ^{13}C-NMR shifts obtained from HSQC- and HMBC-NMR experiments. Spin systems evaluated by HSQC- NMR experiment
[c] Reference data can be found in H. Vuorela et al., Planta Med. 1988, 54, 538-542
[d] Reference data can be found in K.S. Khetwal et al., Planta Med. 1987, 53, 581.

3.3. POSITIVE GABA~A~ RECEPTOR MODULATORS FROM *ACORUS CALAMUS* AND STRUCTURAL ANALYSIS OF (+)-DIOXOSARCOGUAIACOL BY 1D AND 2D NMR AND MOLECULAR MODELING

Zaugg J, Eickmeier E, Ebrahimi SN, Baburin I, Hering S, Hamburger M.
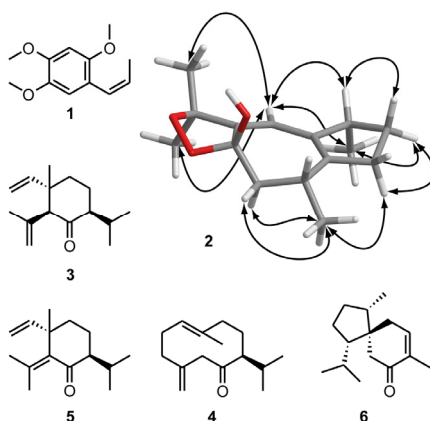
Five sesquiterpenes and β-asarone from *Acorus calamus* roots were identified as positive $\alpha_1\beta_2\gamma_{2S}$ GABA~A~ receptor modulating constituents using HPLC based activity profiling in combination with an *in vitro* functional assay using *Xenopus* oocytes. Structures were elucidated by high resolution mass spectrometry and microprobe NMR. The relative configuration of (+)-dioxosarcoguaiacol was determined by NOESY NMR and conformational analysis.

Eva Eickmeier did upscaled extraction of plant material, isolation of compounds, recording and interpretation of analytical data for structure elucidation (HPLC-PDA-ESI-TOF-MS, microprobe NMR, optical rotation) as part of her master's thesis under my direct supervision. HPLC microfractionation, structure elucidation of (+)-dioxosarcoguaiacol, Xenopus surgery, preparation of oocytes for electrophysiological measurements, two-microelectrode voltage clamp studies on fractions (except for open column fractions) and pure compounds, data analysis, writing of the manuscript, and preparation of figures were my contribution to this publication.

Janine Zaugg

Positive GABA$_A$ Receptor Modulators from *Acorus calamus* and Structural Analysis of (+)-Dioxosarcoguaiacol by 1D and 2D NMR and Molecular Modeling

Janine Zaugg,[†] Eva Eickmeier,[†] Samad Nejad Ebrahimi,[†,‡] Igor Baburin,[§] Steffen Hering,[§] and Matthias Hamburger*[†]

[†]Division of Pharmaceutical Biology, University of Basel, Klingelbergstrasse 50, 4056 Basel, Switzerland

[‡]Departement of Phytochemistry, Medicinal Plant and Drugs Research Institute, Shahid Beheshti University, G. C., Tehran, Iran

[§]Departement of Pharmacology and Toxicology, University of Vienna, Althanstrasse 14, 1090 Vienna, Austria

Ⓢ *Supporting Information*

ABSTRACT: In a two-microelectrode voltage clamp with *Xenopus laevis* oocytes, a petroleum ether extract of *Acorus calamus* rhizomes enhanced the GABA-induced chloride current through GABA$_A$ receptors of the $\alpha_1\beta_2\gamma_{2S}$ subtype by 277% ± 9.7% (100 μg/mL). β-Asarone (**1**), (+)-dioxosarcoguaiacol (**2**), (+)-shyobunone (**3**), and (+)-preisocalamenediol (**4**) were subsequently identified as main active principles through HPLC-based activity profiling and targeted isolation. The compounds induced maximum potentiation of the chloride current ranging from 588% ± 126% (EC$_{50}$: 65.3 ± 21.6 μM) (**2**) to 1200% ± 163% (EC$_{50}$: 171.5 ± 34.6 μM) (**1**), whereas (−)-isoshyobunone (**5**) and (−)-acorenone (**6**) exhibited weak GABA$_A$ modulating properties (**5**: 164% ± 42.9%; EC$_{50}$: 109.4 ± 46.6 μM and **6**: 241% ± 23.1%; EC$_{50}$: 34.0 ± 6.7 μM). The relative configuration of **2** was established as 4R*8S*10R* by NOESY experiments and conformational analysis.

RESULTS AND DISCUSSION
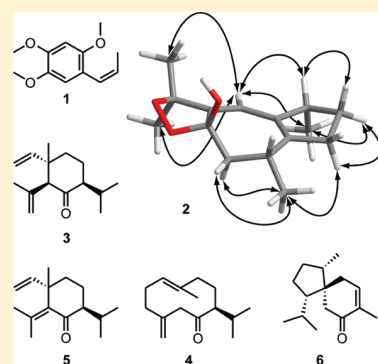
*A*corus calamus L. (Acoraceae), commonly known as "sweet flag", is a polyploidic marsh plant indigenous to Asia and is now distributed along trade routes all over the northern hemisphere.[1] The aromatic rhizome has been widely used as an herbal remedy. It contains 1.7−9.3% of a volatile oil composed of monoterpenes, sesquiterpenes, and phenylpropanoids. The most characteristic constituent of the oil is β-asarone, even though its concentration may vary considerably (96% in the tetraploidic form found in eastern and tropical southern Asia, 5% in the triploidic form found in Europe, Himalayan, and temperate Indian regions, and 0% in the diploidic variety growing from North America to Siberia).[1−4] In European folk medicine, *A. calamus* rhizomes have been mainly used as "*Amarum aromaticum*" to alleviate gastrointestinal ailments such as acute and chronic dyspepsia, gastritis and gastric ulcer, intestinal colic, and anorexia.[5,6] Ayurvedic medicine and traditional Chinese medicine (TCM) use the drug preferably to treat central nervous system (CNS) related diseases such as epilepsy, insanity, mental weakness, or insomnia.[7−9] Several in vivo studies support a sedative and tranquillizing action of the essential oil and of ethanolic and aqueous extracts of *A. calamus*.[10−12] Up to now, the underlying mechanism of action has remained elusive despite various investigations, even though the pharmacological effect could be mainly attributed to α-asarone and β-asarone.[11,13−15]

GABA$_A$ receptors are pentameric ligand-gated chloride ion channels that are activated by GABA, the major inhibitory neurotransmitter in the CNS. Most likely more than 11 different receptor subtypes, assembled from five varying subunits, exist in the human brain. These are involved in distinct neuronal circuits and are targeted by numerous classes of drugs such as benzodiazepines, barbiturates, and some general anesthetics. The most abundant GABA$_A$ receptor in the human brain consists of two α_1, two β_2, and one γ_{2S} subunit.[16−18]

We recently screened a library of 982 extracts using an automated functional two-microelectrode voltage clamp assay with *Xenopus* oocytes[19] that transiently expressed GABA$_A$ receptors of the $\alpha_1\beta_2\gamma_{2S}$ subtype. A petroleum ether extract of *A. calamus* rhizomes showed promising activity. As previously shown, HPLC-based activity profiling is a miniaturized, effective approach to discover new bioactive natural products,[20−24] and we have successfully applied it to the discovery of new GABA$_A$ receptor modulators of natural origin.[25−28] Herein, we describe the identification of GABA$_A$ receptor modulating compounds in *A. calamus* (**1−6**) and provide information suggesting the complete relative configuration of (+)-dioxosarcoguaiacol (**2**), a sesquiterpene previously unknown in this plant.

■ RESULTS AND DISCUSSION

Plant extracts were screened in an automated, fast perfusion system during two-microelectrode voltage clamp measurements with *Xenopus* oocytes that transiently expressed GABA$_A$ receptors of the subunit combination $\alpha_1\beta_2\gamma_{2S}$.[19] At a

concentration of 100 μg/mL, the *A. calamus* petroleum ether extract potentiated the GABA-induced chloride current (I_{GABA}) by 277% $\pm$ 9.7% (Figure 1C). To localize the activity within the extract, it was submitted to HPLC-based activity profiling using a previously validated protocol.[29] The chromatogram (254 nm) of a semipreparative HPLC separation (10 mg of extract) and the corresponding activity profile of the time-based microfractionation (28 microfractions of 90 s each) are shown in Figure 1B and A, respectively. A major peak of activity was found in fraction 14 (potentiation of I_{GABA} by 237% $\pm$ 5.4%), which contained an unresolved complex of peaks containing compounds **3**–**6**. Minor activity was found in fractions 1, 6–8, and 10. Fractions 6 and 7 contained a major compound of the extract and enhanced I_{GABA} by 54.7% $\pm$ 9.3% and 73.9% $\pm$ 17.7%, respectively. Fraction 8, consisting of a minor compound, showed a potentiation of I_{GABA} by 50.6% $\pm$ 17.4%, whereas fraction 10 enhanced I_{GABA} by 33.8% $\pm$ 10.3%. Fraction 1 showed marginal activity (38.3% $\pm$ 2.9%) but was not further pursued.

Preparative isolation was focused on the purification of compounds in the active time-based fractions and was started by an open column separation of the extract. An HPLC-ESIMS analysis of the resulting 21 fractions revealed that the extract was significantly more complex than suggested by the semipreparative HPLC chromatogram at 254 nm (Figure 1B). Peaks with retention times fitting to active microfractions were detected in several fractions. Fractions A–E and L–U were submitted to bioassay at a test concentration of 10 μg/mL (Figure 1C). The most active fractions, A, C, L, and M (potentiation of I_{GABA} by 132% $\pm$ 41.5%, 157% $\pm$ 20.7%, 235% $\pm$ 59.0%, and 158% $\pm$ 72.9%, respectively), contained peaks that corresponded to the active time windows in the HPLC-based activity profiling (Figure 1D) and were further purified. Fraction D was not further pursued since it was very similar to fraction C. Finally, β-asarone (**1**), (+)-dioxosarcoguaiacol (**2**), (+)-shyobunone (**3**), (+)-preisocalamenediol (**4**), (−)-isoshyobunone (**5**), and (−)-acorenone (**6**) were isolated and unambiguously identified by ESI-TOF-MS, 1D and 2D microprobe NMR, optical rotation, and comparison with published data.[30−37] Compounds **1** and **3**–**6** have been previously isolated from *A. calamus*.[38−41] Their spectroscopic data are given as Supporting Information.

(+)-Dioxosarcoguaiacol (**2**), a sesquiterpene new for *A. calamus*, had been described from a Red Sea soft coral (*Sarcophyton glaucum*). However, assignment of the relative configuration was limited to stereocenters 4S* and 10R*, while the configuration at the bridgehead C-8 was not established.[35] Optical rotation and NMR data of **2** were identical to published data. To confirm the relative configuration of the stereocenters at C-4 and C-10, we submitted the four possible stereoisomers of **2** (4R*8S*10R*, 4S*8S*10R*, 4R*8S*10S*, 4S*8S*10S*) to conformational analysis and compared $^3J_{\text{HH}}$ coupling constants from ^{1}H NMR and selective TOCSY experiments, and NOESY correlations with the structures of the calculated conformers (relevant NMR data are summarized in Table 1; NMR spectra of **2** are given as Supporting Information). For each stereoisomer, 1−3 conformers were obtained within a 1 kcal/mol range from the corresponding global energy minimum (Figure S1, Supporting Information). However, only one conformer of each stereoisomer reasonably fit to the observed NMR data. These conformers were then submitted to geometrical optimization using density function theory (B3LYP/6-31G*), prior to comparison of

optimized dihedral angles and interatomic distances with the experimental data.
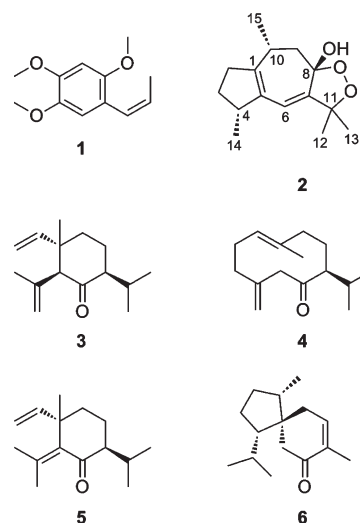
Unambiguous assignment of the methylene protons at C-2 and C-3 was established on the basis of $^3J_{\text{HH}}$ H-2b/H-3b of 0 Hz, indicative of their perpendicular orientation. This was corroborated by a NOESY correlation between H-3b and H-2a. $^3J_{\text{HH}}$ coupling constants H-9b/H-10 (5.2 Hz) and H-9a/H-10 (13.4 Hz) corresponded to dihedral angles of approximately 60° and 180°, respectively. Geometrically optimized conformers matched with the above-mentioned NMR data. However, two stereoisomers (4R*8S*10S*, 4S*8S*10S*) could be discarded since the interatomic distances between H-2a and CH$_3$-15, and between H-6 and both methyl groups at C-11, were not in accord with the observed NOESY correlations. Assignment of the relative configuration at C-4 was supported by NOESY correlations between H-3a and H-4, and H-3b and CH$_3$-14. Hence, only the 4R*8S*10R* stereoisomer fully matched with the NMR data of (+)-dioxosarcoguaiacol (**2**) (Figure 2). A synoptical table (Table S6) of the stereoisomers is given as Supporting Information.

(+)-Dioxosarcoguaiacol[35] was previously published with a 4S*10R* configuration, and with NMR shifts and optical rotation identical to compound **2**. 4R10R-Calamusenone, the 8-oxo, $\Delta^{7,11}$ analogue of **2**, was previously reported from *A. calamus* essential oil, and its absolute configuration determined by X-ray crystallographic analysis.[42] The formation of **2** can be plausibly explained via photo-oxygenation of calamusenone by "ene-type" addition of O$_2$ at C-11 and subsequent ring closure to the endoperoxide.[43] ^{1}H NMR integrals of **2** showed an enantiomeric excess of the 8S* epimer [8-OH: δ 3.08, 8S* and δ 2.94, 8R* (95:5); H-6: δ 5.55, 8S* and δ 5.51, 8R* (95:5)]. The comparison of computationally optimized conformers of **2** with structural information obtained by 1D and 2D NMR experiments allowed us to unambiguously identify the relative configuration of (+)-dioxosarcoguaiacol (**2**) as 4R*8S*10R*, which contradicted the previously reported structure.[35] Our findings were supported by the existence of a putative precursor, 4R10R-calamusenone, with known absolute configuration.

Compounds **1**–**6** were tested in the oocyte assay at concentrations ranging from 0.1 to 1000 μM. To varying degrees, all compounds enhanced I_{GABA} at a GABA EC$_{5-10}$ in a concentration-dependent manner (Figure 3). Compared to other natural products,[25,27,44] compounds **1**–**4** showed high efficiencies on $\alpha_1\beta_2\gamma_{2S}$ GABA$_A$ receptors. Potentiation of I_{GABA} ranged from
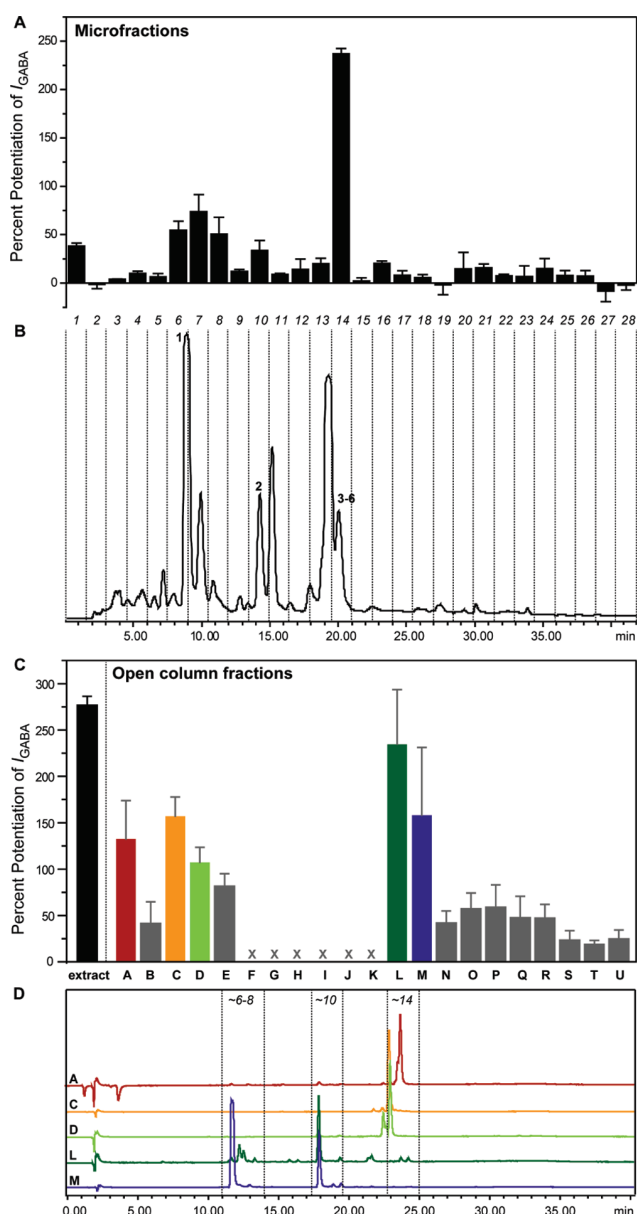
Figure 1. HPLC-based activity profiling of a petroleum ether extract of *Acorus calamus* L. for GABA$_A$ modulating properties. The HPLC chromatogram (254 nm) of a semipreparative separation of 10 mg of extract is shown in B. Peak numbering corresponds to compounds 1−6. The 28 collected time-based fractions, 90 s each, are indicated with dashed lines. Potentiation of the GABA-induced chloride current in *Xenopus* oocytes (I_{GABA}) of microfractions is shown in A. Potentiation of I_{GABA} by the extract (100 μg/mL) and by open column fractions A−E and L−U (10 μg/mL) are shown in C. Fractions F−K were not tested due to limited amounts (<100 μg). Part D shows analytical HPLC traces (254 nm) of open column fractions A, C, D, L, and M. The active time-windows from the HPLC-based activity profiling (approximately corresponding to microfractions 6−8, 10, and 14) are indicated with dashed lines.

588% ± 126% (2) to 1197% ± 163% (1) (Table 2). Compounds with higher efficiency usually displayed lower potencies (higher concentrations for half-maximal stimulation of I_{GABA}; EC$_{50}$) and vice versa. Compound 6 showed the highest potency (34.0 ± 6.7 μM) but a maximum stimulation of I_{GABA} of only 241% ± 23.1%.

Even though the set of compounds tested was too small for a study of structure−activity relationships, some interesting observations were made: (+)-shyobunone (3) and (+)-preisocalamenediol (4), which both derive from acoragermacrone,[40,45] showed comparably high efficiencies. The potency of 4 was lower, which could be due to the high conformational flexibility of the germacrane-type scaffold. (−)-Isoshyobunone (5) was much less efficient than its presumed precursor 3[46] (Figure 3; Table 3), which can only be explained by the varying C-2 substitution and the consequential conformational difference. Interestingly, 5 showed a weak (less than GABA EC$_{5−10}$) direct activation of the $\alpha_1\beta_2\gamma_{2S}$ GABA$_A$ receptor, whereas 3 did not evoke any agonistic effect. Only weak GABA$_A$ receptor modulation was found for (−)-acorenone (6). Compounds 2−6 broaden the spectrum of sesquiterpenes acting at the GABA$_A$ receptors. Up to now only a few sequiterpenes have been reported as GABA$_A$ receptor modulators. The most prominent is picrotoxin, a strong GABA$_A$ receptor inhibitor[47] that is widely used as an experimental compound for animal convulsion models. Valerenic acid from *Valeriana officinalis* roots is a $\beta_{2/3}$-subunit-specific positive allosteric modulator[44,48] with anxiolytic effects in vivo.[48,49] This compound has served as a new scaffold for GABA$_A$ receptor ligands.[49,50]

Among the compounds identified by the profiling of *Acorus* extract, the simple phenylpropanoid β-asarone (1) induced the highest potentiation of I_{GABA} (1200% ± 163% with an EC$_{50}$ of 171.5 ± 34.6 μM). Its efficiency at a GABA EC$_{5−10}$ was significantly higher than that of known GABA$_A$ receptor modulators such as benzodiazepines (triazolam: 253% ± 12%, midazolam: 342% ± 64%, clotiazepam: 260% ± 27%)[51] or natural products such as valerenic acid (400% ± 78%).[44] The structure of 1 is somewhat reminiscent of propofol, a general anesthetic acting at the GABA$_A$ receptor. However, the pharmacological potential of 1 is certainly limited due to its known toxicity.[52−54] There are many reports of sedative and tranquillizing properties of *Acorus* extracts and essential oil in animal models, but the mechanism of action was not established up to now.[10−15,55] Given that β-asarone (1) is a major compound of the essential oil, its sedative and tranquillizing activities may be due to the GABA$_A$ receptor modulating properties of 1. The quantity of β-asarone in *Acorus* rhizome and essential oil, however, depends on the chemotype and thus varies considerably.[3,4] Medicinal preparations made of the diploidic or triplodic form are free of the toxic β-asarone and are, therefore, recommended for therapeutic use.[8] It is interesting to note that there seems to be a correlation between β-asarone content in the three chemotypes of *A. calamus* and their traditional uses. The tetraploidic, β-asarone-rich types growing in Asia have been traditionally used in Ayurvedic medicine and TCM as sedatives, whereas such uses have not been reported from the β-asarone-poor European and North American chemotypes. The reason for "Eastern" traditional usage as a sedative and "Western" traditional usage as an aromatic bitter could possibly be explained by limited access in the past to the geographically separated chemotypes of *A. calamus*.

The essential oil and extracts of *A. calamus* roots have multiple pharmacological and biological effects,[56] but there is not much published data on bioactivity of sesquiterpenes 3−6 and (+)-dioxosarcoguaiacol (2). The compounds represent interesting drug-like structures, since they all fulfill Lipinski's "rule of five".[57] From a pharmacological perspective, however, further investigations may be limited to the highly efficient sesquiterpenes 3 and 4 and to the minor compound 2. Further pharmacological and toxicological studies are needed to substantiate the

Table 1. NMR Spectroscopic Data (500 MHz, CDCl$_3$) for (+)-Dioxosarcoguaiacol (2)

position	$\delta_C{}^a$	mult.	δ_H (J in Hz)	HMBC^b	NOESY^c
1	145.8	C			
2	35.6	CH$_2$	H-2a: 2.58, ddd (16.7, 8.5, 7.2)		H-2a ↔ H-3b, 15
			H-2b: 2.21, ddd (16.7, 10.9, 0)		
3	29.9	CH$_2$	H-3a: 1.95, m		H-3a ↔ 4
			H-3b: 1.40, dddd (16.6, 8.5, 3.5, 0)		H-3b ↔ H-2a, 14
4	44.3	CH	2.63, m		
5	132.5	C			
6	114.6	CH	5.55, s	C-11, 4, 8, 7, 5	H-13, 12, 14, 4
7	153.2	C			
8	103.4	C			
8-OH			3.08, br s		
9	38.0	CH$_2$	H-9a: 1.63, dd (13.4, 13.4)	C-14, 10, 8, 7, 1	H-9a ↔ H-15
			H-9b: 2.03, dd (13.4, 5.2)		H-9b ↔ H-15
10	31.5	CH	2.71, m		
11	85.3	C			
12	28.0	CH$_3$	1.37, s	C-15, 11, 7	H-6
13	24.8	CH$_3$	1.43, s	C-12, 11, 7	H-6
14	20.1	CH$_3$	1.04, d (7.1)	C-3, 4, 5	
15	19.6	CH$_3$	1.12, d (7.1)	C-10, 9, 8, 1	H-9a, 9b, 2a

^{a} ^{13}C shifts are deduced from HSQC and HMBC experiments. ^{b} HMBC correlations from *hmbcgp* experiment (NS: 128, DS: 16), optimized for 10 Hz, are from proton(s) stated to the indicated carbon. ^{c} Critical NOESY correlations from *noesygpphpp* experiment (mixing time 0.75 s, NS: 32, DS: 16)

Figure 2. Geometrically optimized structure of 4R*8S*10R*-(+)-dioxosarcoguaiacol (2). Critical NOESY correlations for assigning the relative configuration are indicated with arrows. The geometrical optimization was performed using density function theory at the B3LYP/6-31G* level.

sedative and tranquillizing properties of pure compounds and of the essential oil.

■ EXPERIMENTAL SECTION

General Experimental Procedures. Optical rotations of compounds **2**−**6** were measured on a Perkin-Elmer polarimeter (model 341) equipped with a 10 cm microcell. The optical rotation for the Na-D-line (589 nm) was extrapolated from the lines of a mercury lamp using the Drude equation.[58] NMR spectra were recorded at room temperature with a Bruker Biospin Avance III spectrometer operating at 500.13 MHz.

^{1}H NMR, COSY, DEPT-edited HSQC, HMBC, 1D-TOCSY, and 2D-NOESY spectra were measured with a 1 mm TXI probe. Spectra were analyzed using Bruker TopSpin 2.1 software. ESI-TOF-MS spectra of compounds **1**−**6** were recorded in positive mode on a Bruker Daltonics microTOF ESIMS system. Nitrogen was used as a nebulizing gas at a pressure of 2.0 bar and as a drying gas at a flow rate of 9.0 L/min (dry gas temperature 240 °C). Capillary voltage was set at 4500 V, hexapole at 230.0 Vpp. Instrument calibration was performed using a reference solution of sodium formate 0.1% in 2-propanol/water (1:1) containing 5 mM NaOH.

HPLC-PDA-ESIMS spectra were obtained in positive mode on a Bruker Daltonics Esquire 3000 Plus ion trap MS system connected via T-splitter (1:5) to an Agilent HP 1100 series system consisting of a binary pump, autosampler, column oven, and diode array detector (G1315B). Data acquisition and processing of all mass spectra was performed using Bruker HyStar 3.0 software.

Semipreparative HPLC separations were performed on a Waters Alliance 2690 separation module connected to a 996 photodiode array detector. Data acquisition and processing was performed using Waters Empower Pro software. Preparative HPLC separation was performed using a Shimadzu LC-8A preparative separation chromatograph equipped with a SPD-M10A VP diode array detector. Medium-pressure liquid chromatography (MPLC) was done on prepacked normal-phase cartridges (40−63 μm, 40 × 150 mm) using a Buchi Sepacore system consisting of a control unit C-620, a fraction collector C-660, and two pump modules C-605. The MPLC unit was controlled with the Buchi SepacoreControl software (version 1.0.3000.1). Deuterated chloroform (100 atom % D, stabilized with Ag) for NMR experiments was purchased from Armar Chemicals. HPLC-grade MeOH (Scharlau Chemie S.A.) and water were used for HPLC separations. Solvents used for extraction, open column chromatography, and MPLC were of technical grade and purified by distillation. Silica gel (63−200 μm, Merck) was used for open column chromatography.

Plant Material. Dried and cut rhizomes of *A. calamus* Ph. Helv. were purchased from Haenseler AG (Herisau, Switzerland) (batch 2009.12.0224). The identity of the plant material was confirmed at

Figure 3. Part A shows the concentration−response curves for compounds **1**−**6** on GABA$_A$ receptors (α_1, β_2, and γ_{2S} subunit composition) using a GABA EC$_{5-10}$. Typical traces for modulation of chloride currents through $\alpha_1\beta_2\gamma_{2S}$ GABA$_A$ receptors for compounds **1**−**6** are given in B.

Table 2. Potencies (EC$_{50}$) and Efficiencies (Maximum Stimulation of the GABA-Induced Chloride Current) of Compounds 1−6 for GABA$_A$ Receptors of the Subunit Composition $\alpha_1\beta_2\gamma_{2S}$

compd	EC$_{50}$ [μM] ± SE	maximum stimulation of I_{GABA} (EC$_{5-10}$) ± SE [%]	Hill coefficient[a] (n_H) ± SE	no. of experiments (n)
1	171.5 ± 34.6	1200 ± 163	1.8 ± 0.2	6
2	65.3 ± 21.6	588 ± 126	1.6 ± 0.3	5
3	64.8 ± 19.8	669 ± 112	1.7 ± 0.3	6
4	135.1 ± 34.4	886 ± 105	1.6 ± 0.2	5
5	109.4 ± 46.6	164 ± 42.9	2.1 ± 0.8	6
6	34.0 ± 6.7	241 ± 23.1	1.6 ± 0.3	5

[a] Indicates the slope of the concentration−response curve at the EC$_{50}$. Hill coefficients > 1 indicate positive cooperativity during receptor binding.[62]

the Division of Pharmaceutical Biology, University of Basel, where a voucher specimen (00 380) is deposited.

Microfractionation for Activity Profiling. An aliquot (approximately 20 g) of ground roots was macerated at room temperature with petroleum ether (3 × 0.5 L, 1 h each). Microfractionation for GABA$_A$ receptor activity profiling was performed as previously described,[25,27−29] with minor modifications; separation was carried out on a Waters SunFire Prep C18 (5 μm, 10 × 150 mm) column with MeOH (solvent A) and H$_2$O (solvent B) using the following gradient: 60% A to 100% A in 30 min, hold for 10 min. The flow rate was 4 mL/min, and 100 μL of the extract (100 mg/mL in DMSO) was injected. A total of 28 time-based microfractions of 90 s each were collected. Microfractions were evaporated in parallel with a Genevac EZ-2 Plus vacuum centrifuge. The dry films were redissolved in 1 mL of MeOH; aliquots of 0.5 mL were dispensed in two vials, dried under N$_2$ gas, and submitted to bioassay.

Preparative Extraction and Isolation. The plant material was ground with a Retsch ZM1 ultracentrifugal mill. Ground roots (630 g)

were extracted by maceration at room temperature with petroleum ether (4 × 2.5 L, 1 h each). The solvent was evaporated at reduced pressure to yield 20.7 g of petroleum ether extract. A portion of the extract (18.8 g) was separated by open column chromatography (9 × 80 cm, 1.2 kg silica gel) using a step gradient of petroleum ether and ethyl acetate (95:5, 10 L; 90:10, 4 L; 80:20, 2 L; 70:30, 2 L; 60:40, 2 L; 50:50, 4 L; 25:75, 1.8 L; 100:0, 2 L). The flow rate was approximately 15 mL/min. The effluents were combined to 21 fractions (A−U) based on TLC patterns (detection at 254 nm and at daylight after staining with anisaldehyde−sulfuric acid reagent). Fractions A−U were analyzed by HPLC-PDA-ESIMS on a Waters SunFire C18 (3.5 μm, 3.0 × 150 mm) column with MeOH (solvent A) and H$_2$O (solvent B), both containing 0.1% formic acid. A gradient of 60% A to 100% A in 30 min, hold for 10 min, and a flow rate of 0.4 mL/min were used. The sample concentration was 10 mg/mL in DMSO, and the injection volume was 5 μL. The fractions were then submitted to bioassay. A portion (700 mg) of fraction A (1.32 g) was separated into 21 fractions (A1−A21) by MPLC using toluene, hexane,

and CH_2Cl_2 in the following gradient: 10:90:0 to 100:0:0 in 3 h, 0:0:100 for 1 h at a flow rate of 30 mL/min. Fractions A10 (60.9 mg), A14 (140.8 mg), and A18 (19.2 mg) consisted of (+)-shyobunone (**3**), (+)-preisocalamenediol (**4**), and (−)-isoshyobunone (**5**), respectively. A portion (750 mg) of fraction C (920 mg) was separated into five fractions (C1−C5) by MPLC using a gradient of hexane and ethyl acetate (100:0 to 95:5 in 1.5 h, flow rate 30 mL/min) to yield 376 mg (fraction C3) of (−)-acorenone (**6**). Fraction L (385 mg) was separated by MPLC using a gradient of a $CHCl_3$/EtOAc [9:1] mixture and hexane (20:80 to 50:50 in 2 h, flow rate 30 mL/min), which yielded 15 fractions (L1−L15). Fraction L13 (29.5 mg) was dissolved in 400 μL of DMSO and separated by preparative HPLC on a Waters SunFire Prep C18 OBD (5 μm, 30 × 150 mm) column using a gradient of $MeOH/H_2O$ (50:50 to 100:0 in 30 min, flow rate 20 mL/min) to obtain 3.8 mg of (+)-dioxosarcoguaiacol (**2**). A portion (790 mg) of fraction M (952 mg) was separated by MPLC using a gradient of a CH_2Cl_2/EtOAc [9:1] mixture and hexane (20:80 to 50:50 in 2 h, flow rate 30 mL/min), which yielded 12 fractions (M1−M12). Fraction M2 (290.9 mg) was identified as β-asarone (**1**). A portion (30 mg) of fraction M5 (83.4 mg) was dissolved in hexane (300 μL) and submitted repeatedly to semipreparative HPLC on a Merck LiChroSorb 100 Diol (10 μm, 10 × 250 mm) column (hexane/2-propanol (97:3) isocratic, flow rate 5 mL/min) to isolate another 18.5 mg of (+)-dioxosarcoguaiacol (**2**).

(+)-**Dioxosarcoguaiacol** (**2**): yellow oil; $[\alpha]^{22}_D$ +36 (c 0.16, $CHCl_3$); UV (MeOH) λ_{max} 260 (sh), 267 nm; NMR data see Table 1 and Supporting Information; ESI-TOF-MS m/z 273.1447 $[M + Na]^+$ (calcd for $C_{15}H_{22}O_3Na$, 273.1463).

Compounds **1** and **3**−**6** were unambiguously identified by means of 1D and 2D NMR experiments, ESI-TOF-MS, and optical rotation in the case of chiral compounds. The data were compared with published values[30−37] and are available as Supporting Information.

Conformational Analysis and Geometrical Optimization. Conformational analysis of the stereoisomers of **2** was performed with Schrödinger 9.1 software at the OPLS_2005 level in $CHCl_3$. Selection of the conformers was done within a 1 kcal/mol energy window. Conformers not fitting to NMR data were discarded (exclusion criteria: (i) dihedral angles clearly mismatching the $^3J_{HH}$ coupling constants between H-10/H-9a and H-10/H-9b or (ii) dihedral angles mismatching $J_{2b,3b}$ 0 Hz and interatomic distances between H-6/H-12 and H-6/H-13 mismatching the corresponding NOESY correlations). The Gaussian 03 package[59] was used for optimizing the remaining starting geometries by means of the density function theory with the B3LYP functional and the 6-31G* basis set in the gas phase.[60] Dihedral angles and interatomic distances were taken from minimized conformers and compared with NMR data.

Expression of $GABA_A$ Receptors. Stage V−VI oocytes from *Xenopus laevis* were prepared and cRNA was injected as previously described by Khom et al. (2006).[51] Female *X. laevis* (NASCO, Fort Atkinson, WI) were anesthetized by exposing them for 15 min to a 0.2% MS-222 (3-aminobenzoic acid ethyl ester methanesulfonate, Sigma-Aldrich, Munich, Germany) solution before surgically removing parts of the ovaries. Follicle membranes from isolated oocytes were enzymatically digested with 2 mg/mL collagenase from *Clostridium histolyticum* (Type 1A, Sigma-Aldrich). Synthesis of capped runoff poly(A+) cRNA transcripts was obtained from linearized cDNA templates (pCMV vector). One day after enzymatic isolation, the oocytes were injected with 50 nL of DEPC-treated H_2O (Sigma-Aldrich) containing different cRNAs at a concentration of approximately 300−3000 pg/nL per subunit. The amount of injected cRNA mixture was determined by means of a NanoDrop ND-1000 (Kisker Biotech, Steinfurt, Germany). Rat cRNAs were mixed in a 1:1:10 ratio to ensure expression of the gamma subunit in $\alpha_1\beta_2\gamma_{2S}$ receptors. Oocytes were then stored at 18 °C in an aqueous solution of 90 mM NaCl, 1 mM KCl, 1 mM $MgCl_2$, 1 mM $CaCl_2$, and 5 mM HEPES (pH 7.4), containing 1% of

penicillin−streptomycin solution (Sigma-Aldrich).[61] Voltage clamp measurements were performed between days 1 and 5 after cRNA injection.

Two-Microelectrode Voltage Clamp Studies. Electrophysiological experiments were performed by the two-microelectrode voltage clamp method at a holding potential of −70 mV making use of a TURBO TEC 03X amplifier (npi Electronic GmbH, Tamm, Germany) and an Axon Digidata 1322A interface (Molecular Devices, Sunnyvale, CA). Data were recorded by using pCLAMP v10.2 data acquisition software (Molecular Devices). Currents were low-pass-filtered at 1 kHz and sampled at 3 kHz. The bath solution contained 90 mM NaCl, 1 mM KCl, 1 mM $MgCl_2$, 1 mM $CaCl_2$, and 5 mM HEPES (pH 7.4). Electrode filling solution contained 2 M KCl.

Fast Solution Exchange during I_{GABA} Recordings. Test solutions (100 μL) of extracts, fractions, and pure compounds were applied to the oocytes at a speed of 300 μL/s by means of the ScreeningTool automated fast perfusion system (npi Electronic GmbH).[19] In order to determine GABA EC_{5-10} (typically between 3 and 10 μM for receptors of the subunit combination $\alpha_1\beta_2\gamma_{2S}$), a concentration−response experiment with GABA concentrations ranging from 0.1 μM to 1 mM was performed. Stock solutions (10 mg/mL in DMSO) of *A. calamus* extract and open column fractions (1−21) were diluted to concentrations of 100 and 10 μg/mL, respectively, with bath solution containing GABA EC_{5-10}. As previously described in a validated protocol, microfractions collected from the semipreparative HPLC separations were dissolved in 30 μL of DMSO and subsequently mixed with 2.97 mL of bath solution containing GABA EC_{5-10}.[29] For concentration−response experiments, bath solution containing compounds **1**−**6** in concentrations ranging from 0.1 to 1000 μM was applied to the oocyte. After a 20 s incubation period, a second application immediately followed containing the corresponding compound solution combined with GABA EC_{5-10}.

Data Analysis. Enhancement of the GABA-induced chloride current (I_{GABA}) was defined as $I_{(GABA+Comp)}/I_{GABA} - 1$, where $I_{(GABA+Comp)}$ is the current response in the presence of a given compound, and I_{GABA} is the control GABA-induced chloride current. Data were analyzed using the ORIGIN 7.0 SR0 software (OriginLab Corporation) and are given as mean ± SE of at least 2 oocytes and ≥2 oocyte batches.

■ ASSOCIATED CONTENT

ⓢ Supporting Information. Spectral characterization data of compounds **1** and **3**−**6** including ^1H and ^{13}C shifts from ^1H NMR and 2D-heteronuclear NMR spectra, critical NOE enhancement data, accurate masses from ESI-TOF-MS spectra, and optical rotation values. Proton NMR, 2D homonuclear, and 2D heteronuclear NMR spectra of compound **2**. Table summarizing the assignment of the relative configuration of **2** by molecular modeling and 1D and 2D NMR. Conformers of the stereoisomers of **2** were found by conformational analysis. This material is available free of charge via the Internet at http://pubs.acs.org.

■ AUTHOR INFORMATION

Corresponding Author
*Tel: +41 61 267 1425. Fax: +41 61 267 1474. E-mail: matthias.hamburger@unibas.ch.

■ ACKNOWLEDGMENT

■ REFERENCES

(1) Motley, T. J. *Econ. Bot.* **1994**, *48*, 397–412.

(2) Keller, K.; Stahl, E. *Planta Med.* **1983**, *47*, 71–74.

(3) Mazza, G. *J. Chromatogr.* **1985**, *328*, 179–194.

(4) Stahl, E.; Keller, K. *Planta Med.* **1981**, *43*, 128–140.

(5) Barnes, J.; Anderson, L. A.; Phillipson, J. D. *Herbal Medicines*; Pharmaceutical Press, RPS Publishing: London, Grayslake, 2007; pp 118–119.

(6) Wichtl, M.; Bauer, R.; Blaschek, W.; Buff, W.; Hiller, K.; Lichius, J. J.; Loew, D.; Stahl-Biskup, E.; Teuscher, E. *Teedrogen und Phytopharmaka*; Wissenschaftliche Vertragsgesellschaft mbH: Stuttgart, 2009; p 98.

(7) Chang, H.-M.; But, P. P.-H., *Pharmacology and Applications of Chinese Materia Medica*; World Scientific Publishing Co. Pte. Ltd.: Singapore, 1987; pp 261–266.

(8) Khare, C. P. *Indian Herbal Remedies*; Springer-Verlag: Berlin, 2004; pp 19–20.

(9) Williamson, E. M. *Major Herbs of Ayurveda*; Churchill Livingstone; Elsevier Science Ltd: London, 2002; pp 16–19.

(10) Dandiya, P. C.; Cullumbine, H.; Sellers, E. A. *J. Pharmacol. Exp. Ther.* **1959**, *126*, 334–337.

(11) Dandiya, P. C.; Menon, M. K. *Br. J. Pharmacol.* **1963**, *20*, 436–442.

(12) Vohora, S. B.; Shah, S. A.; Dandiya, P. C. *J. Ethnopharmacol.* **1990**, *28*, 53–62.

(13) Liao, J. F.; Huang, S. Y.; Jan, Y. M.; Yu, L. L.; Chen, C. F. *J. Ethnopharmacol.* **1998**, *61*, 185–193.

(14) Menon, M. K.; Dandiya, P. C. *J. Pharm. Pharmacol.* **1967**, *19*, 170–175.

(15) Zanoli, P.; Avallone, R.; Baraldi, M. *Phytother. Res.* **1998**, *12*, S114–S116.

(16) Simon, J.; Wakimoto, H.; Fujita, N.; Lalande, M.; Barnard, E. A. *J. Biol. Chem.* **2004**, *279*, 41422–41435.

(17) Olsen, R. W.; Sieghart, W. *Pharmacol. Rev.* **2008**, *60*, 243–260.

(18) Olsen, R. W.; Sieghart, W. *Neuropharmacol.* **2009**, *56*, 141–148.

(19) Baburin, I.; Beyl, S.; Hering, S. *Pflug. Arch. Eur. J. Phy.* **2006**, *453*, 117–123.

(20) Adams, M.; Christen, M.; Plitzko, I.; Zimmermann, S.; Brun, R.; Kaiser, M.; Hamburger, M. *J. Nat. Prod.* **2010**, *73*, 897–900.

(21) Danz, H.; Stoyanova, S.; Wippich, P.; Brattstroem, A.; Hamburger, M. *Planta Med.* **2001**, *67*, 411–416.

(22) Dittmann, K.; Gerhaeuser, C.; Klimo, K.; Hamburger, M. *Planta Med.* **2004**, *70*, 909–913.

(23) Potterat, O.; Hamburger, M. *Curr. Org. Chem.* **2006**, *10*, 899–920.

(24) Potterat, O.; Wagner, K.; Gemmecker, G.; Mack, J.; Puder, C.; Vettermann, R.; Streicher, R. *J. Nat. Prod.* **2004**, *67*, 1528–1531.

(25) Li, Y.; Plitzko, I.; Zaugg, J.; Hering, S.; Hamburger, M. *J. Nat. Prod.* **2010**, *73*, 768–770.

(26) Yang, X.; Baburin, I.; Plitzko, I.; Hering, S.; Hamburger, M. *Mol. Diversity* **2011**, DOI: 10.1007/s11030-010-9297-7.

(27) Zaugg, J.; Baburin, I.; Strommer, B.; Kim, H. J.; Hering, S.; Hamburger, M. *J. Nat. Prod.* **2010**, *73*, 185–91.

(28) Zaugg, J.; Eickmeier, E.; Rueda, D. C.; Hering, S.; Hamburger, M. *Fitoterapia* **2011**, DOI: 10.1016/j.fitote.2010.12.001

(29) Kim, H. J.; Baburin, I.; Khom, S.; Hering, S.; Hamburger, M. *Planta Med.* **2008**, *74*, 521–526.

(30) Baldwin, S. W.; Fredericks, J. E. *Tetrahedron Lett.* **1982**, *23*, 1235–1238.

(31) Delvalle, D. M.; Schwenker, G. *Planta Med.* **1987**, *53*, 230.

(32) Niwa, M.; Terada, Y.; Iguchi, M.; Yamamura, S. *Chem. Lett.* **1977**, 1415–1418.

(33) Patra, A.; Mitra, A. K. *J. Nat. Prod.* **1981**, *44*, 668–669.

(34) Rascher, W.; Wolf, H. *Tetrahedron* **1977**, *33*, 575–577.

(35) Sawant, S. S.; Youssef, D. T. A.; Sylwester, P. W.; Wali, V.; El Sayed, K. A. *Nat. Prod. Commun.* **2007**, *2*, 117–119.

(36) Weyerstahl, P.; Rilk, R.; Marschall-Weyerstahl, H. *Liebigs Ann. Chem.* **1987**, *2*, 89–101.

(37) Zdero, C.; Bohlmann, F.; Solomon, J. C.; King, R. M.; Robinson, H. *Phytochemistry* **1989**, *28*, 531–542.

(38) Baxter, R. M.; Dandiya, P. C.; Kandel, S. I.; Okany, A.; Walker, G. C. *Nature* **1960**, *185*, 466–467.

(39) Iguchi, M.; Nishiyama, A.; Koyama, H.; Yamamura, S.; Hirata, Y. *Tetrahedron Lett.* **1968**, *51*, 5315–5318.

(40) Iguchi, M.; Nishiyama, A.; Yamamura, S.; Hirata, Y. *Tetrahedron Lett.* **1970**, *11*, 855–857.

(41) Vrkoc, J.; Herout, V.; Sorm, F. *Collect. Czech. Chem. Commun.* **1961**, *26*, 3183–3185.

(42) Rohr, M.; Naegeli, P.; Daly, J. J. *Phytochemistry* **1979**, *18*, 279–281.

(43) Wong, H. F.; Brown, G. D. *J. Chem. Res.* **2002**, *S*, 30–33.

(44) Khom, S.; Baburin, I.; Timin, E.; Hohaus, A.; Trauner, G.; Kopp, B.; Hering, S. *Neuropharmacology* **2007**, *53*, 178–187.

(45) Stahl, E.; Keller, K. *Planta Med.* **1983**, *47*, 75–78.

(46) Yamamura, S.; Iguchi, M.; Nishiyama, A.; Niwa, M.; Koyama, H.; Hirata, Y. *Tetrahedron* **1971**, *27*, 5419–5431.

(47) Twyman, R. E.; Rogers, C. J.; Macdonald, R. L. *Neurosci. Lett.* **1989**, *96*, 89–95.

(48) Benke, D.; Barberis, A.; Kopp, S.; Altmann, K. H.; Schubiger, M.; Vogt, K. E.; Rudolph, U.; Mohler, H. *Neuropharmacology* **2009**, *56*, 174–81.

(49) Khom, S.; Strommer, B.; Ramharter, J.; Schwarz, T.; Schwarzer, C.; Erker, T.; Ecker, G. F.; Mulzer, J.; Hering, S. *Br. J. Pharmacol.* **2010**, *161*, 65–78.

(50) Kopp, S.; Baur, R.; Sigel, E.; Mohler, H.; Altmann, K. H. *Chem. Med. Chem.* **2010**, *5*, 678–81.

(51) Khom, S.; Baburin, I.; Timin, E. N.; Hohaus, A.; Sieghart, W.; Hering, S. *Mol. Pharmacol.* **2006**, *69*, 640–9.

(52) Abel, G. *Planta Med.* **1987**, *53*, 251–253.

(53) Goeggelmann, W.; Schirmer, O. *Mutat. Res.* **1983**, *121*, 191–194.

(54) Taylor, J. M.; Jones, W. I.; Hagan, E. C.; Gross, M. A.; Davis, D. A.; Cook, E. L. *Toxicol. Appl. Pharmacol.* **1967**, *10*, 405.

(55) Malhotra, C. L.; Das, P. K.; Dhalla, N. S. *Arch. Int. Pharmacodyn. Ther.* **1962**, *138*, 537–547.

(56) Mukherjee, P. K.; Kumar, V.; Mal, M.; Houghton, P. J. *Pharm. Biol.* **2007**, *45*, 651–666.

(57) Lipinski, C. A.; Lombardo, F.; Dominy, B. W.; Feeney, P. J. *Adv. Drug Delivery Rev.* **1997**, *23*, 3–25.

(58) Fluegge, J. *Grundlagen der Polarimetrie*; Zeiss Verlag: Oberkochen, Ost-Württemberg, 1970; pp 62, 88.

(59) Frisch, M. J.; Trucks, G. W.; Schlegel, H. B.; Scuseria, G. E.; Robb, M. A.; Cheeseman, J. R.; Montgomery, J. A. Jr.; Vreven, T.; Kudin, K. N.; Burant, J. C.; Millam, J. M.; Iyengar, S. S.; Tomasi, J.; Barone, V.; Mennucci, B.; Cossi, M.; Scalmani, G.; Rega, N.; Petersson, G. A.; Nakatsuji, H.; Hada, M.; Ehara, M.; Toyota, K.; Fukuda, R.; Hasegawa, J.; Ishida, M.; Nakajima, T.; Honda, Y.; Kitao, O.; Nakai, H;. Klene, M.; Li, X.; Knox, J. E.; Hratchian, H. P.; Cross, J. B.; Bakken, V.; Adamo, C.; Jaramillo, J.; Gomperts, R.; Stratmann, R. E.; Yazyev, O.; Austin, A. J.; Cammi, R.; Pomelli, C.; Ochterski, J. W.; Ayala, P. Y.; Morokuma, K.; Voth, G. A.; Salvador, P.; Dannenberg, J.J.; Zakrzewski, V. G.; Dapprich, S.; Daniels, A. D.; Strain, M. C.; Farkas, O.; Malick, D. K.; Rabuck, A. D.; Raghavachari, K.; Foresman, J. B.; Ortiz, J. V.; Cui, Q.; Baboul, A. G.; Clifford, S.; Cioslowski, J.; Stefanov, B. B.; Liu, G.; Liashenko, A.; Piskorz, P.; Komaromi, I.; Martin, R. L.; Fox, D. J.; Keith, T.; Al-Laham, M. A.; Peng, C. Y.; Nanayakkara, A.; Challacombe, M.; Gill, P. M. W.; Johnson, B.; Chen, W.; Wong, M. W.; Gonzalez, C.; Pople, J. A. *Gaussian 03*, Revision E.01; Gaussian, Inc.: Wallingford, CT, 2004.

(60) Bringmann, G.; Bruhn, T.; Makismenka, K.; Hemberger, Y. *Eur. J. Org. Chem.* **2009**, *17*, 2717–2727.

(61) Methfessel, C.; Witzemann, V.; Takahashi, T.; Mishina, M.; Numa, S.; Sakmann, B. *Pflug. Arch. Eur. J. Phys.* **1986**, *407*, 577–588.

(62) Krampfl, K.; Wolfes, H.; Dengler, R.; Bufler, J. *Eur. J. Pharmacol.* **2002**, *435*, 1–8.

SUPPORTING INFORMATION

Positive GABA$_A$ Receptor Modulators from *Acorus calamus* L. and Structural Analysis of (+)-Dioxosarcoguaiacol by 1D and 2D NMR and Molecular Modeling

Janine Zaugg[†], Eva Eickmeier[†], Samad Ebrahimi[†], Igor Baburin[‡], Steffen Hering[‡], and Matthias Hamburger*[,†]

[†]Division of Pharmaceutical Biology, University of Basel, Klingelbergstrasse 50, 4056 Basel, Switzerland

[‡]Departement of Pharmacology and Toxicology, University of Vienna, Althanstrasse 14, 1090 Vienna, Austria

*To whom correspondence should be addressed. Tel: +41 61 267 1425. Fax: +41 61 267 1474. E-mail: matthias.hamburger@unibas.ch

Table S1. Spectral characterization data for (**1**) (NMR spectra recorded in CDCl₃)

β-Asarone
CAS Nr.: 5273-86-9
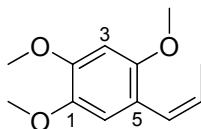
m/z (ESITOFMS)   231. 0998 [M+Na$^+$]   (Calc.: 231.0992)

position	δ_C ^{a,b}	δ_H (I, m, J in Hz)^a
1	142.6	-
1-OCH₃	56.5	3.57 (CH₃, s)
2	148.9	-
2-OCH₃	55.8	3.6 (CH₃, s)
3	98.4	6.30 (CH, s)
4	151.8	-
4-OCH₃	56.0	3.52 (CH₃, s)
5	118.0	-
5-**CH**=CHCH₃	124.9	6.28 (CH, dq, 11.5, 2.0)
5-CH=**CH**CH₃	124.8	5.49 (CH, dq, 11.5, 7.0)
5-CH=CH**CH₃**	14.3	1.61 (CH₃, dd, 7.0, 2.0)
6	115.0	6.64 (CH, s)

^{a}Reference data can be found in A. Patra et al., J. Nat. Prod. 1981, 44, 668-669
^{b}Calculated ^{13}C shift of HSQC- and HMBC-NMR experiments. Spin systems evaluated by HSQC-NMR experiment

Table S2. Spectral characterization data for (**3**) (NMR spectra recorded in CDCl$_3$)

(+)-Shyobunone
CAS Nr.: 21698-44-2
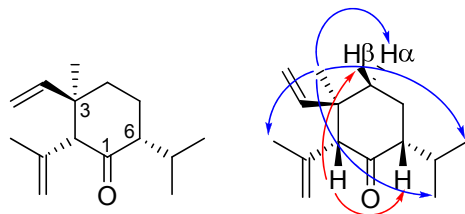
Relative configuration detected by 1D NOE NMR. Critical correlations highlighted by red and blue arrows.

| *m/z* (ESITOFMS) | 243.1722 [M+Na$^+$] | (Calc.: 243.1719) |

$[\alpha]_D$ (21.4°C)   +100° (*c* = 0.19, CHCl$_3$)[a]

position	δ_C [b,c]	δ_H (I, m, *J* in Hz)[c]
1	209.6	-
2	66.9	2.99 (CH, s)
2-**C**CH$_2$CH$_3$	139.7	-
2-C**CH$_2$**CH$_3$	116.5	4.70 (CH$_2$, s)
		4.93 (CH$_2$, s)
2-CCH$_2$**CH$_3$**	24.1	1.70 (CH$_3$, s)
3	46.2	-
3-CH$_3$	18.9	0.98 (CH$_3$, s)
3-**CH**CH$_2$	146.6	5.76 (CH, dd, 11.0, 17.8)
3-CH**CH$_2$**	110.7	4.89 (CH$_2$, dd, 11.0, 1.0)
		4.91 (CH$_2$, dd, 17.8, 1.0)
4	39.3	Hα: 1.56, CH$_2$, m
		Hβ: 1.86, CH$_2$, ddd (5.2, 13.2, 13.2)
5	24.8	1.59 (CH$_2$, m)
		1.96 (CH$_2$, m)
6	56.4	2.09 (CH, m)
6-**CH**(CH$_3$)$_2$	26.3	2.09 (CH, m)
6-CH(**CH$_3$)$_2$**	18.3	0.82 (CH$_3$, d, 6.4)
6-CH(**CH$_3$)$_2$**	21.0	0.86 (CH$_3$, d, 6.4)

[a]No reference value could be found in literature. Relative configuration detected by 1D NOE NMR experiments. Important correlations highlighted by red (plain) and blue (dashed) arrows.
[b]Calculated ^{13}C shift of HSQC-NMR and HMBC-NMR experiments. Spin systems evaluated by HSQC- NMR experiment
[c]Reference data can be found in P. Weyerstahl et al. Liebigs Ann. Chem. 1987, 2, 89-101

Table S3. Spectral characterization data for (**4**) (NMR spectra recorded in CDCl$_3$)

(+)-Preisocalamenediol
CAS Nr.: 25645-19-6
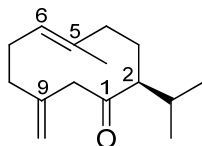
m/z (ESITOFMS)   243.1731 [M+Na$^+$]   (Calc.: 243.1719)

[α]$_D$ (20.3°C)   +61.6° (*c* = 0.71, CHCl$_3$)[a]

position	δ$_C$ [b,c]	δ$_H$ (I, m, *J* in Hz)[a]
1	207.2	-
2	60.0	2.20 (CH, ddd, 1.0, 4.9, 10.9)
2-**CH**(CH$_3$)$_2$	30.5	1.61 (CH, m)
2-CH(**CH$_3$)$_2$**	19.5	0.82 (CH$_3$, d, 6.9)
	20.5	0.77 (CH$_3$, d, 6.9)
3	28.2	1.43 (CH$_2$, dm, 13.5)
		2.03 (CH$_2$, m)
4	40.6	1.75 (CH$_2$, dt, 3.4, 12.8)
		1.98 (CH$_2$, m)
5	137.9	-
6	125.6	5.15 (CH, dd, 3.0, 10.7)
7	29.2	1.96 (CH$_2$, m)
		2.11 (CH$_2$, m)
8	36.7	1.94 (CH$_2$, m)
		2.27 (CH$_2$, m)
9	142.6	-
10	53.4	2.85 (CH$_2$, d, 14.8)
		3.21 (CH$_2$, d, 14.8)
5-CH$_3$	15.2	1.30 (CH$_3$, s)
9=CH$_2$	116.5	4.77 (CH$_2$, s)
		4.90 (CH$_2$, s)

[a]Reference value can be found in C. Zdero et al. Phytochemistry 1989, 28, 531-542
[b]Calculated ^{13}C shift of HSQC- and HMBC-NMR experiments. Spin systems evaluated by HSQC-NMR experiment
[c]Reference data can be found in D.M. Delvalle et al. Planta Med. 1987, 87, 230.

Table S4. Spectral characterization data for (**5**) (NMR spectra recorded in CDCl$_3$)

(-)-Isoshyobunone
CAS Nr.: 21698-46-4
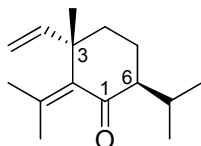
m/z (ESITOFMS)	243.1730 [M+Na$^+$]	(Calc.: 243.1719)

$[\alpha]_D$ (21.5°C)   -156° (*c* = 0.61, CHCl$_3$)[a]

position	δ_C [b, c]	δ_H (I, m, *J* in Hz)[b,c]
1	209.4	-
2	140.1	-
3	44.4	-
4	39.3	1.33 (CH$_2$, ddd, 14.0, 6.8, 3.6)
		1.44 (CH$_2$, ddd, 14.0, 10.7, 3.3)
5	21.4	1.79 (CH$_2$, m)
		1.60 (CH$_2$, m)
6	55.2	2.11 (CH, ddd, 9.0, 9.0, 6.3)
2-**C**(CH$_3$)	146.6	-
2-C(**CH$_3$)$_2$**	23.5	1.69 (CH$_3$, s)
	24.2	1.74 (CH$_3$, s)
3-CH$_3$	24.5	1.29 (CH$_3$, s)
3-**CH**CH$_2$	146.4	5.83 (CH, dd, 10.4, 17.9)
3-CH**CH$_2$**	110.7	4.91 (CH$_2$, dd, 10.4, 1.2)
		4.90 (CH$_2$, dd, 17.9, 1.2)
6-**CH**(CH$_3$)$_2$	29.4	2.00 (CH, m)
6-CH(**CH$_3$)$_2$**	18.4	0.79 (CH3, d, 6.8)
	20.6	0.84 (CH3, d, 6.8)

[a]Reference value can be found in M. Niwa et al. Chem. Lett. 1977, 12, 1415-1418
[b]Calculated ^{13}C shift of HSQC- and HMBC-NMR experiments. Spin systems evaluated by HSQC-NMR experiment
[c]Reference data can be found in P. Weyerstahl et al. Liebigs Ann. Chem. 1987, 2, 89-101

Table S5. Spectral characterization data for (**6**) (NMR spectra recorded in CDCl$_3$)

(-)-Acorenone
CAS Nr.: 5956-05-8
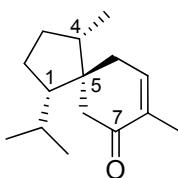
| *m/z* (ESITOFMS) | 243.1730 [M+Na$^+$] | (Calc.: 243.1719) |

[α]$_D$ (21.5°C)   -27° (*c* = 0.37, CHCl$_3$)[a]

position	δ$_C$ [a, b]	δ$_H$ (I, m, *J* in Hz)[a, c]
1	56.9	1.24 (CH, m)
1-**CH**(CH$_3$)$_2$	28.9	1.49 (CH, o, 6.5)
1-CH(**CH$_3$)$_2$**	21.5	0.73 (CH$_3$, d, 6.8)
	24.0	0.84 (CH$_3$, d, 6.8)
2	25.4	1.24 (CH$_2$, m)
		1.60 (CH$_2$, m)
3	29.9	1.14 (CH$_2$, m)
		1.57 (CH$_2$, m)
4	47.0	1.57 (CH, m)
4-CH$_3$	16.1	0.70 (CH$_3$, d, 6.8)
5	47.9	-
6	38.8	2.16 (CH$_2$, d, 16.6)
		2.21 (CH$_2$, d, 16.6)
7	200.3	-
8	134.6	-
8-CH$_3$	15.6	1.63 (CH$_3$, s)
9	144.4	6.54 (CH, s)
10	37.4	2.01 (CH$_2$, dm, 19.9)
		2.53 (CH$_2$, dm, 19.9)

[a]Reference value can be found in S.W. Baldwin et al., Tetrahedron Lett. 1982, 23, 1235-1238
[b]Calculated ^{13}C shift of HSQC- and HMBC-NMR experiments. Spin systems evaluated by HSQC-NMR experiment
[c]Reference data can be found in W. Rascher et al., Tetrahedron, 33, 575-577
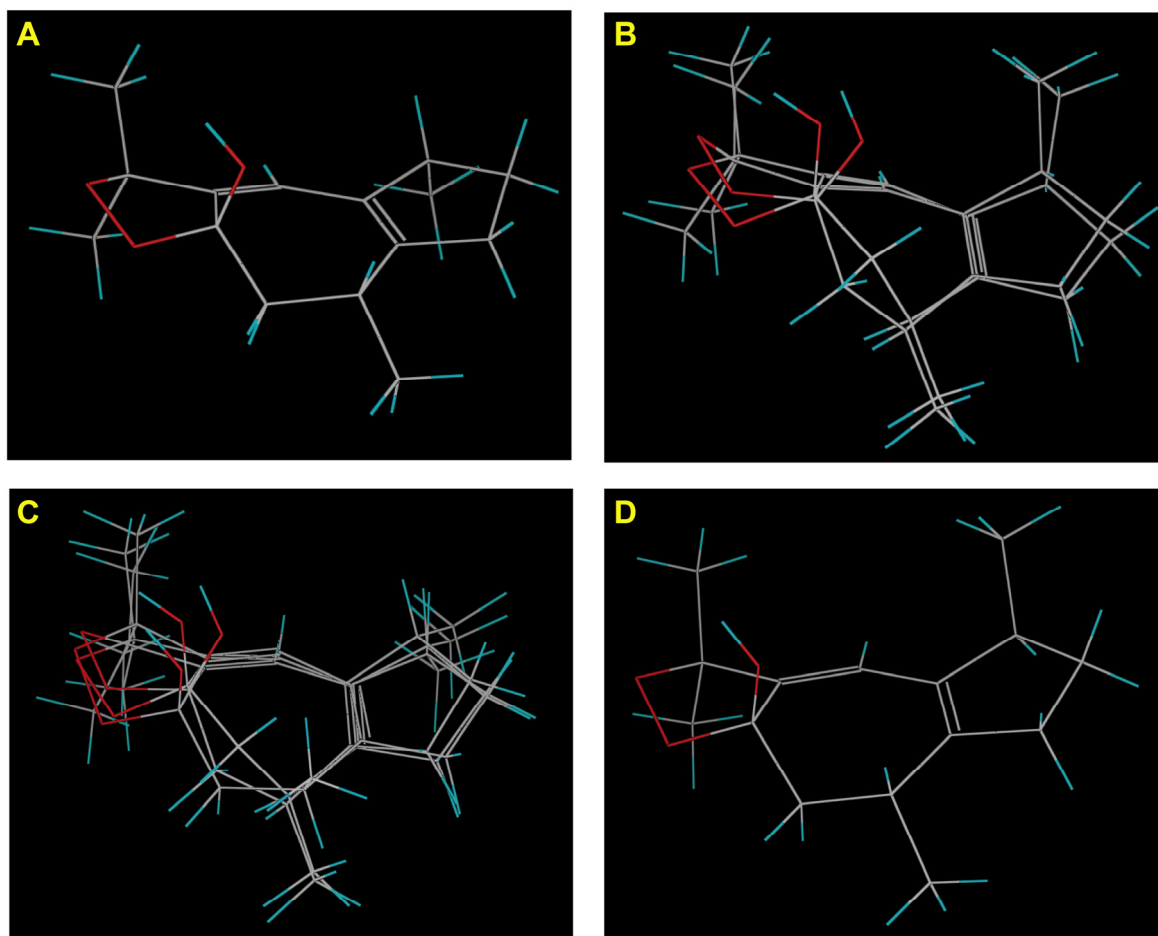
Figure S1: Predominant conformers of the four possible stereoisomers of (+)-dioxosarcoguaiacol (**2**) within a 1 kcal/mol energy window from the particular global minimum. Conformational analysis was performed at the OPLS_2005 level in chloroform. A: 4*R**8*S**10*R**, B: 4*S**8*S**10*S**, C: 4*R**8*S**10*S**, D: 4*S**8*S**10*R**

Table S6. Comparison of NMR Data ($^3J_{HH}$-Coupling Constants and NOESY Correlations) with Geometrically Optimized Conformers of the Four Stereoisomers of (+)-Dioxosarcoguaiacol (**2**)

NMR observations	Matching geometrically optimized conformers[a]			
	4R*8S*10R*	4S*8S*10R*	4R*8S*10S*	4S*8S*10S*
$J_{2b,3b} = 0$ Hz , NOESY: H-3b ↔ H-2a	**yes**	yes	yes	yes
$J_{9b,10} = 5.2$ Hz, $J_{9a,10} = 13.4$ Hz	**yes**	yes	yes	yes
NOESY: H-6 ↔ H-12,13	**yes**	yes	no	no
NOESY: H-2a ↔ H-15	**yes**	yes	no	no
NOESY: H-3a ↔ H-4, H-3b ↔ H-14	**yes**	no	no	yes

[a]Conformers were found by conformational analysis in $CHCl_3$ and further geometrically optimized based on Density function theory (DFT) on the B3LYP/6-31G* level in gas-phase.
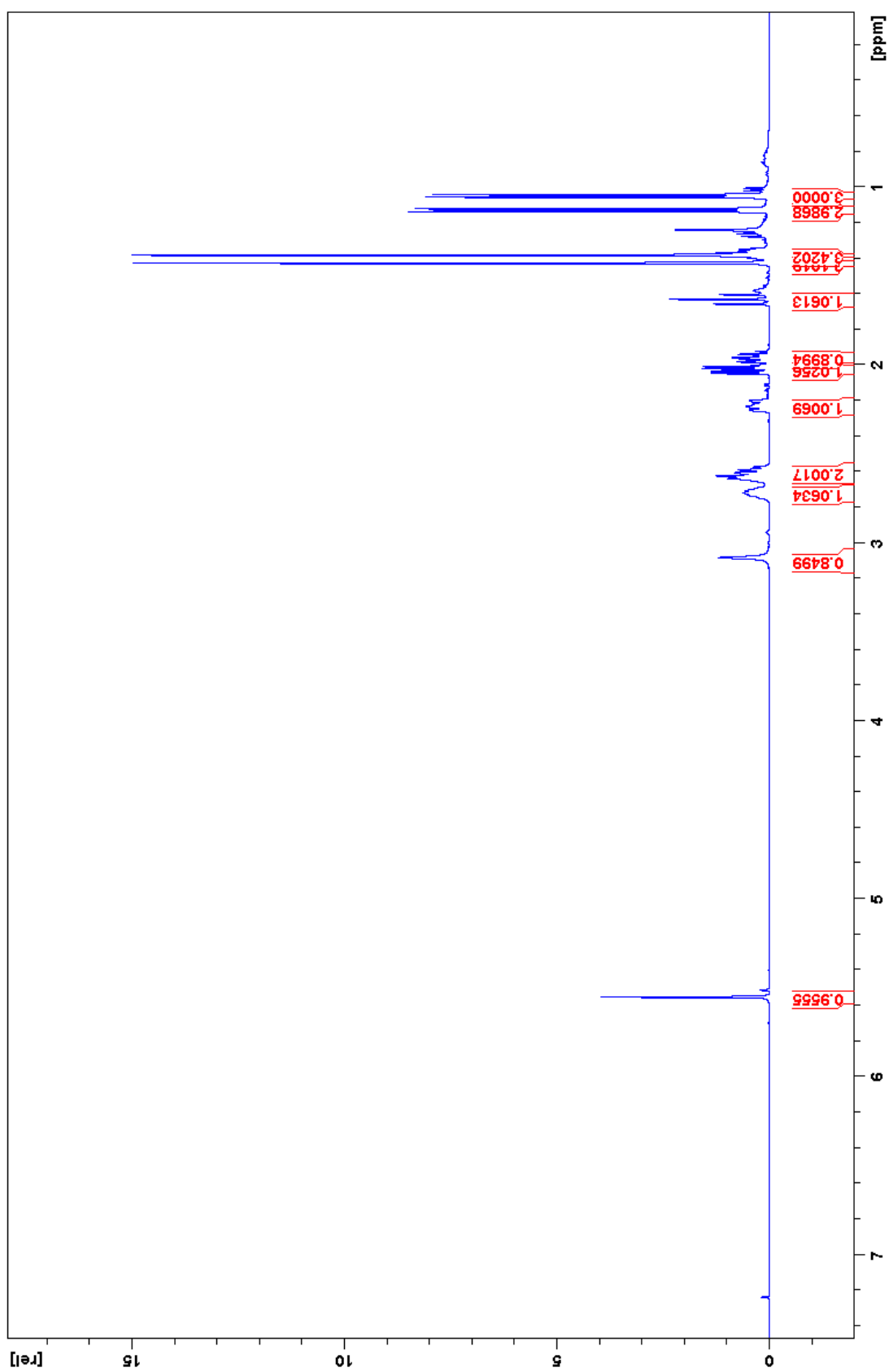
Figure S2. ^{1}H-NMR spectrum of (**2**) (NS: 64, DS: 2, CDCl$_3$).
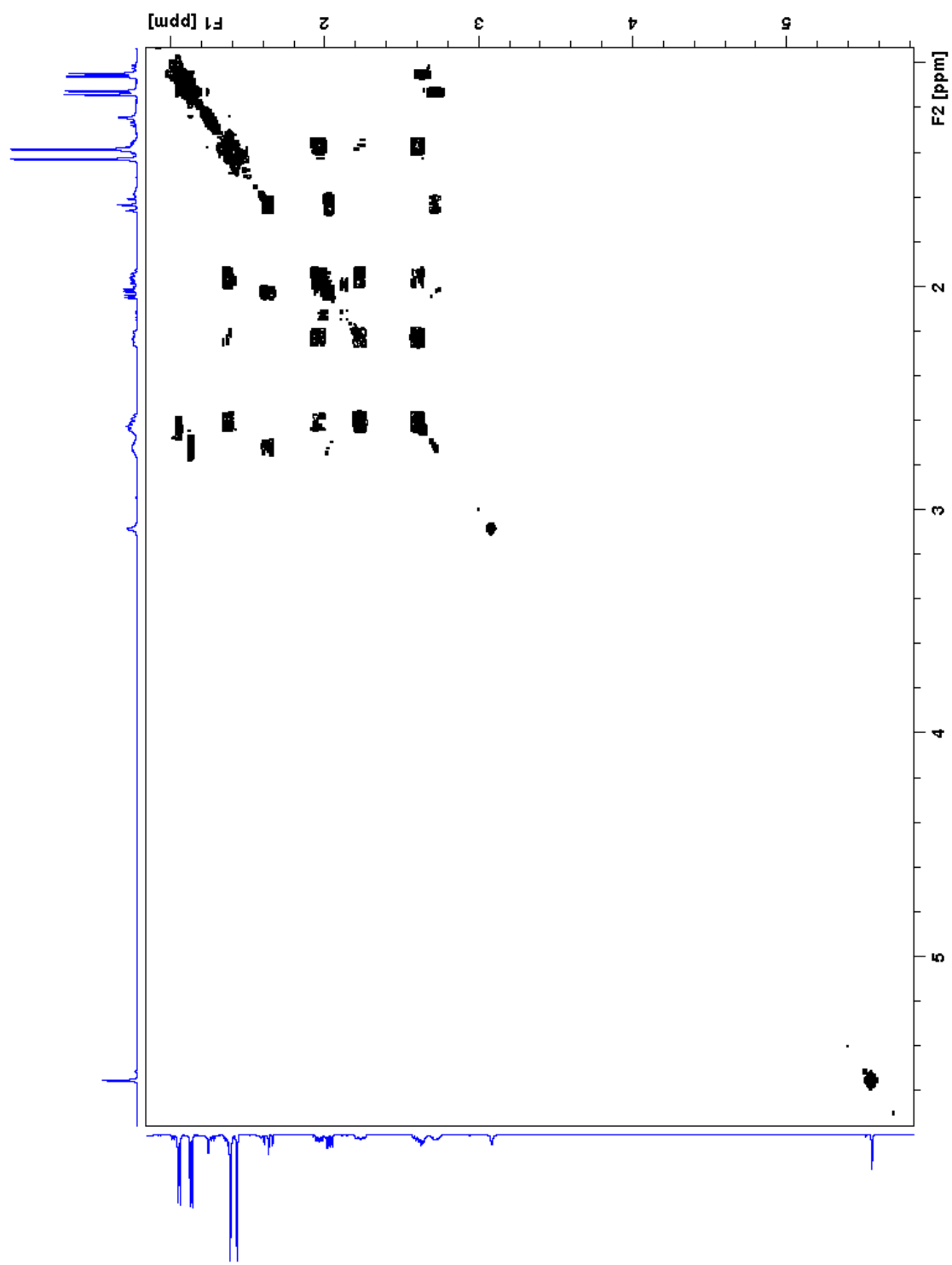
Figure S3. COSY-NMR spectrum (*cosygpqf*, NS: 4, DS: 8) of (**2**) in CDCl$_3$.
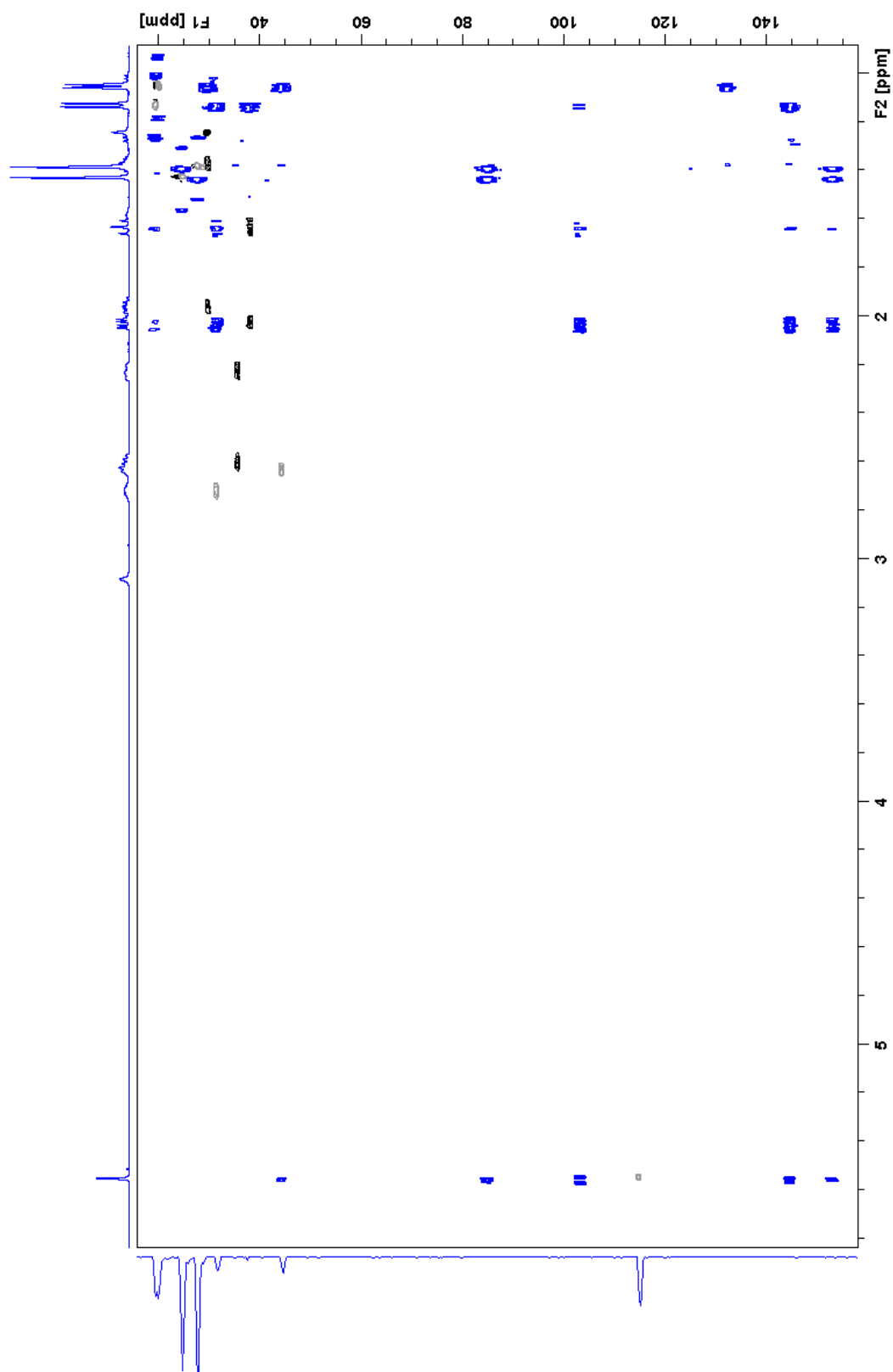
Figure S4. Overlay of DEPTedited HSQC-NMR spectrum (*hsqcedetgp*, NS: 8, DS: 16; black/grey) and HMBC spectrum (*hmbcgp*, NS: 128, DS: 16, optimized for 10 Hz; blue) of (**2**) in CDCl$_3$.
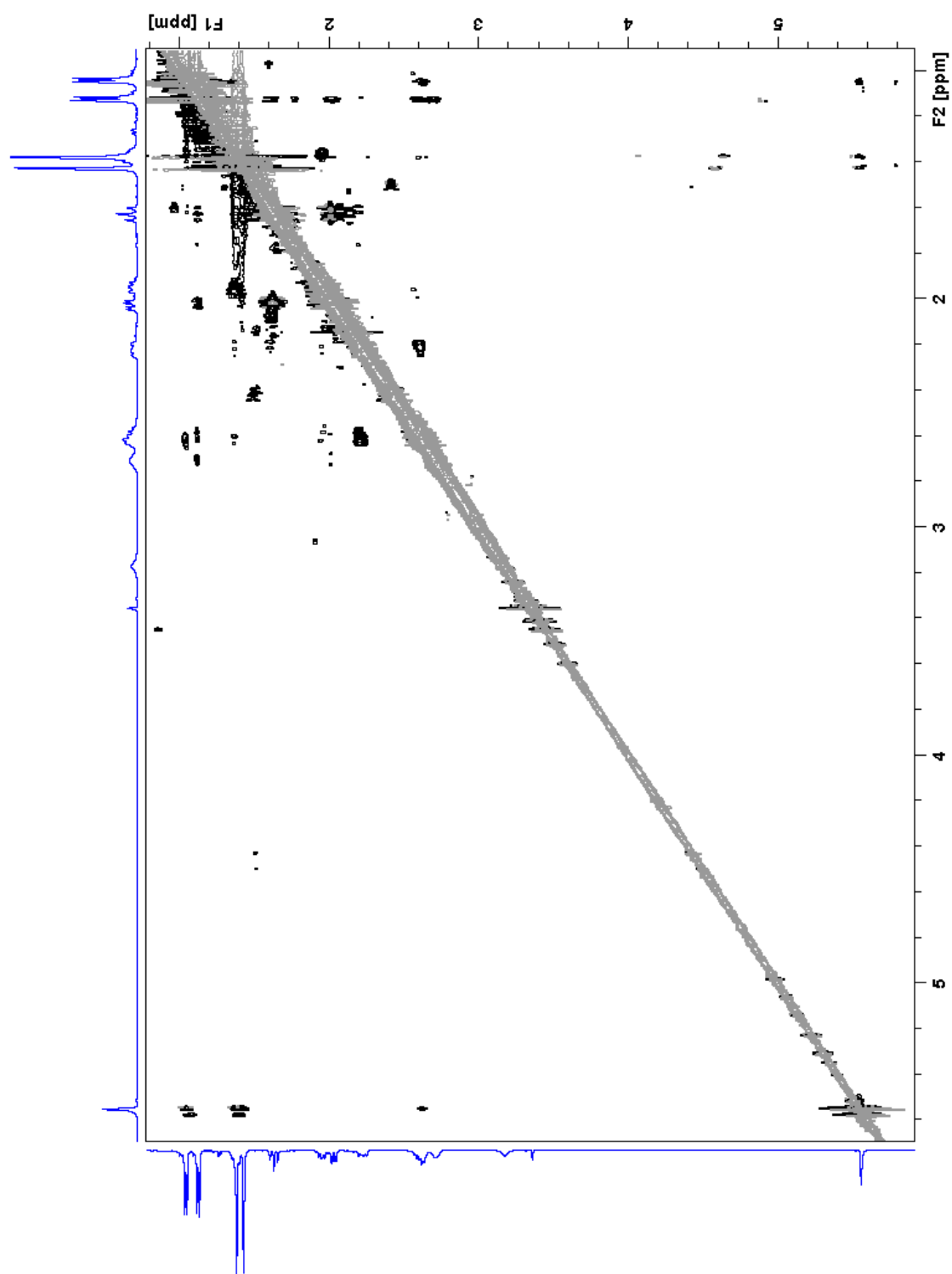
Figure S5. NOESY NMR spectrum (*noesygpphpp*, NS: 32, DS: 16, mixing time 0.75 s) of (**2**) in CDCl₃.

3.4. IDENTIFICATION AND CHARACTERIZATION OF GABA$_A$ RECEPTOR MODULATORY DITERPENES FROM *BIOTA ORIENTALIS* THAT DECREASE LOCOMOTOR ACTIVITY IN MICE

Zaugg J, Khom S, Eigenmann D, Baburin I, Hamburger M, Hering S.
J Nat Prod 2011; 74, 1764-1772.
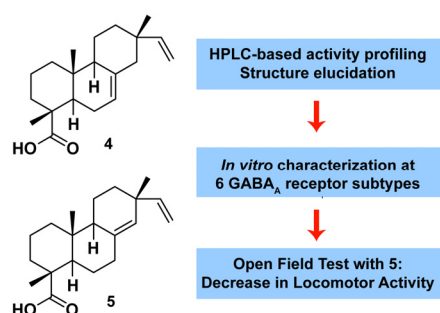
Apart from identification of a new natural product, sandaracopimaric acid and isopimaric acid were identified as main positive GABA$_A$ receptor modulating constituents of *B. orientalis* twigs and leaves. The diterpenes were characterized at six different GABA$_A$ receptor subtypes in a functional assay using *Xenopus* oocytes. Sandaracopimaric acid was tested in the Open Field Test in mice for measuring *in vivo* pharmacological effects.

Daniela Eigenmann did upscaled extraction of plant material, isolation of compounds, recording and interpretation of analytical data for structure elucidation (HPLC-PDA-ESI-TOF-MS, microprobe NMR) as part of her master's thesis under my direct supervision. HPLC microfractionation, Xenopus surgery, preparation of oocytes for electrophysiological measurements, two-microelectrode voltage clamp studies with sandaracopimaric acid and isopimaric acid, data analysis, writing of the manuscript, and preparation of figures (except for Fig. 5) were my contribution to this publication.

Janine Zaugg

Identification and Characterization of GABA$_A$ Receptor Modulatory Diterpenes from *Biota orientalis* That Decrease Locomotor Activity in Mice

Janine Zaugg,[†,§] Sophia Khom,[‡,§] Daniela Eigenmann,[†] Igor Baburin,[‡] Matthias Hamburger,[*,†] and Steffen Hering[‡]

[†]Division of Pharmaceutical Biology, University of Basel, Klingelbergstrasse 50, 4056 Basel, Switzerland

[‡]Institute of Pharmacology and Toxicology, University of Vienna, Althanstrasse 14, 1090 Vienna, Austria

S *Supporting Information*

ABSTRACT: An ethyl acetate extract of *Biota orientalis* leaves potentiated GABA-induced control current by 92.6% ± 22.5% when tested at 100 μg/mL in *Xenopus laevis* oocytes expressing GABA$_A$ receptors ($\alpha_1\beta_2\gamma_{2S}$ subtype) in two-microelectrode voltage clamp measurements. HPLC-based activity profiling was used to identify isopimaric acid (**4**) and sandaracopimaric acid (**5**) as the compounds largely responsible for the activity. Sandaracopimar-adienolal (**3**) was characterized as a new natural product. Compounds **4** and **5** were investigated for GABA$_A$ receptor subtype selectivity at the subtypes $\alpha_1\beta_1\gamma_{2S}$, $\alpha_1\beta_2\gamma_{2S}$, $\alpha_1\beta_3\gamma_{2S}$, $\alpha_2\beta_2\gamma_{2S}$, $\alpha_3\beta_2\gamma_{2S}$, and $\alpha_5\beta_2\gamma_{2S}$. Sandaracopimaric acid (**5**) was significantly more potent than isopimaric acid (**4**) at the GABA$_A$ receptor subtypes $\alpha_1\beta_1\gamma_{2S}$, $\alpha_2\beta_2\gamma_{2S}$, and $\alpha_5\beta_2\gamma_{2S}$ (EC$_{50}$ **4**: 289.5 ± 82.0, 364.8 ± 85.0, and 317.0 ± 83.7 μM vs EC$_{50}$ **5**: 48.1 ± 13.4, 31.2 ± 4.8, and 40.7 ± 14.7 μM). The highest efficiency was reached by **4** and **5** on α_2- and α_3-containing receptor subtypes. In the open field test, ip administration of **5** induced a dose-dependent decrease of locomotor activity in a range of 3 to 30 mg/kg body weight in mice. No significant anxiolytic-like activity was observed in doses between 1 and 30 mg/kg body weight in mice.

HPLC-based activity profiling
Structure elucidation

In vitro characterization at 6 GABA$_A$ receptor subtypes

Open Field Test with **5**: Decrease in Locomotor Activity
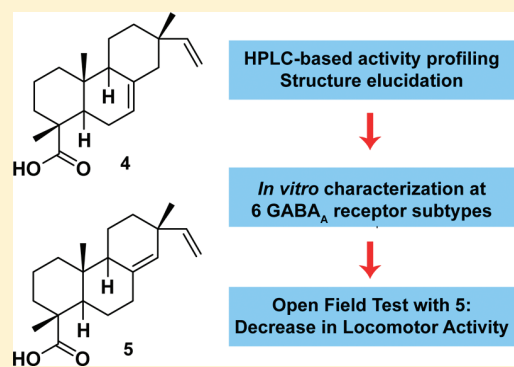
amma-aminobutyric acid (GABA) is the major inhibitory neurotransmitter in the central nervous system (CNS). GABA binding to the GABA$_A$ receptor leads to opening of the intrinsic chloride ion channel. This causes a hyperpolarization of the neuronal membrane and thus to an inhibition of further action potential triggering.[1,2] The quaternary structure of the GABA$_A$ receptor is an assembly of five varying subunits. The human genome encodes for 19 subunits, namely, α_{1-6}, β_{1-3}, γ_{1-3}, ρ_{1-3}, δ, ϵ, π, and θ, which may combine into numerous heteropentamers.[3] So far, 11 GABA$_A$ receptor subtypes with distinct pharmacological properties are known to be expressed in human neurons.[4,5] CNS-related diseases such as insomnia, anxiety, and epilepsy are often treated with GABA$_A$ receptor modulating drugs, such as benzodiazepines or barbiturates, which, however, suffer from various side-effects.[6]

We screened a library consisting of 982 plant and fungal extracts for GABA$_A$ receptor modulatory activity with the objective of identifying new scaffolds for the target. For this purpose, we used an automated, functional, two-microelectrode voltage clamp assay with *Xenopus* oocytes[7] that transiently expressed rat GABA$_A$ receptors of the subunit composition $\alpha_1\beta_2\gamma_{2S}$. An ethyl acetate extract of *Biota orientalis* (L.) Endl. (Cupressaceae) leaves and twigs showed promising activity.

B. orientalis originates from Eastern Asia,[8] but nowadays is also widely cultivated in Europe. In addition to various flavonoids, phenylpropanoids, and some lignans, over 100 different terpenoids have been identified from *B. orientalis* (a synoptical table with secondary metabolites identified in *B. orientalis* is provided as Supporting Information).[8−28] The crude drug consisting of leaves and twigs is known as Cebaye in China and is one of the 50 fundamental herbs of traditional Chinese medicine (TCM). It is used to treat disorders such as diarrhea, respiratory malfunction,[29−31] gout, rheumatism, leukotrichia, and alopecia.[32] The TCM drug Baiziren consists of seeds of *B. orientalis* and is prescribed, among other indications, to treat anxiety.[31]

HPLC-based activity profiling is a miniaturized and highly effective approach for rapid dereplication and characterization of bioactive natural products in extracts[33] and can be combined with various cell-based and biochemical assays.[34−40] We recently developed and validated a profiling protocol for the discovery of new GABA$_A$ receptor ligands,[41] which was successfully applied in the investigation of several active plant extracts.[42−46] Here we report the structural elucidation of a new diterpene, sandaraco-pimaradienolal (**3**), and the identification of isopimaric acid (**4**) and sandaracopimaric acid (**5**) as GABA$_A$ receptor modulatory constituents via HPLC-based activity profiling of the active *B. orientalis* extract. The GABA$_A$ receptor subtype specificity of **4** and **5** was characterized at receptors of the composition $\alpha_1\beta_1\gamma_{2S}$,
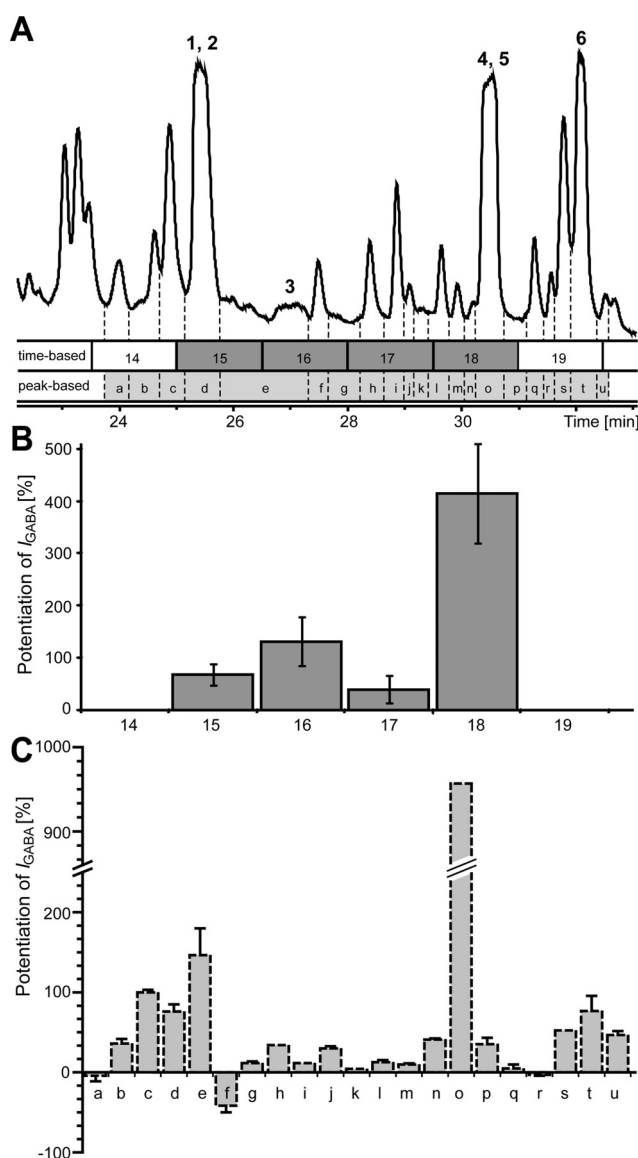
Figure 1. HPLC-based activity profiling of *Biota orientalis* ethyl acetate extract. Part A shows critical time window of a semipreparative HPLC separation (10 mg of extract, detection at 210 nm). Time windows of the time-based microfractionation (90 s each) are highlighted in dark gray, and corresponding potentiation of GABA-induced control current by fractions 14–19 is shown in B. Subsequent peak-based fractionation is shown in light gray bars in A, and potentiation of GABA-induced control current by peak-based microfractions *a*–*u* is displayed in C.

$\alpha_1\beta_2\gamma_{2S}$, $\alpha_1\beta_3\gamma_{2S}$, $\alpha_2\beta_2\gamma_{2S}$, $\alpha_3\beta_2\gamma_{2S}$, and $\alpha_5\beta_2\gamma_{2S}$, and the most potent compound, sandaracopimaric acid (**5**), was examined in a mouse model by means of the open field test.

■ RESULTS AND DISCUSSION

Extracts were screened by means of an automated, fast perfusion system used for two-microelectrode voltage clamp measurements in *Xenopus* oocytes that expressed functional GABA$_A$ receptors with the subunit composition $\alpha_1\beta_2\gamma_{2S}$.[7] When tested at 100 μg/mL, an ethyl acetate extract of *B. orientalis* leaves and twigs enhanced the GABA-induced chloride ion current (I_{GABA}) by 92.6% ± 22.5%. To localize the activity within the

extract, we performed an HPLC-based activity profiling after a validated protocol.[41] The relevant time window of the chromatogram (210 nm) from a semipreparative HPLC separation (10 mg of extract, 28 microfractions of 90 s each) is shown in Figure 1A. GABA$_A$ receptor modulatory activity was concentrated in fractions 15 to 18 (Figure 1A, dark gray bar). Fraction 18 induced the strongest potentiation of I_{GABA} (414.5% ± 95.3%), and fractions 15, 16, and 17 enhanced GABA-induced chloride currents by 67.6% ± 21.0%, 131.5% ± 47.3%, and 39.2% ± 25.8%, respectively (Figure 1B). The active region of the chromatogram was rather complex, and the time-based fractionation did not provide the necessary resolution to track the active peaks. This was achieved by a peak-based fractionation. Peak-based fractions *a*–*u* are shown in Figure 1A by a light gray bar, and the corresponding activity profile is given in Figure 1C. The high activity of time-based fraction 18 could thus be assigned to peak *o* (potentiation of I_{GABA} by 956.9% ± 0.0%). Fraction 16 was resolved into peaks *e*, *f*, and *g*. However, only *e* showed an appreciable potentiation of I_{GABA} (146.45% ± 33.3%). Fraction 15 corresponded to part of peak *e*, to *d*, and to part of *c*. Moderate activity was found in *c* and *d* (potentiation of I_{GABA} by 100.0% ± 3.0% and 76.1% ± 8.9%, respectively). Although time-based fractions 14 and 19 did not show any activity, the corresponding peak-based microfractions were collected and tested. Moderate activity was found in peak-based fraction *t* (enhancement of I_{GABA} by 76.6% ± 18.8%).

For structure elucidation and for further pharmacological testing, compounds corresponding to the active peaks were purified at preparative scale. Liquid–liquid extraction of the EtOAc extract, separation on a silica gel MPLC column, and semipreparative RP-HPLC afforded four pure compounds (**1**–**3**, **6**) and an inseparable mixture of **4** and **5**. Structures were established by 1D NMR and 2D NMR experiments as pinusolide (**1**), sandaracopimaradienediol (**2**), totarol (**6**), and a mixture of isopimaric acid (**4**) and sandaracopimaric acid (**5**) in a ratio of 77:23 (^{1}H NMR). Analytical data of **1**, **2**, **4**, **5**, and **6** are provided as Supporting Information. Structural analysis of minor compound **3** revealed a pimaradiene-type diterpene that differed from **2** only by the oxidation state of C-18. Due to its close relationship to **2** and the aldehyde function at C-18, compound **3** was named sandaracopimaradienolal.
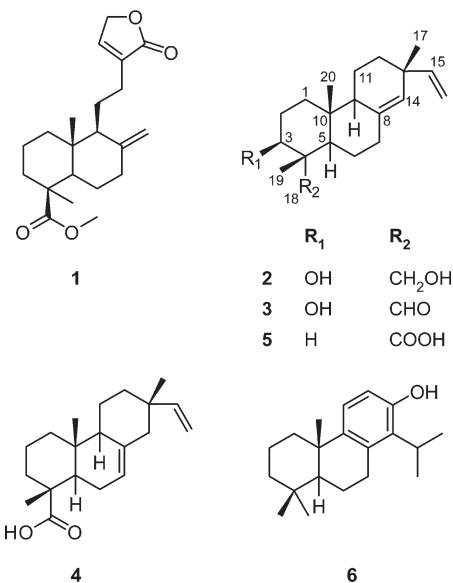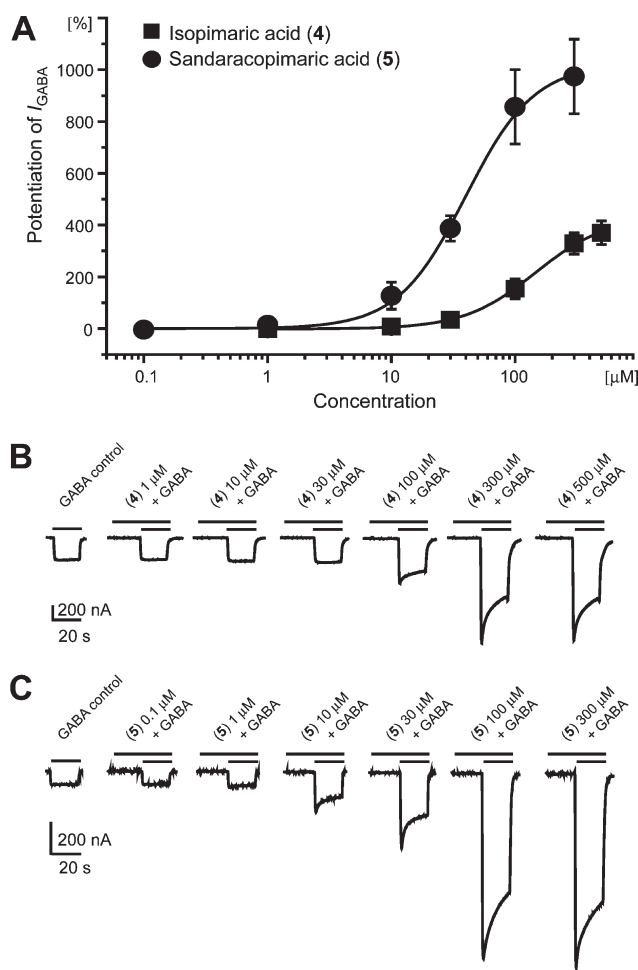
Figure 2. Part A shows concentration—response curves of isopimaric acid (**4**) and sandaracopimaric acid (**5**) at GABA$_A$ receptors of the subunit composition $\alpha_1\beta_2\gamma_{2S}$, using a GABA EC$_{5-10}$. Typical traces for modulation of chloride currents through $\alpha_1\beta_2\gamma_{2S}$ GABA$_A$ receptors without direct activation by **4** and **5** are given in B and C, respectively.

Pure compounds and the isomer mixture were tested at concentrations of 10 and 100 μM in the oocyte assay for a preliminary activity profile at $\alpha_1\beta_2\gamma_{2S}$ receptors. The isomer mixture **4**/**5** potentiated I_{GABA} by 43.9% $\pm$ 1.1% and 318.9% $\pm$ 101.1% at 10 and 100 μM, respectively (n = 2). Rather unexpectedly, none of the other compounds induced a significant potentiation of I_{GABA} at the tested concentrations (10 μM: $-13.4\% \pm 2.0\%$ (**1**), 13.8% $\pm$ 1.3% (**2**), 3.8% $\pm$ 3.8% (**3**), $-10.6\% \pm 4.8\%$ (**6**); 100 μM: $-13.1\% \pm 2.6\%$ (**1**), 7.7% $\pm$ 7.7% (**2**), 3.0% $\pm$ 3.0% (**3**), $-15.1\% \pm 15.1\%$ (**6**) (n = 2)). Therefore, further concentration—response experiments were performed only with **4** and **5**, which were commercially obtained as pure substances. Modulation of I_{GABA} through $\alpha_1\beta_2\gamma_{2S}$ receptors was studied with concentrations ranging from 0.1 to 500 μM. Maximum I_{GABA} potentiation by **4** (425.2% $\pm$ 96.5%, n = 5) was observed at $\sim$500 μM, with an EC$_{50}$ of 141.6 $\pm$ 68.0 μM. Sandaracopimaric acid (**5**) was more potent (EC$_{50}$: 33.3 $\pm$ 8.7 μM) and more efficient than **4** (max. potentiation of I_{GABA}: 855.7% $\pm$ 114.9%, n = 4) (Figure 2; Table 1).

Next, the concentration-dependent I_{GABA} modulation of compounds **4** and **5** was tested on distinct GABA$_A$ receptor subtypes ($\alpha_1\beta_1\gamma_{2S}$, $\alpha_1\beta_3\gamma_{2S}$, $\alpha_2\beta_2\gamma_{2S}$, $\alpha_3\beta_2\gamma_{2S}$, and $\alpha_5\beta_2\gamma_{2S}$) to elucidate potential subunit specificity. As displayed in Figure 3 and summarized in Table 1, sandaracopimaric acid (**5**) showed higher potencies (EC$_{50}$) than isopimaric acid (**4**) on all receptor subtypes, reflected by potency ratios [EC$_{50}$(**4**)/EC$_{50}$(**5**)] of 4.25 ($\alpha_1\beta_2\gamma_{2S}$ receptors) and upward (Table 2). However, only on receptor subtypes $\alpha_1\beta_1\gamma_{2S}$, $\alpha_2\beta_2\gamma_{2S}$, and $\alpha_5\beta_2\gamma_{2S}$ was this difference statistically significant. Moreover, on $\alpha_1\beta_2\gamma_{2S}$ receptors, **5** was twice as efficient in stimulating I_{GABA} compared to **4**, as reflected by the efficiency ratio [I_{max}(**4**)/I_{max}(**5**)] (Table 2). Overall, **5** seemed slightly more efficient, except at subtype $\alpha_1\beta_1\gamma_{2S}$ (differences not statistically significant). The huge discrepancies between potency and efficiency of **4** and **5** are of particular interest in light of the small structural differences between these compounds. The two diterpenes differ only in the position of a double bond ($\Delta^{7,8}$ in **4** vs $\Delta^{8,14}$ in **5**).

However, neither of the compounds exerted significant particular subtype specificity, as reflected by their comparable EC$_{50}$ values at the subtypes of investigation (p > 0.05) (Table 1). The order of efficiency of isopimaric acid (**4**) on GABA$_A$ receptors comprising different α-subunits was $\alpha_1\beta_2\gamma_{2S} \approx \alpha_5\beta_2\gamma_{2S} < \alpha_2\beta_2\gamma_{2S}$ (p < 0.05). The apparently higher efficiency of **4** on $\alpha_3\beta_2\gamma_{2S}$ receptors compared to α_1/α_5-containing subtypes, however, was not statistically significant. A different order of efficiency was observed for **5** with $\alpha_5\beta_2\gamma_{2S} < \alpha_1\beta_2\gamma_{2S} \approx \alpha_2\beta_2\gamma_{2S} \approx \alpha_3\beta_2\gamma_{2S}$ (p-values see Table 1). On GABA$_A$ receptors comprising varying β-subunits, only **5** showed a significant difference in efficiency ($\alpha_1\beta_1\gamma_{2S} < \alpha_1\beta_2\gamma_{2S}$; p < 0.05) (Table 1). When tested at the $\alpha_1\beta_2\gamma_{2S}$ subtype, benzodiazepines (triazolam, midazolam, and clotiazepam) were clearly more potent than **4** and **5** (Table 1). Efficiencies, however, ranged from 253% $\pm$ 12% (triazolam) to 342 $\pm$ 64% (midazolam) potentiation of I_{GABA}[47] and are thus comparable with efficiencies of **4** and **5** (Table 1). To determine a possible dependency on the γ-subunit, which is involved in the benzodiazepine binding site, **4** and **5** were tested on GABA$_A$ receptors comprising α_1 and β_2 subunits only. No significant difference in activity was found between $\alpha_1\beta_2$ and $\alpha_1\beta_2\gamma_{2S}$ subtypes at 30 and 100 μM, which suggested a γ-subunit-independent binding site (Figure 4). Preincubation experiments revealed that neither **4** nor **5** showed direct activation on any of the expressed GABA$_A$ receptor subtypes (Figure 3, parts B, D, F, and H; Figure 4, parts B and D). Therefore, isopimaric acid (**4**) and sandaracopimaric acid (**5**) can be described as positive allosteric GABA$_A$ receptor modulators devoid of direct agonistic activity and particular subtype specificity.

Modulation of GABA$_A$ receptors comprising α_1, α_2, and α_3 subunits by **4** and **5** (Figure 3, Table 1) suggests sedative-like and anxiolytic-like action in vivo (see Mohler et al. 2010 for a recent review).[48] We, therefore, studied the in vivo effects of the more potent compound (**5**) in mice in the open field (OF) test. The OF test is based on the natural behavior of rodents such as an innate fear of open spaces and represents a standard behavioral paradigm for evaluation of anxiolytic-like properties of drugs and for the measurement of locomotor activity.[49] We analyzed the explorative behavior of male c57Bl/6N mice 30 min after intraperitoneal injection of either vehicle (= control) or **5** in the OF test. As illustrated in Figure 5A, ambulation of control mice and mice treated with 1 mg/kg BW **5** did not significantly differ (control: 31.8 $\pm$ 1.7 m, n = 10 vs 1 mg/kg BW: 31.8 $\pm$ 2.3 m, n = 10; p > 0.05). Administration of **5** at a dose of 3 mg/kg BW, however, resulted in significantly reduced ambulation (25.1 $\pm$ 2.0 m, n = 19; p < 0.05), which reached its

Table 1. Potencies and Efficiencies of Compounds 4 and 5 for GABA$_A$ Receptors of Different Subtype Compositions and of Reference Compounds (Benzodiazepines) at the $\alpha_1\beta_2\gamma_{2S}$ Subtype

		Isopimaric Acid (4)		
subtype	EC$_{50}$ [μM]	max. potentiation of I_{GABA} (EC$_{5-10}$) [%](I_{max})	Hill coeff (n_H)[a]	n[b]
$\alpha_1\beta_1\gamma_{2S}$	289.5 ± 82.0	715.9 ± 143.3	1.6 ± 0.2	6
$\alpha_1\beta_2\gamma_{2S}$	141.6 ± 68.0	425.2 ± 96.5[c-h]c	1.6 ± 0.4	5
$\alpha_1\beta_3\gamma_{2S}$	257.0 ± 121.2	475.7 ± 150.9	1.5 ± 0.3	4
$\alpha_2\beta_2\gamma_{2S}$	364.8 ± 85.0	1031.5 ± 173.9[c-h]c,d	1.9 ± 0.3	5
$\alpha_3\beta_2\gamma_{2S}$	724.1 ± 340.7	1074.0 ± 370.5	1.2 ± 0.1	6
$\alpha_5\beta_2\gamma_{2S}$	317.0 ± 83.7	472.2 ± 93.7[c-h]d	2.0 ± 0.3	5
		Sandaracopimaric Acid (5)		
subtype	EC$_{50}$ [μM]	max. potentiation of I_{GABA} (EC$_{5-10}$) [%]	Hill coeff (n_H)[a]	n[b]
$\alpha_1\beta_1\gamma_{2S}$	48.1 ± 13.4	501.6 ± 55.7[c-h]e	1.8 ± 0.3	4
$\alpha_1\beta_2\gamma_{2S}$	33.3 ± 8.7	855.7 ± 114.9[c-h]e,f	1.6 ± 0.4	4
$\alpha_1\beta_3\gamma_{2S}$	24.9 ± 6.3	519.7 ± 83.8	2.1 ± 0.5	4
$\alpha_2\beta_2\gamma_{2S}$	31.2 ± 4.8	1093.7 ± 60.1[c-h]g	2.1 ± 0.3	4
$\alpha_3\beta_2\gamma_{2S}$	56.6 ± 10.6	1101.1 ± 97.8[c-h]h	1.7 ± 0.3	5
$\alpha_5\beta_2\gamma_{2S}$	40.7 ± 14.7	512.7 ± 98.3[c-h]f-h	1.6 ± 0.3	6
	Benzodiazepines at $\alpha_1\beta_2\gamma_{2S}$ (Data by Khom et al., 2006)[47]			
compound	EC$_{50}$ [nM]		max. potentiation of I_{GABA} (EC$_{5-10}$) [%]	
triazolam	22 ± 3		253 ± 12	
midazolam	143 ± 88		342 ± 64	
clotiazepam	184 ± 88		260 ± 27	

[a] Indicates the slope of the concentration−response curve at the EC$_{50}$. Hill coefficients > 1 indicate positive cooperativity during ligand binding.[69] [b] Number of experiments. [c-h] Each letter separately shows significantly different efficiencies ([c-e]$p < 0.05$, [f]$p = 0.06$, [g,h]$p < 0.01$).

maximum at a dose of 30 mg/kg BW (22.3 ± 1.2 m; n = 17; $p < 0.05$). Control mice and mice treated with 1−30 mg/kg BW of **5** spent the same amount of time in the center of the OF (no statistically significant difference observed). Hence no anxiolytic-like effect was observed under influence of **5** (Figure 5B).

With the example of *B. orientalis*, HPLC-based activity profiling led to the identification of two positive GABA$_A$ receptor modulators with a diterpene scaffold that is new for the target. In addition, a new natural product, sandaracopimaradienolal (**3**), was identified. The GABA$_A$ receptor modulation observed with the time-based fractions 15−18 could be located at higher resolution in the peak-based fractions. However, only the compounds responsible for the activity of 18/*o* were finally identified. Further work is required to identify the active compounds located in peak-based microfractions *c*−*e*, *o*, and *t*. A thorough characterization of isopimaric acid (**4**) and sandaracopimaric acid (**5**) at several GABA$_A$ receptor subtypes revealed two novel positive GABA$_A$ receptor modulators with virtually the same efficiencies but varying potencies at the investigated subtypes. The two diterpenes differ only in the position of a double bond ($\Delta^{7,8}$ in **4** vs $\Delta^{8,14}$ in **5**), which seems to affect potency rather than efficiency. Future investigation of structurally related diterpenes could, therefore, provide deeper insights on how potency and efficiency relate to structural features of pimarane diterpenoids. Interestingly, activity of **4** and **5** was independent of the γ-subunit, which clearly indicated that both compounds interact with a non-benzodiazepine binding site (Figure 4).

The reduced locomotor activity observed with intraperitoneal administration of **5** may result from an enhancement of the GABAergic system—in particular a positive allosteric modulation of GABA-induced currents and thus an enhanced inhibitory neurotransmission—but might be also due to interaction with completely different molecular targets. Analysis of the EEG or measurement of body temperature upon administration of the compound would substantiate whether the observed decrease of locomotor activity was due to sedation.[50,51] Interestingly, the observed effects of **5** occurred at doses comparable to those of known GABA$_A$ receptor modulators and sedatives such as midazolam or zolpidem.[52,53]

The absence of an anxiolytic-like effect was inconsistent with the in vitro data (high efficiency at α_2- and α_3-containing subtypes) (Figure 3, Table 1). Other behavioral paradigms for anxiolysis might reveal whether the observed decrease in locomotor activity negatively interfered with an anxiolytic-like effect in the OF. Sandaracopimaric acid (**5**) is a molecule with suitable physicochemical properties for oral bioavailability (H-acceptors/donors 2:1, MW 302, cLogP 4.16, rotatable bonds 2).[54] In addition, a relatively small polar surface area of 37.3 Å^2 is favorable for blood-brain-barrier (BBB) penetration.[54,55] However, further studies on metabolism and BBB penetration of **5** are needed. This first preliminary in vivo evaluation was performed with intraperitoneal administration, which circumvents the liver first-pass. Oral administration and comparison with clinically used GABA$_A$ receptor ligands will be needed to determine the therapeutic potential of **5**.

■ EXPERIMENTAL SECTION

General Experimental Procedures. NMR spectra were recorded at target temperature 18 °C on a Bruker Avance III 500 MHz

113
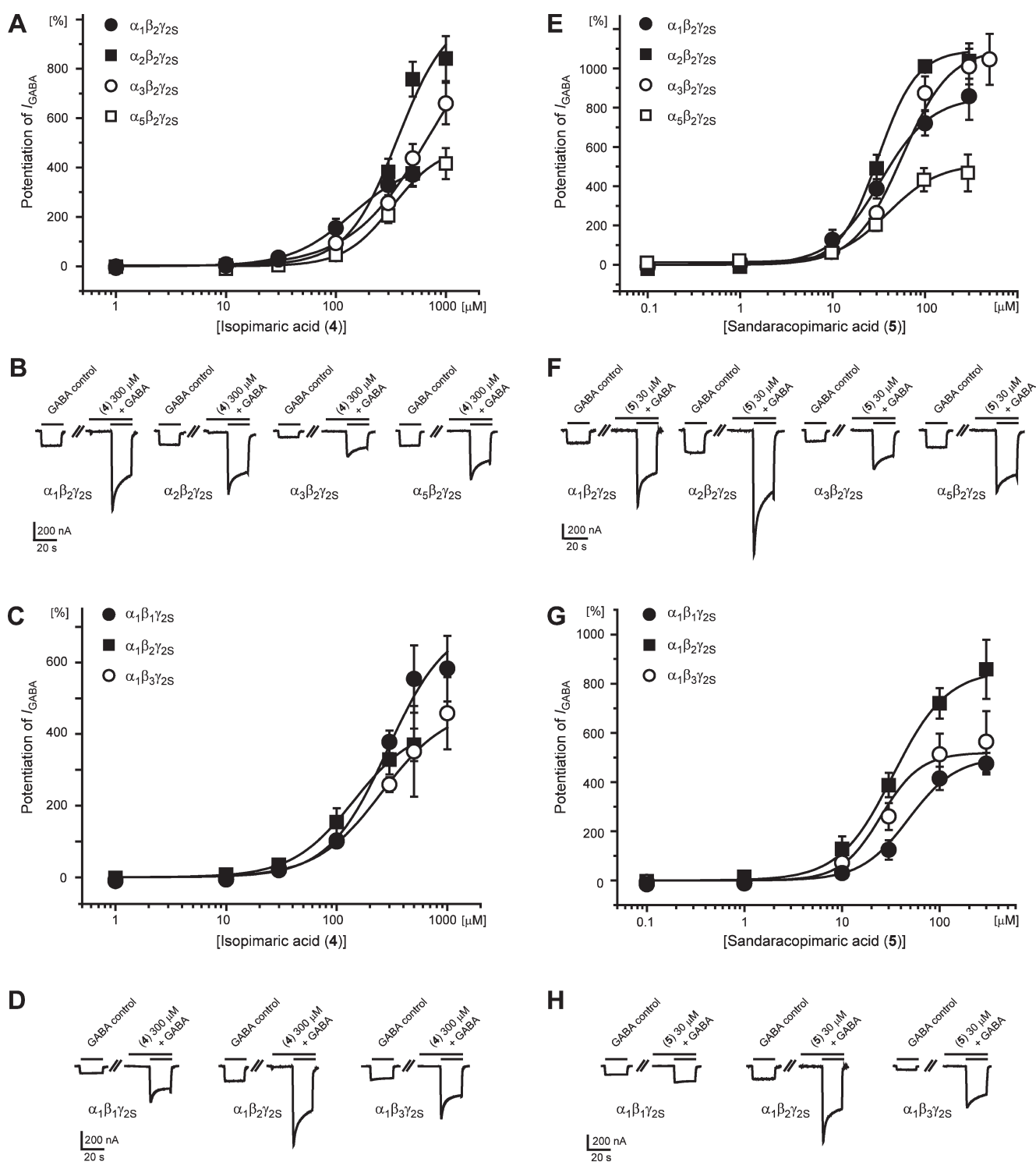
Figure 3. Parts A and E display the α-subunit dependency of isopimaric acid (**4**) and sandaracopimaric acid (**5**), respectively, reflected by concentration−response curves with GABA$_A$ receptors of subunit compositions $\alpha_1\beta_2\gamma_{2S}$, $\alpha_2\beta_2\gamma_{2S}$, $\alpha_3\beta_2\gamma_{2S}$, and $\alpha_5\beta_2\gamma_{2S}$. Parts C and G show the β-subunit dependency of **4** and **5**, respectively, reflected by concentration−response curves at GABA$_A$ receptors of the subunit compositions $\alpha_1\beta_1\gamma_{2S}$, $\alpha_1\beta_2\gamma_{2S}$, and $\alpha_1\beta_3\gamma_{2S}$. Typical traces reflecting modulation of chloride currents without direct activation were recorded with compounds **4** and **5** at all expressed GABA$_A$ receptor subtypes (typical currents of **4** and **5** are displayed in B and D, and F and H, respectively). All measurements were performed with a GABA EC$_{5-10}$.

spectrometer (Bruker BioSpin, Faellanden, Switzerland) operating at 500.13 MHz for ^{1}H and 125.77 MHz for ^{13}C. A 1 mm TXI-microprobe with a z-gradient was used for ^{1}H-detected experiments; ^{13}C NMR

spectra were recorded with a 5 mm BBO-probe head with z-gradient. Spectra were analyzed using Bruker TopSpin 2.1 software. High-resolution mass spectra (HPLC-PDA-ESITOFMS) in positive mode

114

Table 2. Potency Ratio and Efficiency Ratio for Isopimaric Acid (4) and Sandaracopimaric Acid (5)

subtype	$\alpha_1\beta_1\gamma_{2S}$	$\alpha_1\beta_2\gamma_{2S}$	$\alpha_1\beta_3\gamma_{2S}$	$\alpha_2\beta_2\gamma_{2S}$	$\alpha_3\beta_2\gamma_{2S}$	$\alpha_5\beta_2\gamma_{2S}$
potency ratio $[EC_{50}(4)/EC_{50}(5)]$	6.02^a	4.25	10.32	11.69^b	12.79	7.79^a
efficiency ratio $[I_{max}(4)/I_{max}(5)]$	1.43	0.50^a	0.92	0.94	0.98	0.92

^{a} Statistically significant ($p < 0.05$). ^{b} Statistically significant ($p < 0.01$).
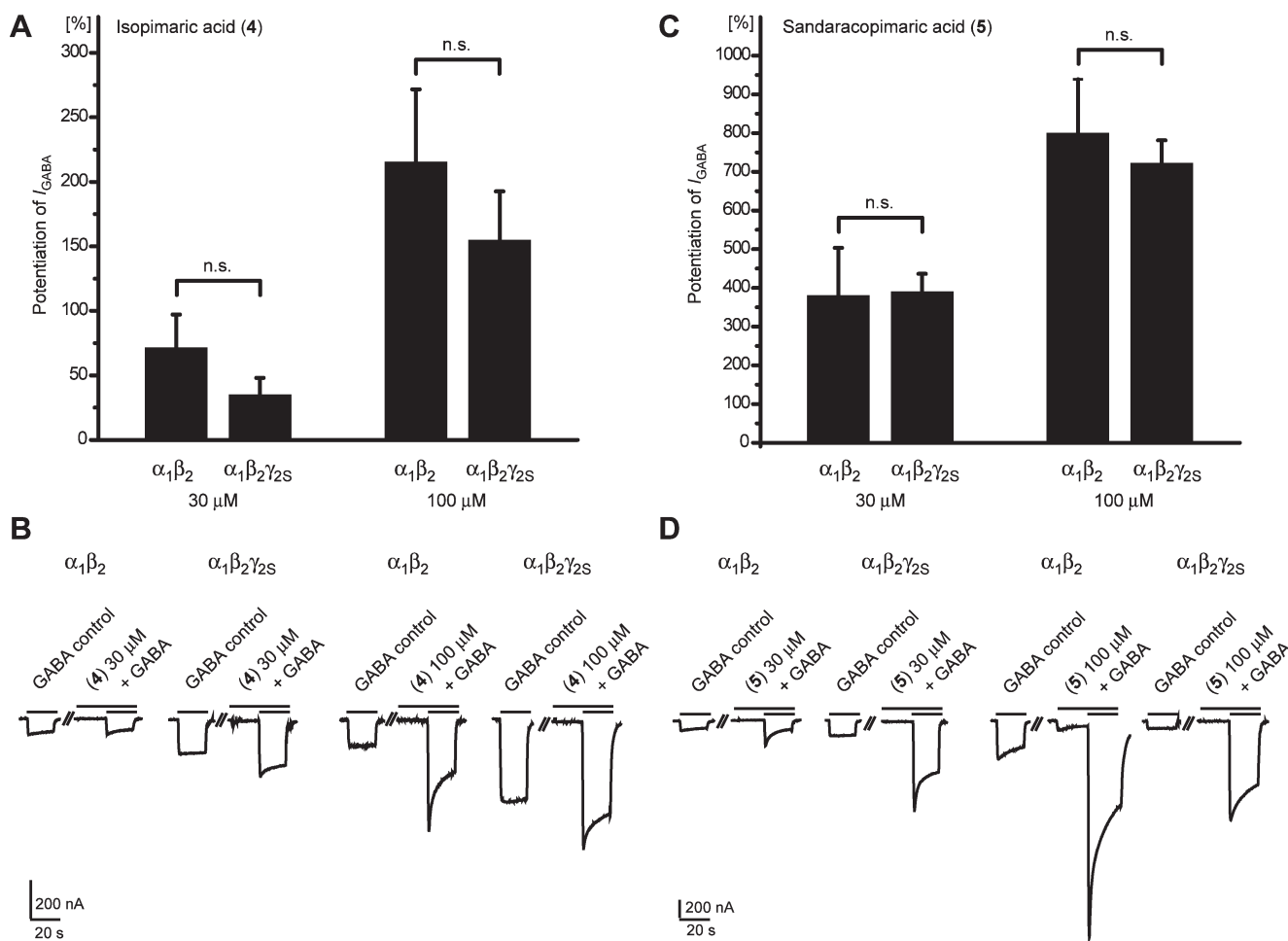
Figure 4. Parts A and C display the γ-subunit dependency of isopimaric acid (4) and sandaracopimaric acid (5), respectively. The bar graphs indicate the potentiation of GABA-induced control currents by 30 and 100 μM of compound, at GABA$_A$ receptors of the subunit compositions $\alpha_1\beta_2$ and $\alpha_1\beta_2\gamma_{2S}$. Traces show typical modulation of chloride currents in GABA$_A$ receptor subtypes by compounds 4 and 5 (parts B and D, respectively).

were obtained on a Bruker micrOTOF ESIMS system (Bruker Daltonics, Bremen, Germany) connected via a T-splitter (1:10) to an Agilent HP 1100 Series system consisting of a binary pump, autosampler, column oven, and diode array detector (G1315B) (Agilent Technologies, Waldbronn, Germany). Nitrogen was used as a nebulizing gas at a pressure of 2.0 bar and as a drying gas at a flow rate of 9.0 L/min (dry gas temperature 240 °C). Capillary voltage was set at 4500 V; hexapole at 230.0 Vpp. Instrument calibration was done with a reference solution of sodium formate 0.1% in 2-propanol/water (1:1) containing 5 mM NaOH. Data acquisition and processing were performed using Bruker HyStar 3.0 software. Semipreparative HPLC separations for activity profiling were carried out with an Agilent HP 1100 Series system consisting of a quaternary pump, autosampler, column oven, and diode array detector (G1315B). HPLC fractions were evaporated with a Genevac EZ-2 Plus vacuum centrifuge (Genevac Ltd., Ipswich, United Kingdom). Waters SunFire C18 (3.5 μm, 3.0 × 150 mm) and SunFire

Prep C18 (5 μm, 10 × 150 mm) columns (Waters, Wexford, Ireland) were used for HPLC-PDA-ESITOFMS and semipreparative HPLC, respectively. Medium-pressure liquid chromatography (MPLC) was performed with a glass column (49 × 460 mm) packed with silica gel (0.015−0.040 μm; Merck) on a Buchi Sepacore system consisting of two C605 pumps, a C635 detector, a C620 control unit, and a C660 fraction collector (Buchi Labortechnik AG, Flawil, Switzerland). Sample introduction was carried out with a precolumn packed with the sample absorbed onto silica gel. The separation was monitored with Buchi Sepacore Control 1.0 software.

Plant Material. Cebaye (dried twigs and leaves of *B. orientalis*) was purchased from a local market in Shanxi Province, China. Identity of the sample was confirmed with the aid of the corresponding monograph of the Chinese Pharmacopoeia IX and other literature[56] at the Division of Pharmaceutical Biology, University of Basel, where a voucher specimen (00 305) is deposited.
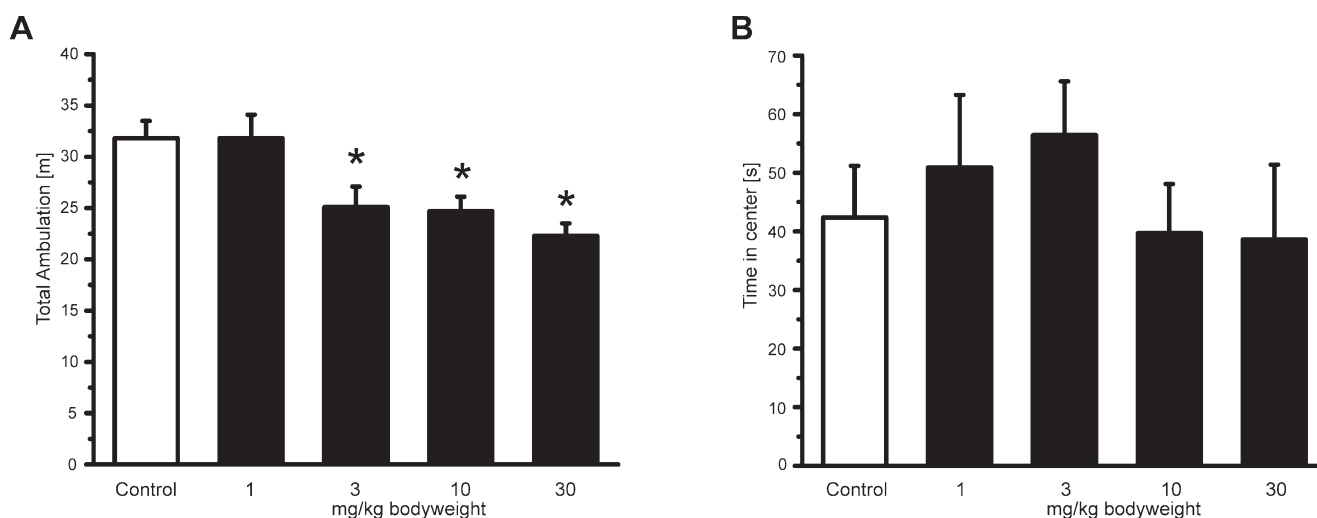
Figure 5. Ambulation and explorative behavior in the open field test assessed over 10 min for control and sandaracopimaric acid (**5**)-treated mice at the indicated doses (doses represent mg/kg BW). Bars indicate the total distance traveled (A) and the time spent in the center (B). Bars represent mean ± SEM from ≥10 mice. The asterisks indicate statistically significant differences ($p < 0.05$).

Extraction. The plant material was frozen with liquid nitrogen and ground with a ZM1 ultracentrifugal mill (Retsch). The EtOAc extract for screening and HPLC-based activity profiling was prepared with an ASE 200 extraction system with solvent module (Dionex, Sunnyvale, CA). Extraction pressure was 120 bar, temperature was set at 70 °C, and three extraction cycles of 5 min each were performed. For preparative isolation, 430 g of ground plant material was macerated overnight with 1.25 L of EtOAc, followed by percolation with EtOAc (2×1 L). The solvent was evaporated at reduced pressure to yield 22.8 g of extract. The extracts were stored at −20 °C until use.

Microfractionation for Activity Profiling. Time-based microfractionation for GABA$_A$ receptor activity profiling was performed as previously described,[41] with minor modifications. Separation for both time-based and peak-based microfractionation was carried out on a semipreparative HPLC column with acetonitrile containing 0.1% formic acid (solvent A) and water containing 0.1% formic acid (solvent B) using the following gradient: 10% A to 100% A for 30 min, hold for 10 min. In the time-based fractionation, 28 microfractions of 90 s each were collected from an injection of 10 mg of extract (in 500 μL of DMSO). The flow rate was 7 mL/min. In peak-based fractionation (10 mg of extract in 100 μL of DMSO), 21 microfractions were collected. The flow rate was 4 mL/min. All microfractions were dried, evenly distributed to two vials, and submitted to activity testing.

Isolation. The EtOAc extract (22.8 g) was dissolved in MeOH and extracted with n-hexane to remove essential oils. The methanolic portion was then redissolved in CHCl$_3$ and extracted with H$_2$O to remove polar constituents. The residue (11.1 g) was coated onto silica gel (44.9 g) and packed into a precolumn prior to elution onto the MPLC column. Elution was done with an n-hexane (solvent A) and EtOAc (solvent B) gradient: 0% B to 30% B in 4 h, followed by 30% A to 100% B in 4 h. The flow rate was set at 15 mL/min. Fractions of 15 mL were collected and were later combined to 20 fractions (1−20) on the basis of a TLC analysis. Selected fractions were submitted to semipreparative gradient HPLC with acetonitrile (solvent C) and H$_2$O containing 0.1% formic acid (solvent D) as eluents. The flow rate was 4 mL/min. Methanolic stock solutions (100 mg/mL) were prepared and repeatedly injected in portions of 30 to 100 μL. A portion (140 mg) of fraction 2 (322.4 mg) afforded compound **6** (12.0 mg). The gradient profile was 30% C to 100% C in 20 min. An aliquot (56 mg) of fraction 7 (265.7 mg) gave a mixture of **4** and **5** (30.5 mg). A gradient of 70% C to 100% C over

20 min was used. The same gradient was used for separation of an aliquot (120 mg) of fraction 13 (281.6 mg). Compounds **1** (24.4 mg) and **3** (2.6 mg) were obtained. Compound **2** (5.2 mg) was isolated from 80 mg of fraction 16 (2.035 g). A gradient of 65% C to 73% C over 16 min was used. Several attempts to separate the mixture of **4** and **5** failed.

Compounds **1**−**6** were identified by comparison of physicochemical data (NMR, ESI-TOF-MS, and UV−vis spectroscopy) with published values.[11,57−66] The purity (except for the mixture of **4** and **5**) was >95% (purity check by ^{1}H NMR).

*Sandaracopimaradienolal (**3**):* ^{1}H NMR (CDCl$_3$, 500.13 MHz) δ 9.38 (1H, s, H-18), 5.73 (1H, dd, $J = 17.7$, 10.7 Hz, H-15), 5.24 (1H, br s, H-14), 4.87 (1H, dd, $J = 17.7$, 2.0 Hz, H-16a), 4.85 (1H, dd, $J = 10.7$, 2.0 Hz, H-16b), 3.77 (1H, dd, $J = 11.6$, 4.5 Hz, H-3), 2.21 (1H, ddd, 14.2, 4.3, 2.3 Hz, H-7a), 2.04 (1H, ddm, $J = 14.2$, 12.9 Hz, H-7b), 1.80 (1H, ddd, $J = 13.7$, 3.0, 3.0 Hz, H-1a), 1.74 (1H, m, H-9), 1.74 (1H, m, H-2a), 1.63 (1H, m, H-2b), 1.60 (1H, m, H-11a), 1.53 (1H, dd, $J = 12.7$, 1.7 Hz, H-5), 1.52 (1H, m, H-11b), 1.47 (1H, m, H-6a), 1.45 (1H, m, H-12a), 1.36 (1H, m, H-12b), 1.22 (1H, ddd, $J = 13.7$, 13.7, 4.5 Hz, H-1b), 1.08 (3H, s, H-19), 1.07 (1H, m, H-6b), 1.02 (3H, s, H-17), 0.84 (3H, s, H-20); ^{13}C shifts (CDCl$_3$, 125.77 MHz) δ 206.86 (CH, C-18), 148.57 (CH, C-15), 135.66 (C, C-8), 129.80 (CH, C-14), 110.41 (CH$_2$, C-16), 72.12 (CH, C-3), 55.30 (C, C-4), 50.06 (CH, C-9), 46.87 (CH, C-5), 37.45 (C, C-13), 37.12 (C, C-10), 36.75(CH$_2$, C-1), 35.21 (CH$_2$, C-7), 34.25 (CH$_2$, C-12), 26.56 (CH$_2$, C-2), 26.02 (CH$_3$, C-17), 24.08 (CH$_2$, C-6), 18.74 (CH$_2$, C-11), 15.36 (CH$_3$, C-20), 9.22 (CH$_3$, C-19); relevant NOESY correlations, H-3 ↔ H-17, H-3 ↔ H-5, H-5 ↔ H-17, H-5 ↔ H-9, H-20 ↔ H-19, H-20 ↔ H-17; HR-ESIMS m/z 325.2153 [M + Na]$^+$ (calcd for C$_{20}$H$_{30}$O$_2$Na, 325.2143). NMR spectra of **3** are available as Supporting Information.

Expression and Functional Characterization of GABA$_A$ Receptors. The preparation of stage V−VI oocytes from *Xenopus laevis*, the synthesis of capped-off runoff poly(A+) cRNA transcripts from linearized cDNA templates (pCMV vector), and cRNA injection into oocytes were performed as previously described.[47] In summary, female *X. laevis* (Nasco, Fort Atkinson, WI) were anesthetized by a 15 min exposure to a 0.2% MS-222 (methanesulfonate salt of 3-amino-benzoic acid ethyl, Sigma-Aldrich, Munich, Germany) solution before surgically removing parts of the ovaries. Follicle membranes from isolated oocytes were enzymatically digested with 2 mg/mL collagenase (Type 1 A, Sigma-Aldrich). One day after enzymatic isolation, the

oocytes were injected with approximately 10—50 nL of DEPC-treated water (diethyl pyrocarbonate, Sigma-Aldrich) containing different cRNAs at a concentration of approximately 300—3000 pg/nL per subunit. The amount of injected cRNA mixture was determined by means of a NanoDrop ND-1000 (Kisker Biotech, Steinfurt, Germany). To ensure expression of the γ_{2S} subunits in $\alpha_1\beta_2\gamma_{2S}$, $\alpha_2\beta_2\gamma_{2S}$, $\alpha_3\beta_2\gamma_{2S}$, $\alpha_5\beta_2\gamma_{2S}$, and $\alpha_1\beta_3\gamma_{2S}$ receptors, cRNAs were mixed in a 1:1:10 ratio, except $\alpha_1\beta_1\gamma_{2S}$ (ratio 3:1:10). For $\alpha_1\beta_2$ receptors, the cRNAs were mixed in a 1:1 ratio. Oocytes were then stored at 18 °C in an aqueous solution of 90 mM NaCl, 1 mM KCl, 1 mM MgCl$_2$, 1 mM CaCl$_2$, and 5 mM HEPES (pH 7.4), containing 1% penicillin—streptomycin solution (Sigma-Aldrich).[67] Voltage clamp measurements were performed between days 1 and 5 after cRNA injection. Electrophysiological experiments on a two-microelectrode voltage clamp setup were performed at a holding potential of −70 mV making use of a TURBO TEC 01C amplifier (npi electronic, Tamm, Germany) and an Axon Digidata 1322A interface (Molecular Devices, Sunnyvale, CA). Data were recorded by using pCLAMP v10.2. Currents were low-pass-filtered at 1 kHz and sampled at 3 kHz. The bath solution contained 90 mM NaCl, 1 mM KCl, 1 mM MgCl$_2$, 1 mM CaCl$_2$, and 5 mM HEPES (pH 7.4). Electrodes with resistances between 1 and 3 MΩ were used and filled with 2 M KCl.

Sample Application during Current Recordings. Of each sample, 100 μL was applied to the oocytes at a perfusion speed of 300 μL/s by the ScreeningTool automated fast perfusion system (npi electronic).[7] Before application of test solutions, concentration—response experiments with GABA concentrations ranging from 0.01 μM to 1 mM were performed to determine the GABA concentration eliciting 5—10% of the maximal current amplitude at 1 mM (GABA EC$_{5-10}$), which typically ranged from 3 to 10 μM for receptors comprising a γ_{2S} subunit and 0.3 to 1 μM for $\alpha_1\beta_2$ receptors. The stock solution (10 mg/mL in DMSO) of *B. orientalis* extract was diluted to a concentration of 100 μg/mL with bath solution containing GABA EC$_{5-10}$. As previously described in a validated protocol, time-based and peak-based microfractions collected from the semipreparative HPLC separations were dissolved in 30 μL of DMSO and mixed with 2.97 mL of bath solution containing GABA EC$_{5-10}$.[41] For concentration—response experiments, bath solution containing compounds **4** and **5** in concentrations ranging from 0.1 to 1000 μM was applied to the oocyte. After a preincubation period of 20 s, a second application immediately followed containing the corresponding compound solution combined with GABA EC$_{5-10}$. Pure isopimaric acid (**4**) (≥98%) and GABA were purchased from Sigma-Aldrich, and sandaracopimaric acid (≥95%) (**5**) was purchased from Orchid Cellmark (Princeton, NJ).

Data Analysis. Enhancement of the GABA-induced chloride current (I_{GABA}) was defined as $I_{(GABA+Comp)}/I_{GABA} - 1$, where $I_{(GABA+Comp)}$ is the current response in the presence of a given compound, and I_{GABA} is the control GABA-induced chloride current. Concentration—response curves were generated, and the data were fitted by nonlinear regression analysis using ORIGIN software (OriginLab Corporation, Northampton, MA). Data were fitted to the equation $1/[1 + (EC_{50}/[Comp])^{n_H}]$, where EC_{50} is the concentration of the compound that increases the amplitude of the GABA-evoked current by 50%, and n_H is the Hill coefficient. The maximum potentiation of I_{GABA} by a given compound was derived from the fit. Data are given as mean ± SE of at least 2 oocytes and ≥2 oocyte batches. Statistical significance was calculated using the paired Student *t*-test with confidence intervals of $p < 0.05$ unless otherwise stated.

In Vivo Experiments. Male mice (C57Bl/6N) were obtained from Charles River Laboratories (Wilmington, MA). For breeding and maintenance mice were group housed with free access to food and water. Temperature was fixed to 23 ± 1 °C and 60% humidity with a 12 h light—dark cycle (lights on 0700—1900 h). Male mice at 3—6 months of age were tested in all experiments. All procedures involving animals were approved by the Austrian Animal Experimentation Ethics Board in compliance with the European convention for the protection of vertebrate

animals used for experimental and other scientific purposes ETS no.: 123. Every effort was taken to minimize the number of animals used.

Chemicals. A stock solution of sandaracopimaric acid was prepared in 100% DMSO (50 mg/mL). Working concentrations were adjusted by dilution with 0.9% NaCl. NaOH was used to adjust the pH to 7.2—7.4. For ip administration the compound was solubilized with 3% Polysorbate 80 and with DMSO, whereby the final DMSO concentrations did not exceed 10% (see Broadwell et al. 1982 for DMSO effects on the permeability of the blood brain barrier).[68] All solutions were freshly prepared every day prior to experiments.

Open Field Test. Ambulation 30 min after ip injection of either control (vehicle without compound) or test solution (vehicle containing compound at the indicated doses) was tested over 10 min in 50 × 50 cm Flexfield boxes equipped with infrared rearing detection. Animals were video monitored, and their explorative behavior was analyzed using ActiMot 2 equipment and software (TSE Systems, Bad Homburg, Germany). Arenas were subdivided into border (up to 8 cm from wall), center (20 × 20 cm, i.e. 16% of total area), and intermediate area according to the recommendations of EMPRESS (European Mouse Phenotyping Resource of Standardised Screens; http://empress.har.mrc.ac.uk).

For comparison of control groups and compound-treated groups the unpaired Student's *t* test is used. Comparison of more than two groups was done by one-way ANOVA. *p*-values of <0.05 were accepted as statistically significant.

■ ASSOCIATED CONTENT

S Supporting Information. ^{1}H and ^{13}C NMR spectra of compound **3**, spectral data of compounds **1**, **2**, and **4**—**6**, and a synoptical table with currently known secondary metabolites from *Biota orientalis*. This material is available free of charge via the Internet at http://pubs.acs.org.

■ AUTHOR INFORMATION

Corresponding Author
*Tel: +41 61 267 1425. Fax: +41 61 267 1474. E-mail: Matthias.hamburger@unibas.ch.

Author Contributions
§These authors contributed equally to the work.

■ ACKNOWLEDGMENT

■ REFERENCES

(1) Jacob, T. C.; Moss, S. J.; Jurd, R. *Nat. Rev. Neurosci.* **2008**, *9*, 331–43.
(2) Stephenson, F. A. *Biochem. J.* **1995**, *310* (Pt 1), 1–9.
(3) Simon, J.; Wakimoto, H.; Fujita, N.; Lalande, M.; Barnard, E. A. *J. Biol. Chem.* **2004**, *279*, 41422–41435.
(4) Olsen, R. W.; Sieghart, W. *Pharmacol. Rev.* **2008**, *60*, 243–60.
(5) Olsen, R. W.; Sieghart, W. *Neuropharmacology* **2009**, *56*, 141–148.
(6) D'Hulst, C.; Atack, J. R.; Kooy, R. F. *Drug Discuss. Today* **2009**, *14*, 866–875.

117

(7) Baburin, I.; Beyl, S.; Hering, S. *Pflug. Arch. Eur. J. Phys.* **2006**, *453*, 117–123.

(8) Sakar, M. K.; Engelshowe, R. *J. Faculty Pharm. Istanbul Univ.* **1985**, *21*, 80–85.

(9) Chizzola, R.; Hochsteiner, W.; Hajek, S. *Res. Vet. Sci.* **2004**, *76*, 77–82.

(10) Koo, K. A.; Sung, S. H.; Kim, Y. C. *Chem. Pharm. Bull.* **2002**, *50*, 834–836.

(11) Kuo, Y. H.; Chen, W.-C. *J. Chin. Chem. Soc.* **1999**, *46*, 819–824.

(12) Lee, H.-K.; Ahn, K.-S.; Park, S. H.; Lee, I. S.; Kim, J. H. Recent Advances in Natural Products Research. *Proceedings of the International Symposium on Recent Advances in Natural Products Research*, 3rd ed.; Shin, K.-H.; Kang, S. S.; Kin, Y. S., Eds.; Seoul, Republic of Korea, 1999; pp 54–62.

(13) Lee, M. K.; Yang, H.; Yoon, J. S.; Jeong, E. J.; Kim, D. Y.; Ha, N. R.; Sung, S. H.; Kim, H. C. *Arch. Pharmacol. Res.* **2008**, *31*, 866–871.

(14) Mehta, B.; Nagar, V.; Shitut, S.; Nagar, S.; Sharma, S. *Indian J. Chem., Sect. B: Org. Chem. Incl. Med. Chem.* **2002**, *41B*, 1088–1092.

(15) Nickavar, B.; Amin, G.; Parhami, S. *Z. Naturforsch., C: J. Biosci.* **2003**, *58*, 171–172.

(16) Ren, X.-Y.; Ye, Y. *J. Asian Nat. Prod. Res.* **2006**, *8*, 677–682.

(17) Singh, A.; Yadaw, A. *Indian Perfum.* **2005**, *49*, 173–177.

(18) Song, G.; Deng, C.; Wu, D.; Hu, Y. *Chromatographia* **2003**, *58*, 769–774.

(19) Tomita, B.; Hirose, Y.; Nakatsuka, T. *Mokuzai Gakkaishi* **1969**, *15*, 47.

(20) Tomita, B.; Hirose, Y.; Nakatsuka, T. *Tetrahedron Lett.* **1968**, *7*, 843–848.

(21) Tomita, B.; Hirose, Y.; Nakatsuka, T. *Mokuzai Gakkaishi* **1969**, *15*, 46.

(22) Fahmy, H. *J. Environ. Sci. (Mansoura, Egypt)* **2003**, *26*, 297–306.

(23) Gadek, P. A.; Quinn, C. J. *Phytochemistry* **1985**, *24*, 267–272.

(24) Khabir, M.; Khatoon, F.; Ansari, W. H. *Curr. Sci.* **1985**, *54*, 1180–1185.

(25) Kim, H. Y.; Kang, M. H. *Food Sci. Technol.* **2003**, *12*, 687–690.

(26) Lie Ken Jie, M. S. F.; Lao, H. B.; Zheng, Y. F. *J. Am. Oil Chem. Soc.* **1988**, *65*, 597–600.

(27) Lu, Y.-H.; Liu, Z.-Y.; Wang, Z.-T.; Wei, D.-Z. *J. Pharm. Biomed. Anal.* **2006**, *41*, 1186–1190.

(28) Yoon, J. S.; Koo, K. A.; Ma, C. J.; Sung, S. H.; Kim, Y. C. *Nat. Prod. Sci.* **2008**, *14*, 167–170.

(29) Huang, K. C. *The Pharmacology of Chinese Herbs*; CRC Press, 1999; p 349.

(30) Nishiyama, N.; Chu, P. J.; Saito, H. *Biol. Pharm. Bull.* **1995**, *18*, 1513–1517.

(31) Zhongzhen, Z., *An Illustrated Chinese Materia Medica in Hong Kong*; School of Chinese Medicine, Hong Kong Baptist University: Hong Kong, 2004; pp 10, 426.

(32) Zhu, J. X.; Wang, Y.; Kong, L. D.; Yang, C.; Zhang, X. *J. Ethnopharmacol.* **2004**, *93*, 133–140.

(33) Potterat, O.; Hamburger, M. *Curr. Org. Chem.* **2006**, *10*, 899–920.

(34) Adams, M.; Christen, M.; Plitzko, I.; Zimmermann, S.; Brun, R.; Kaiser, M.; Hamburger, M. *J. Nat. Prod.* **2010**, *73*, 897–900.

(35) Adams, M.; Zimmermann, S.; Kaiser, M.; Brun, R.; Hamburger, M. *Nat. Prod. Commun.* **2009**, *4*, 1377–1381.

(36) Danz, H.; Stoyanova, S.; Wippich, P.; Brattstroem, A.; Hamburger, M. *Planta Med.* **2001**, *67*, 411–416.

(37) Dittmann, K.; Gerhaeuser, C.; Klimo, K.; Hamburger, M. *Planta Med.* **2004**, *70*, 909–913.

(38) Potterat, O.; Wagner, K.; Gemmecker, G.; Mack, J.; Puder, C.; Vettermann, R.; Streicher, R. *J. Nat. Prod.* **2004**, *67*, 1528–1531.

(39) Adams, M.; Plitzko, I.; Kaiser, M.; Brun, R.; Hamburger, M. *Phytochem. Lett.* **2009**, *2*, 159–162.

(40) Adams, M.; Gschwind, S.; Zimmermann, S.; Kaiser, M.; Hamburger, M. *J. Ethnopharmacol.* **2011**, *135*, 43–47.

(41) Kim, H. J.; Baburin, I.; Khom, S.; Hering, S.; Hamburger, M. *Planta Med.* **2008**, *74*, 521–526.

(42) Li, Y.; Plitzko, I.; Zaugg, J.; Hering, S.; Hamburger, M. *J. Nat. Prod.* **2010**, *73*, 768–70.

(43) Zaugg, J.; Baburin, I.; Strommer, B.; Kim, H. J.; Hering, S.; Hamburger, M. *J. Nat. Prod.* **2010**, *73*, 185–191.

(44) Zaugg, J.; Eickmeier, E.; Rueda, D. C.; Hering, S.; Hamburger, M. *Fitoterapia* **2011**, *82*, 434–440.

(45) Yang, X.; Baburin, I.; Plitzko, I.; Hering, S.; Hamburger, M. *Mol. Diversity* **2011**, *15*, 361–372.

(46) Zaugg, J.; Eickmeier, E.; Ebrahimi, S.; Baburin, I.; Hering, S.; Hamburger, M. *J. Nat. Prod.* **2011**, *74*, 1437–1443.

(47) Khom, S.; Baburin, I.; Timin, E. N.; Hohaus, A.; Sieghart, W.; Hering, S. *Mol. Pharmacol.* **2006**, *69*, 640–649.

(48) Mohler, H. *Neuropharmacology* **2011**, *60*, 1042–1049.

(49) Bourin, M.; Petit-Demouliere, B.; Dhonnchadha, B. N.; Hascoet, M. *Fundam. Clin. Pharmacol.* **2007**, *21*, 567–574.

(50) Chow, N. K.; Fretz, M.; Hamburger, M.; Butterweck, V. *Planta Med.* **2011**, *77*, 795–803.

(51) Kopp, C.; Rudolph, U.; Tobler, I. *Neuroreport* **2004**, *15*, 2299–2302.

(52) Korkosz, A.; Zatorski, P.; Taracha, E.; Plaznik, A.; Kostowski, W.; Bienkowski, P. *Alcohol* **2006**, *40*, 151–157.

(53) Vlainic, J.; Pericic, D. *Neuropharmacology* **2009**, *56*, 1124–1130.

(54) Lipinski, C. A. *Drug Discovery Today: Technol.* **2004**, *1*, 337–341.

(55) Pajouhesh, H.; Lenz, G. R. *NeuroRx* **2005**, *2*, 541–553.

(56) Haensel, R.; Keller, K.; Rimpler, H.; Schneider, G. *Hagers Handbuch der Pharmazeutischen Praxis*; Springer Verlag, 1993; Vol. 5, pp 963–965.

(57) Asili, J.; Lambert, M.; Ziegler, H. L.; Staerk, D.; Sairafianpour, M.; Witt, M.; Asghari, G.; Ibrahimi, I. S.; Jaroszewski, J. W. *J. Nat. Prod.* **2004**, *67*, 631–637.

(58) Banerjee, A. K.; Laya, M. S.; Mora, H. R.; V., C. E. *Curr. Org. Chem.* **2008**, *12*, 1050–1070.

(59) Marcos, I. S.; Cubillo, M. A.; Moro, R. F.; Diez, P.; Basabe, P.; Sanz, F.; Urones, J. G. *Tetrahedron Lett.* **2003**, *44*, 8831–8835.

(60) Morisawa, J.; Kim, C. S.; Kashiwagi, T.; Tebayashi, S.; Horiike, M. *Biosci., Biotechnol., Biochem.* **2002**, *66*, 2424–2428.

(61) Ncanana, S.; Baratto, L.; Roncaglia, L.; Riva, S.; Burton, S. G. *Adv. Synth. Catal.* **2007**, *349*, 1507–1513.

(62) Sakar, M. K.; Er, N.; Ercil, D.; Del Olmo, E.; San Feliciano, A. *Acta Pharm. Turc.* **2002**, *44*, 213–219.

(63) Shults, E. E.; Velder, J.; Schmalz, H.-G.; Chernov, S. V.; Rubalova, T. V.; Gatilov, Y. V.; Henze, G.; Tolstikov, G. A.; Prokop, A. *Bioorg. Med. Chem. Lett.* **2006**, *16*, 4228–4232.

(64) Sung, S. H.; Koo, K. A.; Lim, H. K.; Lee, H. S.; Cho, J. H.; Kim, H. S.; Kim, Y. C. *Korean Soc. Pharmacogn.* **1998**, *29*, 347–352.

(65) Yang, H. O.; Suh, D. Y.; Han, B. H. *Planta Med.* **1995**, *61*, 37–40.

(66) Zgoda-Pols, J.; Freyer, A. J.; Killmer, L. B.; Porter, J. R. *Fitoterapia* **2002**, *73*, 434–438.

(67) Methfessel, C.; Witzemann, V.; Takahashi, T.; Mishina, M.; Numa, S.; Sakmann, B. *Pflug. Arch. Eur. J. Phys.* **1986**, *407*, 577–588.

(68) Broadwell, R. D.; Salcman, M.; Kaplan, R. S. *Science* **1982**, *217*, 164–166.

(69) Krampfl, K.; Wolfes, H.; Dengler, R.; Bufler, J. *Eur. J. Pharmacol.* **2002**, *435*, 1–8.

118

SUPPORTING INFORMATION

Identification and characterization of GABA$_A$ receptor modulatory diterpenes from *Biota orientalis* that decrease locomotor activity in mice

Janine Zaugg[†,§], Sophia Khom[‡,§], Daniela Eigenmann[†], Igor Baburin[‡], Matthias Hamburger[†,]*, Steffen Hering[‡]

Division of Pharmaceutical Biology, University of Basel, Klingelbergstrasse 50, 4056 Basel, Switzerland

Institute of Pharmacology and Toxicology, University of Vienna, Althanstrasse 14, 1090 Vienna, Austria

*To whom correspondence should be addressed. Tel.: +41 612671425; fax: +41 612671474. E-mail address: matthias.hamburger@unibas.ch

[†] University of Basel

[§] Authors equally contributed to the work

[‡] University of Vienna

Index

S1. ^{1}H NMR (500 MHz, CDCl$_3$) of sandaracopimaradienolal (**3**).

S2. ^{13}C NMR (125 MHz, CDCl$_3$) of sandaracopimaradienolal (**3**).

S3. DEPT-edited HSQC NMR (green/blue) and HMBC NMR (red) spectra of sandaracopimaradienolal (**3**), overlaid.
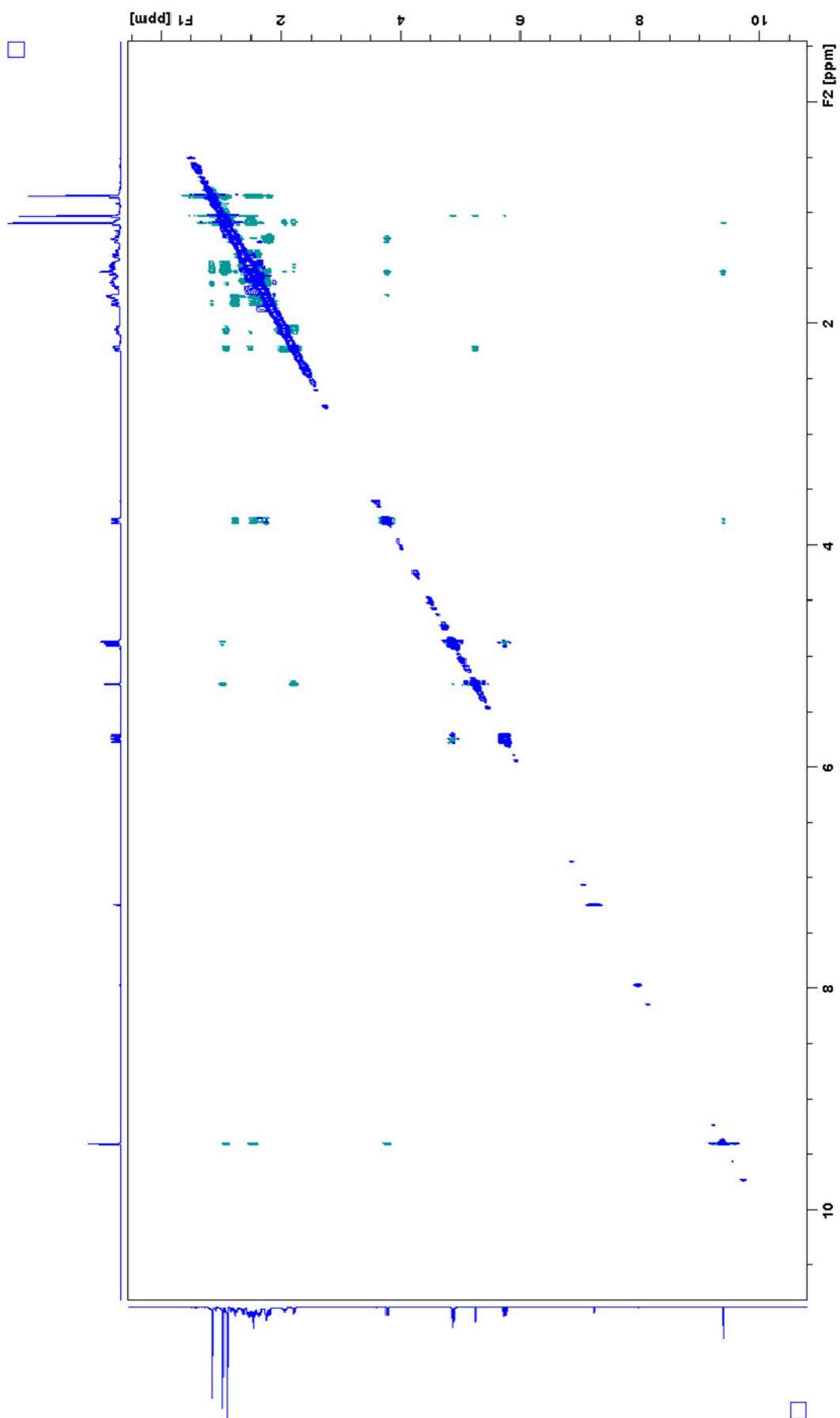
S4. NOESY NMR of sandaracopimaradienolal (**3**)

S5. Analytical data of pinusolide (**1**) (CAS = 31685-80-0)

Experimental data	
m/z (ESI-ion trap, positive mode)[1]	[M+H]$^+$ 347.2; [2M+Na]$^+$ 715.3
m/z (ESI-TOF-MS, positive mode)[1]	[M+Na]$^+$ 369.2152; [2M+Na]$^+$ 715.4238
Sum formula	$C_{21}H_{30}O_4$
UV λ_{max} [nm]	210
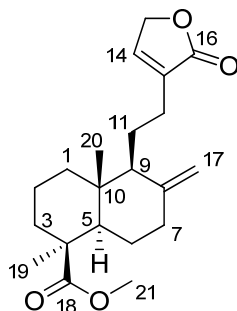
	δ_C (CDCl$_3$)^a [2]	δ_H (I, m, *J* in Hz) (CDCl$_3$) [2]
1	39.7	1.81 (1H, m); *1.06* (1H, m)
2	20.2	1.83 (1H, m); *1.50* (1H, m)
3	38.6	2.16 (1H, m); *1.01* (1H, m)
4	45.3	-
5	56.9	1.59 (1H, dd, *12.6, 3.1*)
6	26.5	1.97 (1H, m); *1.77* (1H, m)
7	39.1	2.40 (1H, m); *1.88* (1H, m)
8	148.0	-
9	56.3	1.60 (1H, br d, *10.8*)
10	40.4	-
11	22.4	1.57 (1H, m); *1.76* (1H, m)
12	25.1	2.45 (1H, m); *2.10* (1H, m)
13	135.3	-
14	144.0	7.06 (1H, dd, *1.8*)
15	70.2	4.73 (2H, dd, *4.3, 1.8*)
16	175.2	-
17	107.3	4.87 (1H, br s); 4.56 (1H, br s)
18	178.7	-
19	29.1	1.16 (3H, s)
20	13.1	0.50 (3H, s)
21	51.4	3.58 (3H, s)

^{a}^{13}C-Shifts from HSQC- and HMBC-NMR-experiments

S6. Analytical data of sandaracopimaradienediol (**2**) (CAS = 59219-64-6)

Experimental data	
m/z (ESI-ion trap, positive mode)	[2M+H]$^+$ 609.3
m/z (ESI-TOF-MS, positive mode)[3]	[M+Na]$^+$ 327.2313
Sum formula	$C_{20}H_{32}O_2$
UV λ_{max} [nm]	210
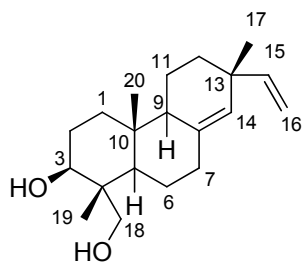
	δ_C (CDCl$_3$)^{a3}	δ_H (I, m, *J* in Hz) (CDCl$_3$)^3
1	37.31	1.74 (1H, m); 1.15 (1H, m)
2	27.57	1.57 – 1.65 (2H, m)
3	77.03	3.66 (1H, m)
4	42.62	-
5	48.88	1.16 (1H, m)
6	22.75	1.38 – 1.45 (2H, m)
7	35.87	2.24 (1H, m); 2.02 (1H, m)
8	136.56	-
9	50.71	1.66 (1H, m)
10	38.34	-
11	19.12	1.58 (1H, m); 1.49 (1H, m)
12	34.93	1.45 (1H, m); 1.34 (1H, m)
13	37.68	-
14	129.45	5.21 (1H, s)
15	149.17	5.74 (1H, dd, *17.6, 10.6*)
16	110.38	4.88 (1H, dd, *17.6, 1.22*); 4.85 (1H, dd, *10.6, 1.22*)
17	26.34	1.02 (3H, s)
18	71.88	3.66 (1H, d, *10.5*); 3.40 (1H, d, *10.5*)
19	11.74	0.90 (3H, s)
20	15.74	0.84 (3H, s)

^{a}^{13}C-shifts measured at 125.77 MHz.

S7. Analytical data of isopimaric acid (**4**) (CAS = 5835-26-7)

Experimental data	
m/z (ESI-ion trap, negative mode)[4]	[M-H]$^-$ 301.2 ; [2M-H]$^-$ 603.1
m/z (ESI-TOF-MS, negative mode)	[M-H]$^-$ 301.2174
Sum formula	$C_{20}H_{30}O_2$
UV λ_{max} [nm]	210
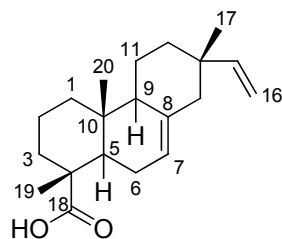
	δ_C (CDCl$_3$)^{a} [5,6]	δ_H (I, m, *J* in Hz) (CDCl$_3$)[7]
1	38.9	1.87 (1H, m); 1.14 (1H, m)
2	18.0	1.58 (2H, m)
3	37.0	1.81 (1H, m); 1.69 (1H, m)
4	46.2	-
5	45.3	1.98 (1H, m)
6	25.1	2.03 (1H, m); 1.73 (1H, m)
7	120.7	5.34 (1H, dd, *5.53, 1.30*)
8	*n.d.*	-
9	52.0	1.78
10	35.1	-
11	20.0	1.59 (1H, m); 1.40 (1H, m)
12	36.0	1.51 (1H, m); 1.39 (1H, m)
13	*n.d.*	-
14	46.3	1.99 (1H, m); 1.94 (1H, m)
15	150.7	5.82 (1H, dd, *17.4, 10.8*)
16	109.9	4.94 (1H, dd, *17.4, 0.8*); 4.88 (1H, dd, *10.8, 0.8*)
17	21.6	0.89 (3H, s)
18	185.9	-
19	17.2	1.30 (3H, s)
20	15.1	0.94 (3H, s)

^{a}^{13}C-Shifts from HSQC- and HMBC-NMR-experiments

S8. Analytical data of sandaracopimaric acid (**5**) (CAS = 471-74-9)

Experimental data

m/z (ESI-ion trap, negative mode)	[M-H]$^-$ 301.2 ; [2M-H]$^-$ 603.1 [4]
m/z (ESI-TOF-MS, negative mode)	[M-H]$^-$ 301.2174
Sum formula	$C_{20}H_{30}O_2$
UV λ_{max} [nm]	210
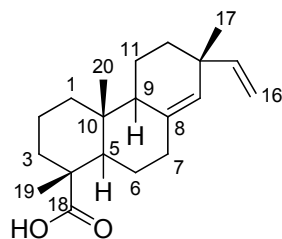
	δ_C (CDCl$_3$)^{a} [5, 6]	δ_H (I, m, *J* in Hz) (CDCl$_3$) [7, 8]
1	38.3	1.78 (1H, m); 1.15 (1H, m)
2	18.0	1.58 (2H, m)
3	37.0	1.81 (1H, m); 1.69 (1H, m)
4	47.9	-
5	48.8	1.94 (1H, m)
6	24.9	1.48 (1H, m); 1.31 (1H, m)
7	35.4	2.25 (1H, m); 2.15 (1H, m)
8	*n.d.*	-
9	50.7	1.83 (1H, m)
10	38.4	-
11	18.4	1.63 (1H, m); 1.49 (1H, m)
12	34.5	1.49 (1H, m); 1.40 (1H, m)
13	37.5	-
14	129.5	5.25 (1H, br s)
15	148.7	5.79 (1H, dd, *17.2, 10.7*)
16	110.0	4.92 (1H, dd, *17.2, 1.2*); 4.89 (1H, dd, *10.7, 1.2*)
17	26.1	1.06 (3H, s)
18	185.9	-
19	16.7	1.23 (3H, s)
20	15.1	0.86 (3H, s)

$^{a\,13}$C-Shifts from HSQC- and HMBC-NMR-experiments

S9. Analytical data of totarol (**6**) (CAS = 511-15-9)

Experimental data
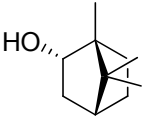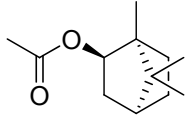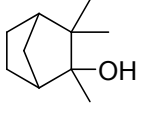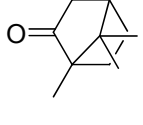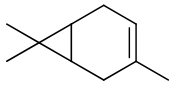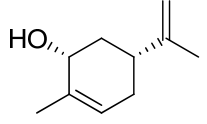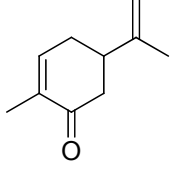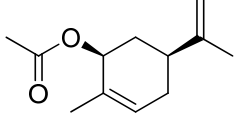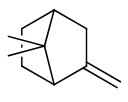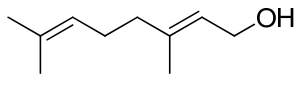
m/z (ESI-ion trap, negative mode)	[M-H]⁻ 285.3
m/z (ESI-TOF-MS, negative mode)[9]	[M-H]⁻ 285.2248
Sum formula	$C_{20}H_{30}O$
UV λ_{max} [nm] [10]	210; 280
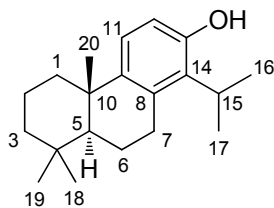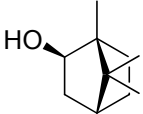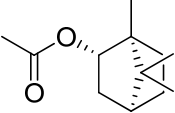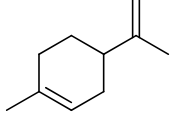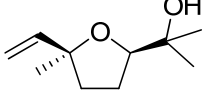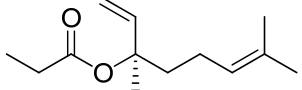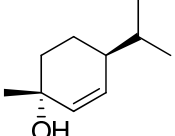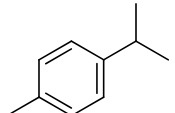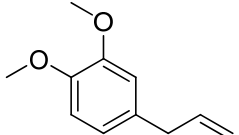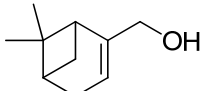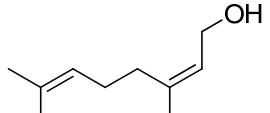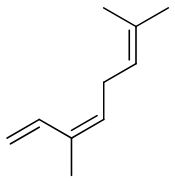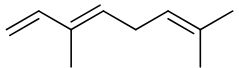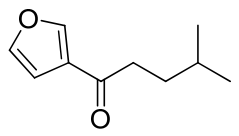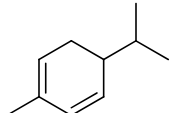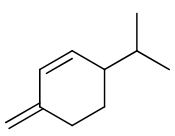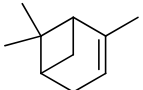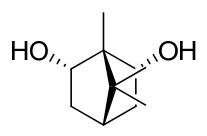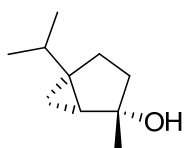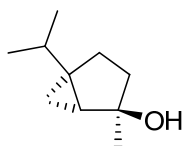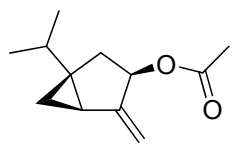
	δ_C (CDCl₃)[a][9,11]	δ_H (I, m, *J* in Hz) (CDCl₃)[11]
1	39.6	2.25 (1H, br d, *12.7*); 1.37 (1H, m)
2	19.5	1.75 (1H, m); 1.61 (1H, m)
3	41.7	1.49 (1H, br d, *13.3*); 1.23 (1H, ddd, *13.3, 13.3, 3.1*)
4	33.2	-
5	49.7	1.29 (1H, dd, *12.6, 2.0*)
6	19.3	1.94 (1H, br dd, *12.6, 7.7*); 1.69 (1H, m)
7	28.6	2.96 (1H, dd, *17.2, 6.7*); 2.78 (1H, ddd, *17.2, 10.1, 7.7*)
8	133.7	-
9	143.2	-
10	37.6	-
11	122.9	7.00 (1H, d, *8.5*)
12	114.3	6.51 (1H, d, *8.4*)
13	151.8	-
14	131.1	-
15	27.1	3.32 (1H, sept, *7.2*)
16/17	20.5	1.38 (3H, d, *7.2*) and 1.36 (3H, d, *7.2*)
18	33.2	0.98 (3H, s)
19	21.6	0.95 (3H, s)
20	25.1	1.20 (3H, s)
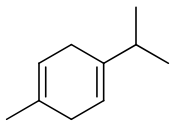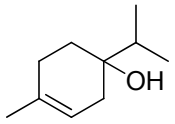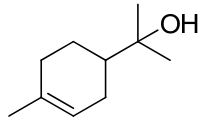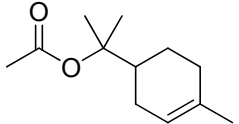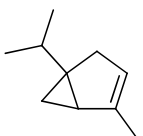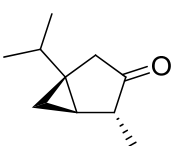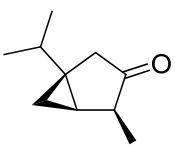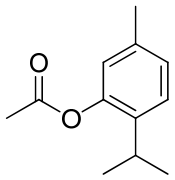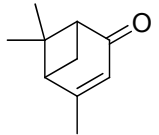
[a] ¹³C-Shifts from HSQC- and HMBC-NMR-experiments

S10. Monoterpenes isolated from *Biota orientalis*
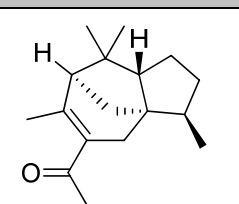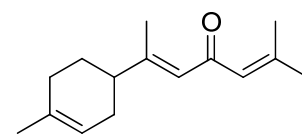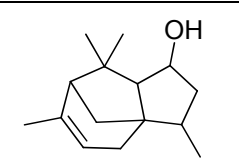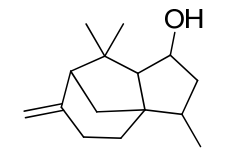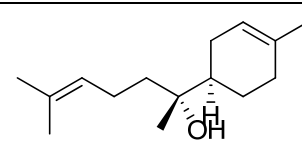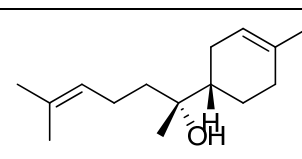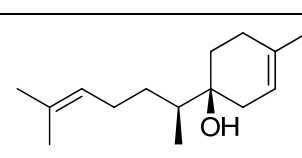
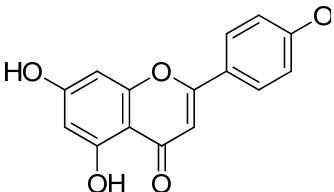| Trivial name	CAS number	Sum formula	MW	Structure	Ref.
Borneol	507-70-0	$C_{10}H_{18}O$	154.25		12
Bornyl acetate	76-49-3	$C_{12}H_{20}O_2$	196.29		13
Camphene hydrate	465-31-6	$C_{10}H_{18}O$	154.25		12
Camphor	76-22-2	$C_{10}H_{16}O$	152.23		12
Δ^3-Carene	13466-78-9	$C_{10}H_{16}$	136.23		12
cis-Carveol	1197-06-4	$C_{10}H_{16}O$	152.23		12
Carvone	99-49-0	$C_{10}H_{14}O$	150.22		12
cis-Carvyl acetate	1205-42-1	$C_{12}H_{18}O_2$	194.27		12
α-Fenchene	471-84-1	$C_{10}H_{16}$	136.23		14
Geraniol	106-24-1	$C_{10}H_{18}O$	154.25		12
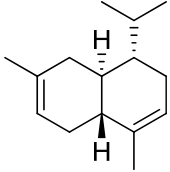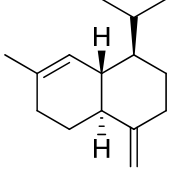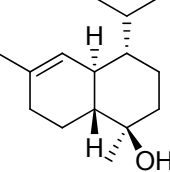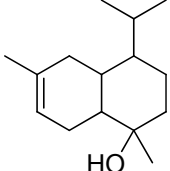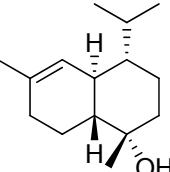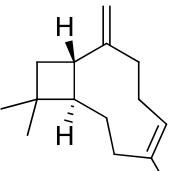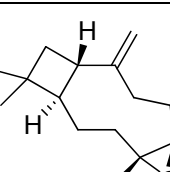
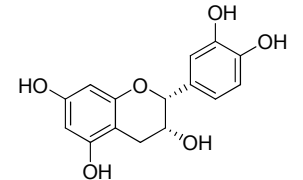| Trivial name	CAS number	Sum formula	MW	Structure	Ref.
Isoborneol	124-76-5	$C_{10}H_{18}O$	154.25		12
Isobornyl acetate	125-12-2	$C_{12}H_{20}O_2$	196.29		12
α-Limonene	138-86-3	$C_{10}H_{16}$	136.23		12
Linalool oxide	5989-33-3	$C_{10}H_{18}O_2$	170.25		12
Linalyl propionate	144-39-8	$C_{13}H_{22}O_2$	210.31		12
trans-*p*-Menth-2-en-1-ol	29803-82-5	$C_{10}H_{18}O$	154.25		12
p-Methyl-cumene (*p*-Cymene)	99-87-6	$C_{10}H_{14}O$	134.22		12
Methyleugenol	93-15-2	$C_{11}H_{14}O_2$	178.23		12
Myrtenol	515-00-4	$C_{10}H_{16}O$	152.23		12
β-Nerol (*cis*-Geraniol)	106-25-2	$C_{10}H_{18}O$	154.25		12
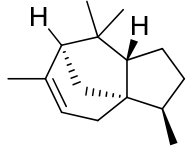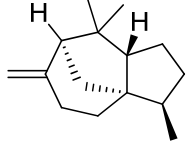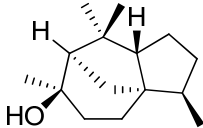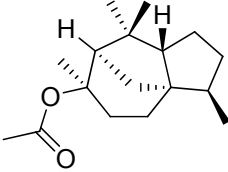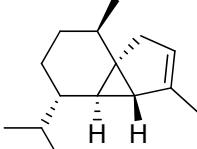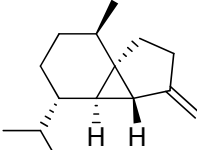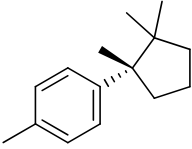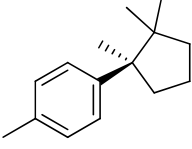
Trivial name	CAS number	Sum formula	MW	Structure	Ref.
cis-β-Ocimene	3338-55-4	$C_{10}H_{16}$	136.23		[12]
trans-β-Ocimene	3779-61-1	$C_{10}H_{16}$	136.23		[12]
Perilla ketone	553-84-4	$C_{10}H_{14}O_2$	166.22		[12]
α-Phellandrene	99-83-2	$C_{10}H_{16}$	136.23		[12]
β-Phellandrene	555-10-2	$C_{10}H_{16}$	136.23		[13]
α-Pinene	80-56-8	$C_{10}H_{16}$	136.23		[12]
Platydiol	70630-07-8	$C_{10}H_{18}O_2$	170.25		[4]
cis-Sabinene hydrate (*cis*-4-Thujanol)	15537-55-0	$C_{10}H_{18}O$	154.25		[12]
trans-Sabinene hydrate (*trans*-4-Thujanol)	17699-16-0	$C_{10}H_{18}O$	154.25		[12]
Sabinyl acetate	53833-85-5	$C_{12}H_{18}O_2$	194.27		[12]
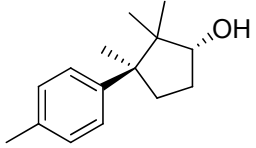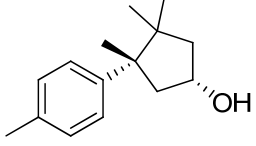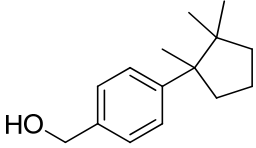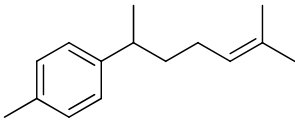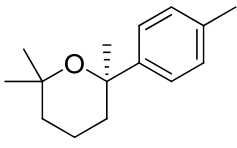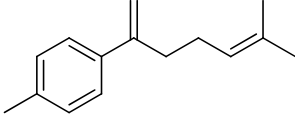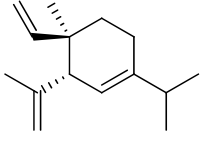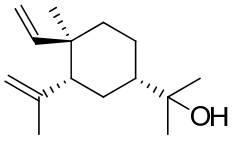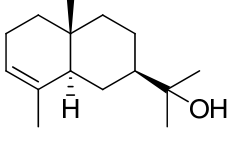
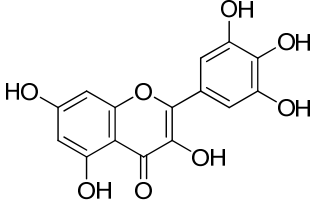| Trivial name	CAS number	Sum formula	MW	Structure	Ref.
γ-Terpinene	99-85-4	$C_{10}H_{16}$	136.23		12
4-Terpineol	562-74-3	$C_{10}H_{18}O$	154.25		12
α-Terpineol	98-55-5	$C_{10}H_{18}O$	154.25		12
α-Terpinyl acetate	80-26-2	$C_{12}H_{20}O_2$	196.29		12
α-Thujene	2867-05-2	$C_{10}H_{16}$	136.23		13
α-Thujone	546-80-5	$C_{10}H_{16}O$	152.23		14
β-Thujone	471-15-8	$C_{10}H_{16}O$	152.23		14
Thymol acetate	528-79-0	$C_{12}H_{16}O_2$	192.25		12
Verbenone	80-57-9	$C_{10}H_{14}O$	150.22		12
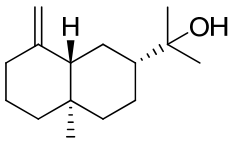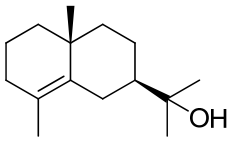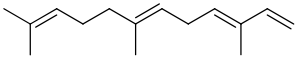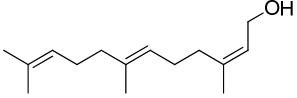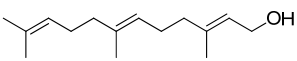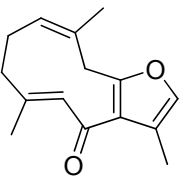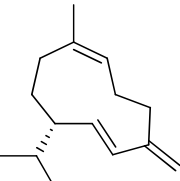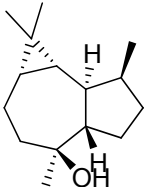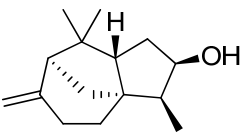
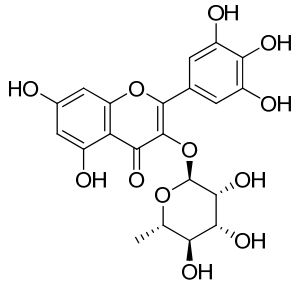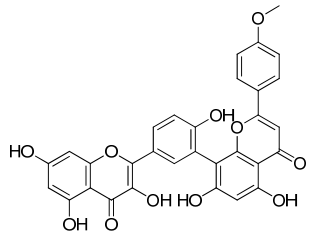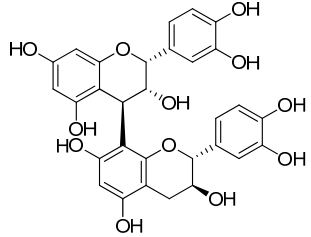**S11.** Sesquiterpenes isolated from *Biota orientalis*
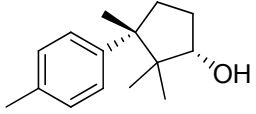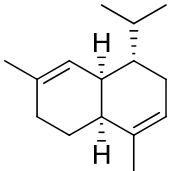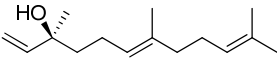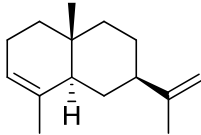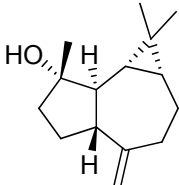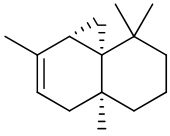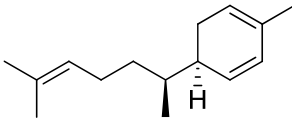
Trivial name	CAS number	Sum formula	MW	Structure	Ref.
Acetylcedrene	32388-55-9	$C_{17}H_{26}O$	246.39		12
trans-α-Atlantone	32207-08-2	$C_{15}H_{22}O$	218.33		12
α-Biotol	19902-30-8	$C_{15}H_{24}O$	220.35		15
β-Biotol	19902-26-2	$C_{15}H_{24}O$	220.35		15
α-Bisabolol	515-69-5	$C_{15}H_{26}O$	222.37		12
epi-α-Bisabolol	78148-59-1	$C_{15}H_{26}O$	222.37		12
β-Bisabolol	15352-77-9	$C_{15}H_{26}O$	222.37		12

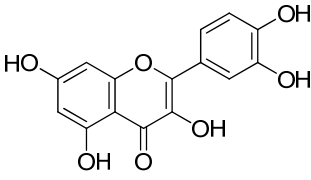| Trivial name	CAS number	Sum formula	MW	Structure	Ref.
β-Cadinene	523-47-7	$C_{15}H_{24}$	204.35		12
γ-Cadinene	39029-41-9	$C_{15}H_{24}$	204.35		12
α-Cadinol	481-34-5	$C_{15}H_{26}O$	222.37		12
β-Cadinol	481-33-4	$C_{15}H_{26}O$	222.37		12
τ-Cadinol	5937-11-1	$C_{15}H_{26}O$	222.37		12
β-Caryophyllene	87-44-5	$C_{15}H_{24}$	204.35		12
β-Caryophyllene oxide (Caryophyllene oxide)	1139-30-6	$C_{15}H_{24}O$	220.35		12

Trivial name	CAS number	Sum formula	MW	Structure	Ref.
α -Cedrene	469-61-4	$C_{15}H_{24}$	204.35		[12]
β-Cedrene	546-28-1	$C_{15}H_{24}$	204.35		[12]
α-Cedrol	77-53-2	$C_{15}H_{26}O$	222.37		[4, 12]
Cedryl acetate	77-54-3	$C_{17}H_{28}O_2$	264.40		[12]
α-Cubebene	17699-14-8	$C_{15}H_{24}$	204.35		[12]
β -Cubebene	13744-15-5	$C_{15}H_{24}$	204.35		[12]
(-)-Cuparene	56324-31-3	$C_{15}H_{22}$	202.34		[12]
(+)-Cuparene	16982-00-6	$C_{15}H_{22}$	202.34		[12]
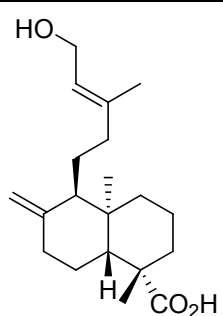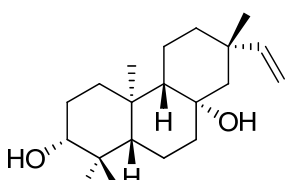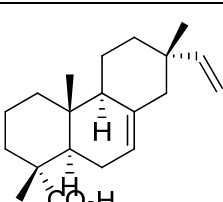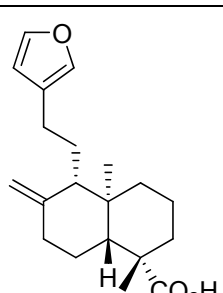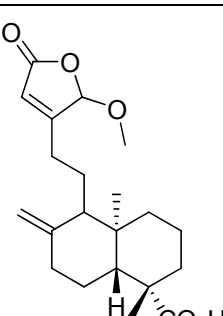
Trivial name	CAS number	Sum formula	MW	Structure	Ref.
α-Cuparenol	21730-88-1	$C_{15}H_{22}O$	218.33		15
β-Cuparenol	24887-33-0	$C_{15}H_{22}O$	218.33		15
γ-Cuparenol	4584-25-2	$C_{15}H_{22}O$	218.33		15
Curcumene	644-30-4	$C_{15}H_{22}$	202.34		12
Curcumene ether	24048-43-9	$C_{15}H_{22}O$	218.33		16
Dehydro-α-curcumene	4999-58-0	$C_{15}H_{20}$	200.32		17
δ-Elemene	20307-84-0	$C_{15}H_{24}$	204.35		12
α-Elemol	639-99-6	$C_{15}H_{26}O$	222.37		12
α-Eudesmol	473-16-5	$C_{15}H_{26}O$	222.37		12
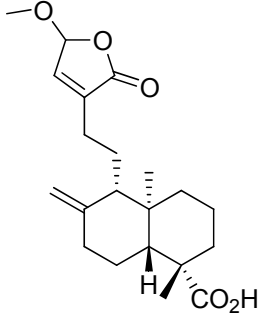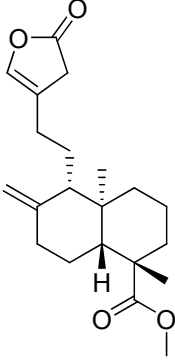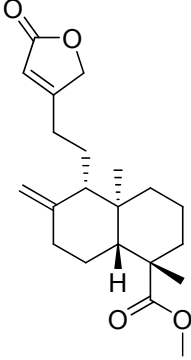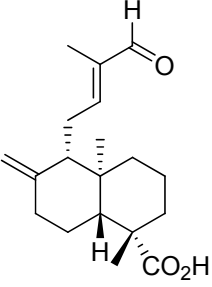
Trivial name	CAS number	Sum formula	MW	Structure	Ref.
β -Eudesmol	473-15-4	$C_{15}H_{26}O$	222.37		[12]
γ-Eudesmol	1209-71-8	$C_{15}H_{26}O$	222.37		[12]
Farnesene	502-61-4	$C_{15}H_{24}$	204.35		[18]
cis,trans-Farnesol	3790-71-4	$C_{15}H_{26}O$	222.37		[12]
trans-Farnesol/ *E,E*-Farnesol	106-28-5	$C_{15}H_{26}O$	222.37		[12]
Furanodienone	24268-41-5	$C_{15}H_{18}O_2$	230.30		[12]
Germacrene D	23986-74-5	$C_{15}H_{24}$	204.35		[12]
Globulol	489-41-8	$C_{15}H_{26}O$	222.37		[12]
β-Isobiotol	24048-41-7	$C_{15}H_{24}O$	220.35		[16]
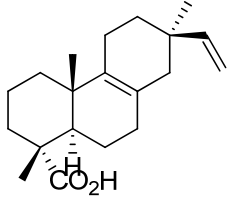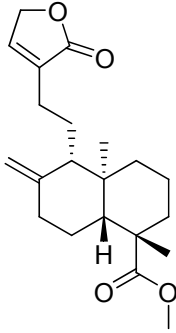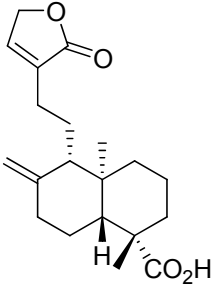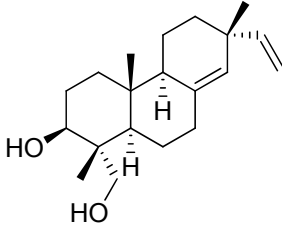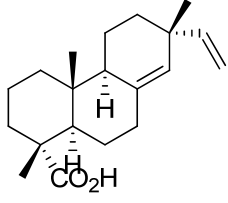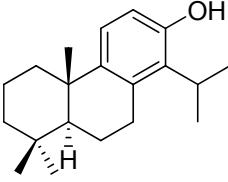
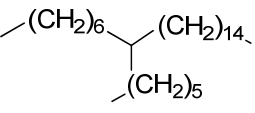| Trivial name	CAS number	Sum formula	MW	Structure	Ref.
α -Isocuparenol	21730-87-0	$C_{15}H_{22}O$	218.33		[15]
α-Muurolene	10208-80-7	$C_{15}H_{24}$	204.35		[12]
Nerolidol	7212-44-4	$C_{15}H_{26}O$	222.37		[12]
α-Selinene	473-13-2	$C_{15}H_{24}$	204.35		[12]
Spathulenol	6750-60-3	$C_{15}H_{24}O$	220.35		[12]
Thujopsene	470-40-6	$C_{15}H_{24}$	204.35		[12]
Zingiberene	495-60-3	$C_{15}H_{24}$	204.35		[12]

S12. Diterpenes isolated from *Biota orientalis*
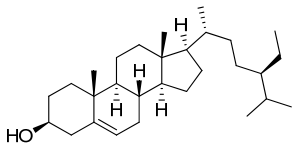
Trivial name	CAS number	Sum formula	MW	Structure	Ref.
14,15-bisnor-13-oxo-8(17),11(*E*)-labdadiene-19-oic acid	98531-41-0	$C_{18}H_{26}O_3$	290.40		4
cis-Communic acid	1231-35-2	$C_{20}H_{30}O_2$	302.45		4
trans-Communic acid	10178-32-2	$C_{20}H_{30}O_2$	302.45		4
15-Hydroxy-pinusolidic acid	131737-65-0	$C_{20}H_{28}O_5$	348.43		4
3-Hydroxy-sandaraco-pimaric acid methyl ester	151384-98-4	$C_{21}H_{32}O_3$	332.48		19

Trivial name	CAS number	Sum formula	MW	Structure	Ref.
Isocupressic acid	1909-91-7	$C_{20}H_{32}O_3$	320.47		[19]
Ent-isopimara-15-en-3α,8α-diol	462122-56-1	$C_{20}H_{34}O_2$	306.48		[20]
Isopimaric acid	5835-26-7	$C_{20}H_{30}O_2$	302.45		[4]
Lambertianic acid (Daniellic acid)	4966-13-6	$C_{20}H_{28}O_3$	316.43		[20]
16-Methoxy labda-8(17),13-dien-15,19-dioic acid butenolide	303176-48-9	$C_{21}H_{30}O_5$	362.46		[19]
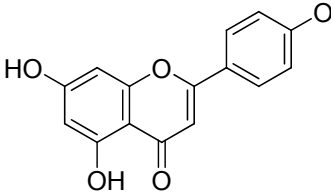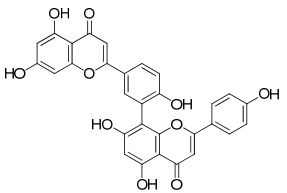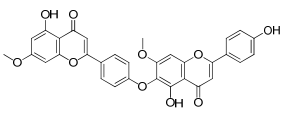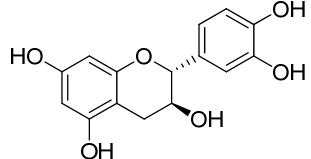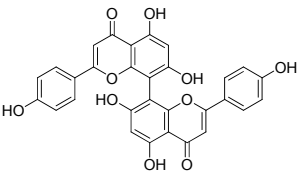
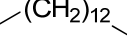| Trivial name	CAS number	Sum formula	MW	Structure	Ref.
15-Methoxypinu-solidic acid	769928-72-5	$C_{21}H_{30}O_5$	362.46		[20]
Methyl 8(17),13(16)-labdadiene-16,15-olide-18-oate	443965-67-1	$C_{21}H_{30}O_4$	346.46		[21]
Methyl 8(17),13-labdadiene-16,15-olide-18-oate	130464-01-6	$C_{21}H_{30}O_4$	346.46		[21]
15-norlabda-8(17),12(E)-diene-14-carboxyaldehyde-19-oic-acid	144125-18-8	$C_{19}H_{28}O_3$	304.42		[4]
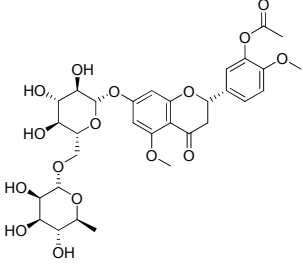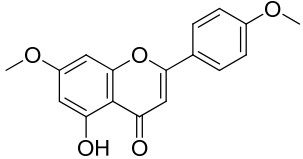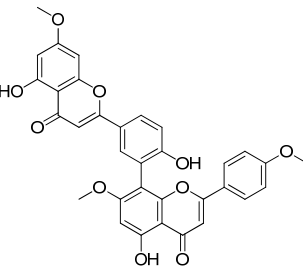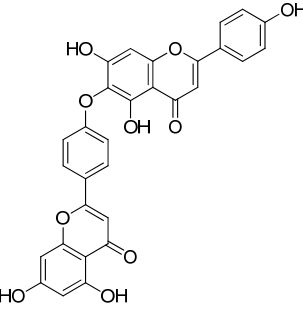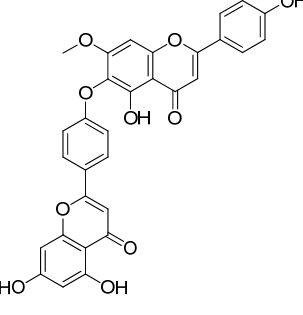
Trivial name	CAS number	Sum formula	MW	Structure	Ref.
8,15-Pimaradien-18-oic acid	7715-76-6	$C_{20}H_{30}O_2$	302.45		4
Pinusolide	31685-80-0	$C_{21}H_{30}O_4$	346.46		4
Pinusolidic acid	40433-82-7	$C_{20}H_{28}O_4$	332.43		4
Sandaraco-pimaradienediol	59219-64-6	$C_{20}H_{32}O_2$	304.47		22
Sandaracopimaric acid	471-74-9	$C_{20}H_{30}O_2$	302.45		4
Totarol	511-15-9	$C_{20}H_{30}O$	286.45		23
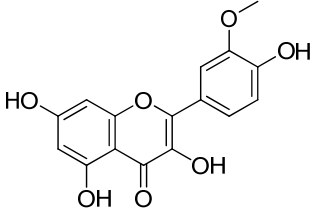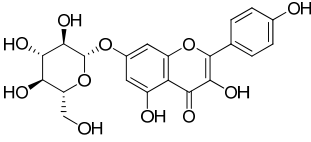
S13. Steroles isolated from *Biota orientalis*
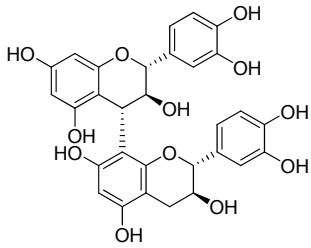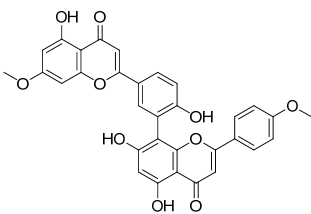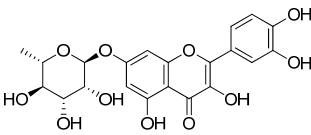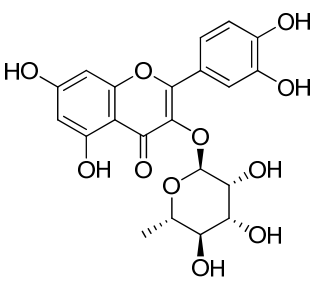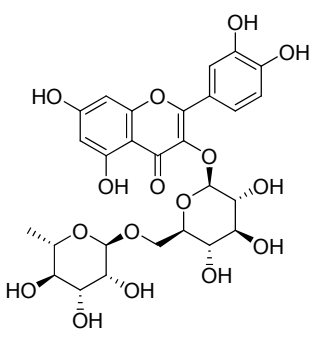
Trivial name	CAS number	Sum formula	MW	Structure	Ref.
β-Sitosterol	83-46-5	$C_{29}H_{50}O$	414.71		4

S14. Flavonoids isolated from *Biota orientalis*
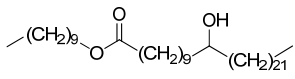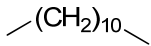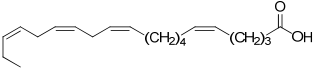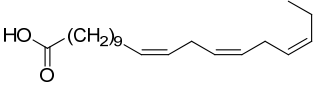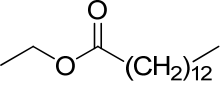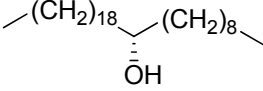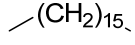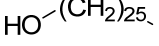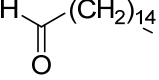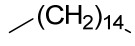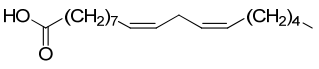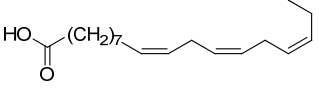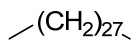
Trivial name	CAS number	Sum formula	MW	Structure	Ref.
Acacetin	480-44-4	$C_{16}H_{12}O_5$	284.26		[19]
Amentoflavone	1617-53-4	$C_{30}H_{18}O_{10}$	538.46		[24]
Apigenin	520-36-5	$C_{15}H_{10}O_5$	270.24		[19, 25]
Chamecyparin	20931-35-5	$C_{32}H_{22}O_{10}$	566.51		[19]
(+)-Catechin	154-23-4	$C_{15}H_{14}O_6$	290.27		[26]
Cupressuflavone	3952-18-9	$C_{30}H_{18}O_{10}$	538.46		[27, 28]
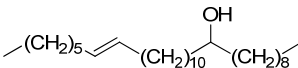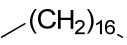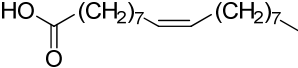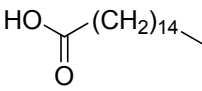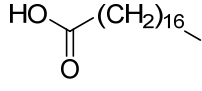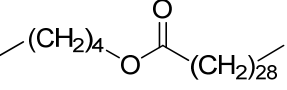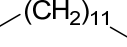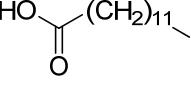
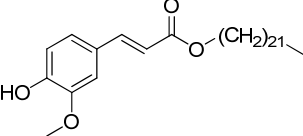| Trivial name	CAS number	Sum formula	MW	Structure	Ref.
5,4'-dimethyl 3'-acetyl eriodicytol 70.β rutinoside	752259-33-9	$C_{31}H_{38}O_{16}$	666.62		29
4',7-Dimethyl-apigenin	5128-44-9	$C_{17}H_{14}O_5$	298.29		4
(-)-Epicatechin	490-46-0	$C_{15}H_{14}O_6$	290.27		26
Heveaflavone	23132-13-0	$C_{33}H_{24}O_{10}$	580.54		19
Hinokiflavone	19202-36-9	$C_{30}H_{18}O_{10}$	538.46		28
Isocryptomerin	20931-58-2	$C_{31}H_{20}O_{10}$	552.48		19

Trivial name	CAS number	Sum formula	MW	Structure	Ref.
Isorhamnetin	480-19-3	$C_{16}H_{12}O_7$	316.26		[25]
Kaempferol 7-O-glucoside	16290-07-6	$C_{21}H_{20}O_{11}$	448.38		[27]
Myricetin	529-44-2	$C_{15}H_{10}O_8$	318.24		[25]
Myricitrine	17912-87-7	$C_{21}H_{20}O_{12}$	464.38		[27]
Podocarpusflavone	22136-74-9	$C_{31}H_{20}O_{10}$	552.48		[28]
Procyanidin B1	20315-25-7	$C_{30}H_{26}O_{12}$	578.52		[26]
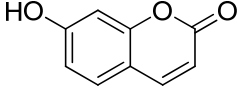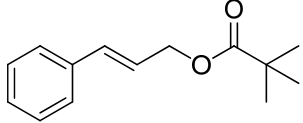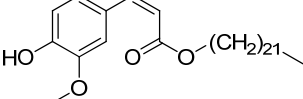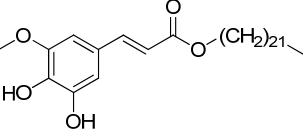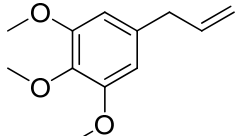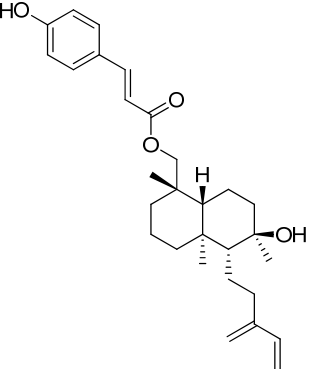
Trivial name	CAS number	Sum formula	MW	Structure	Ref.
Procyanidin B3	23567-23-9	$C_{30}H_{26}O_{12}$	578.52		26
Putraflavone	23624-21-7	$C_{32}H_{22}O_{10}$	566.51		19
Quercetin	117-39-5	$C_{15}H_{10}O_7$	302.24		24, 25, 27, 30
Quercetin 7-*O*-rhamnoside	22007-72-3	$C_{21}H_{20}O_{11}$	448.38		27
Quercitrin	522-12-3	$C_{21}H_{20}O_{11}$	448.38		24
Rutin	153-18-4	$C_{27}H_{30}O_{16}$	610.52		24, 30
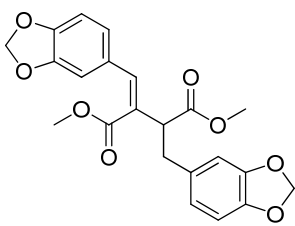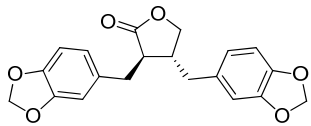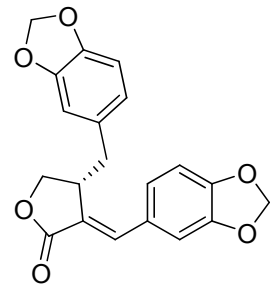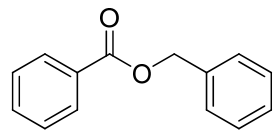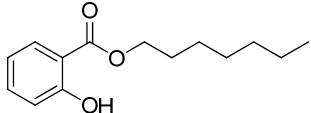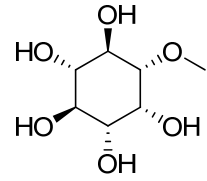
S15. Fatty acids isolated from *Biota orientalis*

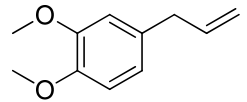| Trivial name	CAS number	Sum formula	MW	Structure	Ref.
Decyl 11-hydroxytritriacontan-oate	444311-96-0	$C_{43}H_{86}O_3$	651.14		21
Dodecane	112-40-3	$C_{12}H_{26}$	170.33		12
5,11,14,17-Eicosatetraenoic acid, (5Z,11Z,14Z,17Z)-	18016-45-0	$C_{20}H_{32}O_2$	304.47		31
11,14,17-Eicosatrienoic acid, (11Z,14Z,17Z)-	17046-59-2	$C_{20}H_{34}O_2$	306.48		31
Ethyl tetradecanoate	124-06-1	$C_{16}H_{32}O_2$	256.42		12
Ginnol	2606-50-0	$C_{29}H_{60}O$	424.79		4
Heptadecane	629-78-7	$C_{17}H_{36}$	240.47		12
1-Hexacosanol	506-52-5	$C_{26}H_{54}O$	382.71		4
Hexadecanal	629-80-1	$C_{16}H_{32}O$	240.42		12
Hexadecane	544-76-3	$C_{16}H_{34}$	226.44		12
8-Hexyltricosane	137280-60-5	$C_{29}H_{60}O_2$	408.79		21
Linoleic acid	60-33-3	$C_{18}H_{32}O_2$	280.45		31
Linolenic acid	463-40-1	$C_{18}H_{30}O_2$	278.43		31
Nonacosane	630-03-5	$C_{29}H_{60}$	408.79		30

149

Trivial name	CAS number	Sum formula	MW	Structure	Ref.
Octacosane-10-ol-21-ene	444311-95-9	$C_{28}H_{56}O$	408.74		[21]
Octadecane	593-45-3	$C_{18}H_{38}$	254.49		[12]
Oleic acid	112-80-1	$C_{18}H_{34}O_2$	282.46		[31]
Palmitic acid	57-10-3	$C_{16}H_{32}O_2$	256.42		[4, 31]
Stearic acid	57-11-4	$C_{18}H_{36}O_2$	284.48		[31]
Tetradecane	629-59-4	$C_{14}H_{30}$	198.39		[12]
Triacontanoic acid	116044-06-5	$C_{35}H_{70}O_2$	522.93		[21]
Tridecane	629-50-5	$C_{13}H_{28}$	184.36		[12]
Tridecanoic acid	638-53-9	$C_{13}H_{26}O_2$	214.34		[12]

S16. Miscellaneous compounds from *Biota orientalis*

Trivial name	CAS number	Sum formula	MW	Structure	Ref.
Coumarins					
Coumarin (Umbelliferon)	93-35-6	$C_9H_6O_3$	162.14		19
Phenylpropanoids					
Cinnamyl valerate	10482-65-2	$C_{14}H_{18}O_2$	218.29		12
Docosyl *cis*-ferulate	133882-81-2	$C_{32}H_{54}O_4$	502.77		4
Docosyl *trans*-ferulate	101927-24-6	$C_{32}H_{56}O_4$	502.77		4
Docosyl *trans*-3-hydroxy-ferulate	252366-72-6	$C_{32}H_{54}O_5$	518.77		4
Elemicin	487-11-6	$C_{12}H_{16}O_3$	208.25		12
8-Hydroxy-labda-13(16),14-dien-19-yl-*E*-coumarate	117254-98-5	$C_{29}H_{40}O_4$	452.63		19

| Trivial name	CAS number	Sum formula	MW	Structure	Ref.
Lignans					
Dehydrohelio-buphthalmin	66547-92-0	$C_{22}H_{20}O_8$	412.39		[32]
Hinokinin	26543-89-5	$C_{20}H_{18}O_6$	354.35		[32]
Savinin	493-95-8	$C_{20}H_{16}O_6$	352.34		[32]
Phenolic compounds					
Methyleugenol	93-15-2	$C_{11}H_{14}O_2$	178.23		[12]
Benzylbenzoate	120-51-4	$C_{14}H_{12}O_2$	212.24		[12]
Heptylsalicylate	6259-77-4	$C_{14}H_{20}O_3$	236.31		[12]
Miscellaneous					
Bornesitol	484-71-9	$C_7H_{14}O_6$	194.18		[4]

References

(1) Shults, E. E.; Velder, J., et al., *Bioorg. Med. Chem. Lett.* **2006,** *16*, 4228.
(2) Yang, H. O.; Suh, D. Y., et al., *Planta Med.* **1995,** *61*, 37-40.
(3) Asili, J.; Lambert, M., et al., *J. Nat. Prod.* **2004,** *67*, 631.
(4) Kuo, Y. H.; Chen, W.-C., *J. Chin. Chem. Soc.* **1999,** *46*, 819.
(5) Sakar, M. K.; Er, N., et al., *Acta Pharm. Turc.* **2002,** *44*, 213-219.
(6) Sung, S. H.; Koo, K. A., et al., *Kor. Soc. Pharmacognosy* **1998,** *29*, 347.
(7) Zgoda-Pols, J.; Freyer, A. J., et al., *Fitoterapia* **2002,** *73*, 434.
(8) Morisawa, J.; Kim, C. S., et al., *Biosci., Biotechnol., Biochem.* **2002,** *66*, 2424-8.
(9) Marcos, I. S.; Cubillo, M. A., et al., *Tetrahedron Lett.* **2003,** *44*, 8831.
(10) Banerjee, A. K.; Laya, M. S., et al., *Curr. Org. Chem.* **2008,** *12*, 1050.
(11) Ncanana, S.; Baratto, L., et al., *Adv. Synth. Catal.* **2007,** *349*, 1507.
(12) Singh, A.; Yadaw, A., *Indian Perfumer* **2005,** *49*, 173.
(13) Nickavar, B.; Amin, G., et al., *Z. Naturforsch., C: J. Biosci.* **2003,** *58*, 171.
(14) Chizzola, R.; Hochsteiner, W., et al., *Res. Vet. Sci.* **2004,** *76*, 77.
(15) Tomita, B.; Hirose, Y., et al., *Tetrahedron Lett.* **1968,** *7*, 843-848.
(16) Tomita, B.; Hirose, Y., et al., *Mokuzai Gakkaishi* **1969,** *15*, 47.
(17) Tomita, B.; Hirose, Y., et al., *Mokuzai Gakkaishi* **1969,** *15*, 46.
(18) Song, G.; Deng, C., et al., *Chromatographia* **2003,** *58*, 769.
(19) Lee, H.-K.; Ahn, K.-S., et al. *Recent Advances in Natural Products Research, Proceedings of the International Symposium on Recent Advances in Natural Products Research, 3rd*, Seoul, Republic of Korea, 1999 Ed.: Shin, K.-H.; Kang, S. S.; Kin, Y. S., pp 54-62.
(20) Koo, K. A.; Sung, S. H., et al., *Chem. Pharm. Bull.* **2002,** *50*, 834.
(21) Mehta, B.; Nagar, V., et al., *Indian J. Chem., Sect. B: Org. Chem. Incl. Med. Chem.* **2002,** *41B*, 1088.
(22) Ren, X.-Y.; Ye, Y., *J. Asian Nat. Prod. Res.* **2006,** *8*, 677.
(23) Lee, M. K.; Yang, H., et al., *Arch. Pharmacal Res.* **2008,** *31*, 866.
(24) Lu, Y.-H.; Liu, Z.-Y., et al., *J. Pharm. Biomed. Anal.* **2006,** *41*, 1186.
(25) Kim, H. Y.; Kang, M. H., *Food Sci. Technol.* **2003,** *12*, 687.
(26) Sakar, M. K.; Engelshowe, R., *J. Faculty Pharm. Istanbul Univ.* **1985,** *21*, 80-85.
(27) Khabir, M.; Khatoon, F., et al., *Curr. Sci.* **1985,** *54*, 1180.
(28) Gadek, P. A.; Quinn, C. J., *Phytochemistry* **1985,** *24*, 267.
(29) Fahmy, H., *J. Environ. Sci. (Mansoura, Egypt)* **2003,** *26*, 297.
(30) Zhu, J. X.; Wang, Y., et al., *J. Ethnopharmacol.* **2004,** *93*, 133.
(31) Lie Ken Jie, M. S. F.; Lao, H. B., et al., *J. Am. Oil Chem. Soc.* **1988,** *65*, 597.
(32) Yoon, J. S.; Koo, K. A., et al., *Nat. Prod. Sci.* **2008,** *14*, 167.

3.5. IDENTIFICATION OF GABA_A RECEPTOR MODULATORS IN *KADSURA LONGIPEDUNCULATA* AND ASSIGNMENT OF ABSOLUTE CONFIGURATIONS BY QUANTUM-CHEMICAL ECD CALCULATIONS

Zaugg J, Ebrahimi SN, Smiesko M, Baburin I, Hering S, Hamburger M.
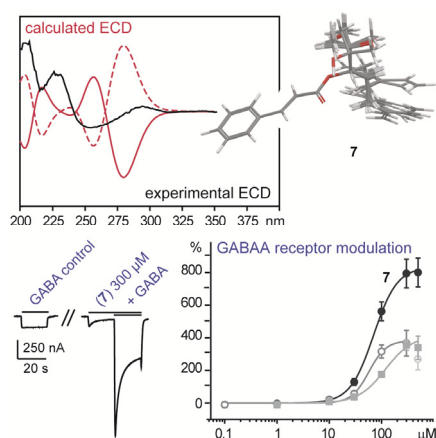
HPLC-based activity profiling enabled the identification of 10 lignans and 3 terpenoids (two of them were new natural products) of *K. longipedunculata* fruits to be tested in the functional *Xenopus* oocyte assay for positive $\alpha_1\beta_2\gamma_{2S}$ GABA_A receptor modulating activity. Concentration-response experiments on 12 compounds revealed interesting new scaffolds at the target. Structures were elucidated by mass spectrometry and microprobe NMR. The absolute configuration of the terpenoids was determined by ECD supported by *in silico* simulation of ECD spectra.

Identification of GABA A receptor modulators in *Kadsura longipedunculata* and assignment of absolute configurations by quantum-chemical ECD calculations

Janine Zaugg [a], Samad Nejad Ebrahimi [a,b], Martin Smiesko [c], Igor Baburin [d], Steffen Hering [d], Matthias Hamburger [a,*]

[a] *Division of Pharmaceutical Biology, University of Basel, Klingelbergstrasse 50, 4056 Basel, Switzerland*
[b] *Departement of Phytochemistry, Medicinal Plant and Drugs Research Institute, Shahid Beheshti University, G.C., Tehran, Iran*
[c] *Division of Molecular Modeling, University of Basel, Klingelbergstrasse 50, 4056 Basel, Switzerland*
[d] *Institute of Pharmacology and Toxicology, University of Vienna, Althanstrasse 14, 1090 Vienna, Austria*

ABSTRACT

A petroleum ether extract of *Kadsura longipedunculata* enhanced the GABA-induced chloride current (I_{GABA}) by $122.5 \pm 0.3\%$ ($n = 2$) when tested at 100 µg/ml in *Xenopus laevis* oocytes expressing GABA A receptors ($\alpha_1\beta_2\gamma_{2S}$ subtype) in two-microelectrode voltage clamp measurements. Thirteen compounds were subsequently identified by HPLC-based activity profiling as responsible for GABA A receptor activity and purified in preparative scale. 6-Cinnamoyl-6,7-dihydro-7-myrcenol and 5,6-dihydrocuparenic acid were thereby isolated for the first time. The determination of the absolute stereochemistry of these compounds was achieved by comparison of experimental and calculated ECD spectra. All but one of the 13 isolated compounds from *K. longipedunculata* potentiated I_{GABA} through GABA A receptors composed of $\alpha_1\beta_2\gamma_{2S}$ subunits in a concentration-dependent manner. Potencies ranged from 12.8 ± 3.1 to 135.6 ± 85.7 µM, and efficiencies ranged from $129.7 \pm 36.8\%$ to $885.8 \pm 291.2\%$. The phytochemical profiles of petroleum ether extracts of *Kadsura japonica* fruits ($114.1 \pm 2.6\%$ potentiation of I_{GABA} at 100 µg/ml, $n = 2$), and *Schisandra chinensis* fruits (inactive at 100 µg/ml) were compared by HPLC-PDA-ESIMS with that of *K. longipedunculata*.

© 2011 Elsevier Ltd. All rights reserved.

1. Introduction

Gamma-aminobutyric acid type A (GABA A) receptors are heteropentameric chloride ion channels and are targets for the major inhibitory neurotransmitter of the central nervous system, gamma-aminobutyric acid (GABA). Chloride channel opening of the GABA A receptor leads to a hyperpolarization of the neuronal membrane and inhibition of further action potentials. To date, 11 GABA A receptor subtypes known to exist in the human brain differ in function and tissue localization, the most prominent being the $\alpha_1\beta_2\gamma_{2S}$ subtype (Olsen and Sieghart, 2008). Numerous sedative-anxiolytics and sedative-hypnotics, such as benzodiazepines and *z*-compounds (zolpidem, zaleplon etc.), and some general anesthetics and antiepileptics, bind to GABA A receptors. However, side-effects of these drugs due to lack of GABA A receptor subtype selectivity limit their clinical use. Thus, there is a continued medical need for GABA A receptor modulators with new structural scaffolds and potential subtype selectivity (Mohler, 2011).

We recently screened a library of fungal and plant extracts in an automated functional two-microelectrode voltage clamp assay on *Xenopus* oocytes (Baburin et al., 2006) which transiently expressed GABA A receptors of the $\alpha_1\beta_2\gamma_{2S}$ subtype. Among the 982 extracts of the library were nine extracts originating from three different species of the Schisandraceae family (*Kadsura longipedunculata*, *Kadsura japonica* and *Schisandra chinensis*). Among these, petroleum ether extracts of *K. longipedunculata* and *K. japonica* showed promising activity.

Kadsura and Schisandra species are scandent, woody vines growing throughout Eastern and Southeastern Asia, with the highest diversity lying in Southern China (Saunders, 1998, 2000). Both genera share highly similar morphologic and anatomic characteristics (Saunders, 1998). In Russia, *S. chinensis* fruits have been used as an adaptogen and stimulant (limonnika kitajskogo nastojka) (Panossian and Wikman, 2008), whereas in traditional Chinese medicine dried fruits of *S. chinensis* (Bei-Wuweizi) and *S. sphenanthera* (Nan-Wuweizi) are officinal drugs to treat respiratory malfunction, spermatorrhoea, enuresis, diarrhea, night sweating, insomnia and hepatitis (Haensel et al., 1993; Hou and Youyu, 2005; Lu and Chen, 2009; Stoeger, 2009). *K. japonica* fruits have more or less the same indications as Schisandra fruits and are used as an unofficial commercial grade of these (Haensel et al., 1993). *K. longipedunculata* is

one of the most common species of Kadsura in China. Traditionally the stems and roots are used for medicinal purposes, while the fruits are eaten locally or serve as a source of fragrant oils (Saunders, 1998). Up to now, only roots and stems of *K. longipedunculata* have been investigated phytochemically, but not the fruits. Due to morphological similarity, *Schisandra* fruits may easily be confused with the dried fruits from *Kadsura* species (Fujita, 1929; Haensel et al., 1993; Xiao et al., 2010).

In this study, 13 natural products from a petroleum ether extract of *K. longipedunculata* fruits were identified as positive GABA A receptor modulators with the aid of HPLC-based activity profiling. This miniaturized approach enables rapid identification of bioactive constituents in extracts (Potterat and Hamburger, 2006) and has been successfully used in combination with various cell-based and biochemical assays (Adams et al., 2009; Danz et al., 2001; Dittmann et al., 2004; Potterat et al., 2004), including the discovery of new GABA A receptor modulators (Kim et al., 2008; Li et al., 2010; Pei et al., 1980; Yang et al., 2011; Zaugg et al., 2010, 2011a, 2011b, submitted for publication).

2. Results and discussion

2.1. Isolation and structure elucidation

A preformatted library of 982 extracts was tested in an automated, fast perfusion system during two-microelectrode voltage clamp measurements with *Xenopus* oocytes which transiently expressed GABA A receptors of the subunit combination $\alpha_1\beta_2\gamma_{2S}$ (Baburin et al., 2006). At a concentration of 100 µg/ml petroleum ether extracts of *K. longipedunculata* and *K. japonica* fruits enhanced the GABA induced chloride current (I_{GABA}) by 122.5 ± 0.3% ($n = 2$) and 114.1 ± 2.6% ($n = 2$), respectively, while ethyl acetate and MeOH extracts of both drugs were not active (data not shown). Interestingly, the petroleum ether, ethyl acetate and MeOH extracts from the taxonomically related *S. chinensis* fruits showed no activity. Next, we performed HPLC-based activity profiling with the active extract of *K. longipedunculata* using a validated protocol (Kim et al., 2008) to identify the constituents responsible for the activity. The chromatogram (266 nm) of a semipreparative HPLC separation (10 mg of extract) and the corresponding activity profile of the time-based microfractionation (28 microfractions of 90 s each) are shown in Fig. 1B and A, respectively. The highest activity was found in fraction 12 which potentiated I_{GABA} by 498.0 ± 150.4% ($n = 3$). Fractions 4 and 13 also were active, albeit to a lesser degree (potentiation of I_{GABA} by 103.2 ± 8.2% ($n = 2$) and 160.5 ± 19.9% ($n = 3$), respectively). Fractions 8 and 14 showed minor activity (potentiation of I_{GABA} by 80.4 ± 7.2% ($n = 3$) and 70.3 ± 11.1% ($n = 3$), respectively). Preparative isolation of active compounds was achieved by liquid–liquid partitioning, normal phase open column chromatography and preparative RP-HPLC. Some structurally related but inactive compounds were also purified in view of preliminary structure–activity considerations. Nine known lignans,
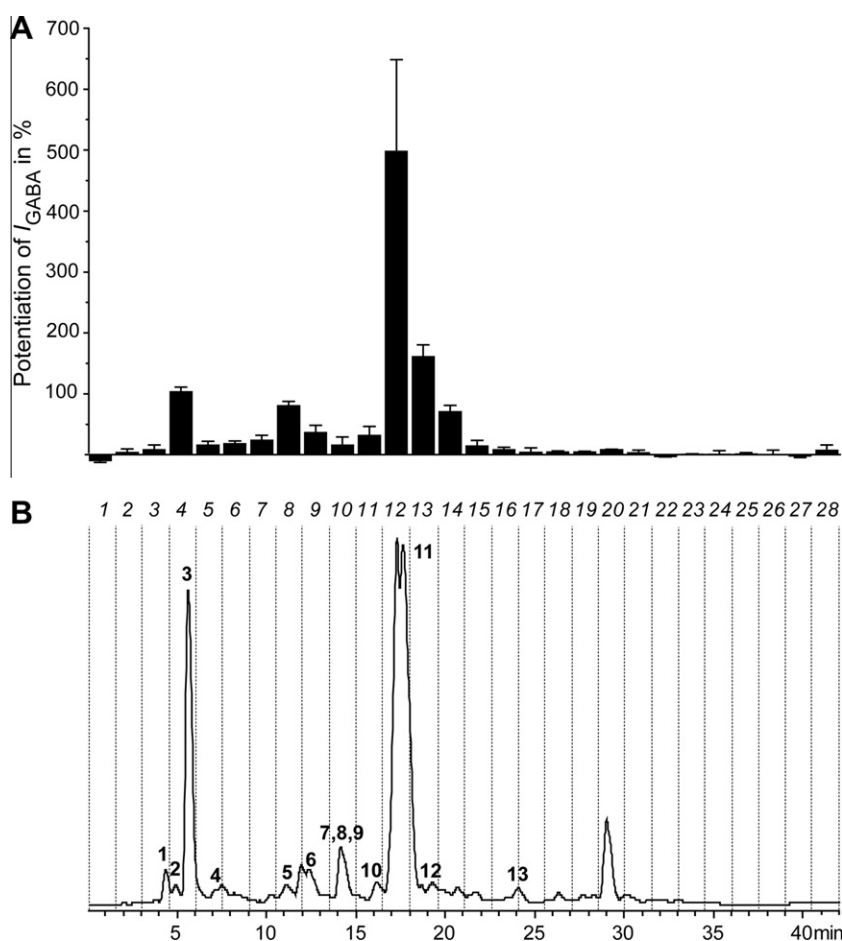

Fig. 1. HPLC-based activity profiling of a petroleum ether extract of *K. longipedunculata* fruits. The chromatogram (266 nm) of a semipreparative separation of 10 mg extract is displayed in part (B). The numbers correspond to the isolated compounds. The 28 collected microfractions (90 s each) are indicated with dashed lines. The corresponding GABA A receptor modulatory activity of each microfraction is shown in part (A) (in percent potentiation of the GABA-induced chloride current, error bars correspond to S.E.).

arisantetralones A–D (**1–4**), dihydroguaiaretic acid (**5**), mono-methyl dihydroguaiaretic acid (**8**), deoxyschizandrin (**9**), zuihonin A (**10**), anwulignan (**11**), and saururenin (**13**), and a known sesqui-terpene, (+)-γ-cuparenol (**6**), were identified by ESI-MS, 1D and 2D NMR spectroscopy, optical rotation, CD, and by comparison with published data (Cheng et al., 2009; da Silva and Lopes, 2004; Ikeya et al., 1980, 1979; Lee, 1981; Miyazawa et al., 1997; Nakatani et al., 1988; Sadhu et al., 2003; Schrecker, 1957; Urzua et al., 1987; Wang et al., 2000, 2006) (Chart 1). Analytical data of the known compounds are given as Supplementary data. In addition, a sesqui-terpene structurally closely related to **6** [(−)-5,6-dihydrocuparenic acid (**12**)] and a monoterpene cinnamic acid ester [(+)-6-cinnam-oyl-6,7-dihydro-7-myrceneol (**7**)] (Chart 1) were identified as pre-viously unreported natural products. Their structures, including absolute configurations, were established with the aid of HR-ESI-MS, 1 and 2 D NMR spectroscopic experiments, optical rotation, and ECD. Multiplicity-edited HSQC NMR and HMBC NMR

unambiguously revealed the covalent structures of compounds **7** and **12** (Chart 1, Tables 1 and 2, for complete NMR spectral datasets see Figures S8–S14 of the Supplementary data). In both cases,

Table 2
^{1}H NMR and ^{13}C NMR spectroscopic data of compound **7**[a].

C[b]		H	
C1	24.5	1	1.21 s
C2	71.3	2	–
C2-CH₃	24.5	2-CH₃	1.21 s
C3	79.6	3	4.98 dd (2.3, 10.3)
C4	27.9	4a	1.98 dddd (14.4, 9.7, 6.4, 2.3)
		4b	1.81 dddd (14.4, 10.3, 9.7, 5.4)
C5	28.2	5a	2.29 ddd (14.6, 5.4, 9.7)
		5b	2.21 ddd (14.6, 9.7, 6.4)
C6	146.0	6	–
C6–CH₂	115.1	6-CH₂	5.01 s
C7	138.9	7	6.36 dd (17.6, 12.0)
C8	112.3	8a	5.22 d (17.6)
		8b	5.04 d (12.0)
C1′	167.5	1′	–
C2′	117.7	2′	6.57 d (16.0)
C3′	145.0	3′	7.75 d (16.0)
C4′	134.4	4′	–
C5′	127.7	5′	7.59 m
C6′	128.7	6′	7.39 m
C7′	130.2	7′	7.39 m
C8′	128.7	8′	7.39 m
C9′	127.7	9′	7.59 m

[a] Recorded in MeOD at 500 MHz (^{1}H) with chemical shift (ppm) of solvent used as internal standard.
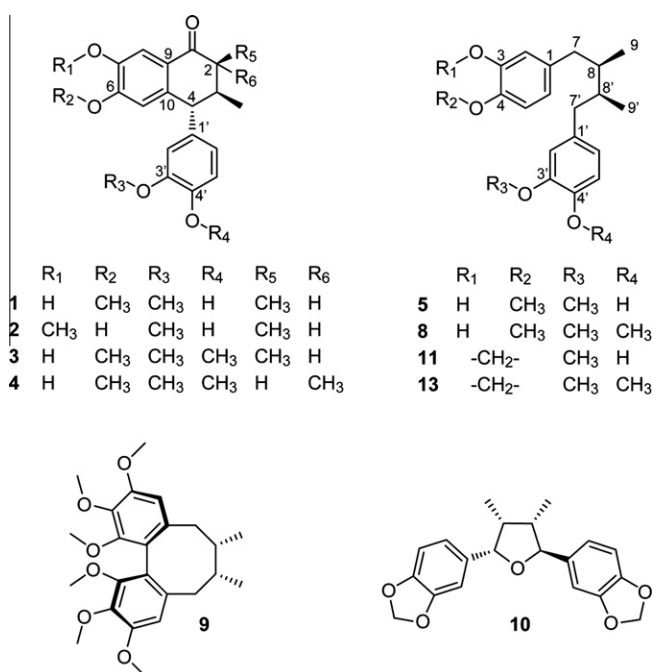[b] ^{13}C shifts from HSQC and HMBC NMR experiment.

Chart 1. Isolated compounds from *K. longipedunculata* fruits.

Table 1
^{1}H NMR and ^{13}C NMR spectroscopic data of compounds **6** and **12**[a].

C	**6**[b]	**12**	H	**6**[b]	**12**
C1	138.0	124.4	1	–	–
C2	126.6	137.3	2	7.26 d (8.7)	7.14 d (6.1)
C3	127.4	118.7	3	7.35 d (8.7)	5.93 d (6.1)
C4	147.4	156.1	4	–	–
C5	127.4	26.0	5	7.35 d (8.7)	2.27 m
C6	126.6	24.7	6	7.26 d (8.7)	2.39 m
C7	65.4	173.3	7	4.63 s	–
C1′	50. 7	52.5	1′	–	–
C2′	44.5	44.1	2′	–	–
C3′	39.9	40.5	3′a	1.70 m β	1.61–1.69 m β
			3′b	1.57 m α	1.50–1.56 m α
C4′	20.0	19.6	4′	1.81 m	1.66 m
C5′	37.0	36.5	5′a	2.51 m α	2.20 m α
			5′b	1.72 m β	1.44–1.50 m β
C1′–CH₃	24.6	22.1	1′-CH₃	1.28 s	1.06 s
C2′–CH₃	24.5 β	25.1 β	2′-CH₃a	1.09 s β	1.03 s β
C2′–CH₃	26.6 α	26.9 α	2′-CH₃b	0.57 s α	0.82 s α

[a] Recorded in CDCl₃ at 500 MHz (^{1}H) and 125 MHz (^{13}C), with chemical shift (ppm) of solvent used as internal standard.
[b] Shift differences between **6** and **12** are due to the anisotropic effect of the aromatic ring.
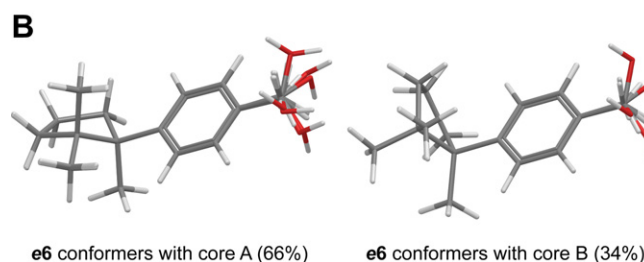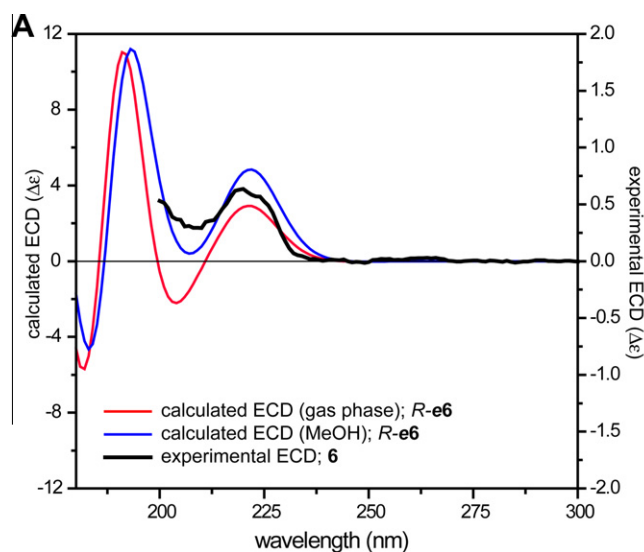

Fig. 2. (A) Minimized conformers of *R*-**e6** in the gas phase using DFT at the B3LYP/6-31G** level. Two major core conformations occurred within a 2 kcal/mol range from the global minimum. According to Boltzmann weights, core conformation A (8 species) accounted for 66%, and core conformation B (4 species) accounted for 34% of the total population. (B) Experimental ECD spectrum of (+)-γ-cuparenol (**6**) in MeOH and calculated ECD spectra of *R*-**e6** in gas-phase and MeOH using density function theory at the B3LYP/6-31G** level.
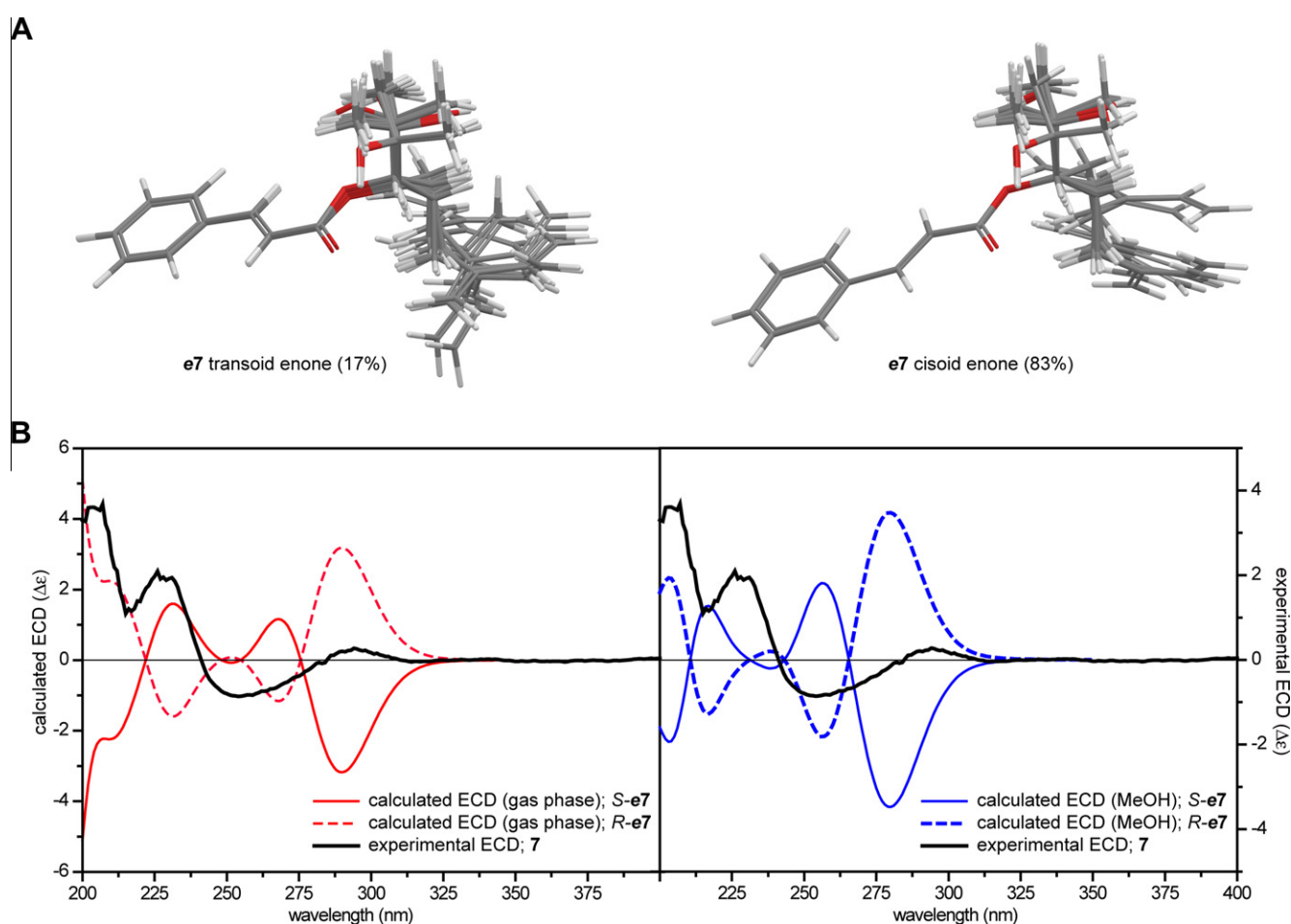
Fig. 3. (A) Minimized conformers of *S*-**e7** in the gas-phase using DFT at the B3LYP/6-31G** level. Two major core conformations occurred within a 1 kcal/mol range from the global minimum. According to Boltzmann weights, a transoid enone core (10 species) accounted for 17%, and a cisoid enone core (7 species) accounted for 83% of the total population. (B) Experimental ECD spectrum of (+)-6-cinnamoyl-6,7-dihydro-7-myrceneol (**7**) in MeOH and calculated ECD spectra of *S*-**e7** in gas-phase and MeOH using density function theory at the B3LYP/6-31G** level. Mirror images reflecting *R*-configuration are displayed with dashed lines.

NOESY NMR allowed the determination of the conformations of the predominant conformers in DMSO. A transoid diene conformation of the myrceneyl moiety of **7** was confirmed by correlations between H-7 and C6–CH$_2$ and between H-8a and H-5. Furthermore, the presence of an *E*-cinnamoyl residue was indicated by the NOESY correlation between H-2′ and H-5′/H-9′. In the case of **12**, NMR shifts of the cyclopentane moiety closely matched with the data of **6** (Table 1). The mutual orientation of the cyclopentane and the cyclohexadiene units was established by a NOESY correlation between H-5′a (α-orientated) and H-3. The absolute configurations of **6, 7** and **12** were determined and that of **6** confirmed by comparison of their CD spectra with ECD spectra calculated in the gas phase and in MeOH using time dependent density functional theory (DFT). For this purpose, 3D structures of *R*-**6** (**e6**), *S*-**7** (**e7**), and *R*-**12** (**e12**) were submitted to a systematic conformational search in H$_2$O (OPLS 2005), within an energy window of 5 kcal/mol. A total of 275 conformational species were found for **e7**, and 24 each were found for **e6** and **e12**. Conformers which were within an energy range of 1 kcal/mol (**e7**: 20) and 2 kcal/mol (**e6**: 16 and **e12**: 7) from the global minima were subject to geometrical optimization (DFT/B3LYP/6-31G**) in the gas-phase combined with calculation of vibrational modes to confirm these minima. No imaginary frequencies were found. For **e6**, **e7**, and **e12**, a total of 12, 7, and 17 species, respectively, could be confirmed (Figs. 2A, Fig. 3A, and Fig. 4A). For these conformations, ECD spectra were calculated (TDDFT/B3LYP/6-31G**) in the gas phase and in MeOH (SCRF/CPCM). Each calculated

ECD spectrum was assigned a Boltzmann weight according to the energy of the minimized conformers at 298.15 K and overlaid prior to comparison with the particular experimental ECD spectrum (Figs. 2B, Figs. 3B, and Figs. 4B). The positive and negative CE of *S*-**e7** at around 300 nm and 250 nm, respectively, appeared inverted in comparison with the experimental ECD spectrum of **7**. Mirror-images of the computed ECD spectra in the gas-phase and MeOH were in agreement with the experimental data. The mirror-image of the ECD calculation in MeOH closely matched the experimental spectrum, especially with respect to Cotton effects (CE) at lower wavelengths. In **7**, differences between calculated and experimental spectra presumably resulted from an overestimation of the UV absorbance in the calculations (Tayone et al., 2011), or may be due to minor differences between calculated and solution conformers (Kamel et al., 2009) of this flexible molecule. The predominant conformers of **e7** (7 species, 83%) had a cisoid enone conformation, while the remaining ones (10 species, 17%) showed a transoid enone conformation. Among these two major conformational groups, individual conformers further varied by bond rotations around C5-C6 and C2-C3 (Fig. 3). Boltzmann-weighted calculated ECD spectra of each conformer in the gas phase and in MeOH are given as Supplementary data (Fig. S3 and S4). Thus, compound **7** was identified as *R*-(+)-6-cinnamoyl-6,7-dihydro-7-myrceneol.

In a conformational search, compound **e6** occurred in two major core conformations A (66% contribution) and B (34% contribution) differing in the orientation of the substituted cyclopentane ring.
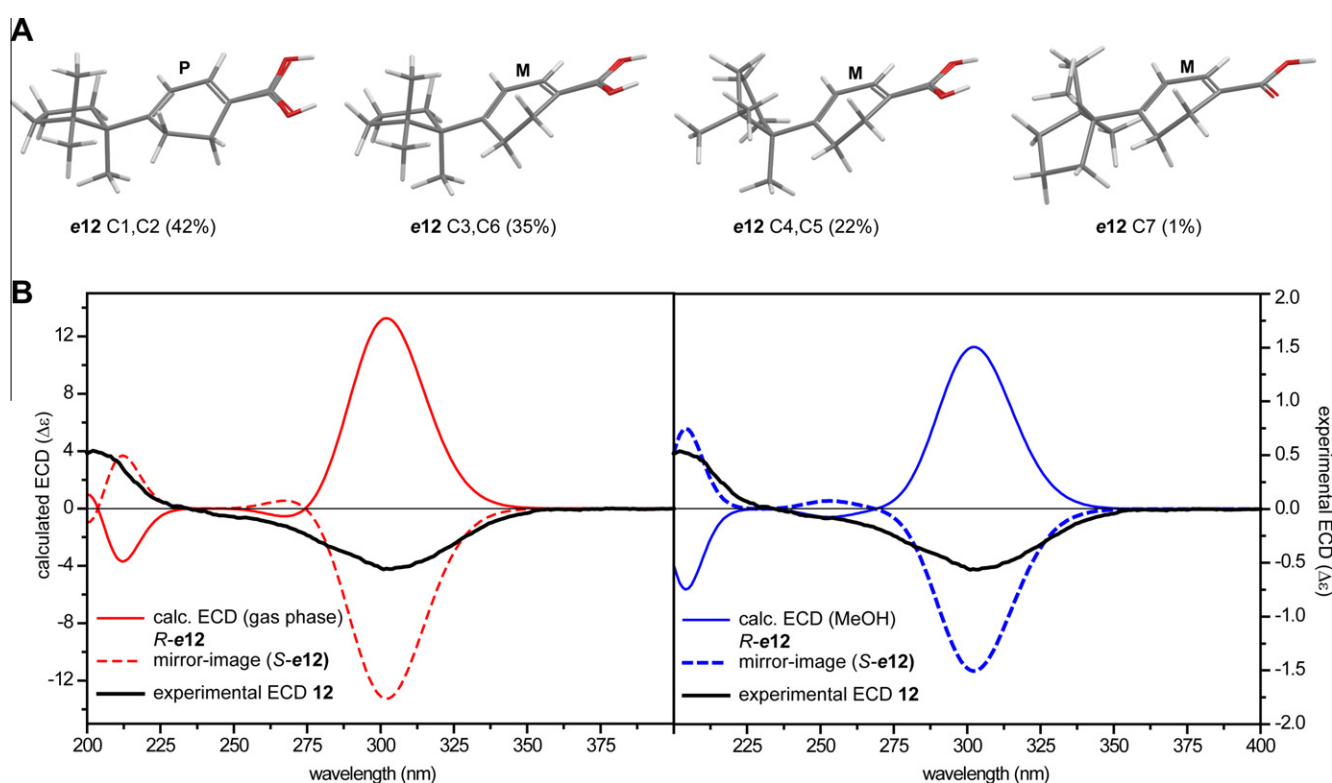
Fig. 4. (A) Minimized conformers of *R*-**e12** in the gas-phase using DFT at the B3LYP/6-31G** level. Two major core conformations occurred within a 2 kcal/mol range from the global minimum. According to Boltzmann weights, two species accounting for nearly half of the total population (42%) showed P-helicity of the cyclic diene. They only differed in the orientation of the carboxylic group. Conformers with an M-helicity (58% in total) showed further conformational variations in the orientation of the cyclopentane residue. (B) Experimental ECD spectrum of (−)-5,6-dihydrocuparenic acid (**12**) in MeOH and calculated ECD spectra of *R*-**e12** in gas-phase and MeOH using density function theory at the B3LYP/6-31G** level. Mirror images reflecting *S*-configuration are displayed with dashed lines.

Further variations arose by bond rotation around C1–C7 and rotation of the hydroxy group itself (Fig. 2A). The calculations of the **e6**-ECD spectra closely matched the experimental spectrum of **6**. The positive CE at around 220 nm was likely due to a $\pi \rightarrow \pi^*$ transition of the aromatic ring system. In agreement with the calculated ECD spectra it indicated an *R*-configuration of the stereocenter at C-1' (Fig. 2B), and compound **6** was thus identified as *R*-(+)-γ-cuparenol (Ito et al., 1965; Nayek et al., 2003). Conformational analysis and geometrical optimization of **e12** provided two major cores with positive helicity (P) (2 species; 42% contribution) and negative helicity (M) of the cyclic diene (5 species; 58% contribution), respectively. The latter further differed in the orientation of the cyclopentane residue (Fig. 4A; dihedral angles of the cyclic diene are listed in Table S2 of the Supplementary data). Inspection of the calculated ECD spectra of each conformer revealed that the change in helicity of the cyclic diene inverted the sign of the CE. P-helicity and M-helicity corresponded to a negative and a positive CE at 302 nm, respectively. Other conformational differences had no pronounced influence on the spectra (Fig. S5). Despite the apparent biosynthetic relation to **6**, calculation of ECD with *R*-**e12** did not match the negative CE at 302 nm observed in the experimental spectrum. The close match with the mirror-inverted calculated curve pointed towards an *S*-configuration of **12**. However, small conformational changes in **e12** strongly affected the sign of the calculated ECD spectra. Hence we feel that independent evidence is needed to unambiguously identify the absolute configuration of **12**.

2.2. Modulation of GABA A receptors

Modulation of GABA A receptors by compounds **1–13** (0.1-500 μM) was assessed in an automated two-microelectrode voltage clamp assay on *Xenopus* oocytes transiently expressing $\alpha_1\beta_2\gamma_{2S}$ receptors. All compounds except the dibenzocyclooctadiene lignan (**9**) enhanced I_{GABA} at a GABA EC_{5-10} in a concentration-dependent manner (see Fig. 5 and Table 3 for details). The potencies (EC_{50} values) of the four arisantetralone lignans (**1–4**) did not significantly differ from each other ($p > 0.05$). In contrast, the structural differences between **2**, and **3** and **4** significantly affected efficiencies in stimulation of I_{GABA} at a GABA EC_{5-10} ($p < 0.05$). Compound **2** had the highest efficiency of I_{GABA} modulation (885.8 ± 291.2%, $n = 4$, Table 3). Interchange of substituents at C-7 and C-6, as in **1**, did not significantly alter the efficiencies of I_{GABA} modulation (**2** ≈ **1**, $p > 0.05$). Replacing the hydroxy group at C-4' of the benzylic moiety by a methoxy group, as in **3**, significantly lowered the activity ($p < 0.05$). Stereochemistry at C-2 had no influence on the efficiencies (**2** > **3** ≈ **4**, $p < 0.05$). However, the inversion of absolute configuration at C-2 apparently affected agonistic and antagonistic potential at $\alpha_1\beta_2\gamma_{2S}$ GABA A receptors: similar to **5,7,8**, and **12**, compounds **1–3** produced small chloride currents in the absence of GABA, as observed in preincubation experiments (Fig. 5 D–F). This partial agonistic activity did not exceed 10% of the maximal current induced by a saturating GABA concentration (1 mM).

The conformationally more flexible acyclic lignans **5**, **8**, **11**, and **13** showed equal to slightly higher potencies than the arisantetralones **1–4** at GABA A receptors of $\alpha_1\beta_2\gamma_{2S}$ subunit composition. Whereas the EC_{50} values of the investigated lignans were not much affected by replacement of the free hydroxy moiety by a methoxy group at C-4' (EC_{50}: **1** ≈ **3**; **5** ≈ **8**; **11** ≈ **13**, $p > 0.05$), this structural change decreased efficiency of acyclic lignans (**8** < **5**; **13** < **11**, $p < 0.05$; **3** ≈ **1**, $p > 0.05$, see Table 3). A dioxomethylene moiety at C–3 and C-4 significantly decreased potency and efficiency in the cases of **5** and **11**, but not of **8** and **13** (EC_{50}: **5** > **11**, $p = 0.06$; efficiency **5** > **11**, $p < 0.05$; EC_{50}, efficiency: **8** ≈ **13**) (Table 3).
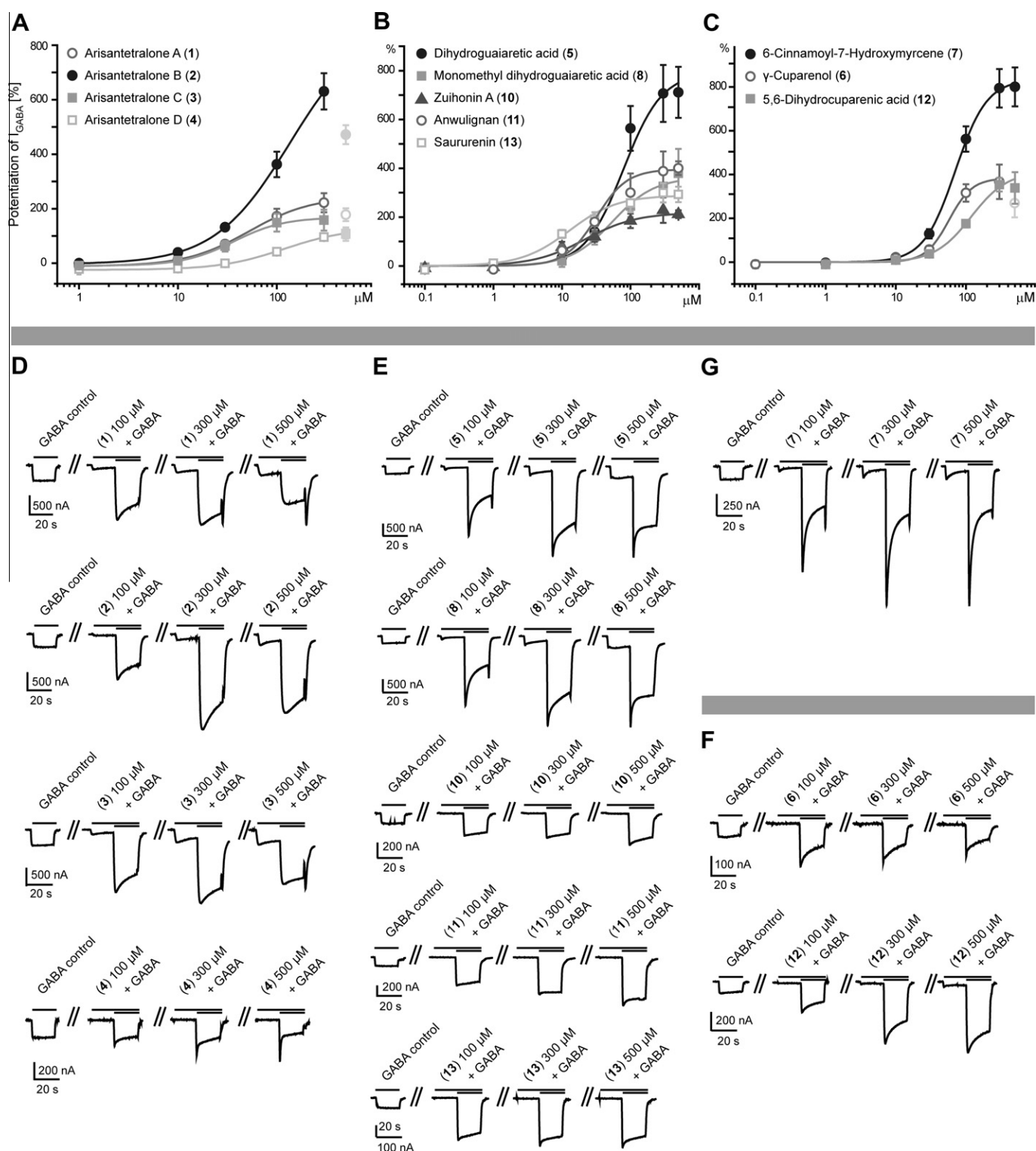
Fig. 5. (A–C) Concentration-dependent potentiation of the GABA-induced chloride current (I_{GABA}) through $\alpha_1\beta_2\gamma_{2S}$ GABA A receptors by compounds **1–8** and **10–13**. (D–F) Typical currents elicited by GABA control samples (GABA EC_{5-10}), and different concentrations of compounds **1–8** and **10–13** in absence and presence of GABA EC_{5-10} (preincubation experiments). Note that compounds **1–3**, **5**, **7**, **8**, and **12** induce small chloride currents in the absence of GABA suggesting partial agonist activity.

However, it visibly influenced the mode of action at the GABA A receptor. Interestingly, compounds **5** and **8** exerted partial agonistic activity, but not the dioxomethylene derivatives **11** and **13** (evident from the absence of chloride currents during the preincubation period in absence of GABA). Different kinetics of the I_{GABA} may be related structural differences among the studied

compounds. Furthermore, near plateau-like currents induced by **11** and **13** are in contrast to the fast decaying I_{GABA} induced by **5** and **8** (similar to **4**, **6**, and **7**), reflecting either pronounced desensitization of GABA A receptors or an open channel block. Zuihonin A (**10**) and deoxyschizandrin (**9**) are structurally too different from the other lignans for structure–activity considerations. Compound

Table 3
Potencies and Efficiencies of Compounds **1–13** at the GABA A receptor ($\alpha_1\beta_2\gamma_{2S}$).

Compounds	EC$_{50}$ μM	Max. stimulation of I$_{GABA}$ at EC$_{5-10}$%	Hill-Coeff. n_H	Nr of exp. (n)
Arisantetralone lignans (Fig. 5A and D)				
1	52.2 ± 24.8	245.0 ± 59.6	1.4 ± 0.5	6
2	135.6 ± 85.7	885.8 ± 291.2[a,b]	1.1 ± 0.3	4
3	36.6 ± 16.4	168.7 ± 41.5[a]	1.7 ± 0.8	5
4	118.7 ± 54.4	129.7 ± 36.8[b]	1.3 ± 0.5	4
Acyclic lignans (Fig. 5B and E)				
5	79.2 ± 19.4[cd]	793.4 ± 107.4[egh]	1.5 ± 0.2	4
8	54.6 ± 28.8	362.5 ± 87.1[e]	1.4 ± 0.6	4
11	31.5 ± 7.1[d]	395.6 ± 27.2[f,g]	1.9 ± 0.7	4
13	12.8 ± 3.1[c]	288.8 ± 23.7[f,h]	1.2 ± 0.2	4
Other lignans (Fig. 5B and E)				
9	n.d.	n.d.	n.d.	0
10	21.8 ± 7.5	218.1 ± 20.8	1.2 ± 0.5	4
Sesquiterpenes (Fig. 5C and F)				
6	57.3 ± 19.7	383.5 ± 89.3	2.6 ± 1.0	4
12	118.4 ± 29.9	413.4 ± 66.3	1.7 ± 0.3	4
Monoterpene derivatives (Fig. 5C and G)				
7	70.6 ± 12.2	834.6 ± 77.5	1.9 ± 0.3	4

[a–h] Statistically significant differences between the measured values in the columns are indicated by letters.
[d] $p = 0.06$; $p < 0.05$.
[g] $p < 0.01$.

10, however, can be grouped with anwulignan (**11**) and saururenin (**13**) considering potency, efficiency, and also with respect to the slowly decaying I$_{GABA}$ induced by this compound. The cuparene sesquiterpenes **6** and **12** showed little to no agonistic activity at GABA A receptors of $\alpha_1\beta_2\gamma_{2S}$ subunit composition, but reasonably potent modulation of I$_{GABA}$ with comparable potency and efficiency. The monoterpene cinnamic acid ester (**7**) showed partial agonistic activity as lignans **1–3**, and potent maximal I$_{GABA}$ stimulation (834.6 ± 77.5%) (Fig. 5, Table 3; Chart 1).

2.3. Phytochemical differences between the genera Kadsura and Schisandra

Kadsura and *Schisandra* are closely related genera which share a similar phytochemical profile (Haensel et al., 1993; Saunders, 1998). Therefore, *Kadsura* fruits were often used as a substitute for *Schisandra* (Haensel et al., 1993; Ookawa et al., 1981; Saunders, 1998). In the initial extract screening only the *Kadsura* species exerted GABA A receptor modulatory activity. We compared the phytochemical profiles of the petroleum ether extracts of *S. chinensis* and both *Kadsura* species by HPLC-PDA-ESIMS. The HPLC-based activity profiling of *K. longipedunculata* led to the identification of constituents (**1–8** and **10–13**) which were responsible, to varying degrees, for the GABA A receptor modulatory activity of the crude extract. Most of these compounds could also be detected in the *K. japonica* extract, which had previously shown comparable activity in the oocyte assay as *K. longipedunculata* (Fig. 6). In contrast, the HPLC profile of the inactive petroleum ether extract of *S. chinensis* strongly differed from those of the *Kadsura* extracts. Only traces of some of the active compounds could be detected by comparison of UV and mass spectra (Fig. 6).

The lignan content of *Schisandra sp.* fruits varies depending on geographical origin and time of harvest (Lu and Chen, 2009; Tang and Eisenbrand, 2011; Zhu et al., 2007), and constituents such as (+)-anwulignan (**11**) or meso-dihydroguaiaretic acid (**5**), which we identified as GABA A receptor active, have already been isolated from this source, however not as major compounds (Lu and Chen, 2009; Wei et al., 2010). Nonetheless, our results suggest that, despite a rather similar phytochemical profile of *Kadsura* and *Schisandra* species, their specific lignan patterns are decisive for the GABA A receptor activities of the extracts. More samples should be tested

to draw a more general conclusion on this issue. Interestingly, deoxyschisandrin (**9**), one of the extensively studied pharmacologically-active dibenzocyclooctadiene lignans (Hancke et al., 1999; Opletal et al., 2004) and a major compound of *S. sphenanthera* (Lu and Chen, 2009), does not affect GABA A receptors of the $\alpha_1\beta_2\gamma_{2S}$ composition. It is possible that a sedative action of *S. sphenanthera* in rodents is not due to GABA A receptor activity, but due to other mechanisms as Huang et al. conjectured (Huang et al., 2007). In contrast, the GABA A receptor modulating lignans of *Kadsura* species indeed reach a concentration sufficient for GABA A receptor activity of the crude extract. Animal behavioral experiments and pharmacokinetic studies with extracts and pure compounds are needed to assess the GABA A receptor related activity *in vivo*.

2.4. Conclusions

Compared to other natural products previously isolated and tested for GABA A receptor activity (Li et al., 2010; Yang et al., 2011; Zaugg et al., 2010, 2011a), the lignans of *K. longipedunculata* showed medium to high potencies and moderate efficiencies (except for **2**,**4**, and **5**). Apart from neolignans honokiol and magnolol (Ai et al., 2001), this is the first time that lignans are described as GABA A receptor modulators. With exception of **11** and **13**[1], all lignans possessed physico-chemical properties favorable for oral bioavailability and blood–brain-barrier penetration (H-acceptors ⩽7, H-donors ⩽3, MW ⩽450, cLogP: ⩽5, number of rotatable bonds ⩽8, polar surface area (PSA) ⩽60–70 (−90) Å^2) (Pajouhesh and Lenz, 2005). Arisantetralones A–C (**1–3**) showed an interesting mode of action, combining partial agonistic activity, positive modulation, and possibly an open channel block at high concentrations, which warrants a more detailed investigation of their binding site(s), and potential GABA A receptor subtype selectivity of this compound class.

Interestingly, two different compound classes, lignans and isoprenoids, contribute to the GABA A receptor modulating activity of the *K. longipedunculata* extract. Among the 3 active terpenoids **6**, **7** and **12**, two were newly-described natural products. Their absolute configurations were determined by comparison of experimental and calculated ECD. ECD calculations have been

---

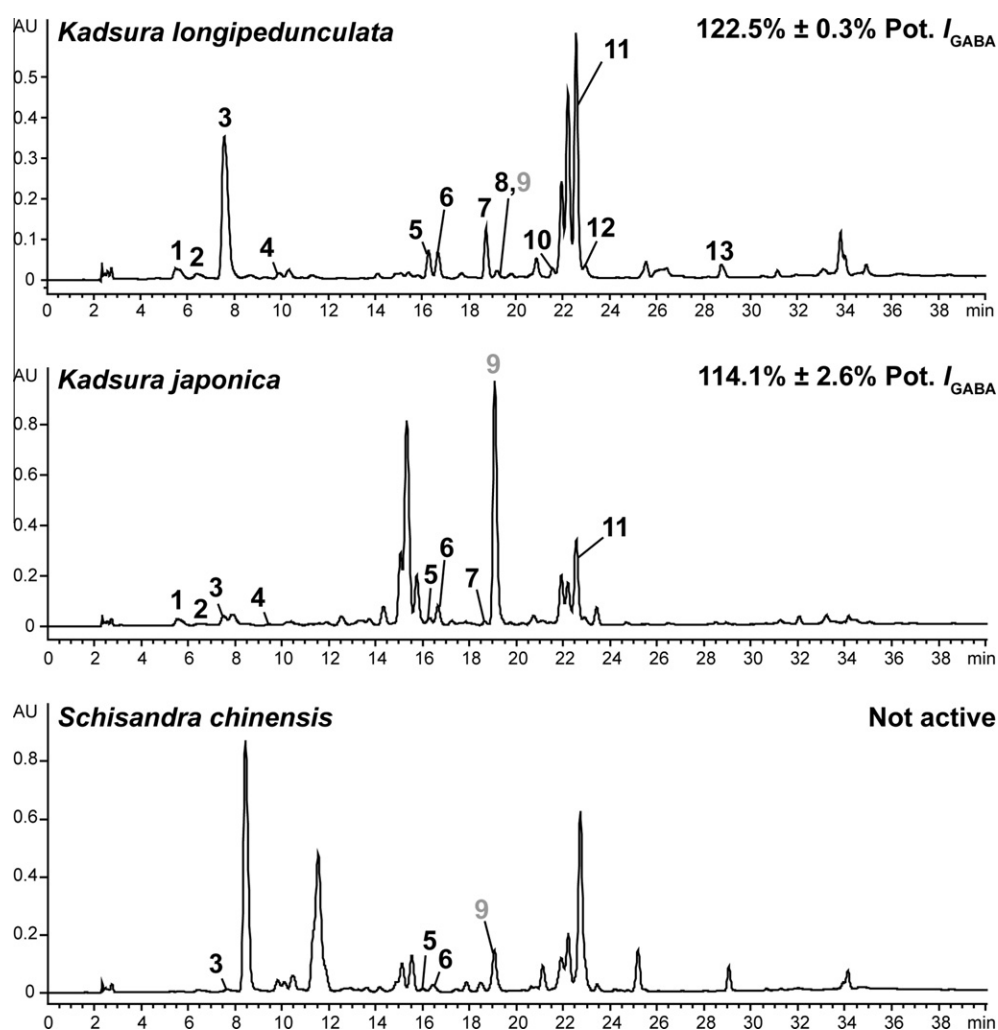[1] Compounds **11** and **13** have a cLogP of 5.59. The other criteria are fulfilled.

Fig. 6. HPLC-PDA-ESIMS analysis of *K. longipedunculata*, *Kadsura japonica* and *Schisandra chinensis* fruits (gradient 65% to 100% MeOH + HCO$_2$H 0.1% in 30 min). Numbers correspond to isolated compounds from *K. longipedunculata* with (black) and without (grey) GABA A receptor modulatory activity. The potentiation of the GABA induced chloride current by the crude extract (100 μg/ml) is indicated on the upper right side of each chromatogram. UV traces recorded at 266 nm are shown. (For interpretation of the references to colour in this figure legend, the reader is referred to the web version of this article.)

increasingly used for the interpretation of CD spectra (Bringmann et al., 2009), However, the example of **12** shows the current limitations of this approach and highlights the sensitivity of circular dichroism to conformational changes. Therefore, proper conformational analysis and geometrical optimizations of the conformers prior to calculations of energy transitions is essential.

3. Experimental

3.1. General experimental procedures

Optical rotation was measured on a Perkin Elmer polarimeter (model 341) equipped with a 10 cm microcell. The optical rotation for the sodium D line (589 nm) was extrapolated from the lines of a mercury lamp using the Drude equation (Fluegge, 1970). CD spectra of compounds **1–4** were recorded in MeOH (50 μg/ml) on a Chirascan CD spectrometer and analyzed with the Pro-Data V2.4 software. CD spectra of other compounds were measured on an AVIV CD Spectrometer Model 62ADS and analyzed with the AVIV 60DS V4.1 software. NMR spectra were recorded at target temperature of 18 °C on a Bruker Avance III 500 MHz spectrometer operating at 500.13 MHz for ^{1}H and 125.77 MHz for ^{13}C. A 1 mm TXI-microprobe with a z-gradient was used for ^{1}H-detected experiments; ^{13}C-NMR

spectra were recorded with a 5 mm BBO-probe head with z-gradient. Spectra were analyzed using Bruker TopSpin 2.1 software. High resolution mass spectra (HPLC-PDA-ESI-TOF-MS) in positive mode were obtained on a Bruker micrOTOF ESI-MS system connected via T-splitter (1:10) to an Agilent HP 1100 series system consisting of a binary pump, autosampler, column oven and diode array detector (G1315B) with settings as previously reported (Zaugg et al., 2010). Data acquisition and processing was performed using Bruker HyStar 3.0 software. Semi-preparative HPLC separation for activity profiling and compound isolation was performed on an Alliance 2690 Separation module connected to a 996 photodiode array detector. Data acquisition and processing was performed using Waters Empower Pro Software. Waters SunFire C18 (3.5 μm, 3.0 × 150 mm) and SunFire Prep C18 (5 μm, 10 × 150 mm) columns were used for analytical HPLC and semipreparative RP-HPLC, respectively. Semipreparative NP-HPLC was performed on a Merck LiChroSorb 100 Diol (10 μm, 10 × 250 mm) column. Medium pressure liquid chromatography (MPLC) was done on a pre-packed normal phase cartridge (40-63 μm, 40 × 150 mm) using a Buchi Sepacore system consisting of a control unit C-620, two pump modules C-605, and a fraction collector C-660. The MPLC unit was controlled with the SepacoreControl software (version 1.0.3000.1). Preparative HPLC separation was performed with a Waters SunFire Prep C18 OBD (5 μm, 30 × 150 mm) column on a Shimadzu LC-8A preparative separation

chromatograph equipped with a SPD-M10A VP diode array detector. HPLC-grade MeOH (Scharlau Chemie S.A.) and H_2O were used for HPLC separations. HPLC solvents contained 0.1% HCO_2H for analytical separations. $CDCl_3$ (100 Atom% D, stab. with Ag) and DMSO-d_6 (100 Atom%) for NMR was purchased from Armar Chemicals. Solvents used for extraction, open column chromatography, and MPLC were of technical grade and purified by distillation. Silica gel (63–200 μm, Merck) was used for open column chromatography.

3.2. Plant material

Dried fruits of *K. longipedunculata* Finet & Gagnep., *K. japonica* (L.) Dunal, and *S. chinensis* (Turczaninow) Baillon were purchased by Mr. Jinfu Wan, Yunnan Baiyao group Co. Ltd., Kunming, China, at the Juhuayan herbal market in Kunming, Yunnan, China, and identified at the labs of Yunnan Baiyao group. Voucher specimens (00 450, 00 440, and 00 451, respectively) are deposited at the Institute of Pharmaceutical Biology, University of Basel. The organoleptic, macroscopic, and microscopic characteristics of apocarps and seeds were confirmed by Janine Zaugg by comparison with lit. (Fujita, 1929; Saunders, 1998, 2000). A detailed description of the plant material is provided as Supplementary data.

3.3. Extraction

The plant material was frozen with liquid N_2 and ground with a Retsch ZM1 ultracentrifugal mill. The extract for the screening and HPLC-based activity profiling was prepared with a Dionex ASE 200 extraction system with solvent module by extraction with pet-ether, b.p. 40–60°, redistilled. In total, 3 extraction cycles were performed at an extraction pressure of 120 bar and a temperature of 70 °C. For compound isolation 1.08 kg of ground fruits were macerated at room temperature with *n*-hexane (4 × 3.2 l, 1 h each). The solvent was evaporated at reduced pressure to yield 109.7 g of extract. The extracts were stored at −20 °C until use.

3.4. HPLC microfractionation

Microfractionation for GABA A receptor activity profiling was performed as previously described (Kim et al., 2008), with minor modifications: separation was carried out on a semipreparative RP-HPLC column with MeOH (solvent A) and H_2O (solvent B) using the following gradient: 65% A–100% A in 30 min, hold for 10 min. The flow rate was 4 ml/min, and 100 μl of the extract (100 mg/ml in DMSO) were injected. A total of 28 time-based microfractions of each 90 s each were collected. Microfractions were evaporated in parallel with a Genevac EZ-2 plus vacuum centrifuge. The dry films were redissolved in 1 ml of MeOH; aliquots of 0.5 ml were dispensed in two vials, dried under N_2 gas, and submitted to bioassay.

3.5. Isolation

A portion of the extract (51.4 g) was partitioned by liquid–liquid extraction with *n*-hexane and MeOH:H_2O [9:1] to yield a lipophilic fraction (36.0 g) and a polar fraction (14.8 g). The latter was separated by open column chromatography (9 × 42 cm, 1.0 kg silica gel) using a step gradient of *n*-hexane–EtOAc–MeOH (100:0:0, 2 l; 95:5:0, 2 l; 90:10:0, 2 l; 80:20:0, 2 l; 70:30:0, 2 l; 60:40:0, 2 l; 50:50:0, 1 l; 40:60:0, 1 l; 30:70:0, 1 l; 20:80:0, 1 l; 10:90:0, 1 l; 0:100:0, 2 l, 0:50:50, 1 l; 0:0:100, 1 l). The flow rate was ca. 50 ml/min. The effluent was combined to 23 fractions (1–23) according to TLC patterns (detection at 254 nm, 366 nm and at daylight after staining with anisaldehyde–sulphuric acid reagent). Crystallization of fraction 9 (1.68 g) yielded 692 mg of the major compound anwulignan (**11**). The mother liquor of fraction 9 as well as other fractions

used for compound isolation were diluted in MeOH (125–500 mg/ml) and separated by preparative HPLC with different gradients of MeOH and H_2O and a flow rate of 20 ml/min as follows: 50 mg of fraction 7 (102 mg), gradient of 70:30 to 85:15 in 14 min, yielded (+)-Zuihonin A (**10**) (10 mg); 200 mg of the mother liquor of fraction 9, gradient of 80:20 to 100:0 in 17 min yielded more anwulignan (**11**) (111 mg) and saururenin (**13**) (19.5 mg), 100 mg of fraction 11 (474 mg), gradient of 73:27–90:10 in 22 min, yielded 8 mg of a cinnamic acid ester of 6,7-dihydro-6,7-myrcenediol (Bohlmann et al., 1983), 6-cinnamoyl-6,7-dihydro-7-myrceneol (**7**) and the dibenzocyclooctadiene lignan deoxyschizandrin (**9**) (1.3 mg); 60 mg of fraction 12 (322 mg), gradient of 73:27–90:10 in 22 min, yielded *meso*-dihydroguaiaretic acid (**5**) (17 mg) and *meso*-monomethyldihydroguaiaretic acid (**8**) (1 mg); 100 mg of fraction 14 (770 mg), gradient of 65:35–70:30 in 5 min, yielded arisantetralone A (**1**) (2 mg), B (**2**) (1 mg), C (**3**) (29 mg), and D (**4**) (1 mg) (Cheng et al., 2009; da Silva and Lopes, 2004; Liu et al., 1988).

An aliquot (980 mg) of fraction 10 (5.95 g) was separated by MPLC using a CH_2Cl_2:THF mixture [97:3] and *n*-hexane in a gradient ranging from 10:90 to 90:10 in 2 h, followed by 90:10–100:0 in 10 min, hold for 30 min. The flow rate was set at 15 ml/min and 12 fractions (A–L) were collected based on TLC analysis. Fractions 10B (76 mg), 10C (28 mg), and 10G (61 mg) were dissolved in *n*-hexane containing ⩽4% *iso*-PrOH (100 mg/ml) and separated by semipreparative NP-HPLC using *n*-hexane and *iso*-PrOH (0.01% HCO_2H) as mobile phase. Isocratic conditions (10B, 10C: [98:2]; 10G: [99.8:0.2]) were used; the flow rate was 5 ml/min. Manual peak collection yielded anwulignan (**12**) (21 mg of fraction 10B and 10 mg of fraction 10C) and γ-cuparenol (**7**) (4.5 mg) of fraction 10G. A part (960 mg) of fraction 15 (1.52 g) was separated by MPLC using a gradient of dichloromethane and MeOH (100:0–90:10 in 2 h, followed by 90:10–0:100 in 30 min, flow rate 15 ml/min). Five fractions (A–E) were collected based on TLC pattern. Repeated injections of fraction 15B (55 mg) onto semipreparative NP-HPLC using *n*-hexane and *iso*-PrOH (0.01% HCO_2H) in an isocratic mode [99.5:0.5] and a flow rate of 5 ml/min yielded the 5,6-dihydro derivative of cuparenic acid (Enzell and Erdtman, 1958) (**13**) (4 mg).

3.6. Spectroscopic data of new compounds

3.6.1. R-(+)-γ-cuparenol (Ito et al., 1965; Nayek et al., 2003) (**6**)

White amorphous substance; $[\alpha]_D^{20}$:+20.7° (MeOH; *c* 0.38); UV: λ_{max} (nm) 222, 263 sh; CD (MeOH, *c* = 1.8 × 10^{-3} M, 0.1 cm pathlength): $[\theta]_{200}$ + 2 667, $[\theta]_{209}$ + 1 009, $[\theta]_{220}$ + 2 127; ESIMS *m/z* 219 $[M + H]^+$. For ^1H and ^{13}C NMR data see Table 1.

3.6.2. R-(+)-6-cinnamoyl-6,7-dihydro-7-myrceneol (**7**)

Colorless oil; $[\alpha]_D^{20}$:+15.2° ($CHCl_3$; *c* 0.66); UV: λ_{max} (nm) 218, 222, 230 sh; 278.5, 230 sh; CD (MeOH, *c* = 6.6 × 10^{-4} M, 0.1 cm pathlength): $[\theta]_{205}$ + 13 380, $[\theta]_{216}$ + 2 207, $[\theta]_{229}$ + 6 677, $[\theta]_{239}$ 0, $[\theta]_{253}$-3 025, $[\theta]_{282}$ 0, $[\theta]_{294}$ + 1 059; HRESIMS *m/z* 323.1649 (calcd. for $C_{19}H_{24}NaO_3$: 323.1618). For ^1H and ^{13}C NMR data see Table 2.

3.6.3. S-(−)-5,6-Dihydrocuparenic acid (**12**)

White amorphous substance; $[\alpha]_D^{20}$: −31.3° ($CHCl_3$; *c* 0.47); UV: λ_{max} (nm) 215, 302; CD (MeOH, *c* = 1.7 × 10^{-3} M, 0.1 cm pathlength): $[\theta]_{205}$ + 1 938, $[\theta]_{233}$ 0, $[\theta]_{302}$ − 1 905; HRESIMS *m/z* 257.1519 (calcd. for $C_{15}H_{22}NaO_2$: 257.1512). For ^1H and ^{13}C NMR data see Table 1.

3.7. Conformational analysis, geometrical optimization, and CD calculation

Conformational analyses of compounds **e6**, **e7** and **e12** were performed with Schrödinger MacroModel 9.1 software using the OPLS 2005 (Optimized Potential for Liquid Simulations) force field

in H_2O. Conformers of $e7$ and $e6/e12$ occurring within a 1 and 2 kcal/mol energy window from the particular global minimum, respectively, were chosen for geometrical optimization and energy calculation using density functional theory (DFT) with the B3LYP functional and the 6-31G** basis-set in the gas-phase with the Gaussian 03 program package (Frisch et al., 2004). Vibrational analysis was done at the same level to confirm minima (Bringmann et al., 2009). TD-DFT/B3LYP/6-31G** (in the gas phase and in MeOH using the "self-consistent reaction field" method (SCRF) with the CPCM polarizable conductor calculation model) was employed to calculate excitation energy (denoted by wavelength in nm) and rotatory strength R in dipole velocity (R_{vel}) and dipole length (R_{len}) forms. ECD curves were calculated based on rotatory strengths using half bandwidth of 0.2 eV with conformers of $e6$, $e7$ and $e12$. The spectra were combined after Boltzmann-weighting according to their population contribution.

3.8. Expression of GABA A receptors

Stage V–VI oocytes from *Xenopus laevis* were prepared and cRNA was injected as previously described (Khom et al., 2006). Female *X. laevis* (Nasco) were anesthetized by exposing them for 15 min to a 0.2% MS-222 (3-aminobenzoic acid ethyl ester methanesulfonate, Sigma–Aldrich) solution before surgically removing parts of the ovaries. Follicle membranes from isolated oocytes were enzymatically digested with 2 mg/ml collagenase from *Clostridium histolyticum* (Type 1A, Sigma–Aldrich). Synthesis of capped run-off poly(A+) cRNA transcripts was obtained from linearized cDNA templates (pCMV vector). One day after enzymatic isolation, the oocytes were injected with 50 nL of DEPC-treated H_2O (Sigma–Aldrich) containing different cRNAs at a concentration of ca. 300-3000 pg/nL per subunit. The amount of injected cRNA mixture was determined by means of a NanoDrop ND-1000 (Kisker Biotech). Rat cRNAs were mixed in a 1:1:10 ratio to ensure expression of the γ-subunit in $α_1β_2γ_{2S}$ receptors. Oocytes were then stored at 18 °C in an aqueous solution of 90 mM NaCl, 1 mM KCl, 1 mM $MgCl_2$, 1 mM $CaCl_2$ and 5 mM HEPES (pH 7.4), containing 1% of Penicillin–Streptomycin solution (Sigma–Aldrich) (Methfessel et al., 1986). Voltage clamp measurements were performed between days one and five after cRNA injection.

3.9. Two-microelectrode voltage clamp studies

Electrophysiological experiments were performed by the two-microelectrode voltage clamp method making use of a TURBO TEC 03X amplifier (npi electronic) at a holding potential of −70 mV and pCLAMP 10 data acquisition software (Molecular Devices). Currents were low-pass-filtered at 1 kHz and sampled at 3 kHz. The bath solution contained 90 mM NaCl, 1 mM KCl, 1 mM $MgCl_2$, 1 mM $CaCl_2$ and 5 mM HEPES (pH 7.4). Electrode filling solution contained 2 M KCl.

3.10. Fast solution exchange during I_{GABA} recordings

Test solutions (100 μL) of extracts, fractions and pure compounds were applied to the oocytes at a speed of 300 μL/s by means of the ScreeningTool automated fast perfusion system (npi electronics) (Baburin et al., 2006). In order to determine GABA EC_{5-10} (typically between 3 and 10 μM for receptors of the subunit combination $α_1β_2γ_{2S}$), a concentration-response experiment with GABA concentrations ranging from 0.1 μM to 1 mM was performed. Stock solution of plant extracts (10 mg/ml in DMSO) were diluted to a concentration of 100 μg/ml with bath solution containing GABA EC_{5-10} according to a validated protocol (Kim et al., 2008). As previously described, microfractions of the *K. longipedunculata* extract collected from the semi-preparative HPLC sepa-

ration were dissolved in 30 μl DMSO and subsequently mixed with 2.97 ml of bath solution containing GABA EC_{5-10} (Kim et al., 2008). For concentration–response experiments, stock solutions of compounds **1–13** (100 mM in DMSO) were diluted to concentrations ranging from 0.1 to 500 μM with bath solution and applied to the oocyte for measuring agonistic activity. After a preincubation period of 20 s, a second application immediately followed containing the corresponding compound solution combined with GABA EC_{5-10} to measure GABA A receptor modulation.

3.11. Analyzing concentration–response curves

Enhancement of the GABA-induced chloride current (I_{GABA}) was defined as $I_{(GABA + Comp)}/I_{GABA}-1$, where $I_{(GABA + Comp)}$ is the current response in the presence of a given compound, and I_{GABA} is the control GABA-induced chloride current.

Concentration–response curves were generated, and the data were fitted by nonlinear regression analysis using ORIGIN software (OriginLab Corporation, Northampton, MA, USA). Data were fitted to the equation $\frac{1}{1+\left(\frac{EC_{50}}{[Comp]}\right)^{n_H}}$, where EC_{50} is the concentration of the compound that increases the amplitude of the GABA-evoked current by 50%, and n_H is the Hill coefficient. The maximum potentiation of I_{GABA} by a given compound was derived from the fit.

Data are given as mean ± S.E. of at least 2 oocytes and $\geqslant 2$ oocyte batches. Statistical significance was calculated using t-test by ANOVA with confidence intervals of $p < 0.05$ and $p < 0.01$.

Acknowledgments

Appendix A. Supplementary data

Supplementary data associated with this article can be found, in the online version, at doi:10.1016/j.phytochem.2011.08.014.

References

Adams, M., Zimmermann, S., Kaiser, M., Brun, R., Hamburger, M., 2009. A protocol for HPLC-based activity profiling for natural products with activities against tropical parasites. Nat. Prod. Comm. 4, 1377–1381.
Ai, J., Wang, X., Nielsen, M., 2001. Honokiol and magnolol selectively interact with GABAA receptor subtypes in vitro. Pharmacology 63, 34–41.
Baburin, I., Beyl, S., Hering, S., 2006. Automated fast perfusion of Xenopus oocytes for drug screening. Pflug. Arch. Eur. J. Phy. 453, 117–123.
Bohlmann, F., Ahmed, M., King, R.M., Robinson, H., 1983. Acetylenic compounds from Bidens graveolens. Phytochemistry 22, 1281–1283.
Bringmann, G., Bruhn, T., Makismenka, K., Hemberger, Y., 2009. The assignement of absolute stereostructures through quantum chemical circular dichroism calculations. Eur. J. Org. Chem. 17, 2717–2727.
Cheng, Y.B., Chang, M.T., Lo, Y.W., Ho, C.J., Kuo, Y.C., Chien, C.T., Chen, S.Y., Liou, S.S., Kuo, Y.H., Shen, Y.C., 2009. Oxygenated lignans from the fruits of Schisandra arisanensis. J. Nat. Prod. 72, 1663–1668.
da Silva, T., Lopes, L.M.X., 2004. Aryltetralone lignans and 7, 8-seco-lignans from Holostylis reniformis. Phytochemistry 65, 751–759.
Danz, H., Stoyanova, S., Wippich, P., Brattstroem, A., Hamburger, M., 2001. Identification and isolation of the cyclooxygenase-2 inhibitory principle in Isatis tinctoria. Planta Med. 67, 411–416.
Dittmann, K., Gerhaeuser, C., Klimo, K., Hamburger, M., 2004. HPLC-based activity profiling of Salvia miltiorrhiza for MAO A and iNOS inhibitory activities. Planta Med. 70, 909–913.
Enzell, C., Erdtman, H., 1958. The chemistry of the natural order Cupressales–XXI Cuparene and Cuparenic acid, two sesquiterpenic compounds with a new carbon skeleton. Tetrahedron 4, 361–368.
Fluegge, J., 1970. Grundlagen der Polarimetrie. De Gruyter-Verlag, Berlin.
Frisch, M. J., Trucks, H. B., Schlegel, H. B., Gaussian 03, Revision E.01, M. J. Frisch, G. W. Trucks, H. B. Schlegel, G. E. Scuseria, M. A. Robb, J. R. Cheeseman, J. A. Montgomery, Jr., T. Vreven, K. N. Kudin, J. C. Burant, J. M. Millam, S. S. Iyengar, J. Tomasi, V. Barone, B. Mennucci, M. Cossi, G. Scalmani, N. Rega, G. A. Petersson,

H. Nakatsuji, M. Hada, M. Ehara, K. Toyota, R. Fukuda, J. Hasegawa, M. Ishida, T. Nakajima, Y. Honda, O. Kitao, H. Nakai, M. Klene, X. Li, J. E. Knox, H. P. Hratchian, J. B. Cross, V. Bakken, C. Adamo, J. Jaramillo, R. Gomperts, R. E. Stratmann, O. Yazyev, A. J. Austin, R. Cammi, C. Pomelli, J. W. Ochterski, P. Y. Ayala, K. Morokuma, G. A. Voth, P. Salvador, J. J. Dannenberg, V. G. Zakrzewski, S. Dapprich, A. D. Daniels, M. C. Strain, O. Farkas, D. K. Malick, A. D. Rabuck, K. Raghavachari, J. B. Foresman, J. V. Ortiz, Q. Cui, A. G. Baboul, S. Clifford, J. Cioslowski, B. B. Stefanov, G. Liu, A. Liashenko, P. Piskorz, I. Komaromi, R. L. Martin, D. J. Fox, T. Keith, M. A. Al-Laham, C. Y. Peng, A. Nanayakkara, M. Challacombe, P. M. W. Gill, B. Johnson, W. Chen, M. W. Wong, C. Gonzalez, and J. A. Pople, Gaussian, Inc., Wallingford CT., 2004.

Fujita, N., 1929. Über die Früche der *Schizandra chinensis* Bail Und *Kadsura japonica* Dun. Arch. Pharm. Ber. Deutsch. Pharm. Ges. 267, 532–540.

Haensel, R., Keller, K., Rimpler, H., Schneider, G., 1993. Hagers Handbuch der pharmazeutischen Praxis. Springer Verlag.

Hancke, J.L., Burgos, R.A., Ahumada, R., 1999. *Schisandra chinensis* (Turcz.) Baill. Fitoterapia 70, 451–471.

Hou, J.P., Youyu, J., 2005. The Healing Power of Chinese Herbs and Medicinal Recipes. The Haworth Press, New York, London, Oxford.

Huang, F., Xiong, Y., Xu, L., Ma, S., Dou, C., 2007. Sedative and hypnotic activities of the ethanol fraction from Fructus *Schisandrae* in mice and rats. J. Ethnopharmacol. 110, 471–475.

Ikeya, Y., Taguchi, H., Sasaki, H., Nakajima, K., Yosioka, I., 1980. The constituents of *Schizandra chinensis* BAILL. VI. 13C nuclear magnetic resonance spectroscopy of dibenzocyclooctadiene lignans. Chem. Pharm. Bull 28, 2414–2421.

Ikeya, Y., Taguchi, H., Yosioka, I., Kobayashi, H., 1979. The constituents of *Schizandra chinensis* BAILL V. The structures of four new lignans, gomisin N, gomisin O, epigomisin O and gomisin E, and transformation of gomisin N to deangeloylgomisin. B. Chem. Pharm. Bull. 27, 2695–2709.

Ito, S., Endo, K., Honma, H., Ota, K., 1965. New constituents of *Thujopsis dolabrata*. Tetrahedron Lett. 42, 3777–3781.

Kamel, H.N., Ding, Y., Li, X.C., Ferreira, D., Fronczek, F.R., Slattery, M., 2009. Beyond Polymaxenolide: Cembrane-Africane Terpenoids from the Hybrid Soft Coral *Sinularia maxima × S Polydactyla*. J. Nat. Prod. 72, 900–905.

Khom, S., Baburin, I., Timin, E.N., Hohaus, A., Sieghart, W., Hering, S., 2006. Pharmacological properties of GABA(A) receptors containing gamma1 subunits. Mol. Pharmacol. 69, 640–649.

Kim, H.J., Baburin, I., Khom, S., Hering, S., Hamburger, M., 2008. HPLC-based activity profiling approach for the discovery of GABA(A) receptor ligands using an automated two microelectrode voltage clamp assay on *Xenopus* oocytes. Planta Med. 74, 521–526.

Lee, C.-L., 1981. The extractive components of formosan lauraceous plants I Four lignans from the bark of *Machilus zuihoensis* forma *longipaniculata*. Kexue-Fazhan 9, 578–583.

Li, Y., Plitzko, I., Zaugg, J., Hering, S., Hamburger, M., 2010. HPLC-based activity profiling for GABA(A) receptor modulators: a new dihydroisocoumarin from *Haloxylon scoparium*. J. Nat. Prod. 73, 768–770.

Liu, J., Tao, Y., Huang, M., 1988. Studies on the constituents of Schisandra henryi. V. Structures of wulignan A1, A2, epiwulignan A1 and epischisandrone Huaxue Xuebao 46, 483–488.

Lu, Y., Chen, D.F., 2009. Analysis of *Schisandra chinensis* and *Schisandra sphenanthera*. J. Chromatogr. A 1216, 1980–1990.

Methfessel, C., Witzemann, V., Takahashi, T., Mishina, M., Numa, S., Sakmann, B., 1986. Patch clamp measurements on *Xenopus laevis* oocytes: currents through endogenous channels and implanted acetylcholine receptor and sodium channels. Pflug. Arch. Eur. J. Phy. 407, 577–588.

Miyazawa, M., Kasahara, H., Kameoka, H., 1997. *O*-Demethylation of meso-dimethyldihydroguaiaretic acid in *Spodoptera litua*. Phytochemistry 46, 1173–1175.

Mohler, H., 2011. The rise of a new GABA(A) pharmacology. Neuropharmacology 60, 1042–1049.

Nakatani, N., Ikeda, K., Kikuzaki, H., Kido, M., Yamaguchi, Y., 1988. Diaryldimethylbutane lignans from *Myristica argentea* and their antimicrobial action against *Streptococcus mutans*. Phytochemistry 27, 3127–3129.

Nayek, A., Drew, M.G.B., Ghosh, S., 2003. Convenient route to enantiopure aryl cyclopentanes via Diels-Alder reaction of assymetric dienes. Total synthesis of (+)-herbertene and (+)-cuparene. Tetrahedron 59, 5175–5181.

Olsen, R.W., Sieghart, W., 2008. International Union of Pharmacology LXX. Subtypes of gamma-aminobutyric acid(A) receptors: classification on the basis of subunit composition, pharmacology, and function. Update. Pharmacol. Rev. 60, 243–260.

Ookawa, N., Ikeya, Y., Taguchi, H., Yosioka, I., 1981. The constituents of *Kadsura japonica* Dunal I. The structures of three new lignans, acetyl- angeloyl- and caproyl-binankadsurin. A. Chem. Pharm. Bull. 29, 123–127.

Opletal, L., Sovova, H., Bartlova, M., 2004. Dibenzo[a, c]cyclooctadiene lignans of the genus Schisandra: importance, isolation and determination. J. Chromatogr. B 812, 357–371.

Pajouhesh, H., Lenz, G.R., 2005. Medicinal chemical properties of successful central nervous system drugs. NeuroRx 2, 541–553.

Panossian, A., Wikman, G., 2008. Pharmacology of *Schisandra chinensis* Bail.: an overview of Russian research and uses in medicine. J. Ethnopharmacol. 118, 183–212.

Pei, Y.Q., Yue, W., Cui, J.R., Yao, H.Y., 1980. A study of the central pharmacological action of piperine and its derivatives. Yao Xue Xue Bao 15, 198–205.

Potterat, O., Hamburger, M., 2006. Natural products in drug discovery - concepts and approaches for tracking bioactivity. Curr. Org. Chem. 10, 899–920.

Potterat, O., Wagner, K., Gemmecker, G., Mack, J., Puder, C., Vettermann, R., Streicher, R., 2004. BI-32169, a bicyclic 19-peptide with strong glucagon receptor antagonist activity from *Streptomyces sp*. J. Nat. Prod. 67, 1528–1531.

Sadhu, S.K., Okuyama, E., Fujimoto, H., Ishibashi, M., 2003. Separation of *Leucas aspera*, a medicinal plant of Bangladesh, guided by prostaglandin inhibitory and antioxidant activities. Chem. Pharm. Bull. 51, 595–598.

Saunders, R.K.M., 1998. Monograph of *Kadsura* (Schisandraceae). Systematic Botany Monographs 54, 1–106.

Saunders, R.K.M., 2000. Monograph of *Schisandra* (Schisandraceae). Systematic Botany Monographs 58, 1–146.

Schrecker, A.W., 1957. Meso-Dihydroguaiaretic acid and its derivatives. J. Am. Chem. Soc. 79, 3823–3827.

Stoeger, E.A., 2009. Arzneibuch der Chinesischen Medizin. Monographien des Arzneibuches der Volksrepublik China 2000 und 2005. Deutscher Apotheker Verlag, Stuttgart.

Tang, W., Eisenbrand, G., 2011. Handbook of Chinese Medicinal Plants. Chemistry, Pharmacology, Toxicology. Wiley-VCH, Weinheim.

Tayone, W.C., Honma, M., Kanamaru, S., Noguchi, S., Tanaka, K., Nehira, T., Hashimoto, M., 2011. Stereochemical Investigations of Isochromenones and Isobenzofuranones Isolated from *Leptosphaeria* sp. KTC 727. J. Nat. Prod. 74, 425–429.

Urzua, A., Freyer, A.J., Shamma, M., 1987. 2, 5-Diaryl-3, 4-dimethyltetrahydrofuranoid lignans. Phytochemistry 26, 1509–1511.

Wang, B.G., Hong, X., Li, L., Zhou, J., Hao, X.J., 2000. Chemical constituents of two Chinese Magnoliaceae plants, *Tsoongiodendron odorum* and *Manglietiastrum sinicum*, and their inhibition of platelet aggregation. Planta Med. 66, 6107–6112.

Wang, Q., Yang, Y., Li, Y., Yu, W., Hou, Z.J., 2006. An efficient method for the synthesis of lignans. Tetrahedron 62, 6107–6112.

Wei, H., Sun, L., Tai, Z., Gao, S., Xu, W., Chen, W., 2010. A simple and sensitive HPLC method for the simultaneous determination of eight bioactive components and fingerprint analysis of *Schisandra sphenanthera*. Anal. Chim. Acta 662, 97–104.

Xiao, P.-G., Xu, L.-J., Xiao, W., Peng, Y., 2010. Argument on the correct Chinese name of genus *Kadsura* Kaempf.ex Juss. Yao Xue Xue Bao 45, 1064–1066.

Yang, X., Baburin, I., Plitzko, I., Hering, S., Hamburger, M., 2011. HPLC-based activity profiling for GABA(A) receptor modulators from the traditional Chinese herbal drug Kushen (*Sophora flavescens* root). Mol. Diversity DOI: 10.1007/s11030-010-9297-7.

Zaugg, J., Baburin, I., Strommer, B., Kim, H.J., Hering, S., Hamburger, M., 2010. HPLC-based activity profiling: discovery of piperine as a positive GABA(A) receptor modulator targeting a benzodiazepine-independent binding site. J. Nat. Prod. 73, 185–191.

Zaugg, J., Eickmeier, E., Ebrahimi, S., Baburin, I., Hering, S., Hamburger, M., 2011a. HPLC-based activity profiling for positive GABA(A) receptor modulators in *Acorus calamus* L. J. Nat. Prod. dx.doi.org/10.1021/np200181d.

Zaugg, J., Eickmeier, E., Rueda, D.C., Hering, S., Hamburger, M., 2011b. HPLC-based activity profiling of Angelica pubescens roots for new positive GABA(A) receptor modulators in *Xenopus* oocytes. Fitoterapia 82, 434–440.

Zaugg, J., Khom, S., Eigenmann, D., Baburin, I., Hamburger, M., Hering, S., 2011c. Identification and characterization of GABA(A) receptor modulatory and sedative diterpenes from *Biota orientalis* twigs and leaves. J. Nat. Prod. submitted for publication.

Zhu, M., Chen, X.-S., Wang, K.-X., 2007. Variation of the lignan content of *Schisandra chinensis* (Turcz.) Baill And *Schisandra sphenanthera* Rehd. et Wils. Chromatographia 66, 125–128.

Supplementary Data

Identification of GABA$_A$ Receptor Modulators in *Kadsura longipedunculata* and assignment of absolute configurations by quantum-chemical ECD calculations

Janine Zaugg[a], Samad Nejad Ebrahimi[a,b], Martin Smiesko[c], Igor Baburin[d], Steffen Hering[d], Matthias Hamburger[a,*]

Divisions of [a]Pharmaceutical Biology and [c]Molecular Modeling, University of Basel, Klingelbergstrasse 50, 4056 Basel, Switzerland

[b]*Departement of Phytochemistry, Medicinal Plant and Drugs Research Institute, Shahid Beheshti University, G. C., Tehran, Iran*

[d]*Institute of Pharmacology and Toxicology, University of Vienna, Althanstrasse 14, 1090 Vienna, Austria*

*Corresponding author. Tel.: +41 612671425; fax: +41 612671474.
  E-mail addresses: martin.smiesko@unibas.ch (M. Smiesko), steffen.hering@univie.ac.at (S. Hering) matthias.hamburger@unibas.ch (M. Hamburger)

S1. Plant material

Kadsura longipedunculata (Syn.: *K. peltigera* Rehder & Wilson; *K. Discigera* Finet & Gagnep. ; *K. omeiensis* S.F. Lan). Material: dried apocarps purple to dark brown, 5-7 mm long, 3-5 mm wide; 1-2 reniform seeds found per apocarp, 3-4 mm long and wide. Seed testa smooth, dark brown (in accordance to lit. (Saunders, 1998). Tastes aromatic, slightly sour.

Kadsura japonica (L.) Dunal (Syn.: *K. matsudai* Hayata). Material : dried apocarps purple to dark brown, 5-7 mm long, 3-4 mm wide; 1-2 reniform seeds found per apocarp, approx. 4 mm long, 3-4 mm wide. Seed testa smooth, redish brown to dark brown. (in accordance to literature (Saunders, 1998). Tastes aromatic, slightly sour. Microscopic characteristics were in agreement with lit. (Fujita, 1929)

Schisandra chinensis (Turczaninow) Baillon (Syn.: *Maximowiczia amurensis* Ruprecht; *Sphaerostema japonicum* A. Gray) Material: dried apocarps dark puple, with hoarfrost like coating, 5-7 mm long, 4-5 mm wide; 2 reniform seeds found per apocarp; approx. 4 mm long, 3-4 mm wide. Seed testa smooth, orange-brown (in accordance to literature (Saunders, 2000). Tastes aromatic and very sour. Microscopic characteristics were in agreement with lit. (Fujita, 1929)

S2. Analytical Data of Isolated Compounds
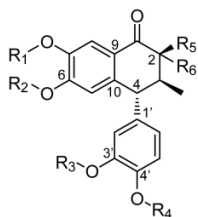
	R_1	R_2	R_3	R_4	R_5	R_6
1	H	CH_3	CH_3	H	CH_3	H
2	CH_3	H	CH_3	H	CH_3	H
3	H	CH_3	CH_3	CH_3	CH_3	H
4	H	CH_3	CH_3	CH_3	H	CH_3

S2.1 (2S,3S,4R)-Arisantetralone A (1) (Cheng et al., 2009; da Silva and Lopes, 2004)

$[\alpha]^{20}_D$: -32.3° (CHCl$_3$; *c* 0.15); CD (MeOH, *c* = 1.46 × 10^{-4} M, 1 cm pathlength): $[\theta]_{213}$ +23 796, $[\theta]_{226}$ +6 370, $[\theta]_{240}$ +24 118, $[\theta]_{252}$ 0, $[\theta]_{256}$ -1 330, $[\theta]_{261}$ 0, $[\theta]_{273}$ +7 013, $[\theta]_{281}$ 0, $[\theta]_{290}$ -10 031, $[\theta]_{302}$ -4 020, $[\theta]_{324}$ -5 820; ^{13}C NMR (shifts from HSQC and HMBC experiment; MeOD): δ 10.6 (CH$_3$-2), 14.5 (CH$_3$-3), 42.2 (C-3), 42.8 (C-2), 49.9 (C-4), 54.9 (OCH$_3$-6), 55.1 (OCH$_3$-3'), 111.8 (C-8), 111.9 (C-5), 112.2 (C-2'), 114.6 (C-5'), 121.1 (C-6'), 125.5 (C-9), 135.3 (C-1'), 138.2 (C-10), 145.0 (C-4'), 145.5 (C-7), 148.0 (3'), 153.1 (C-6), 201.6 (C-1); ^{1}H NMR (500.13 MHz, MeOD): δ 0.97 (3H, *d*, *J* = 7.0 Hz, C3-CH$_3$), 1.09 (3H, *d*, *J* = 7.2 Hz, C2-CH$_3$), 2.42 (1H, *ddq*, $J_{3,2}$ = 4.0 Hz, $J_{3,4}$ = 5.9, *J* = 7.0 Hz, C3-H), 2.73 (1H, *dq*, *J* = 4.0 Hz, *J* = 7.2 Hz, C2-H), 3.75 (3H, s, C6-OCH$_3$), 3.76 (3H, s, C3'-OCH$_3$), 4.00 (1H, d, *J* = 5.9 Hz, C4-H), 6.48 (1H, dd, $J_{6',2'}$ = 2.0 Hz, $J_{6',5'}$ = 8.1 Hz, C6'-H), 6.51 (1H, s, C5-H), 6.67 (1H, d, *J* = 2.0 Hz, C2'-H), 6.74 (1H, d, *J* = 8.1 Hz, C5'-H), 7.41 (1H, s, C8-H); ESI-MS *m/z* 343 [M+H]$^+$

S2.2 (2S,3S,4R)-Arisantetralone B (2) (Cheng et al., 2009; da Silva and Lopes, 2004)

$[\alpha]^{20}_D$: -90.7° (CHCl$_3$; *c* 0.12); CD (MeOH, *c* = 1.46 × 10^{-4} M, 1 cm pathlength): $[\theta]_{213}$ +21 218, $[\theta]_{233}$ +3 533, $[\theta]_{241}$ +6 937, $[\theta]_{256}$ 0, $[\theta]_{274}$ +7 334, $[\theta]_{283}$ 0, $[\theta]_{290}$ -6 737, $[\theta]_{304}$ -2 755, $[\theta]_{317}$ -2 539, $[\theta]_{328}$ 0, $[\theta]_{341}$ +1 515; ^{13}C NMR (shifts from HSQC and HMBC experiment; MeOD): δ 11.8 (CH$_3$-2), 16.12 (CH$_3$-3), 43.2 (C-3), 44.8 (C-2), 50.7 (C-4), 56.4 (OCH$_3$-7), 56.5 (OCH$_3$-3'), 109.6 (C-8), 113.8 (C-2'), 116.2 (C-5'), 117.6 (C-5), 122.7 (C-6'), 125.5 (C-9), 135.1 (C-1'), 142.4 (C-10), 144.8 (C-4'), 148.9 (C-7 and C-3'), 152.8 (C-6), 202.7 (C-1); ^{1}H NMR (500.13 MHz, MeOD): δ 0.95 (3H, *d*, *J* = 7.2 Hz, C3-CH$_3$), 1.10 (3H, *d*, *J* = 7.2 Hz, C2-CH$_3$), 2.43 (1H, *ddq*, $J_{3,2}$ = 4.1 Hz, $J_{3,4}$ = 6.5, *J* = 7.2 Hz, C3-H), 2.71 (1H, *dq*, *J* = 4.1 Hz, *J* = 7.2 Hz, C2-H), 3.77 (3H, s, C3'-OCH$_3$), 3.80 (3H, s, C7-OCH$_3$), 3.91 (1H, d, *J* = 6.5 Hz, C4-H), 6.39 (1H, s, C5-H), 6.50 (1H, dd, $J_{6',2'}$ = 1.8 Hz, $J_{6',5'}$ = 8.1 Hz, C6'-H) 6.67 (1H, d, *J* = 1.8 Hz, C2'-H), 6.74 (1H, d, *J* = 8.1 Hz, C5'-H), 7.52 (1H, s, C8-H); ESI-MS *m/z* 343 [M+H]$^+$

S2.3 (2S,3S,4R)-Arisantetralone C (3) (Cheng et al., 2009; da Silva and Lopes, 2004)

$[\alpha]^{20}_D$: -36.9° (CHCl₃; *c* 0.61); CD (MeOH, *c* = 1.40 × 10⁻⁴ M, 1 cm pathlength): $[\theta]_{213}$ +21 559, $[\theta]_{226}$ +7 680, $[\theta]_{238}$ +20 568, $[\theta]_{256}$ +2017, $[\theta]_{274}$ +7 346, $[\theta]_{287}$ +428, $[\theta]_{298}$ +2 518, $[\theta]_{320}$ 0, $[\theta]_{325}$ -376, $[\theta]_{333}$ 0; ¹³C NMR (shifts from HSQC and HMBC experiment; MeOD): δ 11.9 (CH₃-2), 16.0 (CH₃-3), 43.5 (C-3), 44.0 (C-2), 51.3 (C-4), 56.3 (OCH₃-6 and OCH₃-3'), 56.5 (OCH₃-4'), 113.1 (C-5, C-8, and C-5'), 113.9 (C-2'), 122.4 (C-6'), 126.3 (C-9), 137.5 (C-1'), 139.4 (C-10), 146.8 (C-7), 149.4 (C-4'), 150.5 (C-3'), 154.3 (C-6), 202.3 (C-1); ¹H NMR (500.13 MHz, MeOD): δ 0.98 (3H, *d*, *J* = 7.0 Hz, C3-CH₃), 1.09 (3H, *d*, *J* = 7.0 Hz, C2-CH₃), 2.72 (1H, *dq*, *J* = 4.0 Hz, *J* = 7.0 Hz, C2-H), 2.43 (1H, *ddq*, $J_{3,2}$ = 4.0 Hz, $J_{3,4}$ = 5.7, *J* = 7.0 Hz, C3-H), 3.75 (3H, s, C6-OCH₃ and C3'-OCH₃), 3.81 (3H, s, C4'-OCH₃), 4.04 (1H, d, *J* = 5.7 Hz, C4-H), 6.52 (1H, s, C5-H), 6.58 (1H, dd, $J_{6',2'}$ = 1.9 Hz, $J_{6',5'}$ = 8.1 Hz, C6'-H), 6.73 (1H, d, *J* = 1.9 Hz, C2'-H), 6.88 (1H, d, *J* = 8.1 Hz, C5'-H), 7.42 (1H, s, C8-H); ESI-MS *m/z* 357 [M+H]⁺

S2.4 (2R,3S,4R)-Arisantetralone D (4) (Cheng et al., 2009; da Silva and Lopes, 2004)

$[\alpha]^{20}_D$: +2.7° (CHCl₃; *c* 1.00); CD (MeOH, *c* = 1.46 × 10⁻⁴ M, 1 cm pathlength): $[\theta]_{214}$ +27 701, $[\theta]_{225}$ +9 144, $[\theta]_{241}$ +20 771, $[\theta]_{256}$ +4 273, $[\theta]_{270}$ +10 375, $[\theta]_{284}$ 0, $[\theta]_{288}$ -1 950, $[\theta]_{295}$ -372, $[\theta]_{304}$ -1 188, $[\theta]_{313}$ 0, $[\theta]_{331}$ +9 437; ¹³C NMR (shifts from HSQC and HMBC experiment; MeOD): δ 11.6 (CH₃-2), 16.9 (CH₃-3), 43.8 (C-3), 48.3 (C-2), 52.8 (C-4), 54.6 (OCH₃-6), 55.3 (OCH₃-3' and OCH₃-4'), 111.1 (C-5), 111.5 (C-8), 111.8 (C-5') 112.8 (C-2'), 122.0 (C-6'), 125.7 (C-9), 136.9 (C-1'), 141.3 (C-10), 145.3 (C-7), 147.9 (C-4'), 149.9 (C-3'), 152.6 (C-6), 199.5 (C-1); ¹H NMR (500.13 MHz, MeOD): δ 0.93 (3H, *d*, *J* = 7.0 Hz, C3-CH₃), 1.26 (3H, *d*, *J* = 7.0 Hz, C2-CH₃), 2.37 (1H, *dq*, *J* = 12.2 Hz, *J* = 7.0 Hz, C2-H), 2.43 (1H, *ddq*, $J_{3,2}$ = 12.2 Hz, $J_{3,4}$ = 10.5, *J* = 7.0 Hz, C3-H), 3.59 (3H, s, C6-OCH₃), 3.73 (1H, d, *J* = 10.5 Hz, C4-H), 3.77 (3H, s, C3'-OCH₃), 3.84 (3H, s, C4'-OCH₃), 6.21 (1H, s, C5-H), 6.73 (1H, d, *J* = 1.8 Hz, C2'-H), 6.77 (1H, dd, $J_{6',2'}$ = 1.8 Hz, $J_{6',5'}$ = 7.8 Hz, C6'-H), 6.98 (1H, d, *J* = 7.8 Hz, C5'-H), 7.38 (1H, s, C8-H); ESI-MS *m/z* 357 [M+H]⁺
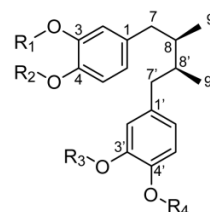
	R₁	R₂	R₃	R₄
5	H	CH₃	CH₃	H
8	H	CH₃	CH₃	CH₃
11	-CH₂-		CH₃	H
13	-CH₂-		CH₃	CH₃

S2.5 Meso-dihydroguaiaretic acid (5) (Schrecker, 1957; Wang et al., 2006)

$[\alpha]^{20}_D$: +4.1° (CHCl₃; *c* 1.00); ¹³C NMR (shifts from HSQC and HMBC experiment; MeOD): δ 15.1 (C-9 and C-9'), 38.3 (C-7 and C-7'), 38.7 (C-8 and C-8'), 55.1 (OCH₃-3 and OCH₃-3'), 112.4 (C-2 and C-2'), 114.5 (C-5 and C-5'), 121.2 (C-6 and C-6'), 133.5 (C-1 and C-1'), 144.1 (C-4 and C-4'), 147.3 (C-3 and C-3'); ¹H NMR (500 MHz, MeOD) δ 0.83 (6H, d, *J* = 6.7 Hz, C9-H, C9'-H), 1.74 (2H, dqdd, *J* = 9.0, 6.7, 5.4, 5.0 Hz, C8-H, C8'-H), 2.26 (2H, dd, *J* = 13.5, 9.0 Hz, C7-Hᵦ and C7'-Hᵦ), 2.70 (2H, dd, *J* = 13.5, 5.4 Hz, C7-Hₐ and C7'-Hₐ), 3.78 (6H, s, C3-OCH₃ and C3'-OCH₃), 6.58 (2H, dd, *J* = 8.0, 1.8 Hz, C5-H and C5'-H), 6.65 (2H, d, *J* = 1.8 Hz, C2-H and C2'-H), 6.71 (2H, d, *J* = 8.0 Hz, C6-H and C6'-H); Critical NOESY correlations: 7.28 ↔ 1.03, 1.22, 2.47; 2.47 ↔ 0.52; ESI-MS *m/z* 331 [M+H]⁺

S2.6 Quasi-meso-monomethyl dihydroguaiaretic acid (8) (Miyazawa et al., 1997)

$[\alpha]^{20}_D$: 0° (CHCl₃; *c* 0.09); ¹³C NMR (shifts from HSQC and HMBC experiment; MeOD): δ 15.1 (C-9 and C-9'), 38.2 (C-7 and C-7'), 38.7 (C-8 and C-8'), 55.2 (OCH₃-3, OCH₃-3', and OCH-4'), 112.1 (C-5)[a], 112.5 (C-2')[b], 113.0 (C-2)[b], 114.5 (C-5')[a], 121.2 (C-6')[c], 121.3 (C-6)[c], 133.4 (C-1')[d], 134.8 (C-1)[d], 143.9 (C-4 and C-4'), 147.2 (C-3')[e], 148.9 (C-3)[e]; ¹H NMR (500 MHz, MeOD) δ 0.84 (3H, d, *J* = 6.7 Hz, C9-H)[f], 0.85 (3H, d, *J* = 6.7 Hz, C9'-H)[f], 1.76 (2H, m, C8-H and C8'-H), 2.28 (1H, dd, *J* = 13.5, 9.1 Hz, C7-Hᵦ)[g], 2.30 (1H, dd, *J* = 13.5, 9.1Hz, C7'-Hᵦ)[g], 2.71 (1H, dd, *J* = 13.5, 5.1 Hz, C7-Hₐ)[h], 2.74 (1H, dd, *J* = 13.5, 5.1 Hz, C7'-Hₐ)[h], 3.77 (3H, s, C3-OCH₃)[i], 3.79 (3H, s, C3'-OCH₃)[i], 3.80 (3H, s, C4'-OCH₃)[i], 6.59 (1H,

169

dd, J = 8.0, 1.9 Hz, C6'-H)^j, 6.67 (1H, d, J = 1.9 Hz, C2'-H)^k, 6.69 (1H, d, J = 1.9 Hz, C2-H) ^{k}, 6.70 (1H, dd, J = 8.0, 1.9 Hz, C6-H)^j, 6.70 (1H, d, J = 8.0 Hz, C5'-H)^l, 6.84 (1H, d, J = 8.0 Hz, C5-H)^l; ESI-MS *m/z* 345 [M+H]$^+$
$^{a-l}$ Interchangeable

S2.7 Anwulignan (11) (Nakatani et al., 1988)

$[\alpha]^{20}_D$: +1.1° (CHCl$_3$; *c* 1.0); ^{13}C NMR (shifts from HSQC and HMBC experiment; CDCl$_3$): δ 16.1 (C-9 and C-9'), 38.9 (C-7'), 39.3 (C-7), 39.4 (C-8 and C-8'), 55.8 (OCH$_3$-3'), 100.6 (-OCH$_2$O-), 107.9 (C-5), 109.3 (C-2), 111.7 (C-2'), 114.1 (C-5'), 121.7 (C-6), 121.7 (C-6'), 133.7 (C-1'), 135.7 (C-1), 143.9 (C-4'), 145.4 (C-4), 146.3 (C-3'), 147.5 (C-3); ^{1}H NMR (500 MHz, CDCl$_3$) δ 0.84 (3H, d, J = 6.7 Hz, C9-H), 0.85 (3H, d, J = 6.7 Hz, C9'-H), 1.74 (2H, m, C8-H and C8'-H), 2.25 (1H, dd, J = 13.5, 9.6 Hz, C7'-H$_b$), 2.28 (1H, dd, J = 13.5, 9.6 Hz, C7-H$_b$), 2.72 (2H, dd, J = 13.5, 4.8 Hz, C7'-H$_a$ and C7-H$_a$), 3.85 (3H, s, C3'-OCH$_3$), 5.90 (2H, m, C3,C4-OOCH$_2$), 6.60 (1H, dd, J = 8.0, 1.4 Hz, C6-H), 6.62 (1H, d, J = 1.4 Hz, C2'-H), 6.64 (1H, dd, J = 8.0, 1.4 Hz, C6'-H), 6.65 (1H, d, J = 1.4 Hz, C2-H), 6.72 (1H, d, J = 8.0 Hz, C5-H), 6.82 (1H, d, J = 8.0 Hz, C5'-H); ESI-MS *m/z* 329 [M+H]$^+$

S2.8 Saururenin (13) (Wang et al., 2000)

$[\alpha]^{20}_D$: +2.3° (MeOD; *c* 0.33); ^{13}C NMR (shifts from HSQC and HMBC experiment; CDCl$_3$): δ 16.2 (C-9 and C-9'), 39.0 (C-7 and C-7'), 39.5 (C-8 and C-8'), 55.9 (OCH$_3$-3' and OCH$_3$-4'), 100.6 (-OCH$_2$O-), 108.0 (C-5), 109.0 (C-2), 112.5 (C-2'), 111.9 (C-5'), 121.5 (C-6), 121.2 (C-6'), 134.5 (C-1'), 135.6 (C-1), 147.6 (C-4'), 145.6 (C-4), 149.4 (C-3'), 147.8 (C-3); ^{1}H NMR (500 MHz, CDCl$_3$) δ 0.84 (3H, d, J = 6.7 Hz, C9-H)^a, 0.85 (3H, d, J = 6.7 Hz, C9'-H)^a, 1.70 – 1.80 (2H, m, C8-H and C8'-H), 2.26 (1H, dd, J = 13.3, 9.0 Hz, C7'-H$_b$), 2.29 (1H, dd, J = 13.3, 9.0 Hz, C7-H$_b$), 2.71 (2H, dd, J = 13.3, 6.2 Hz, C7-H$_a$), 2.73 (2H, dd, J = 13.3, 6.2 Hz, C7'-H$_a$), 3.82 (3H, s, C4'-OCH$_3$), 3.83 (3H, s, C3'-OCH$_3$), 5.86 (2H, s, C3,C4-OOCH$_2$), 6.59 (1H, dd, J = 8.2, 1.3 Hz, C6-H), 6.64 (1H, d, J = 1.3 Hz, C2-H), 6.67 (1H, dd, J = 7.8, 1.4 Hz, C6'-H), 6.70 (1H, d, J = 8.2 Hz, C5-H), 6.65 (1H, d, J = 1.4 Hz, C2'-H), 6.77 (1H, d, J = 8.2 Hz, C5'-H); ESI-MS *m/z* 343 [M+H]$^+$
^{a} Interchangeable
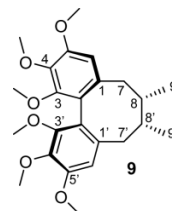
S2.9 Deoxyschizandrin (9) (Ikeya et al., 1980; Ikeya et al., 1979)

CD (MeOH, *c* = 1.20 × 10^{-4} M, 1 cm pathlength): $[\theta]_{213}$ -39 102, $[\theta]_{223}$ 0, $[\theta]_{238}$ +45 446 sh., $[\theta]_{249}$ +56 876, $[\theta]_{272}$ +14 681 sh.; ^{13}C NMR (shifts from HSQC and HMBC experiment; MeOD): δ 12.9 (C-9), 21.9 (C-9'), 35.2 (C-8), 36.4 (C-7'), 40.0 (C-7), 42.2 (C-8'), 56.5 (OCH$_3$-5 and OCH$_3$-5'), 60.8 (OCH$_3$-3 and OCH$_3$-3'), 61.3 (OCH$_3$-4 and OCH$_3$-4'), 108.9 (C-6'), 112.4 (C-6), 123.3 (C-2'), 124.4 (C-2), 135.5 (C-1), 140.5 (C-1'), 140.8 (C-4'), 141.4 (C-4), 152.3 (C-3'), 152.3 (C-3), 152.9 (C-5), 154.0 (C-5'); ^{1}H NMR (500 MHz, MeOD) δ 0.74 (3H, d, J = 7.2 Hz, C9-H), 1.01 (3H, d, J = 7.2 Hz, C9'-H), 1.78 (1H, dqdd, $J_{8',7'a}$ = 9.5 Hz, $J_{8',9'}$ = 7.2 Hz, $J_{8',8}$ = 2.9 Hz, $J_{8',7'b}$ = 1.4 Hz, C8'-H), 1.92 (1H, dqdd, $J_{8,7a}$ = 7.7 Hz, $J_{8,9}$ = 7.2 Hz, $J_{8,8'}$ = 2.9 Hz, $J_{8,7b}$ = 1.8 Hz, C8-H), 2.10 (1H, dd, J = 13.3, J = 1.4 Hz, C7'-H$_b$), 2.26 (1H, dd, J = 13.3 Hz, J = 9.5 Hz, C7'-H$_a$), 2.48 (1H, dd, J = 13.6, J = 1.8 Hz, C7-H$_b$), 2.63 (1H, dd, J = 13.6, J = 7.7 Hz, C7-H$_a$), 3.47 (6H, s, C3-OCH$_3$ and C3'-OCH$_3$), 3.83 – 3.84 (6H, s, C4-OCH$_3$ and C4'-OCH$_3$), 3.87 (6H, s, C5-OCH$_3$ and C5'-OCH$_3$), 6.66 (1H, s, C6'-H), 6.68 (1H, s, C6-H); ESI-MS *m/z* 417 [M+H]$^+$
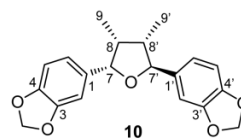
S2.10 (+)-Zuihonin A (10) (Lee, 1981; Sadhu et al., 2003; Urzua et al., 1987)

$[\alpha]^{20}_D$: +104.8° (CHCl$_3$; *c* 0.99); CD (MeOH, *c* = 5.9 × 10^{-4} M, 0.1 cm pathlength): $[\theta]_{200}$ -17 295, $[\theta]_{207}$ +85 087, $[\theta]_{224}$ +3 031, $[\theta]_{239}$ +9 702, $[\theta]_{270}$ +10 375, $[\theta]_{260}$ 0, $[\theta]_{294}$ +3 875, $[\theta]_{304}$ 0; ^{13}C NMR

(shifts from HSQC and HMBC experiment; CDCl$_3$): δ 9.2 (C-9'), 11.7 (C-9), 47.3 (C-8'), 43.3 (C-8), 84.7 (C-7'), 85.6 (C-7), 100.3 (-OCH$_2$O-), 106.2 (C-2), 107.0 (C-2'), 107.6 (C-5 and C-5'), 119.3 (C-6 and C-6'), 134.5 (C-1'), 137.5 (C-1), 147.3 (C-3, C-3', C-4, and C-4'); ^{1}H NMR (500 MHz, CDCl$_3$) δ 0.62 (3H, d, *J* = 7.4 Hz, C9'-H), 0.99 (3H, d, *J* = 7.4 Hz, C9-H), 2.39 (1H, m, C8'-H), 2.40 (1H, m, C8-H), 4.60 (1H, d, *J* = 9.6 Hz, C7-H), 5.34 (1H, d, *J* = 4.4 Hz, C7'-H), 5.90 (4H, m, OCH$_2$O), 6.75 – 6.82 (4H, m, C5-H, C6-H, C5'-H, and C6'-H), 6.85 (1H, br s, C2'-H), 6.92 (1H, br s, C2-H); ESI-MS 703 *m/z* [2M+Na]
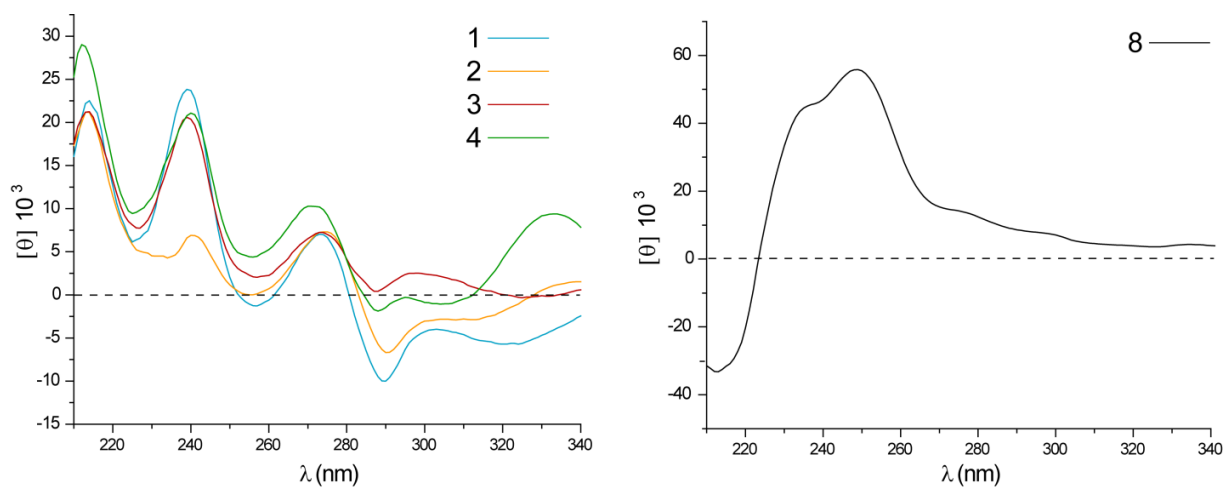
Figure S1. Experimental ECD curves for compounds **1-4** and **8** in MeOH.
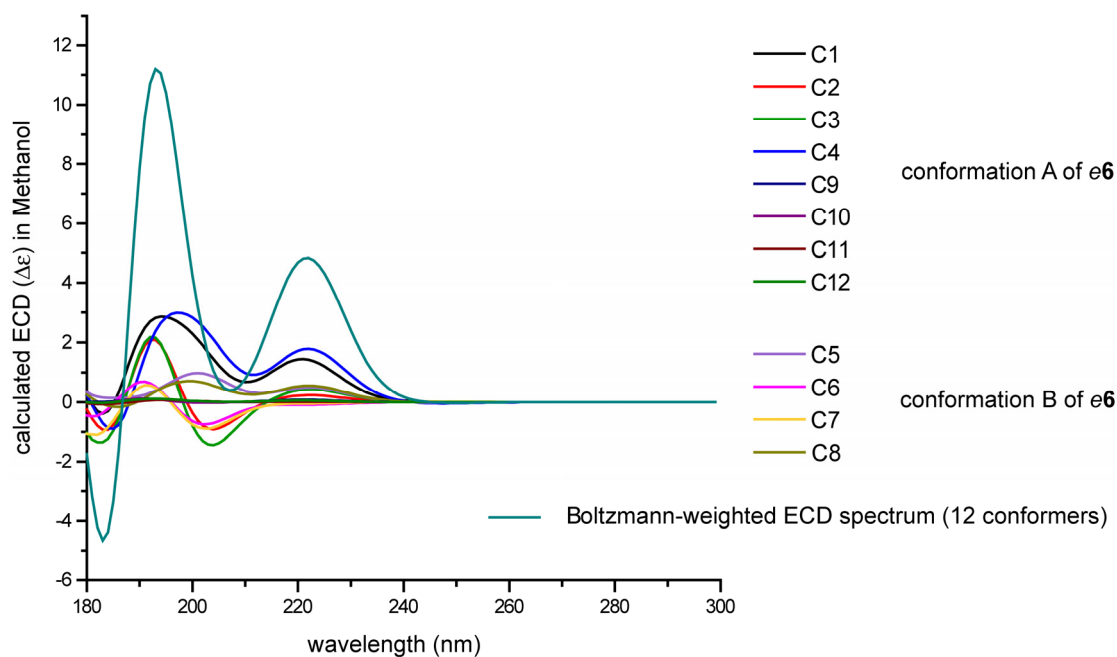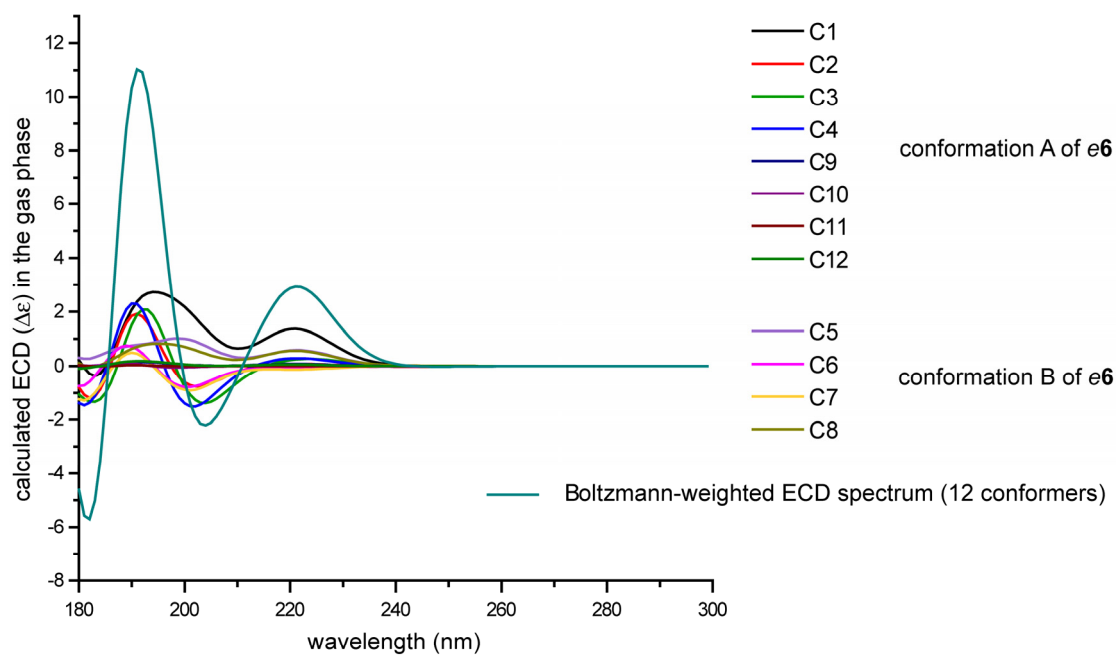
Figure S2. Calculated ECD spectra in the gas-phase and in MeOH (CPCM) of each minimized conformer (DFT/B3LYP/6-31G**) of *e*6 occurring within an energy range of 2 kcal/mol from the global minimum.
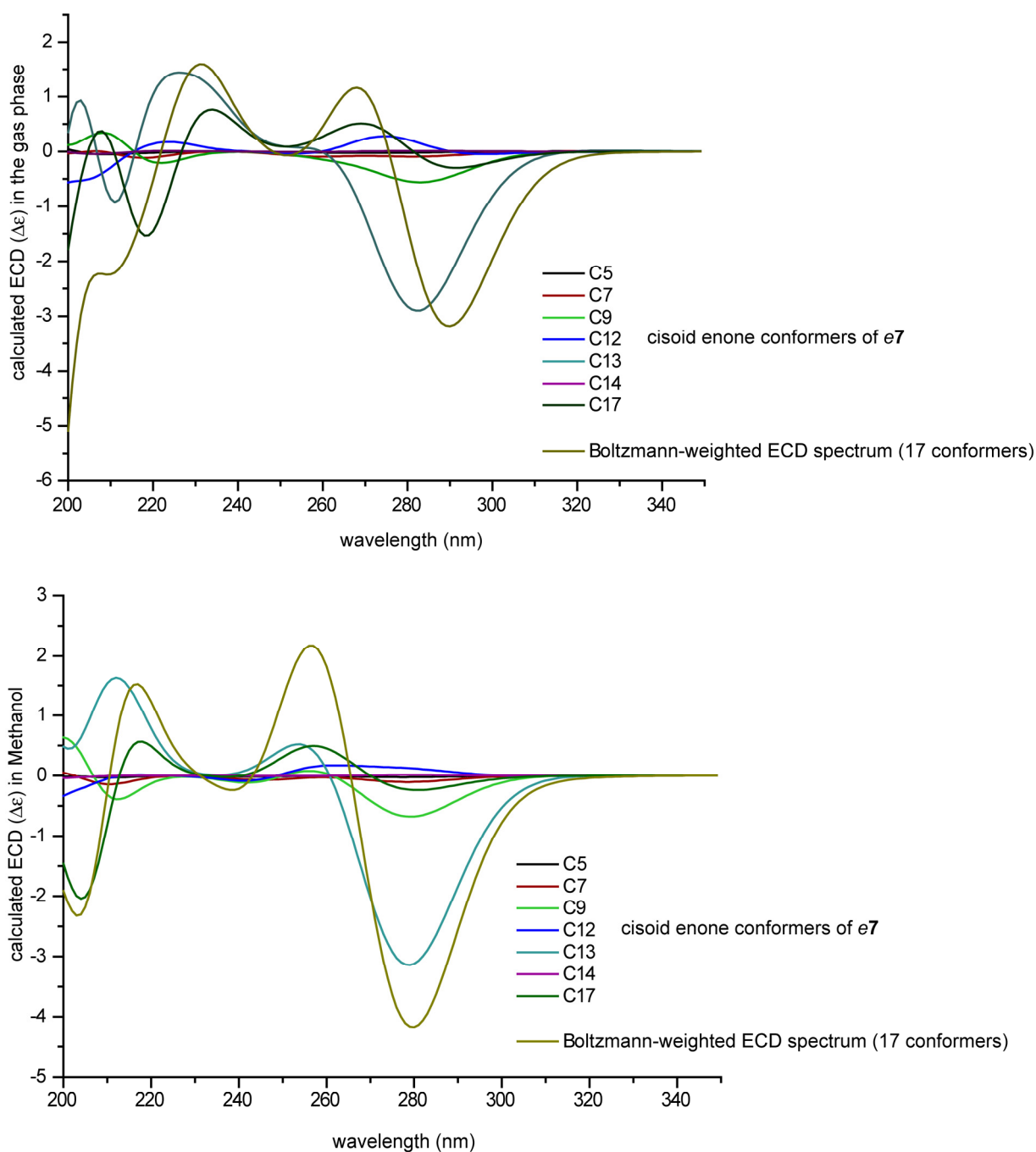
Figure S3. Calculated ECD spectra in the gas-phase and in MeOH (CPCM) of the minimized conformers (DFT/B3LYP/6-31G**) of *e7* with a cisoid enone conformation occurring within an energy range of 1 kcal/mol.
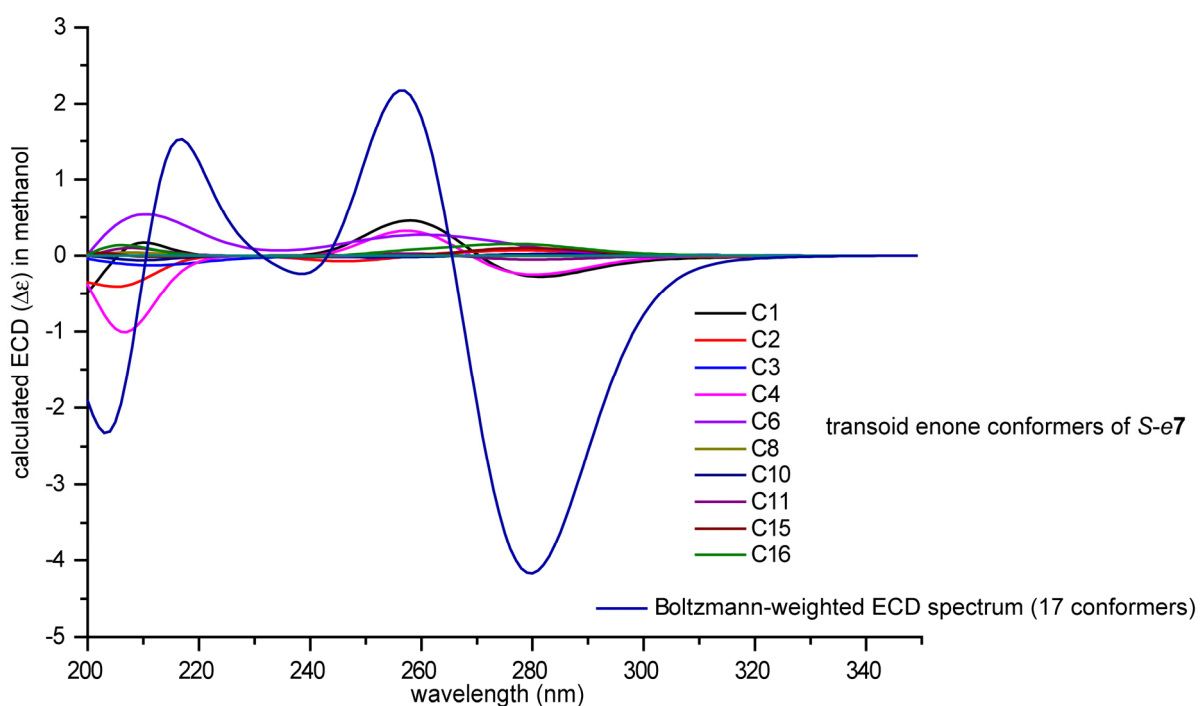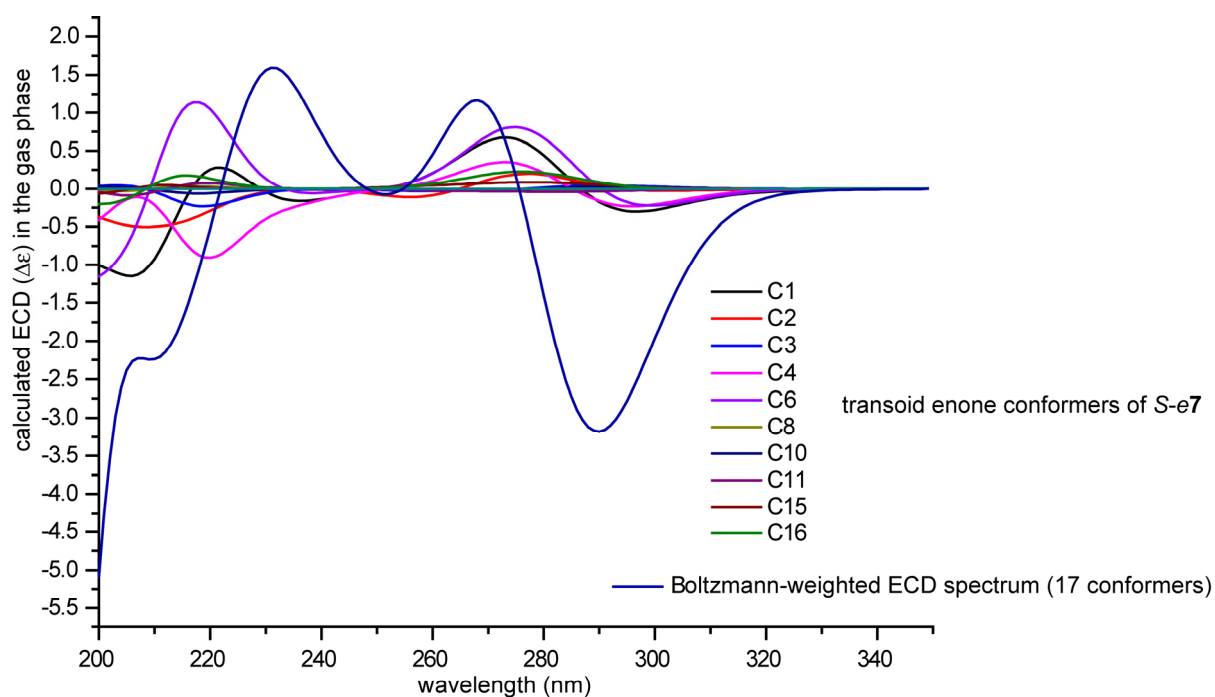
Figure S4. Calculated ECD spectra in the gas-phase and in MeOH (CPCM) of the minimized conformers (DFT/B3LYP/6-31G**) of *e***7** with a transoid enone conformation occurring within an energy range of 1 kcal/mol.
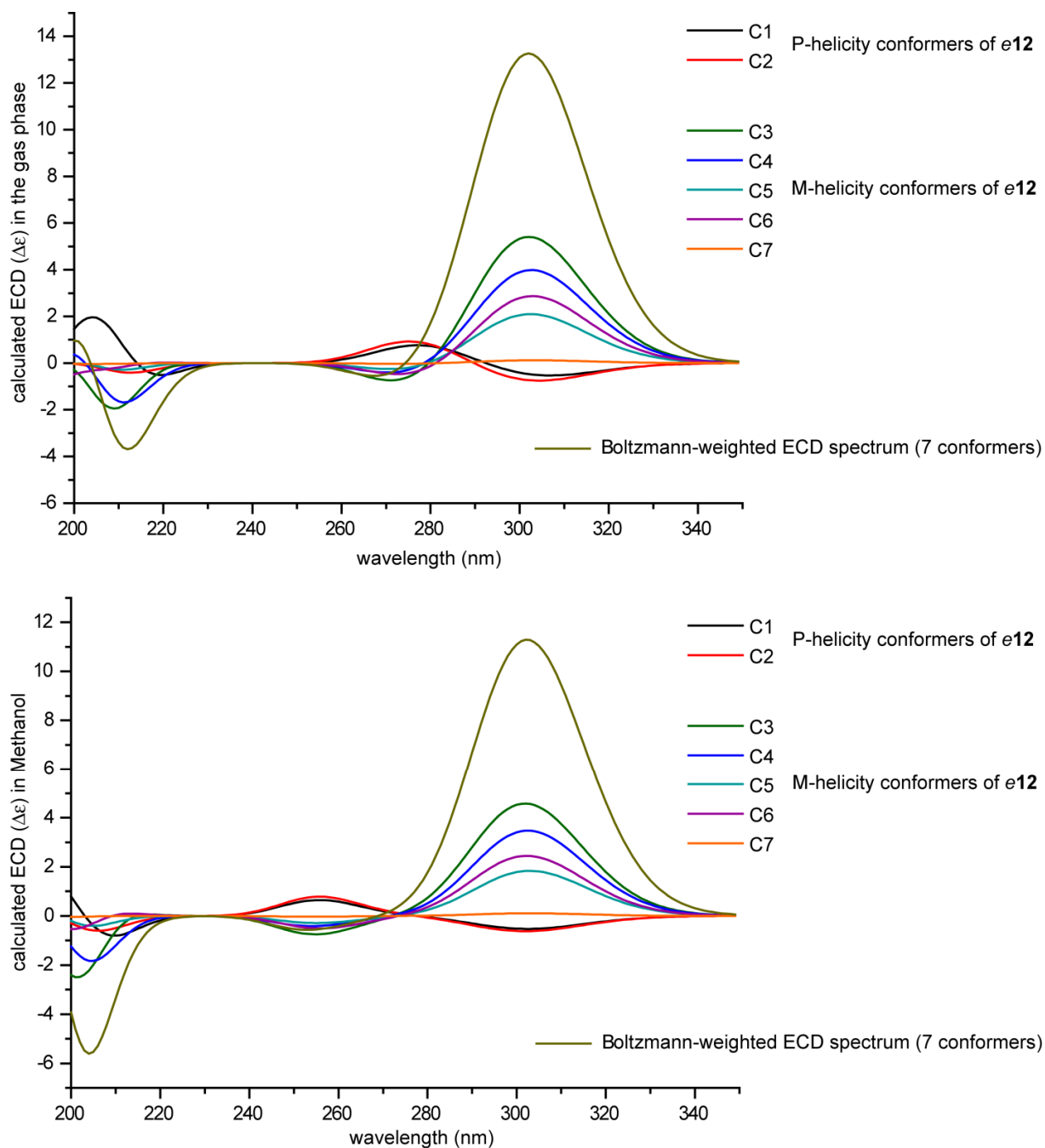
Figure S5. Calculated ECD spectra in the gas-phase and in MeOH (CPCM) of each minimized conformer (DFT/B3LYP/6-31G**) of *e***12** occurring within an energy range of 2 kcal/mol.

Table S1. Conformational analysis of compound *e*7, *e*12, and *e*6 in the gas phase.

Compound *e*7			Compound *e*12			Compound *e*6		
Species[a]	ΔE^{b}	$PE\%^{c}$	Species[a]	ΔE^{a}	$PE\%^{b}$	Species[d]	ΔE^{a}	$PE\%^{b}$
C1	1.2	4.8	**C1**	**0.0**	**26.6**	C1	0.0	15.4
C2	2.8	0.3	C2	0.3	15.1	C2	0.0	15.4
C3	3.8	0.1	C3	0.1	22.6	C3	0.0	15.6
C4	1.3	4.1	C4	0.4	14.3	**C4**	**0.0**	**16.7**
C5	2.6	0.5	C5	0.7	7.9	C5	0.4	8.6
C6	1.2	4.6	C6	0.4	12.6	C6	0.4	8.4
C7	1.7	2.1	C7	2.0	0.9	C7	0.4	8.9
C8	2.9	0.3				C8	0.4	8.3
C9	1.0	7.2				C9	1.9	0.7
C10	2.8	0.3				C10	1.9	0.7
C11	2.3	0.8				C11	1.9	0.7
C12	1.0	6.8				C12	1.9	0.7
C13	**0.0**	**36.3**						
C14	2.7	0.4						
C15	2.5	0.5						
C16	2.1	1.0						
C17	0.2	25.6						

[a]Occurring within a 1 kcal/mol window in the conformational search using OPLS 2005 force field. [b]Relative energy (kcal/mol) *ab initio* calculated. [c]Boltzmann weights for different conformers calculated by using DFT/B3YLP/6-31G** in the gas phase. [d] Occurring within a 2 kcal/mol window in the conformational search using OPLS 2005 force field.

Table S2. Dihedral angles causing diene helicity in compound *e***12.**

Species	*C1-C2-C3-C4*	*Helicity*
C1	15.9	P
C2	15.8	P
C3	-14.8	M
C4	-14.5	M
C5	-14.5	M
C6	-14.8	M
C7	-15.6	M
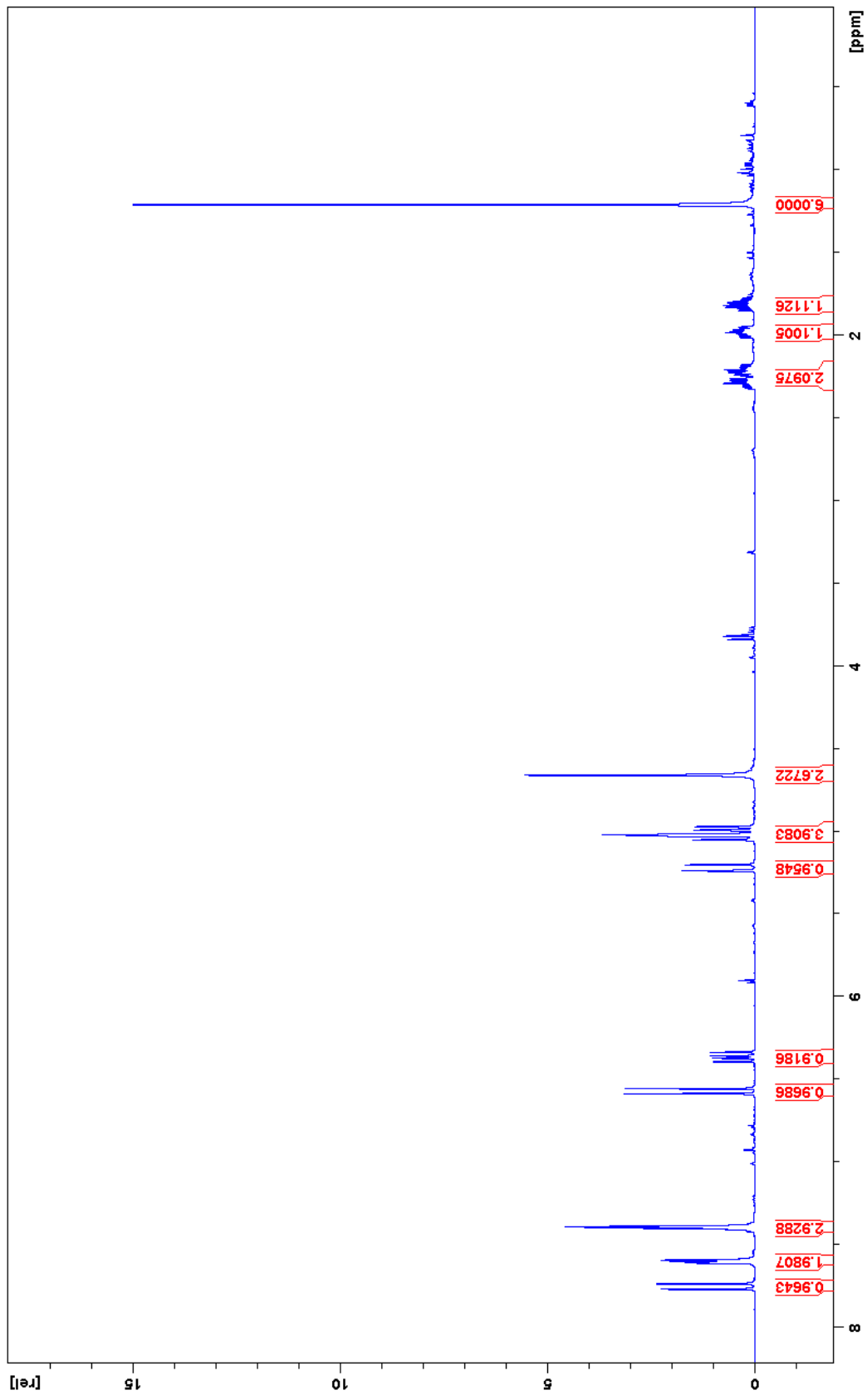
Figure S6. ^{1}H NMR spectrum of compound **7** (recorded in MeOD, 32 scans).
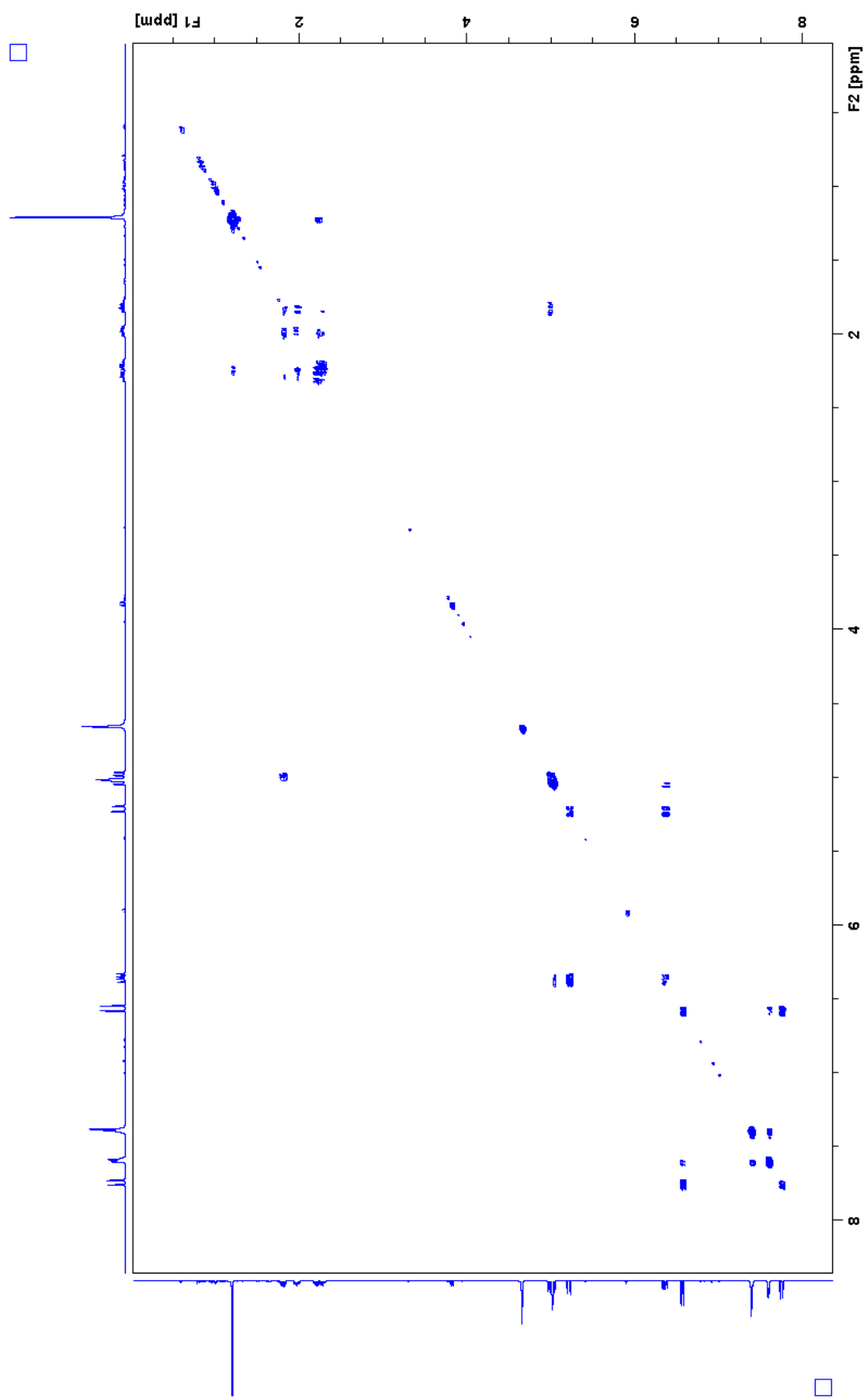
Figure S7. COSY NMR spectrum of compound **7** (recorded in MeOD, 1 scan)
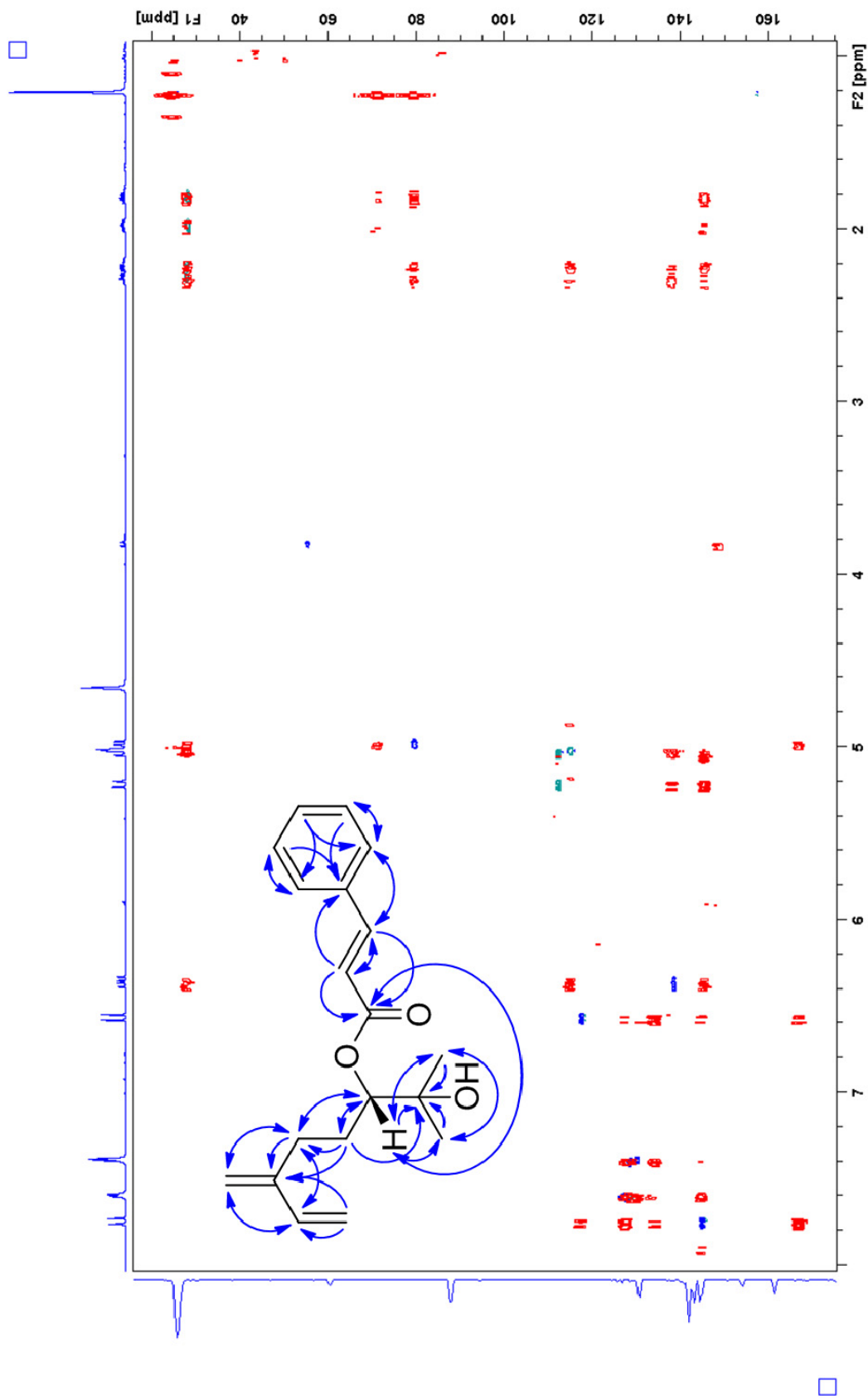
Figure S8. Overlay of HSQC and HMBC NMR spectra of compound **7**. HMBC correlations indicated with arrows (recorded in MeOD, HSQC: 2 scans, HMBC: 16 scans).
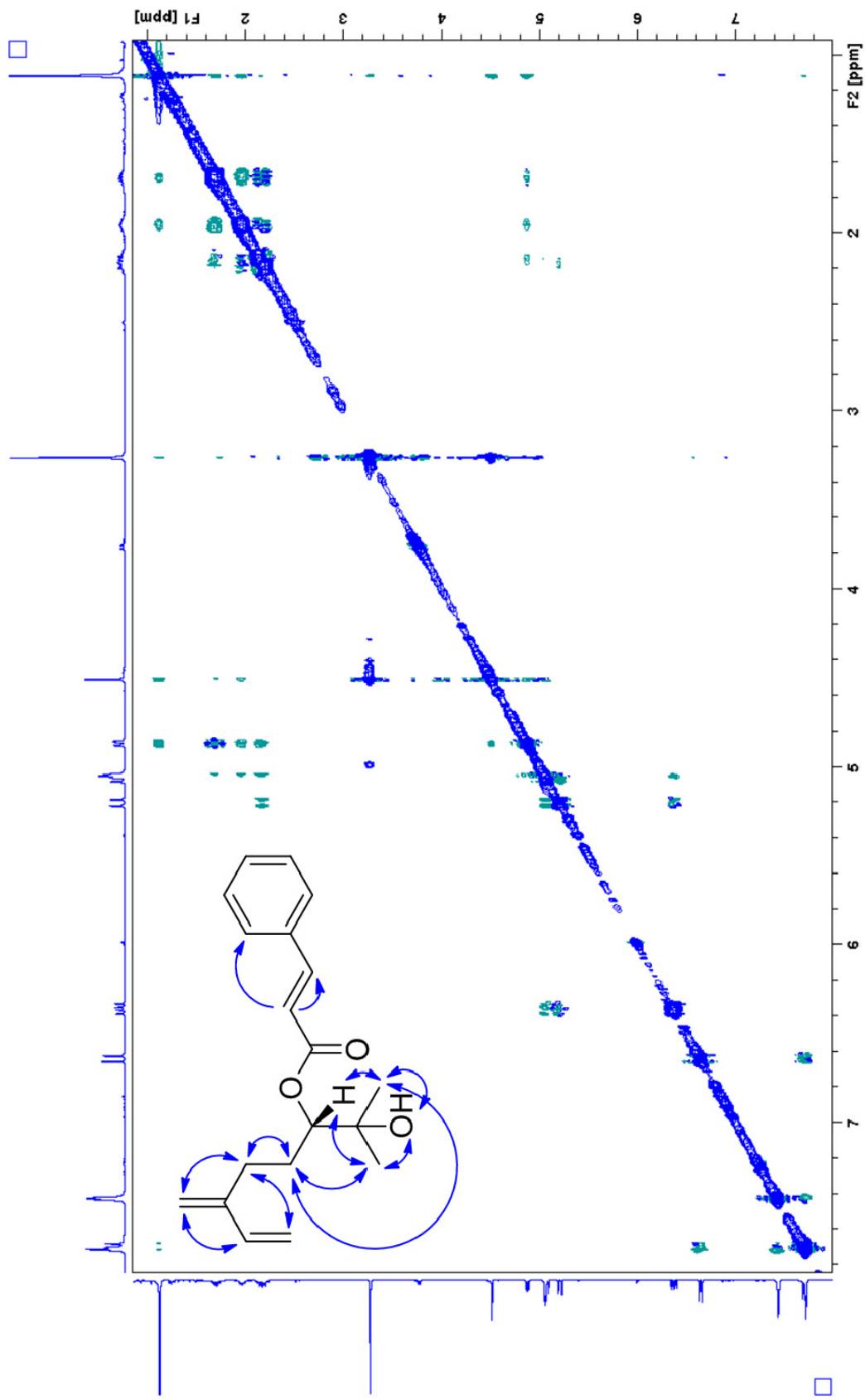
Figure S9. NOESY NMR spectrum of compound **7** (recorded in DMSO-*d6*, 64 scans, mixing time: 300 ms). Correlations indicated with arrows.
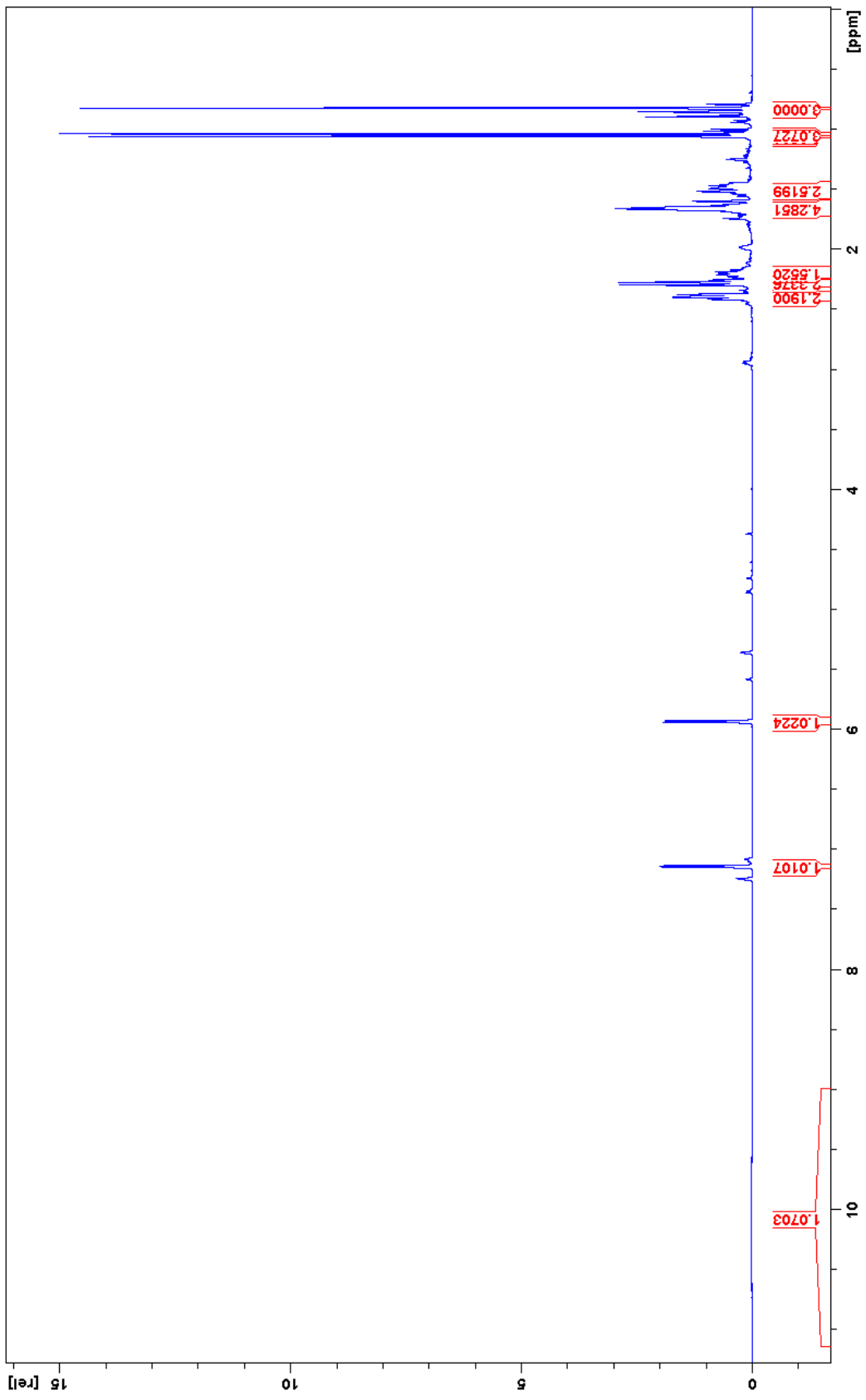
Figure S10. ^1H NMR spectrum of compound **12** (recorded in CDCl$_3$, 128 scans)
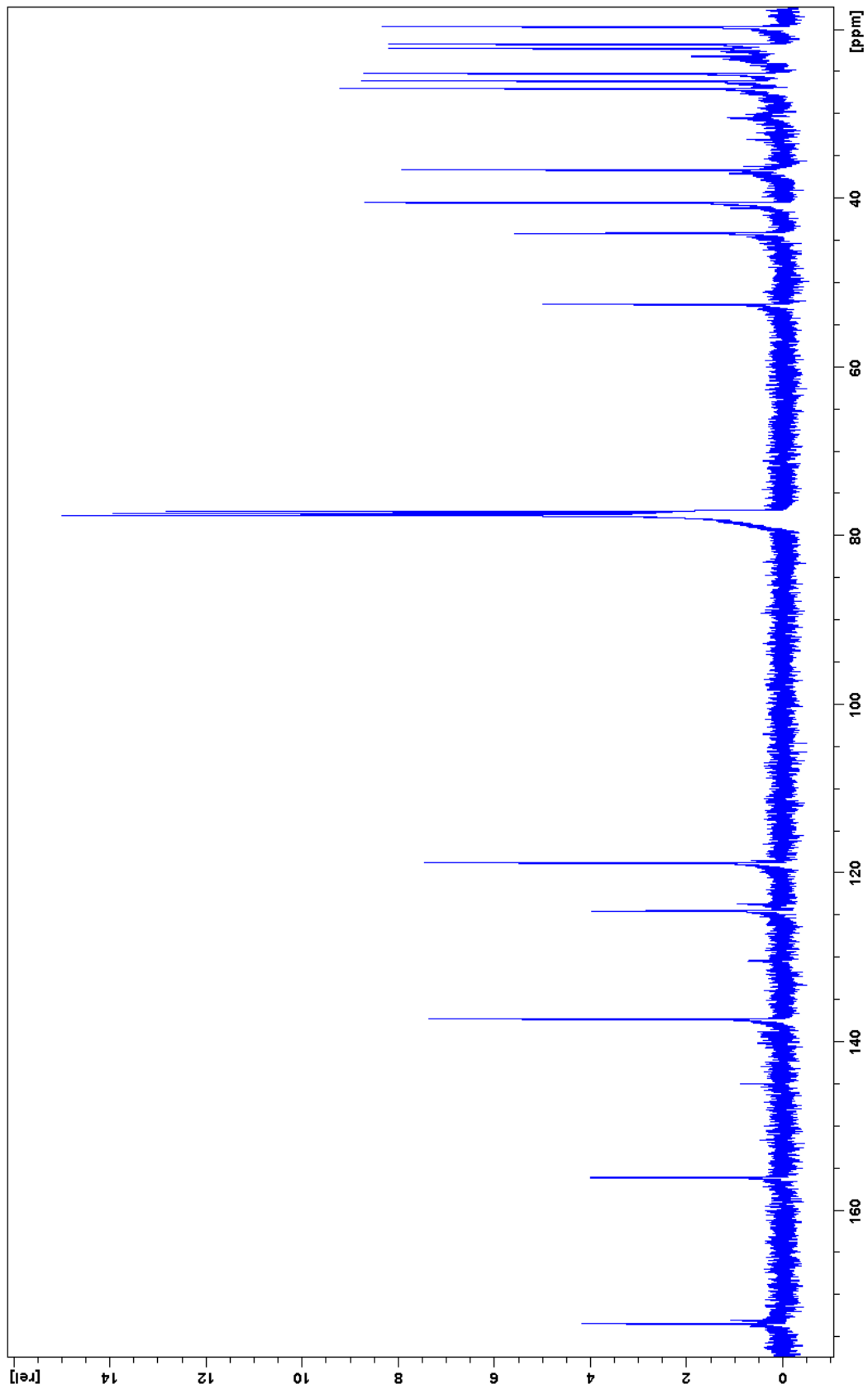
Figure S11. ^{13}C NMR spectrum of compound **12** (recorded in CDCl$_3$, 8192 scans).
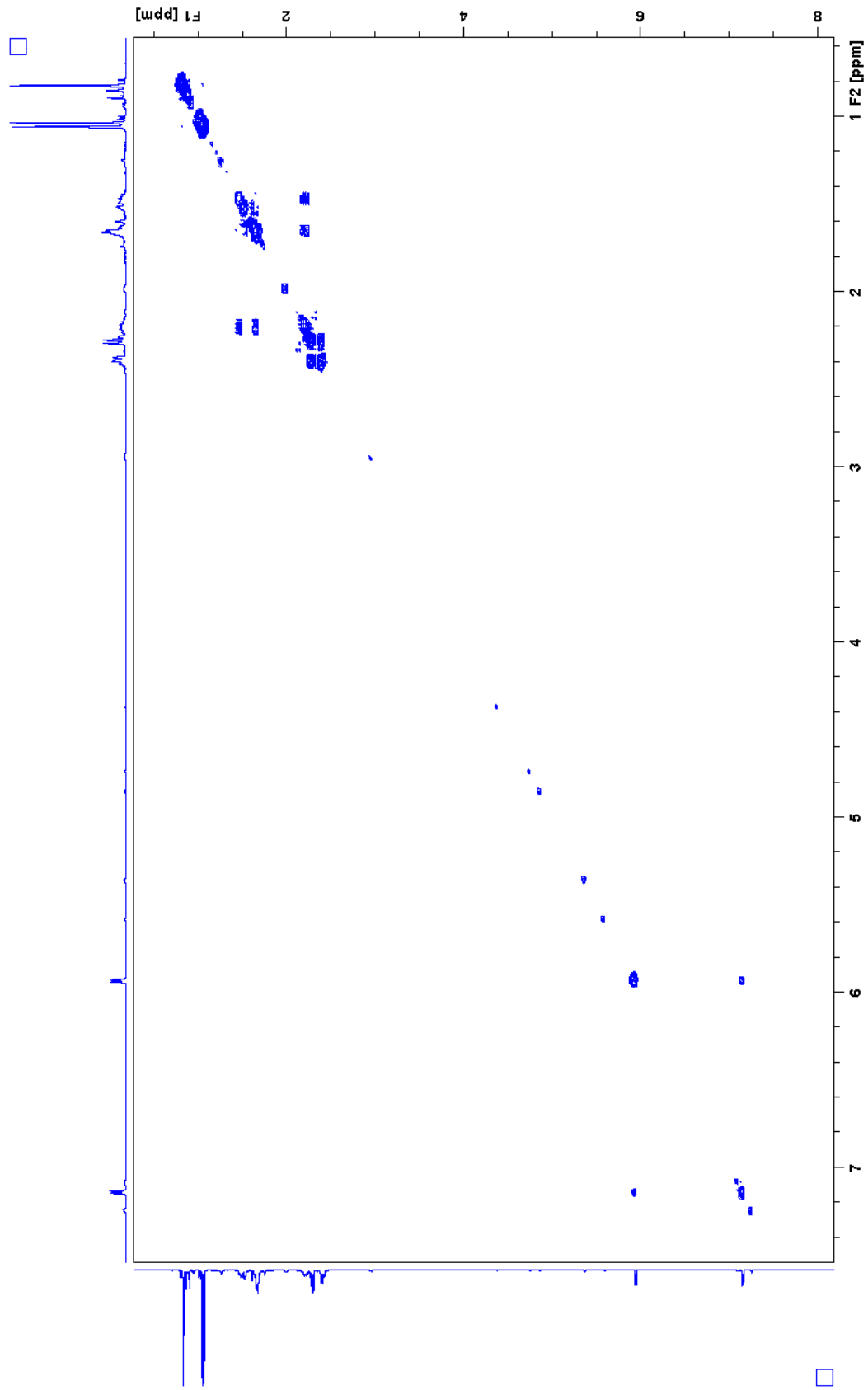
Figure S12. COSY NMR spectrum of compound **12** (recorded in CDCl$_3$, 4 scans)
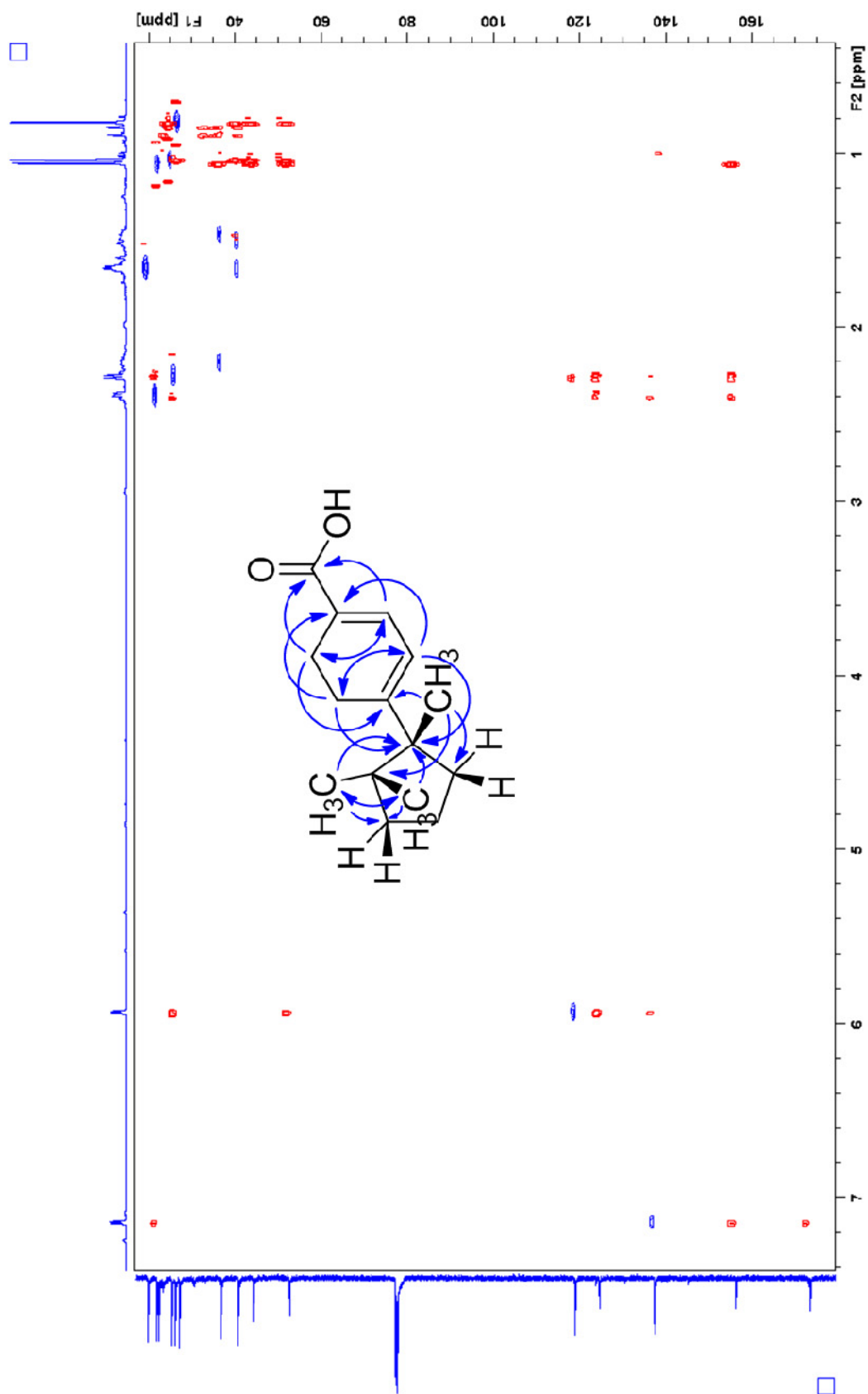
Figure S13. Overlay of HSQC and HMBC NMR spectra of compound **12** (recorded in CDCl$_3$, HSQC: 4 scans, HMBC: 8 scans). HMBC correlations indicated with arrows.

186

Figure S14. NOESY NMR spectrum of compound **12** (recorded in *d6*-DMSO, 64 scans, mixing time: 300 ms).
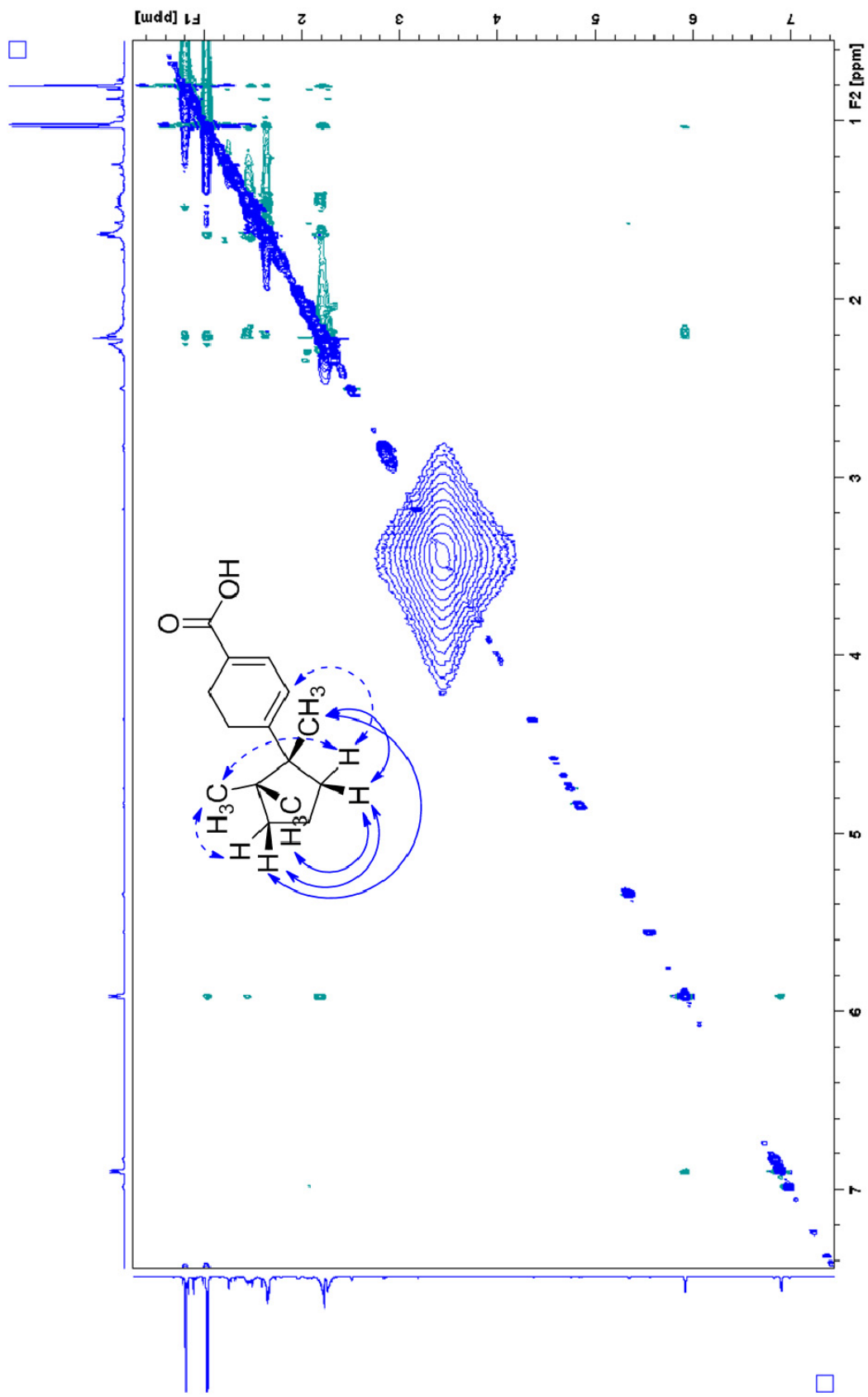
References

Cheng, Y. B., Chang, M. T., Lo, Y. W., Ho, C. J., Kuo, Y. C., Chien, C. T., CHen, S. Y., Liou, S. S., Kuo, Y. H., Shen, Y. C., 2009. Oxygenated lignans from the fruits of *Schisandra arisanensis*. J. Nat. Prod. 72, 1663-1668.

da Silva, T., Lopes, L. M. X., 2004. Aryltetralone lignans and 7,8-seco-lignans from *Holostylis reniformis*. Phytochemistry 65, 751-759.

Fujita, N., 1929. Über die Früche der *Schizandra chinensis* Bail. und *Kadsura japonica* Dun. Arch. Pharm. Ber. Deutsch. Pharm. Ges. 267, 532-540.

Ikeya, Y., Taguchi, H., Sasaki, H., Nakajima, K., Yosioka, I., 1980. The constituents of *Schizandra chinensis* BAILL. VI. 13C nuclear magnetic resonance spectroscopy of dibenzocyclooctadiene lignans. Chem. Pharm. Bull. 28, 2414-2421.

Ikeya, Y., Taguchi, H., Yosioka, I., Kobayashi, H., 1979. The constituents of *Schizandra chinensis* BAILL. V. The structures of four new lignans, gomisin N, gomisin O, epigomisin O and gomisin E, and transformation of gomisin N to deangeloylgomisin B. Chem. Pharm. Bull. 27, 2695-2709.

Lee, C.-L., 1981. The extractive components of formosan lauraceous plants I. Four lignans from the bark of *Machilus zuihoensis* forma *longipaniculata*. Kexue-Fazhan 9, 578-583.

Miyazawa, M., Kasahara, H., Kameoka, H., 1997. *O*-Demethylation of meso-dimethyldihydroguaiaretic acid in *Spodoptera litua*. Phytochemistry 46, 1173-1175.

Nakatani, N., Ikeda, K., Kikuzaki, H., Kido, M., Yamaguchi, Y., 1988. Diaryldimethylbutane lignans from *Myristica argentea* and their antimicrobial action against *Streptococcus mutans*. Phytochemistry 27, 3127-3129.

Sadhu, S. K., Okuyama, E., Fujimoto, H., Ishibashi, M., 2003. Separation of *Leucas aspera*, a medicinal plant of Bangladesh, guided by prostaglandin inhibitory and antioxidant activities. Chem. Pharm. Bull. 51, 595-598.

Saunders, R. K. M., 1998. Monograph of *Kadsura* (Schisandraceae). Systematic Botany Monographs 54, 1-106.

Saunders, R. K. M., 2000. Monograph of *Schisandra* (Schisandraceae). Systematic Botany Monographs 58, 1-146.

Schrecker, A. W., 1957. meso-Dihydroguaiaretic acid and its derivatives. J. Am. Chem. Soc. 79, 3823-3827.

Urzua, A., Freyer, A. J., Shamma, M., 1987. 2,5-Diaryl-3,4-dimethyltetrahydrofuranoid lignans. Phytochemistry 26, 1509-1511.

Wang, B. G., Hong, X., Li, L., Zhou, J., Hao, X. J., 2000. Chemical constituents of two Chinese Magnoliaceae plants, *Tsoongiodendron odorum* and *Manglietiastrum sinicum*, and their inhibition of platelet aggregation. Planta Med. 66, 6107-6112.

Wang, Q., Yang, Y., Li, Y., Yu, W., Hou, Z. J., 2006. An efficient method for the synthesis of lignans. Tetrahedron 62, 6107-6112.

4. CONCLUSIONS AND OUTLOOK

The extracts of *Piper nigrum* fruits, *Angelica pubescens* roots, *Acorus calamus* roots, *Biota orientalis* leaves and twigs, and *Kadsura longipedunculata* fruits fulfilled the selection criteria for an investigation of their GABA$_A$ receptor modulating constituents due to the following reasons: (i) they all exhibited pronounced potentiation of the GABA induced chloride current in the screening, (ii) they all originated from plants related to TCM, and (iii) the plants belong to different families of distinct orders. These are good preconditions to afford pharmacologically favorable, GABA$_A$ receptor modulating compounds from diverse secondary metabolite classes.

The HPLC-based activity profiling approach [1] was used for the identification of the active constituents of all extracts investigated in this study. The virtues of this miniaturized approach were exemplified with the piperamides from *Piper nigrum* (**Chapter 3.1**). Using only milligram amounts of extract, we were able to identify compounds responsible for the activity (piperine (**1**) as main new scaffold) along with other, structurally related, inactive constituents. The generation of this "virtual" library allowed preliminary structure-activity considerations useful for further medicinal chemistry efforts (Chart 4). Structure elucidation using minute amounts of material could only be realized due to off-line use of highly sensitive microprobe NMR for semi-preparative HPLC fractions and on-line HPLC-PDA-TOF-MS. Our work on *Piper nigrum* demonstrated that these are core analytical tools for the HPLC-based activity profiling approach.

In the case of *Angelica pubescens* (**Chapter 3.2**), HPLC-based activity profiling allowed the early dereplication of the coumarin osthol as a major active compound. Despite being aware of the neurotoxicity of this compound, we decided to pursue further the investigation with *A. pubsecens* since reports on GABA$_A$ receptor activity of coumarins were fairly limited [2]. Preliminary *in vitro* tests using the *Xenopus* assay, however, revealed only moderate GABA$_A$ receptor modulation by all compounds isolated from *A. pubescens*, and the project was discontinued.

Determination of the configuration of a chiral compound is difficult and often complicates the process of structure elucidation as it is shown by the examples of *Acorus calamus* (**Chapter 3.3**) and *Kadsura longipedunculata* (**Chapter 3.5**). With (+)-dioxosarcoguaiacol from *A. calamus*, we demonstrated the applicability of *in silico* conformational analysis and geometrical optimization as complementary for determining the relative configuration by NMR experiments. Hence, we were able to rectify and complete the previously reported relative configuration of this compound (Figure 10) [3].

After full elucidation of the covalent structure by NMR experiments, we were able to identify the absolute configuration of the isoprenoids isolated from *K. longipedunculata*. Again, experimental data (ECD) could be interpreted with the aid of conformational analysis and quantum-chemical calculations. Both examples highlight the value of a multidisciplinary approach for successful structure elucidation.
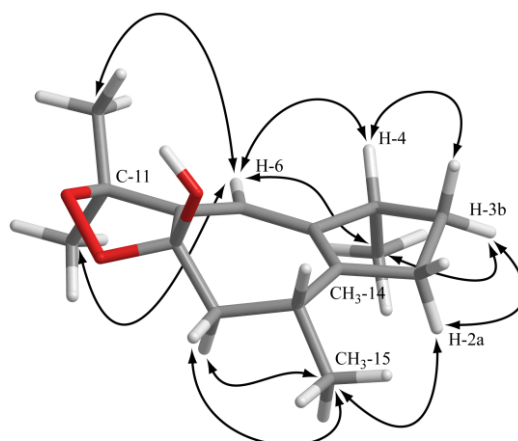
Figure 10: 4*R**8*S**10*R**-(+)-dioxosarcoguaiacol

The ultimately identified novel GABA$_A$ receptor modulators within this study belong to distinct classes of secondary metabolites, as assumed from the targeted choice of active extracts for investigation (Figure 11). Scaffold similarities allowed insights into structural features critical for GABA$_A$ receptor modulation (Chart 4). Several compounds fulfilled the criteria for being a relevant hit for further pharmacological investigations (Figure 11, Table 2, Chart 4). These criteria include (i) adequate potency and efficiency at the target in comparison with known drugs (Figure 11), (ii) "drug-likeness" by answering Lipinski's rule-of-five [4] and physico-chemical properties favorable for blood-brain barrier (BBB) penetration [4, 5] (Table 2), (iii) scaffold novelty, and not unimportant, (iv) the possibility of resupply for *in vivo* experiments and medicinal chemistry efforts.

Table 2: Physico-chemical properties of "drug-like" scaffolds isolated within this thesis with potential for further investigation at the GABA$_A$ receptor.[a]

Compound	H-acceptors	H-donors	MW (g/mol)	cLogP	Rotatable bonds	PSA
1	4	0	285	3.3	0	38.8
2	2	1	302	4.2	2	37.3
4	4	1	328	5.6	6	47.9
5	4	0	342	5.6	7	36.9
6, 7	5	2	342	3.6	3	76.0
8	5	1	356	4.1	4	65.0
10	1	0	220	4.6	3	17.1
12	1	0	220	4.4	1	17.1

[a] Physico-chemical properties favorable for oral bioavailability and blood-brain barrier penetration were enunciated by Pajouhesh and Lenz, 2005 [5], on the basis of Lipinski's rule-of-five [4]. They include: H-acceptors ≤ 7, H-donors ≤ 3, MW ≤ 450 g/mol, cLogP ≤ 5, rotatable bonds ≤ 8, polar surface area (PSA) ≤ 60-70 (-90) Å^2
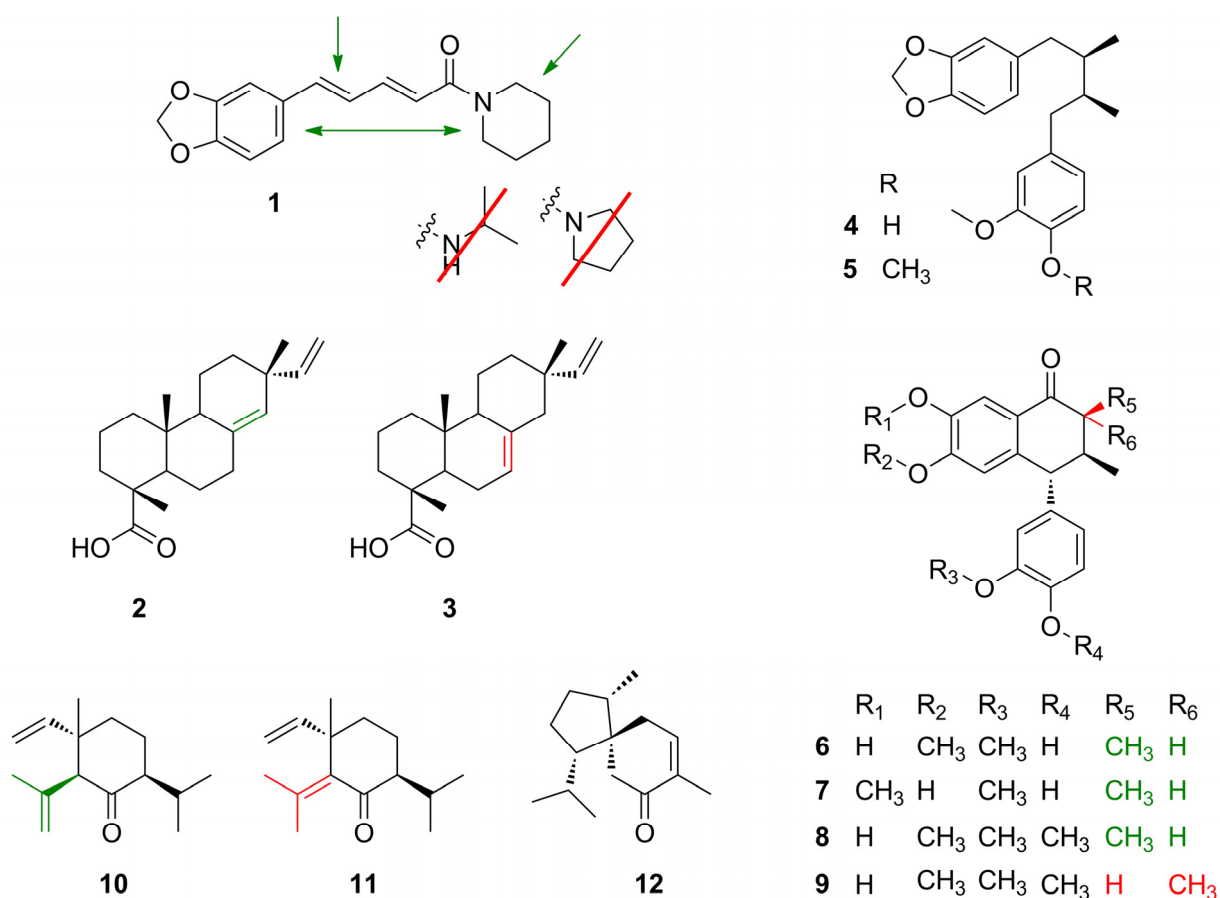
Chart 4: Selected novel scaffolds at the $\alpha_1\beta_2\gamma_{2S}$ GABA$_A$ receptor from natural origin. Structural features positively influencing potency and efficiency are highlighted in green, structural features impairing GABA$_A$ receptor activity, are indicated in red.

As a consequence of our findings, the GABA$_A$ receptor subtype specificity of piperine (**1**) has been characterized, the scaffold was used for medicinal chemistry, and *in vivo* experiments assessing the sedative-like and anxiolytic-like activity of this natural product have been conducted. These soon to be published data will provide more information about the relevance of this scaffold for further development. Piperine (**1**) is, however, a pharmacologically promiscuous compound and inhibits phase I and phase II metabolism [6-10] hence auguring side effects and drug-drug interactions. Therefore it must be investigated to what extent structural modifications of the piperine scaffold can positively influence target selectivity.

Sandaracopimaric acid (**2**) equally answered the criteria for being a relevant hit (Table 2). It binds as well independently from the BZD binding site, thus presenting an interesting scaffold for the development of GABA$_A$ receptor modulating drugs.
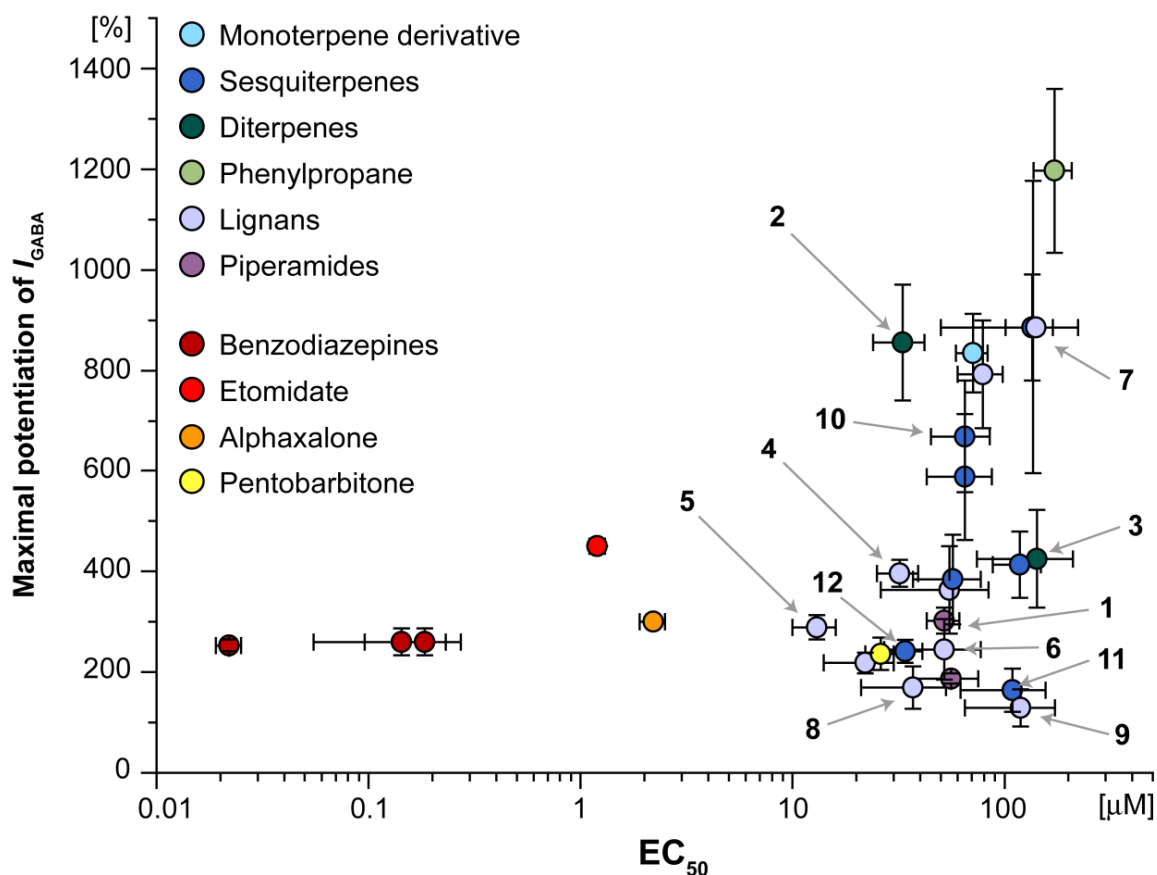
Figure 11: Overview on GABA$_A$ receptor modulatory efficiency and potency at the $\alpha_1\beta_2\gamma_{2S}$ subtype by compounds isolated from *Piper nigrum* fruits, *Acorus calamus* roots, *Biota orientalis* leaves and twigs, and *Kadsura longipedunculata* fruits. The compounds are grouped according to their structure. Compounds from *Angelica pubescens* are missing since potencies and efficiencies were not determined. Numbers indicate the compounds shown in Chart 4: piperine (**1**), sandaracopimaric acid (**2**), isopimaric acid (**3**), anwulignan (**4**), saururenin (**5**), arisantetralones A-D (**6-9**), sesquiterpenes of *A. calamus* (**10-12**). Potentiation of the GABA-induced chloride current (I_{GABA}) was measured at a GABA EC$_{5-10}$. Reference data of benzodiazepines (triazolam, midazolam, clotiazepam) are taken from Khom et al. 2006 [11]. Etomidate and Alphaxalone values were measured by Pau et al. 2003 [12]. Pentobarbitone was investigated by Thompson et al, 1996 [13], however, using a GABA EC$_{20}$ which means that pentobarbitone efficiency is underestimated compared to the rest.

We conducted experiments to investigate GABA$_A$ receptor subtype specificity with **2** and assessed pharmacological effects in preliminary animal experiments (**Chapter 3.4**). However, a rather strong efficiency *in vitro* occurring at α_2, α_3, or β_2 subunit-containing receptors, could not be confirmed *in vivo*, reflected by comparatively weak anxiolytic-like effects. Further *in vivo* experiments using different paradigms complementary to ours might give deeper insight into the pharmacological action and the potency and efficiency of this molecule. Despite slightly superior efficiencies at the above mentioned receptors, it is advisable to further improve subtype

selectivity of **2** by medicinal chemistry. An important issue is pharmacokinetics and toxicity, which should soon be addressed for sandaracopimaric acid (**2**) with appropriate experiments.

Intraperitoneal drug administration has been chosen by many researchers for *in vivo* behavioral experiments investigating GABA$_A$ receptor related effects, inclusively our publication (**Chapter 3.4**). However, this route of drug administration is disputable, since the liver first-pass is disregarded. Oral administration is a much more realistic route including all pharmacokinetic hurdles for a drug to leap and is well applicable when investigating GABA$_A$ receptor active drugs or extracts [2].

Anwulignan (**4**) and saururenin (**5**) showed favorable potencies and efficiencies at the $\alpha_1\beta_2\gamma_{2S}$ GABA$_A$ receptor (**Chapter 3.5**, Figure 11). Moreover, compounds **4** and **5** were devoid of agonistic effects, can be isolated in reasonable amounts, and show "drug-like" physico-chemical properties (except for a slightly high clogP value of 5.6) (Table 2). Therefore, they present new candidates to be evaluated for GABA$_A$ receptor subtype specificity. Other lignans, such as the arisantetralones A-D (**6-9**), attracted attention due to their exceptional influence on I_{GABA} kinetics (**Chapter 3.5**). Such compounds are interesting from the perspective of possibly exploring yet unknown binding sites and mode of interactions at the GABA$_A$ receptor.

Shyobunone (**10**) and acorenone (**12**), isolated from *A. calamus*, are promising in terms of their GABA$_A$ receptor modulatory activity and they also fulfill the criteria for orally available CNS drugs (Figure 11, Table 2). However, careful evaluation of whether further efforts with these compounds are worthwhile is advised. Their small size is a drawback for high affinity hydrophobic interactions [14] but could possibly be overcome by structural modification. Double bonds as well as the carbonyl group may be targeted for this purpose.

The "privileged" scaffolds summarized in Table 2 and Chart 4 are highly lipophilic compounds which are indeed favorable for BBB penetration and oral availability, but implicate solubility problems at sample preparation. For this purpose, often dimethyl sulfoxide is used despite of influencing BBB permeability and brain metabolism [15]. Alternative pharmaceutical formulations for drug delivery devoid of DMSO may be considered for further animal studies.

The compounds that were isolated, structurally characterized, and pharmacologically evaluated in an *in vitro* functional assay enlarge the spectrum of natural products acting as positive GABA$_A$ receptor modulators at the $\alpha_1\beta_2\gamma_{2S}$ subtype (Figure 11). On the whole, a few highlights could be identified which should be pursued further. We can conclude that the pharmacologic potential of some of these compounds is smaller than of others due to known

toxicity (β-asarone, osthol, and linear furanocoumarins), low to moderate activity [angular furanocoumarins, bisabolangelone, isoshyobunone (**11**), piperanine, and arisantetralone D (**9**)] and/or very low potency [preisocalamenediol and isopimaric acid (**3**)], or difficulty in resupply [(+)-dioxosarcoguaiacol (Fig. 1), cuparenes, dihydroguaiaretic acids, zuihonin A, 6-cinnamoyl-7-hydroxymyrcene) (see **Chapters 3.2, 3.3, and 3.5** for structures). In the latter case, literature research for alternative source material might be helpful.

References

1   *Potterat O, Hamburger M*. Natural products in drug discovery - concepts and approaches for tracking bioactivity. Curr Org Chem 2006; 10: 899-920
2   *Moser AD*. Naturstoffe mit GABAA-Rezeptor-Aktivität. Division of Pharmaceutical Biology, University of Basel, Basel, 2009. Master's thesis
3   *Sawant SS, Youssef DTA, Sylwester PW, Wali V, El Sayed KA*. Antiproliferative sesquiterpenes from the red sea soft coral *Sarcophyton glaucum*. Nat Prod Comm 2007; 2: 117-9
4   *Lipinski CA*. Lead- and drug-like compounds: the rule-of-five revolution. Drug Discov Today: Technol 2004; 1: 337-41
5   *Pajouhesh H, Lenz GR*. Medicinal chemical properties of successful central nervous system drugs. NeuroRx 2005; 2: 541-53
6   *McNamara FN, Randall A, Gunthorpe MJ*. Effects of piperine, the pungent component of black pepper, at the human vanilloid receptor (TRPV1). Br J Pharmacol 2005; 144: 781-90
7   *Bajad S, Bedi KL, Singla AK, Johri RK*. Piperine inhibits gastric emptying and gastrointestinal transit in rats and mice. Planta Med 2001; 67: 176
8   *Bhardwaj RK, Glaeser H, Becquemont L, Klotz U, Gupta SK, Fromm MF*. Piperine, a major constituent of black pepper, inhibits human P-glycoprotein and CYP3A4. J Pharmacol Exp Ther 2002; 302: 645
9   *Volak LP, Ghirmai S, Cashman JR, Court MH*. Curcuminoids inhibit multiple human cytochromes P450, UDP-glucuronosyltransferase, and sulfotransferase enzymes, whereas piperine is a relatively selective CYP3A4 inhibitor. Drug Metab Dispos 2008; 36: 1594-605
10 *Anand P, Kunnumakkara AB, Newman RA, Aggarwal BB*. Bioavailability of curcumin: problems and promises. Mol Pharm 2007; 4: 807-18
11 *Khom S, Baburin I, Timin EN, Hohaus A, Sieghart W, Hering S*. Pharmacological properties of GABA(A) receptors containing gamma1 subunits. Mol Pharmacol 2006; 69: 640-9
12 *Pau D, Belelli D, Callachan H, Peden DR, Dunlop JI, Peters JA, Guitart X, Gutierrez B, Lambert JJ*. GABA(A) receptor modulation by the novel intravenous general anaesthetic E-6375. Neuropharmacology 2003; 45: 1029-40
13 *Thompson SA, Whiting PJ, Wafford KA*. Barbiturate interactions at the human GABA(A) receptor: dependence on receptor subunit combination. Br J Pharmacol 1996; 117: 521-7
14 *Böhm H-J, Klebe G, Kubinyi H*, Wirkstoffdesign. Heidelberg, Berlin, Oxford: Spektrum Akademischer Verlag; 1996: 110
15 *Nasrallah FA, Garner B, Ball GE, Rae C*. Modulation of brain metabolism by very low concentrations of the commonly used drug delivery vehicle dimethyl sulfoxide (DMSO). J Neurosci Res 2008; 86: 208-14

ACKNOWLEDGMENTS / DANKSAGUNGEN